Synthesis and Characterization of Transition Metal Amino-phenolate Complexes and Their Reactivity Towards the Oxidation of Lignin Model Compounds and Cyclic Carbonate Formation

By

© Ali Elkurtehi

A thesis submitted to the School of Graduate Studies

in partial fulfillment of the requirements for the degree of

Doctor of Philosophy

Department of Chemistry

Memorial University of Newfoundland

November 2017

St. John's Newfoundland

Abstract

Vanadium and manganese complexes supported by amino-bis(phenolate) ligands, were synthesized and characterized. The catalytic activity of the vanadium complexes in the aerobic oxidation of 4-methoxybenzyl alcohol and 1,2-diphenyl-2-methoxyethanol was explored. Whereas, the complexes showed limited reactivity in H_2O_2-mediated oxidation of diphenylether and benzylphenylether. The manganese complexes showed low activity for the aerobic oxidation of 4-methyoxybenzylalcohol and 1,2-diphenyl-2-methoxyethanol.

The catalytic synthesis of cyclic carbonates under solvent free conditions using vanadium and manganese complexes, epoxides and carbon dioxide was attempted and monitored by in situ IR and NMR spectroscopic techniques. Variable temperature kinetic studies were performed and the activation energies for cyclic carbonate formation were determined experimentally using this *situ* IR spectroscopic data. The catalysts showed excellent activity and good stability in these reactions.

Acknowledgements

Alhamdulillah - all praises to God

First, I offer my sincere gratitude to my supervisor, Dr. Francesca Kerton for giving me the opportunity to join her research group and for her valuable guidance, suggestions, expertise, continuous encouragement and support throughout the course of this study. I would also thank Dr. Francesca Kerton for the useful comments and revisions during the writing of this thesis, which made it possible for me to complete this thesis. My special thanks to Dr. Chris Kozak for his useful suggestions and support in the lab and group meetings. I would want to use this opportunity to express my profound gratitude to my supervisory committee members: Dr. Chris Kozak, Dr. Karen Hattenhauer for their useful discussion and suggestions throughout the period of my studies.

My thanks also go to all the MUN Chemistry Department staff. My especial gratitude to people in Chemistry main office, especially, Mary Flinn, Rosalind Collins, Ebony Penney and Melissa Norris. A special thanks to Dr. Louise Dawe for solving all the crystal structures contained in this thesis. I would also extend my thanks to C-CART (Center for Chemical Analysis, Research and Training): Dr. Celine Schneider, Julie Collins and Linda Windsor for their knowledge and advice with instrumentation (NMR and MALDI-TOF MS).

I would like to thank all the present and past members of Green Chemistry and Catalysis group, especially the undergraduates including Andrew G. Walsh who help contributed to the successful completion of my study. I also thank Yi and Dalal.

Special thanks to Nduka and Katalin for many helpful discussions and encouragement.

I would also like to thank Ministry of Higher Education & Scientific Research - Libya for funding. My regards and gratitude go to those who supported me in any respect during the course of this study. I offer my profound and earnest gratitude to the person who deserves the most gratitude of all is my father. I want to express my deep thanks to my

siblings and all my relatives for their understanding, patience, support and encouragement during the period of this research work and special thanks to my brother Moftah for his encouragement and support.

Lastly, my sincere and profound gratitude go to my wife Fatma. She not only supported me during the entire period of this study but she also made the ultimate sacrifice and give me the strength and courage and took care of my kids, no amount of gift or word can express my heartfelt appreciation for the patience, prayers, and encouragement she has shown to me. She has been my source of inspiration. Especial thanks go to my lovely daughters (Alaa and Saja) and my sons (Mohamed and Omar).

Dedicated to

To

My father and my wife and my kids

My brothers and my sisters

The souls of my mother, step mother, my sisters and father in law

The souls of all those heroes who sacrificed by their souls to defend my country

I dedicate this work with love.

Table of Contents

List of Tables

List of Figures

List of Schemes

List of Appendices

List of Abbreviations and Symbols

(°): degree

Å: Angstrom (10^{-10} m)

BDI: β-diketiminate

BnOH: benzyl alcohol

bp: boiling point

BPA: bisphenol A

br: broad

BuLi: butyllithium

C_5D_5N: deuterated pyridine

C_7D_8: deuterated toluene

calcd: calculated

Cat.: catalyst

$CDCl_3$: deuterated chloroform

CH_2Cl_2: dichloromethane

CHC: cyclohexene carbonate

$CHCl_3$: chloroform

CHO: cyclohexene

CHC: cyclohexene carbonate

Cl^-: chloride ion

DMAP: (4-dimethylamino)pyridine

E_a: activation energy

et al.: and co-workers

GC-MS: gas chromatography mass spectrometry

MALDI-TOF: matrix assisted laser desorption/ionization time-of-flight

NMR: Nuclear magnetic resonance

PC: propylene carbonate

PO: propylene oxide

PPNCl: bis(triphenylphosphoranylidene)iminium chloride

RT: room temperature

SC: styrene carbonate

SO: styrene oxide

TBAB: tetrabutylammonium bromide

^{t}Bu: tertiary-butyl

THF: tetrahydrofuran

TOF: turnover frequency

TON: turnover number

UV: ultraviolet

Vis: visible

1 Introduction

1.1 Biomass as a New Renewable Feedstock

In recent years, concerns about greenhouse gas emissions, global warming as well as the world's energy demands and the potential crisis surrounding the depletion of petroleum resources have increased. Taking such environmental and economic considerations into account and, considering the advantages of renewable resources, including their abundance, sustainability and often low cost,[1] the use of renewable and sustainable feedstocks such as CO_2 or biomass as an energy source is becoming essential.

Recently, biomass (in particular, lignocellulose) has received great interest as a desirable alternative to petroleum as a feedstock for the production of chemicals and fuels. Therefore, the development of new catalytic methods to convert non-food biomass (lignocellulose) into useful chemicals and fuels will become an area of focus for research for many decades to come.[2]

Lignocellulose biomass refers to plant biomass, which is typically composed of microfibrils of cellulose, hemicelluloses, and lignin with varying properties of chain length and degrees of polymerization, and together form a complex and rigid structure (Figure 1.1).[3] The proportion of these polymers is not uniform. They are associated with each other in a hetero-matrix to different degrees and varying relative composition depending on the type, species, and even source of the biomass, Table 1-1.[4]

Although not discussed in detail here, another component group in wood is extractives, which constitute several percent of the wood. The structure of extractives varies considerably between wood types, with their primary function being to protect the tree against fungi and insects.[5]

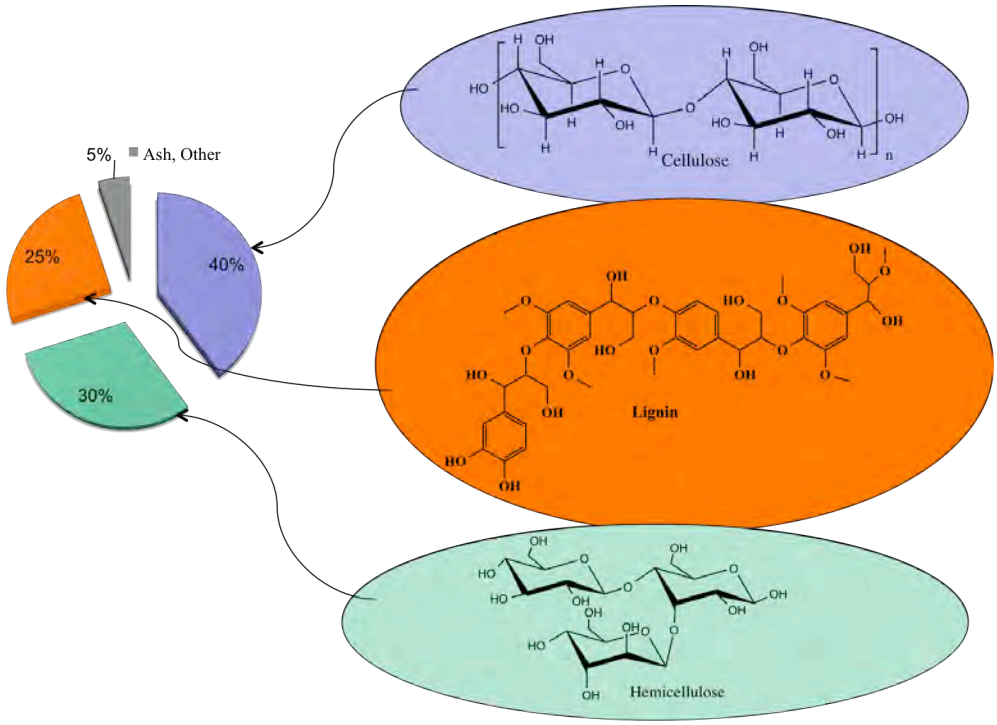

Figure 1.1. The main components and structure of lignocellulose

Table 1-1. Chemical composition of different types of wood

Wood type	Cellulose (%)	Hemicellulose (%)	Lignin (%)
Soft wood	40-45	25-30	25-30
Hard wood	40-45	30-35	20-25
Eucalypt	45	20	30

1.1.1 Cellulose

Cellulose is the most abundant natural carbon bio-resource polymer on Earth and the major component of lignocellulosic materials, representing 40-60% of the total dry weight in wood.[6] It contains carbon, hydrogen and oxygen [C (44.44%), H (6.17%) & O (49.39%)] with a chemical formula of $(C_6H_{10}O_5)_n$. Cellulose is a linear homopolysaccharide of linked sugar molecules, connected by β-1,4-glycosidic bonds,[7] with an average degree of polymerization for wood cellulose is between 5000-10000.[8] [9] The crystalline structure of cellulose extends in three dimensions via intermolecular interactions including ordered hydrogen bonds and Van der Waals forces.[10] This leads to the formation of microfibrils that are hydrophobic and highly crystalline, which contribute greatly to the structural integrity of biomass. The main function of the cellulose in the plant cells is to act as a structural component and give rigidity to the cells. Cellulose has versatile uses in many industries such as paper production, bioethanol manufacturing, fibers and clothes, and the cosmetic and pharmaceutical industries.[11]

1.1.2 Hemicelluloses

Hemicelluloses, the second most abundant polysaccharide, are a group of hetero polysaccharides with shorter chains, and more branches compared to cellulose and are found in the primary and secondary cell walls. Hemicelluloses consist primarily of pentoses (xylose and arabinose) with hexoses (glucose and mannose) and function as supporting material in the cell walls. They are typically defined as alkali soluble materials and have very low molecular weights and a lower degree of polymerization (100–200) compared with cellulose (5000-10000).[9] [12] Hemicelluloses are a class of polysaccharides that have variable composition and structure depending on the plant source. For example, hemicelluloses isolated from softwood species, such as pines, are predominantly composed of galactoglucomannans, with a backbone of β-1,4-linked D-mannopyranose and D-glucopyranose units. On the other hand, hemicelluloses in herbaceous grass species, such as switchgrass, are composed of glucuronoarabinoxylans, complex, branched polysaccharides composed mainly of pentose (five carbon) sugars.[13]

1.1.3 Lignin

Lignin is the most abundant renewable carbon source on Earth after cellulose. It is a natural phenolic copolymer composed of three main phenylpropane units including coniferyl alcohol (G), sinapyl alcohol (S) and p-coumaryl alcohol (H) Figure 1.2. Depending on its origin, the lignin structure varies in its monolignol composition. Generally, the monomeric units of native lignins are connected through more than eight different types of linkages, with examples shown in (Figure 1.3) of β-O-4 (aryl glycerol ether linkage) (45–48% in softwood) , the β-5 phenyl coumaran bond (9–12%), the β–β′ pinoresinol (3%), dibenzodioxocine 5-5′-α, β-O-4′(5%), the diphenyl ether 5-O-4′ (5–8%) and β-1′diphenyl ethane (7–10%).[14]

The very complex structure of lignin consists of a three-dimensional randomized network linked to hemicelluloses. The main function of lignin in the plant is as the glue that keeps hemicelluloses and celluloses linked, shaping the cell wall and acting as a biological barrier. Even though lignin is the second-most most abundant renewable carbon source on Earth, contributing as much as 30% of the weight, and as much as 40% of the energy content of lignocellulosic biomass, it is often viewed as a useless waste product of the pulp and paper industries, as between 40 and 50 million tons of non-commercialized waste products are produced annually.[2b, 15]

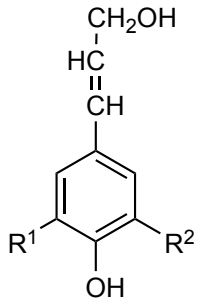

R^1 = OMe, R^2 = H: Coniferyl alcohol guaiacyl
R^1 = R^2 = OMe: Sinapyl alcohol syringyl
R^1 = R^2 = H: *p*-Coumaryl alcohol

Figure 1.2. The most common monolignols in lignin. H: *p*-coumaryl alcohol. G: coniferyl alcohol

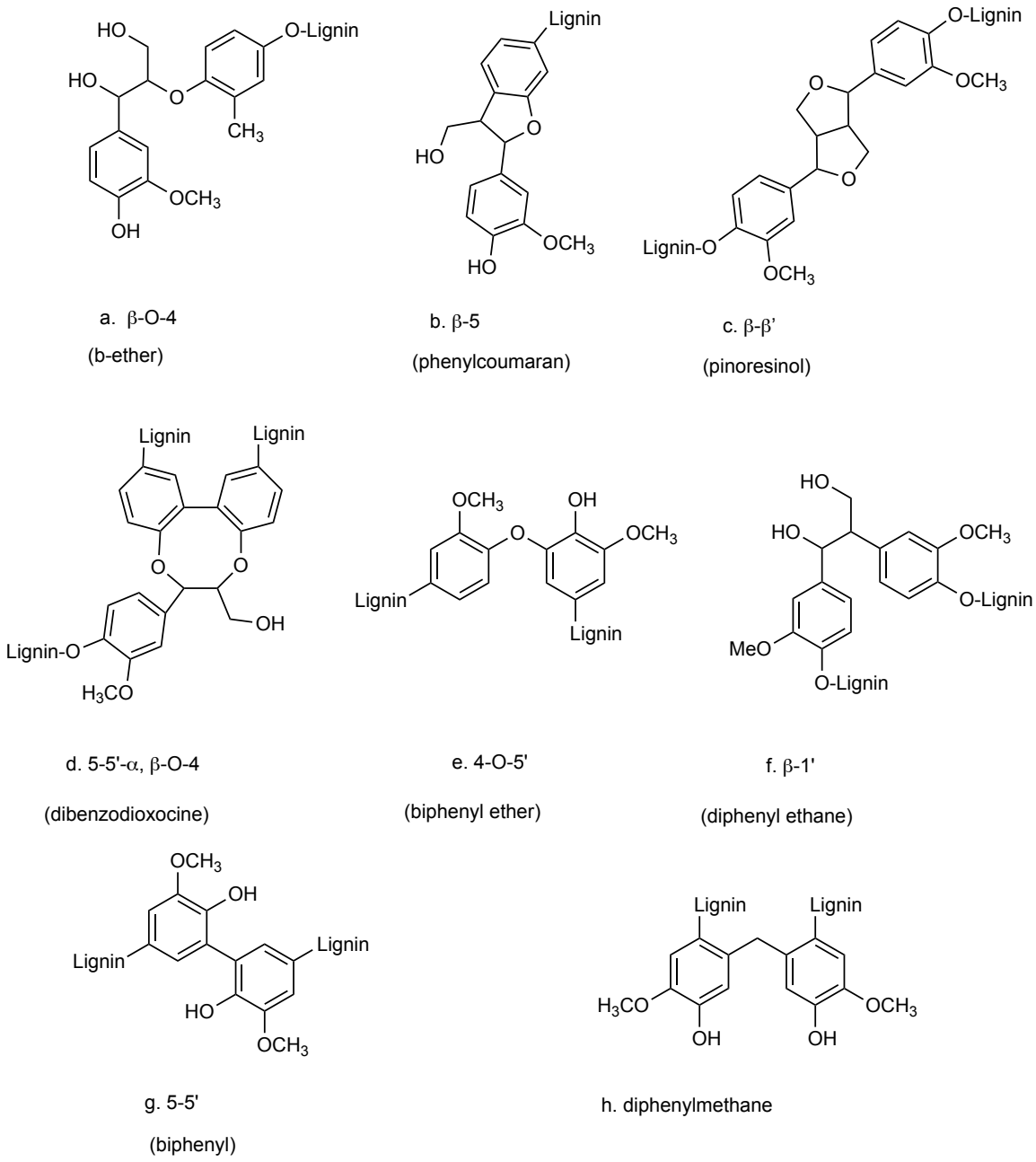

Figure 1.3. Lignin interunit linkages

1.1.3.1 Structure of Lignin

1.1.3.2 Lignin Model Compounds

The development of new methods to break lignin down in a selective fashion is an attractive goal that could provide access to renewable building blocks for chemicals or fuels. Lignin is the only viable renewable and sustainable source for the production of aromatic compounds.[2b] Cleaving of primary linkages is the first stage in the chemical production of monomeric aromatics with various substituted functional groups. However, the study of the depolymerization of lignin has challenges as a result of the large variety of C-C and C-O bonds. It is very difficult to purify and extensively characterize the detailed functionality of lignin samples and product mixtures derived thereof, using conventional analytical methods. On the other hand, studying model compounds representative of the various linkages that occur in lignin, rather than actual lignin, makes it possible to gain a better understanding of the kinetics and the oxidative transformation pathways that take place in lignin depolymerization and conversion studies. Figure 1.4 illustrates examples of model compounds that have been used in the study of lignin.

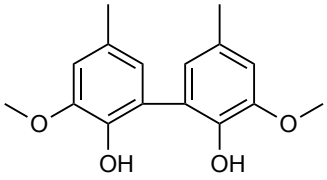

3,3'-dimethoxy-5-5'-diethl-biphenyl-2-2'-diol
5-5' model

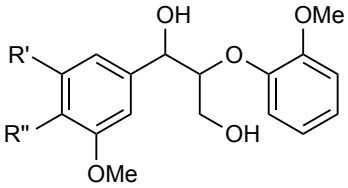

1-(4-ethoxy-3-methoxyphenol)-2-
(2,6-dimethoxyphenoxy)propane-1,3-diol
β-O-4 model
R' = H; R'' = OMe
R' = OMe; R'' = H
R' = OEt; R'' = H
R' = OH; R'' = OMe

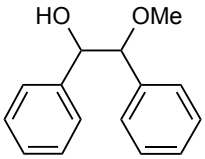

1,2-diphenyl-2-methoxyethanol
(DPME)
β-1 model

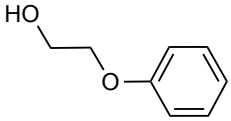

2-phenoxyethanol
β-O-4 model

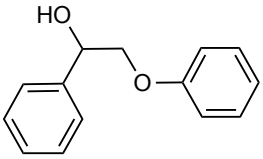

1-phenyl-2-phenoxyethanol
β-O-4 model

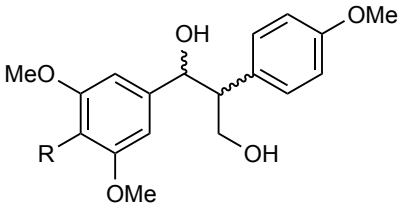

1-(4-hydroxy-3,5-dimethoxyphenyl)-
2-(4-methoxyphenyl)-propane-1,3-diol
β-1 model

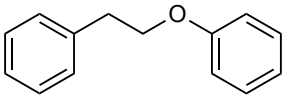

2-phenylethylphenyl ether
β-O-4 model

Figure 1.4. Examples of model compounds of lignin

1.1.3.3 Lignin depolymerization strategies

Even though lignin represents a major component of lignocellulosic biomass, lignin depolymerization is challenging mainly due to the complexity and robustness of its structure.[2c, 16] Nonetheless, the reported approaches of lignin depolymerization such as solvolysis, hydrolysis, hydrogenolysis, pyrolysis, and alkaline oxidation systems to date do not match the principles of green chemistry in terms of selectivity, activity, atom economy and environmental impacts despite the fact that lignin is a renewable feedstock. [2b, 15c] Thus, catalytic oxidative transformations via selective cleavage of C–O and C–C bonds that connect the monomers in lignin are attractive route for the chemical utilization of lignocellulosic biomass, and can offer phenolic platform chemicals, which subsequently can be suitable for fine chemicals applications.[15c, 17] A variety of chemical routes including reduction and oxidation approaches have been explored in detail to produce valuable, useful bulk and platform chemicals. Lignin reduction reactions have been studied as a potential approach to produce fuels or bulk aromatic and phenolic compounds and other alkane derivatives.[18] Lignin oxidation reactions also show promise in generating valuable aromatic chemicals and highly functionalized compounds for the production of fine chemicals.[2a, 19] A number of studies have focused on lignin heterogeneous hydrogenation. Toward this end, many conventional heterogeneous catalysts such as Raney Ni, Pd/C, Rh/C, Rh/Al_2O_3, Ru/C, Ru/Al_2O_3, Co-Mo, Ni-Mo, Ni-W, Ni, Co, Pd, Cu-CrO, Co-Mo, Ni-Mo, Ni-W, Ni, Co, Pd, Cu-CrO, $Mo/SiO_2/Al_2O_3$, $Co-Mo/Al_2O_3$, Ni- Mo/Al_2O_3, Fe_2O_3/Al_2O_3-S, $NiO-MoO_3/Al_2O_3$, and MoO_3/TiO_2-S[15c] [2b] have been examined in the past for use in reductive lignin and lignin model conversion.

1.1.3.4 Homogeneous Catalysis

Homogeneous catalysts offer a number of important advantages that are key in developing methods for lignin valorization. A wide range of ligands with easily adjustable electronic and steric properties which affect the catalyst activity and stability of the catalysts can be used and their activity screened. With respect to this thesis, it is

possible to tune the chemoselectivity and reactivity of a catalyst towards the oxidation of specific lignin linkages.

Furthermore, unlike heterogeneous catalysts, all homogeneous catalysts sites are accessible due to the catalyst solubility and they could potentially penetrate the network structure of the lignin. Catalytic oxidative depolymerization of lignin using base metal homogeneous catalysts is technology worthy of extensive investigation due to the large number of hydroxyl groups in lignin, which should interact favourably with these sorts of metal centers. As a result of the oxidative degradition of lignin, aromatic aldehydes and carboxylic acids are formed as the main products and could be used in the production of fine chemicals from lignin.[20]

1.1.3.5 Transition-Metal Catalyzed Valorization of Lignin

Biomimetic catalysts, such as metalloporphyrin complexes based on Mn, Fe, were inspired by efficient enzymatic catalyst systems found in nature in white rot fungi and are capable of the transformation mentioned above. Schiff-base catalysts, particularly, Co(salen), and polyoxometalates (polyoxotungstate/molybdate) Mn(III), Co(III), and Ru(IV) have also been reported as catalysts for the C–C bond cleavage of lignin model systems and for lignin transformations. In addition, ionic liquids have shown exceptionally high activity towards the transformation of lignin. Many studies have focused on the oxidation and C–C bond cleavage reactions of lignin using a catalytic system consisting of metal catalysts with hydrogen peroxide or other strong chemical oxidants.[2b, 14]

As mentioned in section 1.1.3.3, there are generally two main approaches for lignin depolymerization: the reductive methods and the oxidative methods. The reductive methods for lignin valorization have been primarily based on heterogeneous catalysts and depend on a catalytic system that can perform a tandem catalytic dehydrogenation and cleave the β-O-4 bond of the lignin fragment.[15c, 17c] However, catalytic oxidative lignin depolymerization has also been widely explored for the transformation of lignin and

lignin model systems to break selected bonds, such as aryl ether bonds, carbon–carbon bonds or the β-O-4 bonds in lignin.[15c]

1.1.3.6 Oxidative Homogeneous Methods for Lignin Conversion

Oxidative methods are the preferred technique chosen by nature, with several species of white-rot fungi showing a high capacity to degrade lignin through the action of lignin peroxidase or laccase.[21] Typically, these enzymes work via one-electron oxidation of the aromatic groups found in lignin (Scheme 1-1). Upon oxidation of the substrate, the resultant arene radical cations subsequently undergo either: 1) Cα-Cβ cleavage, which causes a break in the polymeric backbone yielding the corresponding aldehyde and radical, which easily undergoes further oxidation, yielding carboxylic acid and quinones; or 2) deprotonation of H_α from the intermediate generating a ketyl radical, which can undergo direct oxidation to the benzylic ketone or undergo β-O-4 fragmentation to yield β-hydroxyketone, Scheme -1-1.[17c]

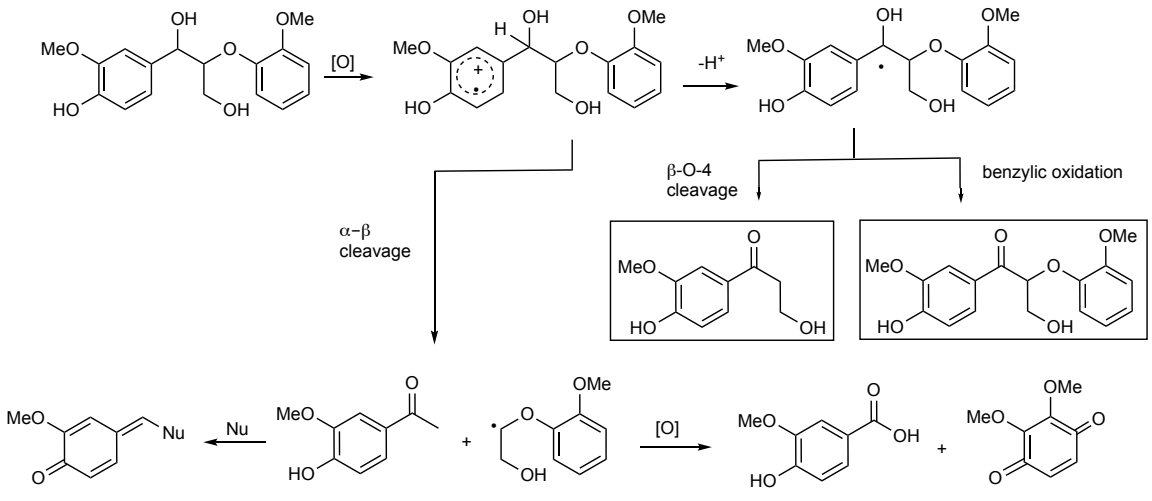

Scheme -1-1. Depolymerization mechanism of lignin by delignifying enzymes. Nu = nucleophile[17c]

The oxidative approaches towards cleavage of lignin have several advantages over the reductive methodologies. The reactions are conducted under milder conditions including lower pressures and temperature and they do not require an inert atmosphere. Also, they require only inexpensive oxidants such as peroxides or air. The oxidation of lignin can be divided into several categories including metal-free systems, and catalytic systems based on transition metals.

Historically, in the 1940s, and later in the 1980s, two different oxidation methods for the quantification and identification of lignin were established as analytical techniques. One method involved the hydrolysis of lignin using an alkaline/CuO system producing several methoxylated phenols,[22] whereas the second method involved the oxidative cleavage of lignin using the alkaline nitrobenzene method producing aldehydes and aromatic carboxylic acids in quantitative yields.[23] These methods have many disadvantages such as the use of stoichiometric amounts of reagents, poor conversions and poor yields.

More recently, Stahl and co-workers[2d, 20] developed an entirely metal-free catalyst system, (**1.1**), based on a readily available radical, TEMPO = 2,2,6,6-tetramethylpiperidine-*N*-oxyl, and mineral acids for the oxidation and depolymerization of aspen lignin (typical hardwood lignin). Two-dimensional NMR data showed that all the guaiacyl [4-(2-methoxyphenol)] and syringyl [4-(2,6-dimethoxyphenol)] units of lignin were transformed, and confirmed that the β-O-4 linkages that were oxidized yielded the aryl ketone-containing β-ether units (Scheme 1-2). Then, a redox-neutral cleavage of the C-O bond afforded low molecular weight fractions and syringyl and guaiacyl-derived diketones.[20] [2d]

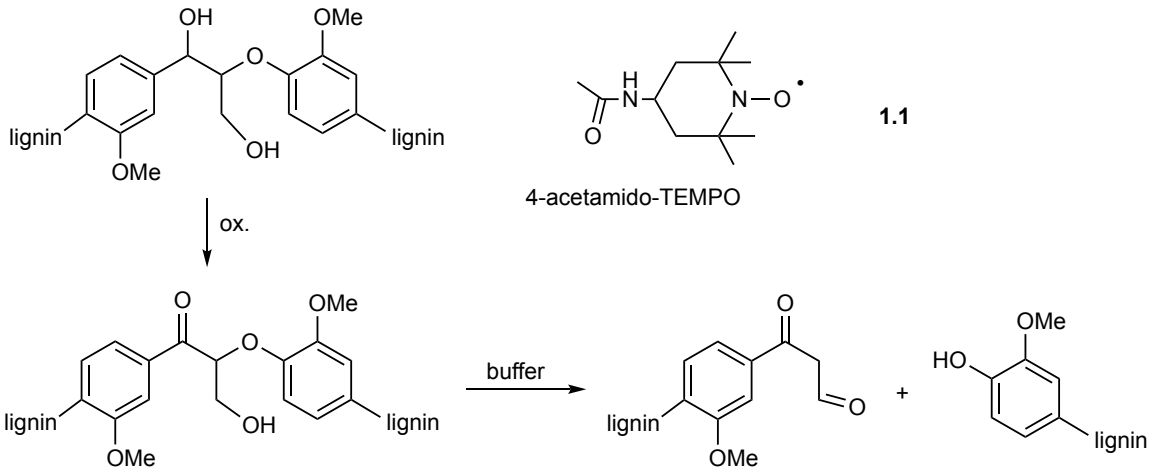

Scheme 1-2. Metal-free systems for depolymerization of lignin

Inexpensive and readily available first row transition metal-catalysts for oxidations of model compounds and real lignin samples have been studied. For instance, the Cu/TEMPO catalyst and related systems with different nitroxyl radicals have been reported by many research groups as effective catalytic systems for the oxidation of primary and secondary alcohols.[24] Nevertheless, only a few reports on the oxidation of lignin models or real lignin extracts using copper catalysts have been reported. Baker and co-workers reported a highly efficient method for the selective C-C bond cleavage of aryl ethers, β-aryl glycerol and β-1 lignin models using Cu(I)/TEMPO in combination with 2,6-lutidine as a solvent and co-ligand (Scheme 1-3).[25] The catalyst system showed high selectivity for the cleavage of C-C bonds of all examined lignin model compounds. However, the Cu(I)/TEMPO/2,6-lutidine catalyst showed no reactivity toward depolymerization of ethanol organosolv lignin (ethanol as the solvent to solubilise lignin).[26]

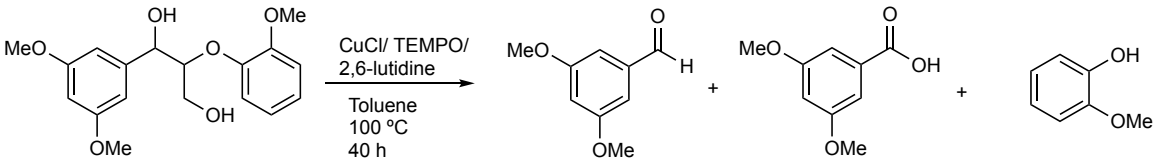

Scheme 1-3. Cu(I)/TEMPO/2,6-lutidine catalyst for the C-C bond cleavage of β-aryl glycerol lignin models

Cobalt Schiff base complexes have emerged as potential catalysts for aerobic oxidation. Specifically, novel asymmetric Co–salen catalysts (**1.2** and **1.3)** were developed by Bozell and co-workers. The catalytic activity of these catalysts toward para-substituted phenol models was investigated and afforded the corresponding benzoquinones (Scheme 1-4).[27]

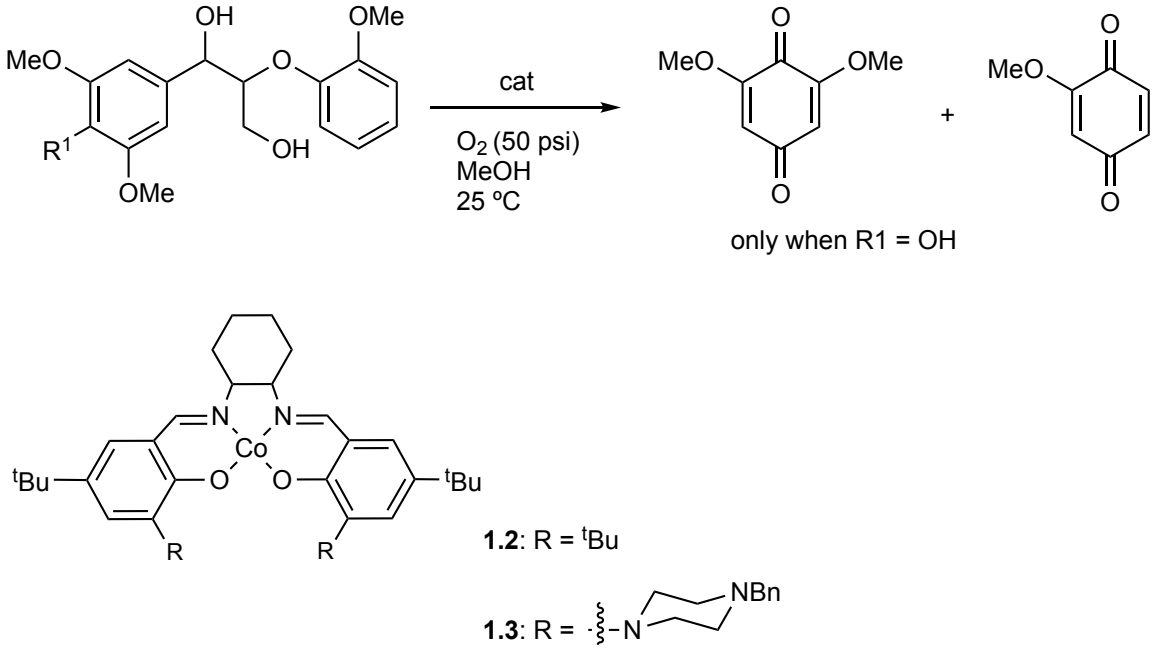

Scheme 1-4. Co-Schiff base catalyst for the selective C_{aryl}-C_{alkyl} bond cleavage[27-28]

Iron complexes have also displayed exceptional oxidative reactivity in various green chemistry applications including hydrocarbon oxidation reactions (e.g., Fe-TAML [tetraamido tetracyclic ligands] water-soluble complexes with peroxides) that normally produce CO_2.[29] Andrioletti and co-workers[30] reported that using a similar Fe(TAML)Li catalyst, (**1.4**, Figure 1.5), for the oxidation of various lignin model compounds afforded mixed reactivity towards β-aryl ether lignin models. Use of the Fe(TAML)Li catalyst combined with 2 equiv. of diacetoxy iodobenzene as an oxidant under mild conditions (25 °C, 1 h) yielded the C-C bond cleavage products benzaldehydes and benzoic acids, and C-H bond cleavage products ketones.

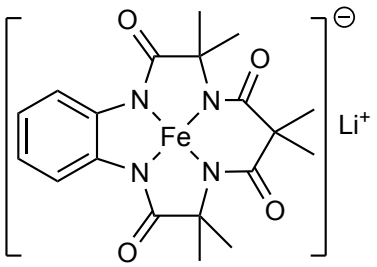

1.4

Figure 1.5. Fe(TAML)Li, a catalyst for lignin disassembly

Recently, Bolm and co-workers[31] demonstrated the use of $FeCl_3$ combined with DABCO (DABCO = 1,4-diazabicyclo[2.2.2]octane) in the presence of H_2O_2 as an oxidant in DMSO for the oxidation of lignin β-O-4 model compounds and lignin. The oxidation reaction produced a mixture of C-O and C-C bond cleavage products including benzaldehydes and methoxyphenols, respectively. The same catalytic system could also depolymerize lignin samples. The results as observed by 2D NMR revealed the cleavage of all the β-O-4 linkages and resinol structures and yielded low-molecular weight degradation products as confirmed by GPC analysis.[31]

Manganese complexes bearing TACN((1,4,7-triaza-cyclononane)-based ligands) such as (**1.5**) are well known as efficient catalysts for the oxidation of substituted phenyl ethanol together with peroxides (Figure 1.6).[32] Phenyl ethanols are considered to be models for some of the functional groups in lignin.

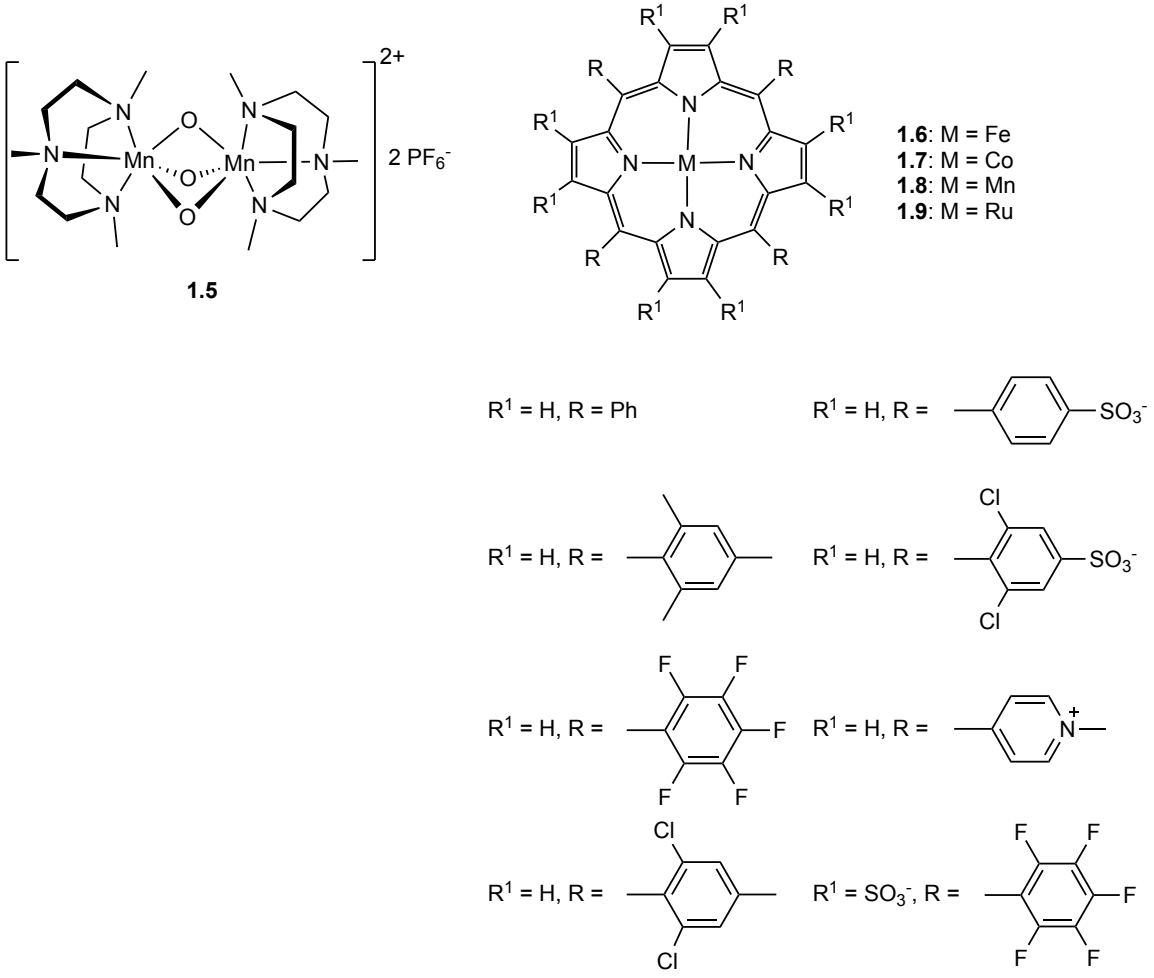

Figure 1.6. Mn-TACN and metalloporphyrins

Several homogeneous catalysts based on metalloporphyrins using Fe, Co, Mn and Ru (Figure 1.6, **1.6-1.9**) as models of the cytochrome P450 enzyme were reported by Ying and co-workers. The catalysts combined with oxidants such as oxone have been

successfully employed for the oxidation of β-aryl ether lignin models under mild reaction conditions with the Co(II) complex (**1.7**) showing the best catalytic activity of the family with 100% conversion at RT in water as the solvent.[33] Furthermore, a catalytic system under similar reaction conditions was also applied for the oxidation of the lignin, and high yields up to 33.4 wt % of an oily liquid fraction yield and up to 49% of aromatic monomeric products were obtained.[33]

Catalytic systems based on second- and third-row metals such as Mo[34] and Re[17d] have also been widely studied for the selective oxidative of lignin model compounds. Kühn *et al.* demonstrated a novel methyltrioxorhenium (MTO) catalyst for the selective cleavage of C-O bonds in β-aryl ether lignin models.[35] The selective cleavage of these C-O bonds using 5 mol% $MeReO_3$ catalyst under mild conditions (110 $^{\circ}$C, 4 h) led to the generation of phenols and aldehydes.[35]

1.1.4 General Chemistry of Vanadium and Manganese

As vanadium and manganese coordination compounds were prepared and studied in the course of the current research, a small summary of important facts regarding these metals is included in the following sections.

1.1.4.1 Vanadium

Vanadium is a transition metal found in Group 5 of the periodic table. Vanadium occurs naturally as a mixture of two isotopes, ^{51}V (99.76%) and ^{50}V (0.24%). The most important sources of the metal are the minerals vanadinite [$Pb(VO_4)_3Cl$] and carnotite [$K_2(UO_2)_2(VO_4)_2$]. It is also present in the form of organic complexes in some crude oils and some aquatic organisms bioaccumulate vanadium in their bodies. For example, members of an order of tunicates (*Ascidiacea*) concentrate vanadium in specialized blood cells.[36] Vanadium occurs with an abundance of 0.014% in the Earth's crust,[37] but it is the second most abundant transition metal in the oceans (50 nM).[38] In 1983, vanadium bromoperoxidase (V-BrPO) as a naturally occurring vanadium-containing enzyme was discovered in the marine brown algae.[39] Numerous other vanadium haloperoxidases

have since been isolated and studied,[40] and are often obtained from red or brown seaweeds.[41] Vanadium has been found in many marine organisms,[42] as well as in many species of terrestrial fungi.[43]

Vanadium has an electronic configuration of [Ar] $3d^3 4s^2$, and its chemistry is dominated by four common oxidation states in its complexes and compounds, including +5, +4, +3, and +2. V exhibits "hard" behaviour in complexing readily with O and N donor ligands.[44] However, only the three highest, +3, +4 and +5 are important in biological systems,[44] [36] with the most stable states under normal conditions being oxidation states of +4 and +5.[45] Compounds which contain the VO^{2+} unit (vanadyl ion) are the most common form of vanadium(IV). These types of compounds commonly adopt square pyramidal or trigonal bipyramidal geometries with an axial oxo ligand.

The chemistry of vanadium has attracted extensive attention due to the promising applications of vanadium complexes as catalysts in different catalytic reactions,[46] in organic synthesis,[47] materials science, and their biological activities as insulin mimics, anticancer, antitumour, and antimicrobial agents.[47] Also, the chemistry of oxovanadium(IV) and (V) ions of the type VO^{2+}, VO^{3+}, VO^{2+}[37] and V_2O^{4+} [38] with a variety of ligands has been widely studied.[48] The VO^{3+} ion in particular, because of its hard acidic nature, is known to exhibit a rich chemistry with oxygen and nitrogen donor ligands.

1.1.4.2 Manganese

Manganese is a relatively abundant metal, making it the 12th most abundant element and the third most abundant transition element (exceeded only by iron and titanium). Commercial sources are secondary deposits of oxides and carbonates such as pyrolusite (MnO_2), hausmannite (Mn_3O_4), and rhodochrosite ($MnCO_3$). Manganese has an electronic configuration of [Ar] $3d^5 3s^2$ and the most common oxidation states of manganese are +2, +3, +4, +6 and +7, though oxidation states from −3 to +7 are observed. The most obvious feature is the relative position of the +2 oxidation state,

which is the most stable, with the +3, +4, +5 and +6 states becoming increasingly less stable. Manganese shows similarities to iron in its physical and chemical properties but is harder and more brittle, though less refractory (mp 1247 ^{o}C). Despite it being quite electropositive, at room temperature manganese metal is not particularly reactive to air; however, it reacts vigorously when heated in O_2 to form the manganese oxide Mn_3O_4, in N_2 to yield the nitride Mn_3N_2, and in reactions with halogens to form MnX_2.[49] Manganese(II) exhibits "hard" behavior in complexing readily with O-donor ligands rather than N-donor ligands. Also, there are a few compounds with P, As, and S-donor ligands.[45] Therefore, both manganese and vanadium should readily form complexes with amino-phenolate ligands and this is one of the hypotheses tested in this thesis. Furthermore, as the amino-phenolate ligands are easily tailored (steric and electronic properties), the reactivity of any complexes in catalytic reactions should be easily controlled and potentially selectivity optimized.

1.1.5 Vanadium (V) and Manganese (III) Complexes for Selective Oxidation of Lignin Model Compounds and Lignin

1.1.5.1 Vanadium Catalysts for Oxidation of Lignin Model Compounds and Lignin

Since the discovery of vanadium-dependent enzymes such as haloperoxidases and nitrogenases and inspired by the role of theses enzymes in different biological catalytic processes in nature, the development of bioinorganic vanadium metal catalysts for several oxidative transformations has attracted broad scientific attention.[50] In the early 1980s, novel oxovanadium(V) peroxo complexes were reported by Mimoun as very active complexes for the oxidation of alkanes to alcohols and ketones, and aromatic hydrocarbons to phenols. It is worth mentioning that the mechanisms of these reactions are closely related to the mechanisms of enzyme cytochrome P_{450} monooxygenases.[51] Later, Thorn and co-workers reported a set of phosphatovanadium(V) complexes based on "(O,N,O)" supporting ligands (pyridine-2,6-dicarboxylic acid ("dipic")). The

complexes were simply synthesized by reacting the ligand with $VO(O^iPr)_3$ in CH_3CN and then the alkoxide-coordinated oxovanadium complexes could be readily produced by exchange with alcohols (**1.10**-**1.13**, Scheme 1-5).[52]

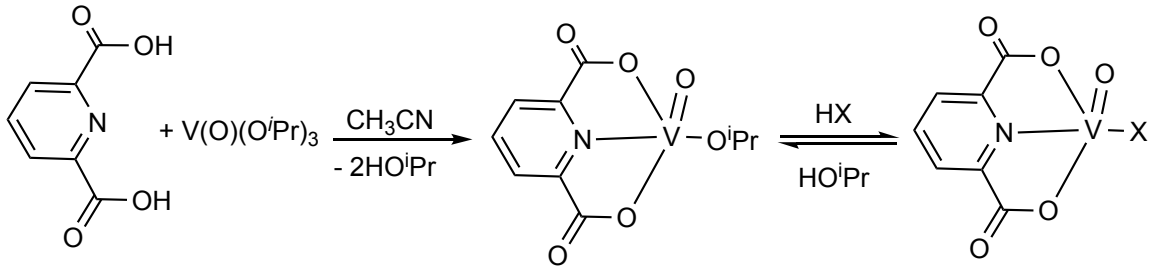

Scheme 1-5. Thorn's vanadium complexes

In the late 2000s, Baker and Hanson began to extensively study the oxovanadium(V) isopropoxide complexes (**1.14**[53] and **1.15**)[54] for their applications in alcohol oxidation and lignin model disassembly (Figure 1.7). It was shown that the reactivity and selectivity of the oxovanadium catalysts for oxidative cleavage of the tested model compounds could be altered and affected depending on different ligand environments and reaction conditions such as the solvent and temperature.[53-54]

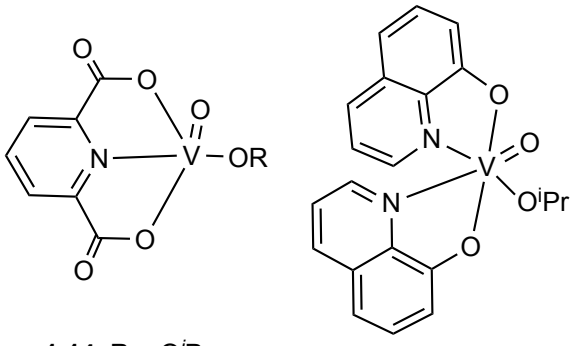

1.14: R = O^{i}Pr
1.15: R = OEt

1.16

Figure 1.7. First generation of oxovanadium(V) catalysts studied by Baker and Hanson

Baker and co-workers investigated the aerobic oxidation of four different 1,2-hydroxyether model systems: pinacol monomethyl ether, 2-phenoxyethanol, 1-phenyl-2-phenoxyethanol, and 1,2-diphenyl-2-methoxyethanol (Figure 1.8), using a V catalyst, bearing dipicolinate ligands (**1.14**) Figure 1.7.[53] These substrates allowed the authors to elucidate the effects and reactivity on the β-O-4 and β-1 lignin motifs, and the effects of the substituted backbones.[53] The catalytic system has been reported to affect the aerobic oxidative cleavage of Cα-Cβ or C-H bond of simple β-1 model compound **A** Figure 1.8 depending on the reaction solvent.[53] Dipicolinate vanadium catalyst (**1.14**) with β-O-4 model substrate **B** afforded a low conversion (20%) with phenol (18%) and formic acid (6%) as major products. Improved catalytic performance was obtained with vanadium-HQ catalyst (HQ = 8-quinolinate) (**1.16**) (69% conversion *vs.* 20% conversion), whereby the major products obtained were 2-phenoxyethylformate (18%), phenol (55%), formic acid (3%) and CO_2. Vanadium-dipic (**1.14**) was reported to afford 95% conversion for the more activated and bulky substrate **C** to benzoic acid (81%), phenol (77%), formic acid (46%) and 1-phenyl-2-phenoxyethanone (9%) after heating at 100 ^oC for 1 week in DMSO-d_6 (Scheme 1.4).[53] Catalyst (**1.16**) was only able to consume 58% of **C** after heating to 100 ^oC for 48 h in pyr-*d5*. The major products of the reaction were comparable to the earlier report and included benzoic acid (46%), phenol (45%), 1-phenyl-2-

phenoxyethanone (16%) and a smaller amount of formic acid (2% vs. 46%) (Scheme1.4). The ketone, 1-phenyl-2-phenoxyethanone, was shown to be the intermediate for the formation of benzoic acid and phenol for this reaction as the same products were observed, starting from the ketone when reacted under the same reaction conditions.

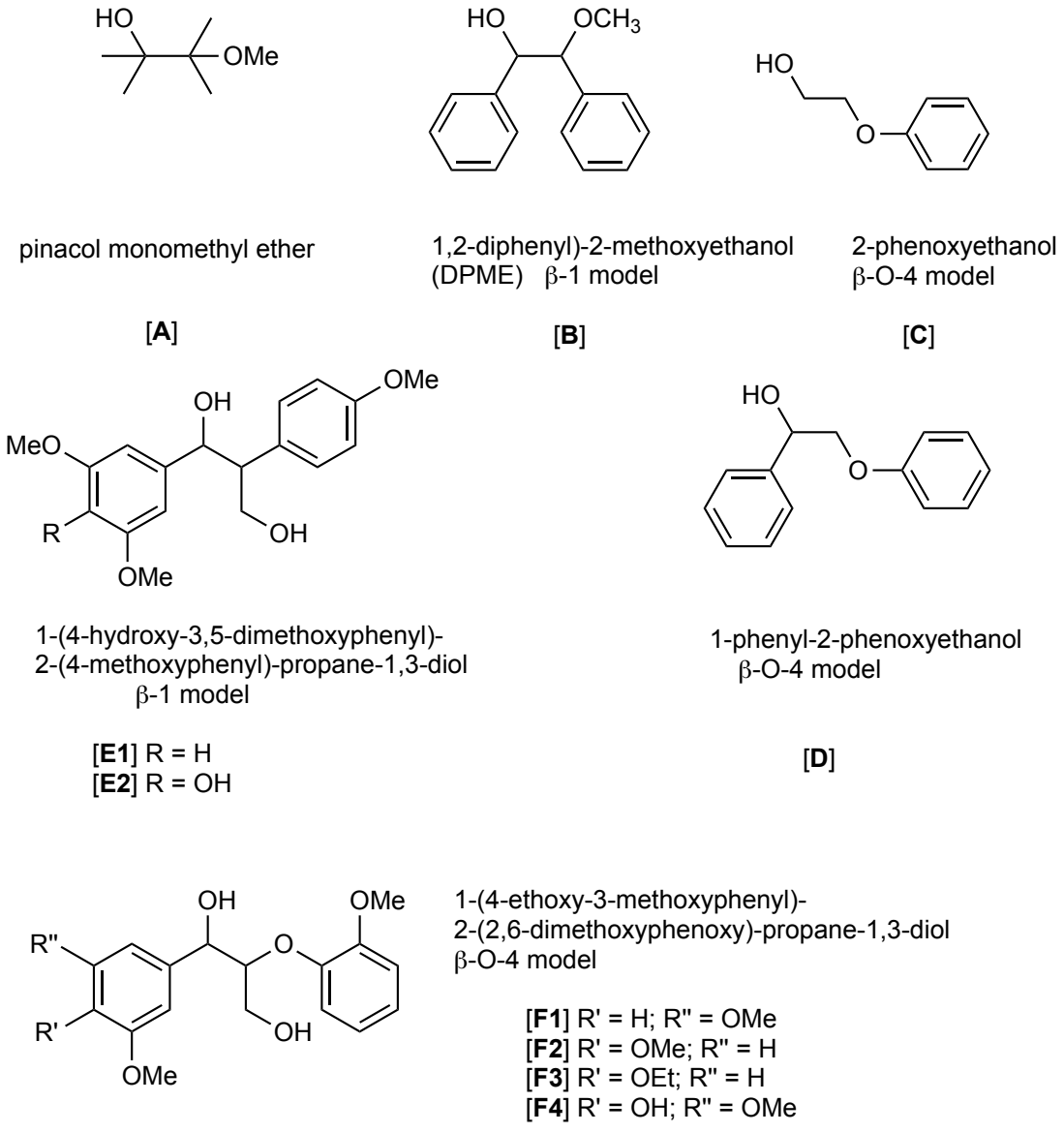

Figure 1.8. Lignin model compounds

Hanson *et al.* soon after also explored the reactivity of the vanadium catalyst (**1.14**) toward the aerobic oxidation of lignin models.[26] The catalyst (**1.14**) catalyzed the aerobic oxidation of the lignin model compound 1,2-diphenyl-2-methoxyethanol and producing benzoic acid (85%) and methyl benzoate (84%) as the major products via the intermediate ketone benzoin methyl ether as evident in Scheme 1-6. The more complex lignin model system, 1-(3,5-dimethoxyphenyl)-2-(2-methoxyphenoxy) propane-1,3-diol, was oxidized under air by the vanadium catalyst (**1.14**), affording ketone as a major product (65%), along with a small amount of the corresponding dehydrated ketone or alkene product, 3,5-dimethoxybenzoic acid, 3,5-dimethoxybenzaldehyde, 2-methoxyphenol, and formic acid (Scheme 1-7).[26]

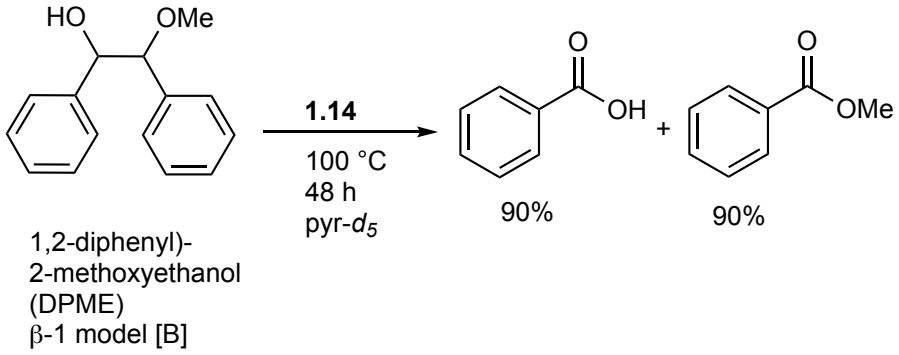

Scheme 1-6. Catalytic oxidation of 1,2-diphenyl-2-methoxyethanol

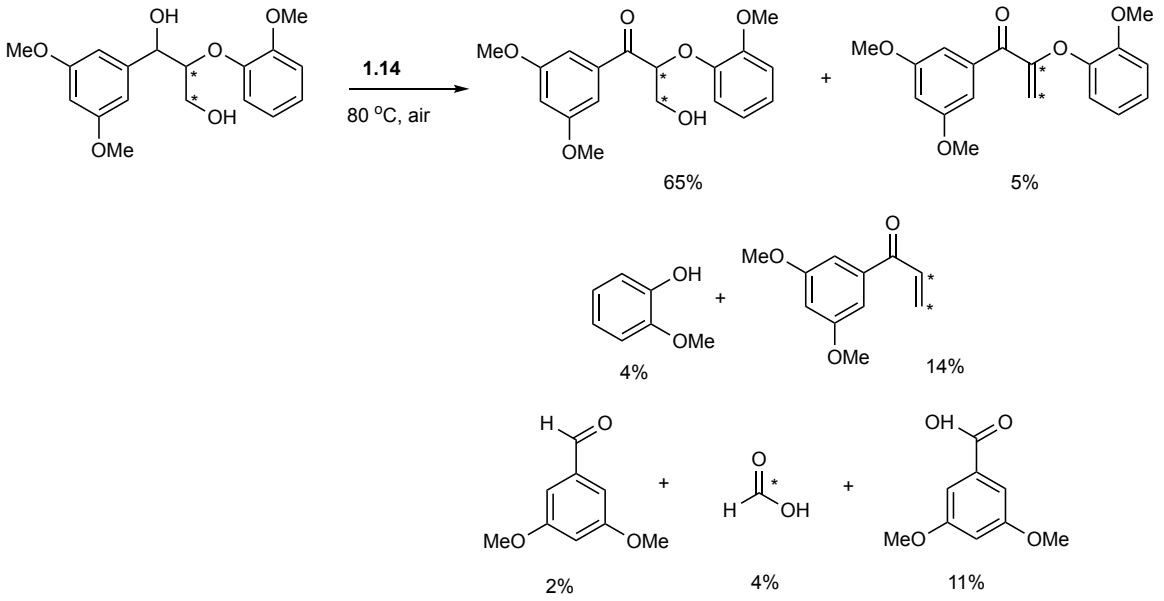

Scheme 1-7. Catalytic oxidation of 1-(3,5-dimethoxyphenyl)-2-(2-methoxyphenoxy) propane-1,3-diol

Hanson *et al.* demonstrated the use of a 8-quinolinate vanadium complex (**1.16**) ($(HQ)_2V^V(O)(OiPr)$, HQ = 8-quinolinate)) for the aerobic oxidation of benzylic, allylic, and propargylic alcohols using air. The reactions proceed in a variety of solvents under mild conditions (air, 40−100 °C, 24−72 h), and all substrates oxidized to the corresponding aldehyde or ketone in high yields (Scheme 1-8). It is worth mentioning that a base promoter was required for the catalytic oxidation.[55]

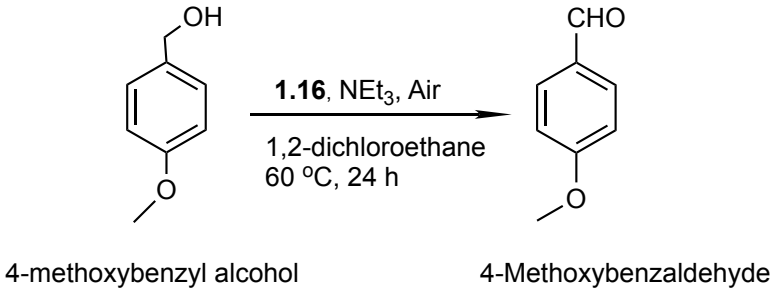

Scheme 1-8. Catalytic oxidation of 4-methoxybenzyl alcohol

The Toste group has also been extensively studying these sorts of reactions using vanadium catalysts. For example, they investigated a series of vanadium-oxo complexes bearing Schiff base ligands (**1.17-1.21** Figure 1.9) as catalysts for C–O bond cleavage of lignin model compounds.[16, 56] Catalyst (**1.17**) showed the highest catalytic activity with the dimeric lignin model resulting in various degradation products via β-O-4′ bond cleavage and a small degree of benzyl alcohol oxidation under optimal conditions with a 95% conversion. In contrast, when the benzylic hydroxy group was replaced with a methoxy group, the reaction proceeded with only 12% conversion to afford a conjugated aldehyde as the product, indicating the importance of ligand exchange on compound (**1.17**) with the benzylic hydroxy group (Scheme 1.9).[16]

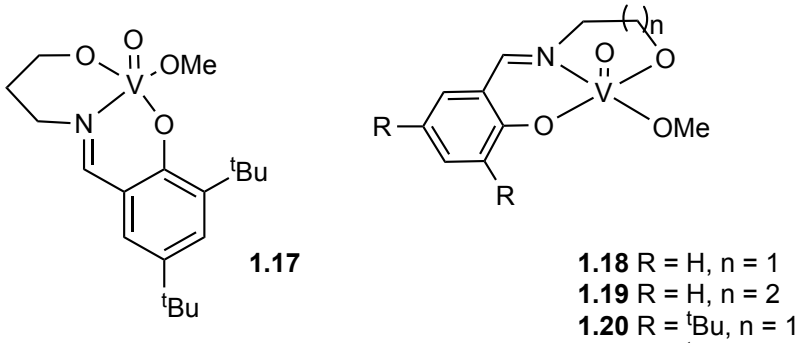

Figure 1.9. Structures of vanadyl-based complexes

Vanadium catalyst (**1.16**) and Schiff base-type vanadium catalyst (**1.21**) have been reported to affect the aerobic oxidative cleavage of Cα-Cβ and C-H bonds, respectively, of a dimeric phenolic β-O-4 model compound as shown in Scheme 1-9. This difference in selectivity between catalyst (**1.16** and **1.21**) suggests a separately evolved mechanism in which catalyst (**1.16**) follows a two-electron base-assisted redox dehydrogenation pathway in contrast to catalyst (**1.21**) which involves a one-electron aryloxy radical mechanism.[16, 54a]

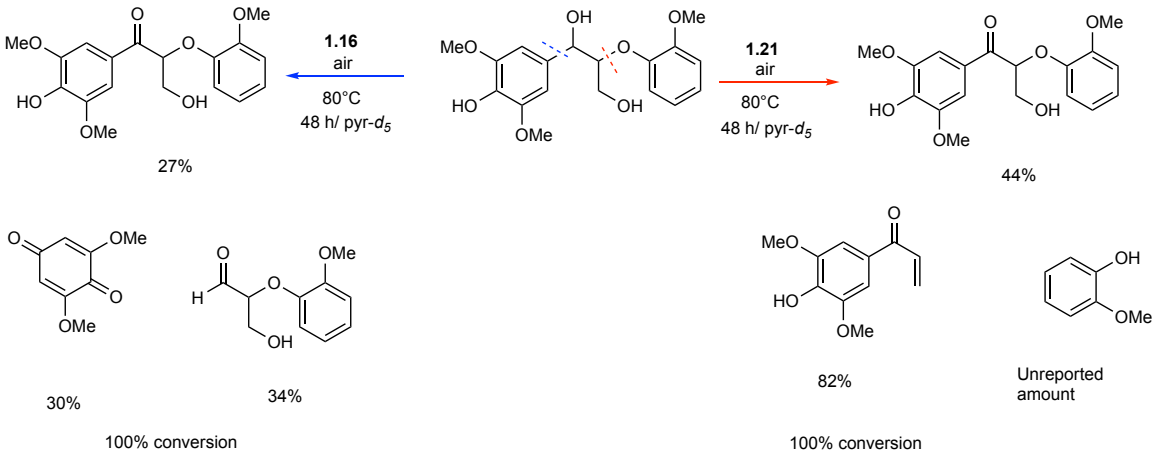

Scheme 1-9. Catalytic oxidation of dimeric phenolic β-O-4 model compound

In another reaction, the vanadium-dipic catalyst (**1.21**) was able to produce at most a trace amount of 3,5-dimethoxybenzaldehyde and some ene-one (29%, 14%) and the ketone (27%, 65%) in pyr-d_5 and DMSO-d_6, respectively. In contrast, for the vanadium-HQ catalyst (**1.16**) only moderate conversion (65%) of C–H bond cleavage products was observed (Scheme 1-10).

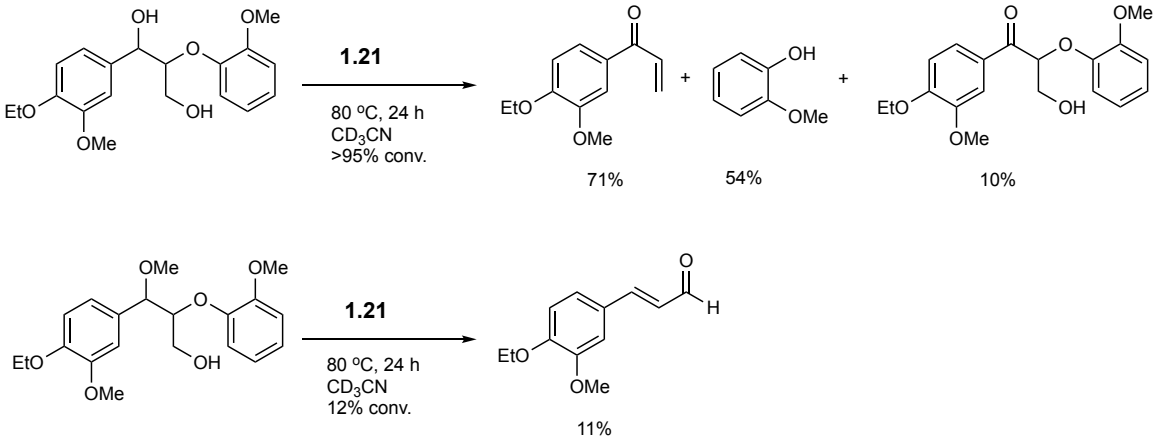

Scheme 1-10. Catalytic oxidation of dimeric phenolic and nonphenolic β-O-4 model compounds

Hanson and co-workers explored the electron-donating nature of the ligand backbone on the catalytic oxidative cleavage of lignin models. They envisioned that a tridentate scaffold with phenolate donors would have the advantage of providing a more electron-rich environment and facilitating the reaction of V^{III} or V^{IV} with O_2 by opening an additional coordination site as well as increasing solubility and activity in nonpolar solvents.[57] As a result, vanadium(V) complexes of bis(phenolate) pyridine (**1.22**) and bis(phenolate)amine ligands as seen in (**1.23**) Figure 1.10, have been found to work as effective catalysts in toluene to convert a non-phenolic lignin to C–O and C–H bond cleavage products.[57] This was analogous to the selectivity observed from the previously reported V-catalyst (**1.14**). However, complex (**1.22**) has been shown to be a more reactive catalyst for oxidation of the lignin model compounds in toluene-d_8 than (**1.23**) Scheme 1-11and Scheme 1-12.

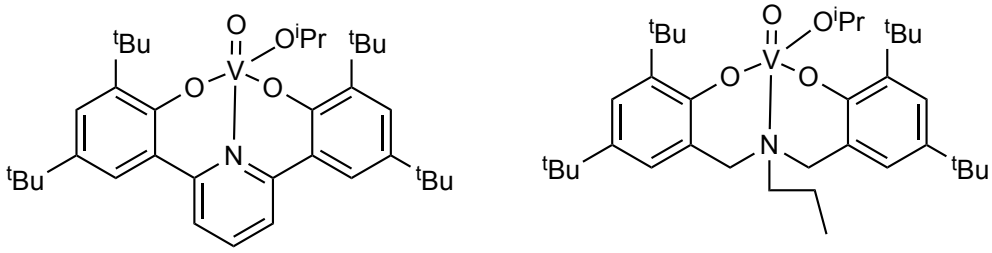

1.22 **1.23**

Figure 1.10. Vanadium (V) complexes of bis(phenolate) ligands

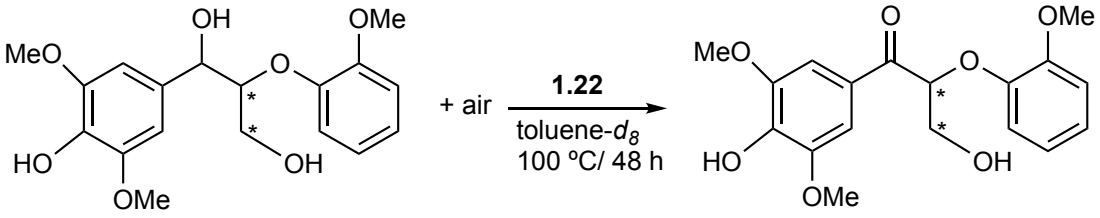

20% conversion

Scheme 1-11. Aerobic oxidation of phenolic lignin model compound using vanadium catalyst **1.22**

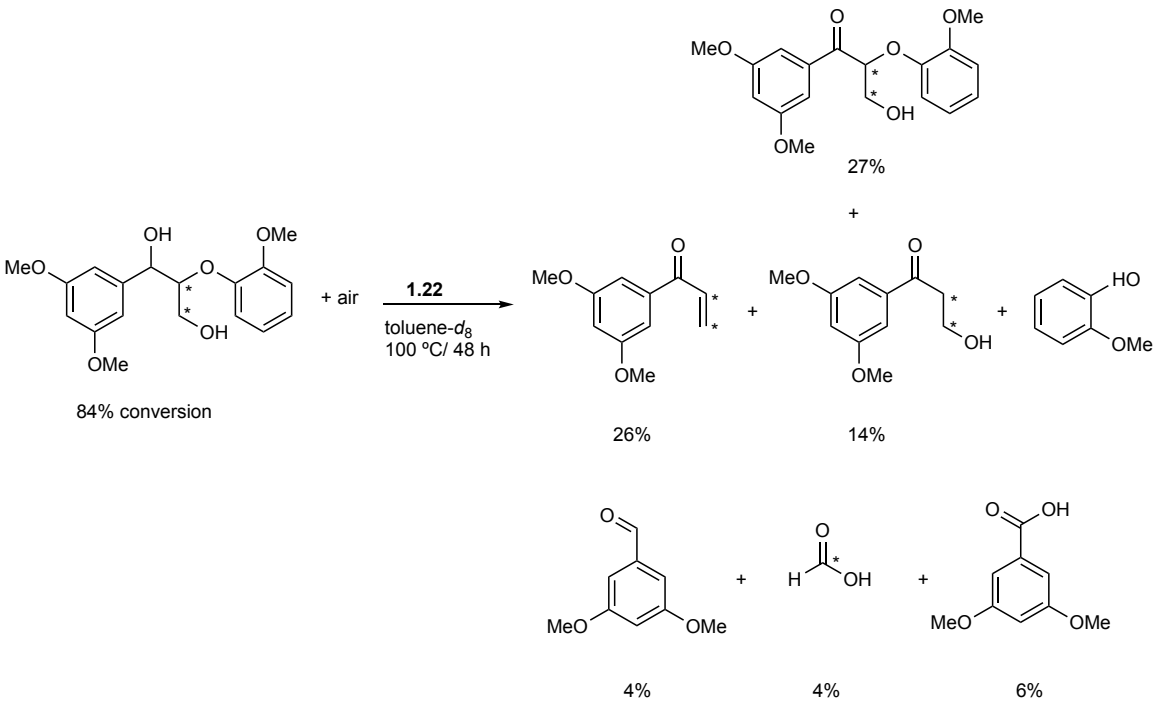

Scheme 1-12. Aerobic oxidation of non-phenolic lignin model compound using vanadium catalyst **1.22**

In a later study, using various solvents, Toste and co-workers in explored the reactivity of the same vanadium catalysts (**1.17-1.21** Figure 1.9)[16] toward lignin samples extracted from *Miscanthus giganteus* known as dioxasolv, acetosolv and ethanosolv lignin as s result of being dioxane, acetone, and ethanol extracted samples, respectively.[58] The results showed that the catalytic system was effective in depolymerizing actual lignin at the β-O-4′ linkages and low molecular weight products were detected by gel permeation chromatography (GPC) analysis. Also, the samples were selectively cleaved at the β-O-4′ linkages in the degradation process, just as in the case of lignin models.

1.1.5.2 Manganese Catalysts Catalysed Lignin Models/Lignin Oxidation

Biomimetic catalysts, such as metalloporphyrins, have been proposed as catalysts for the oxidation of lignin and lignin models. These catalysts aim to mimic the active center of LiP (lignin peroxidases), or Mn-P (manganese peroxidases), two metalloenzymes isolated from the white-rot fungus, which are capable of catalyzing the depolymerization of native lignin by wood-rotting fungi.[21, 59] The proposed mechanism for the catalytic cycle of these enzymes is depicted in Scheme 1-13 begins with the native enzyme of iron(III) protoporphyrin reacting with hydrogen peroxide to give the oxo-iron(IV)- protoporphyrin IX radical- a highly reactive species intermediate (Scheme 1-13, compound I). Further reaction converts compound I to compound II by reacting one equivalent of Mn(II) and forming Mn(III) which is stabilized by chelating agents such as oxalate or maleate. The MnP compound I is then able to oxidize phenolic lignin structures. Similarly, a second Mn(II) is then used to reduce compound II back to the native enzyme.

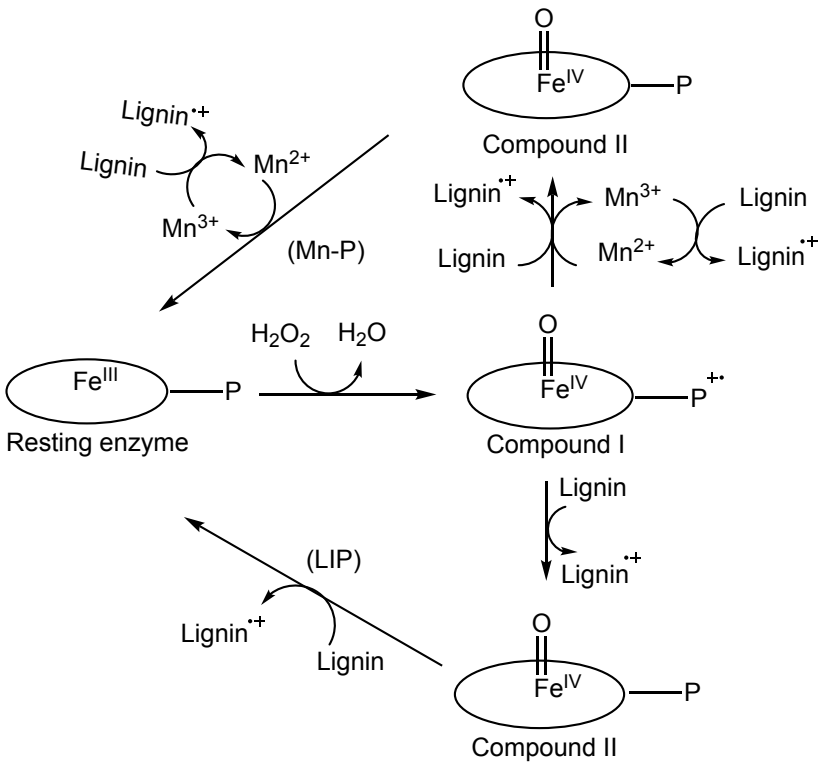

Scheme 1-13. Catalytic cycle of lignin peroxidase (LiP) and manganese peroxidase (Mn-P). The first step (compound I formation) is common for both the enzymes

More specifically, in nature, the lignin laccases and peroxidases from white rot fungi have the unique ability to catalyze the oxidative cleavage of C−O and C−C bonds.[60] Inspired by this fact, many manganese[61] and cobalt[28, 62] complexes of porphyrins and salen ligands have been investigated as biomimetic catalysts for lignin and lignin model compound degradation. A series of Mn^{III}(salen) catalysts based on macrocyclic ligands was reported by Fernández and co-workers which showed excellent performance in alkene epoxidation as a catalytic system for the oxidative C-C bond cleavage of vicinal diols to aldehydes with oxygen as an oxidant.[63] In another study, several metalloporphyrins such as manganese porphyrin metal complexes were synthesized and used as lignin peroxidase models and several studies have evaluated their

potential for lignin transformations.[64] The complexes which displayed the highest activity for lignin oxidation are similar to those generated from Li-P and Mn-P.[21]

Sun and co-workers in 2003[65] synthesized a series of manganese complexes supported by ONNO-tetradentate Schiff-base ligands (**1.24**-**1.26**, Figure1.11) for oxidative kinetic resolution of α-methylbenzyl alcohol catalyzed by Mn(salen) complexes as catalysts in water. The Mn(salen) complexes along with $PhI(OAc)_2$ as the co-oxidant and tetraethylammonium bromide as phase-transfer catalysts (PTC) were used in the aqueous system to overcome the solubility issue of the substrate and catalyst in the water. The results showed that the catalytic system is active and had an unexpected 51.7 % conversion and 85.2 % *ee* at room temperature in 0.5-1 h. They also concluded that water is important for the reaction, Scheme 1-14.[65]

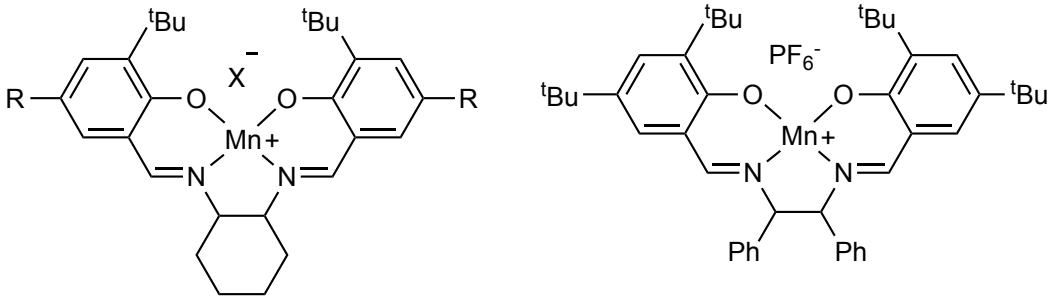

1.24a: R = ^{t}Bu, X = Cl; **1.24b**: R = ^{t}Bu, X = PF_6
1.25: R = Me, X = PF_6

1.26

Figure1.11. Manganese complexes of Schiff-base ligands

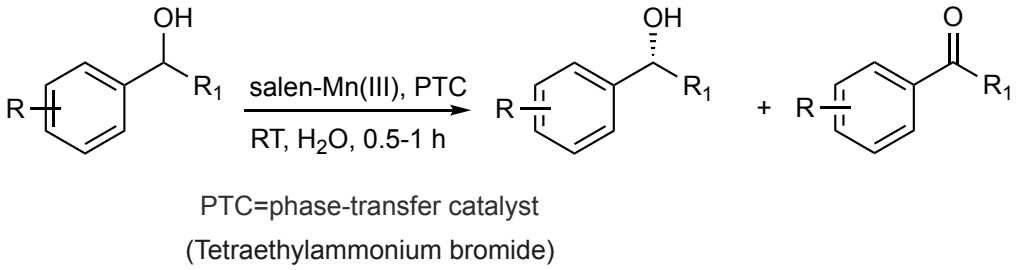

Scheme 1-14. Catalytic oxidation of α-methylbenzyl alcohol catalyzed by Mn(salen) complexes

Mardani and co-workers reported a very efficient Mn(III) Schiff-base complex (**Figure 1.12**) for the selective oxidation of various alcohols under mild conditions.[66] Oxidation of benzylic and aliphatic alcohols to the corresponding ketones and carboxylic acids was achieved in the presence of a catalytic amount of the Mn(III) complex (1.24) using H_2O_2 as the oxidant (Scheme 1-15 & Scheme 1-16) under solvent-free conditions. The catalytic system was found to be an efficient method for the oxidation reactions at 50 °C, and within 8 h, yielded up to 80% conversion and 100% of selectivity.[66]

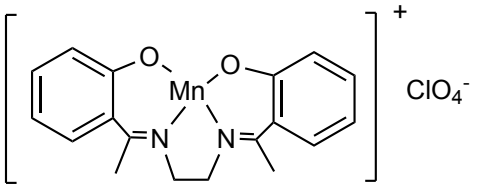

1.27

Figure 1.12. Mn(III) Schiff-base complex for alcohols oxidation reactions

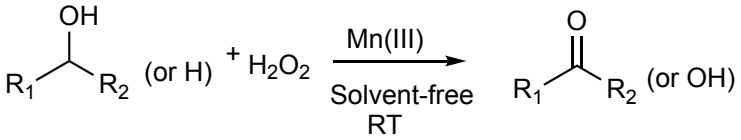

Scheme 1-15. Oxidation of benzylic and aliphatic alcohols using hydrogen peroxide catalyzed by Mn-complex **1.27**

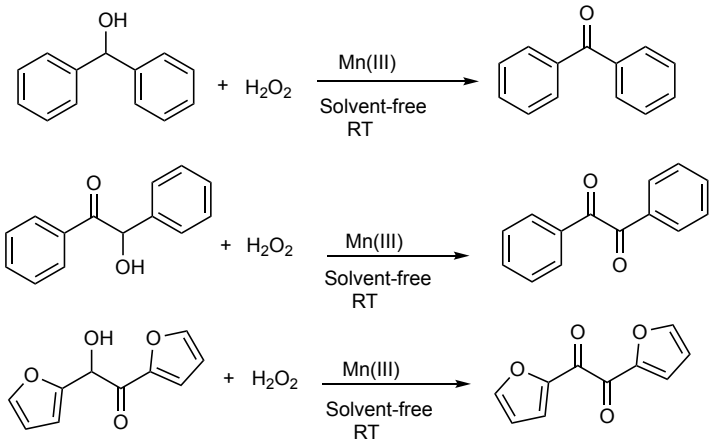

Scheme 1-16. Oxidation of aromatic alcohols with hydrogen peroxide catalyzed by the Mn(III) complex **1.27**

González and co-workers[67] reported the use of a set of Mn(III) complexes of various Schiff base ligands including *N*,*N*'-bis(3-methoxy-5-bromo-salicylidene)propane-1,2-diamine (**1.28**); *N*,*N*'-bis(3-methoxysalicylidene)ethylenediamine (**1.29**); *N*,*N*'-bis(3-methoxy-5-bromo-salicylidene)propane-1,3-diamine (**1.30**) and *N*,*N*'-bis(3-methoxysalicylidene)-2,2'-dimethylpropane-1,3-diamine (**1.31**) (Figure 1.13) as catalysts for the degradation of the lignin model compound, veratryl alcohol, along with dioxygen or hydrogen peroxide as co-oxidants. The oxidation reactions yielded up to 30% of veratraldehyde in the presence of air flow at room temperature.[67]

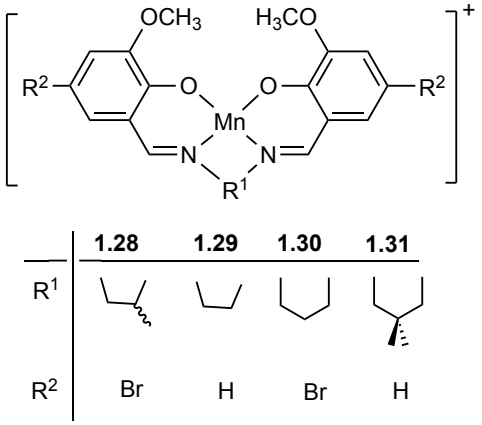

Figure 1.13. Structure of the manganese(III) complexes

1.2 Carbon Dioxide Activation and Uses as a Chemical Feedstock

1.2.1 Introduction

In the early 19th century, scientists recognized that accumulation of gases include water vapor, carbon dioxide CO_2, methane, nitrous oxide (N_2O) and other gases in the atmosphere may cause the greenhouse effect, which is primarily attributed to for raising the global temperature by trapping heat in our atmosphere. This phenomenon is now referred to as climate change. In particular, CH_4 and CO_2 as primary anthropogenic 'greenhouse' gas is the most effective heat-trapping gas due to its long lifetime and ability to absorb and re-emit infrared energy.[68] The combustion of fossil fuels is required to meet the world's energy needs[69] and is considered the primary form of energy production on a worldwide basis with 85% of global energy production coming from non-renewable energy sources including coal, oil and natural gas.[70] The remaining 15% comes from nuclear power and renewable sources, including solar, wind and wave energy, and biomass.[71] Consequently, fossil fuels have become the primary source of non-natural (CO_2) emissions.[72] Nonetheless, CO_2 is considered to be a green, environmentally benign reaction medium and a reactant that is cheap, abundant, renewable and nontoxic. Moreover, since it is a nontoxic carbon source, it can sometimes be used as an alternative for toxic chemicals such as carbon monoxide, phosgene or isocyanates, which could lead to finding new efficient and economical routes to create existing products.[73] Furthermore, CO_2 offers the possibility to create a renewable carbon economy through the chemical valorization of CO_2 into valuable chemicals. Because CO_2 is the most oxidized form of carbon and is kinetically inert and thermodynamically stable, in cases where its transformation is desired, the need for it energy input often renders its use for the synthesis of chemicals problematic and the activation and utilization of CO_2 is still considered a challenge. Chemical fixation of CO_2 is therefore, one of the most important topics in synthetic organic chemistry, and much effort has been spent over a considerable number of years to develop this particular subject.[73-74]

Although several methods have been developed for CO_2 fixation, they currently suffer from a narrow synthetic scope, poor reactivity and harsh conditions. Non-catalytic reactions to form C-C bonds with CO_2 such as carboxylation reactions, Kolbe–Schmitt reactions and using Grignard reagents are well-known chemical fixations of CO_2, but these approaches have shortcomings and environmental concerns. On the other hand, catalytic reactions involving efficient interactions of CO_2 with specific substrates, often in the presence of a suitable catalyst, play a fundamental and important role in these types of reactions. A variety of inorganic, organic, and particularly transition metal[75] catalysts have been used for various chemical CO_2 transformation as successful method of atom efficiency and sustainable development which is consistent and in line with the principles of green chemistry. Consequently, numerous investigations have been widely conducted and remarkable developments have been achieved for the catalytic activation of CO_2 and its transformation. The use of CO_2 as a C1 feedstock in carboxylation reactions, its reduction to yield formic acid and of particular relevance to this thesis the catalytic coupling of CO_2 with highly active substrates, such as epoxides, to generate polycarbonates and/or cyclic carbonates has been receiving increasing attention from the scientific community for over four decades.[73a, 76] Some reactions that utilize CO_2 to produce chemicals are summarized in Figure 1.14.[77] All types of reactions require a suitable catalyst, which is in most cases a metal-containing complex.

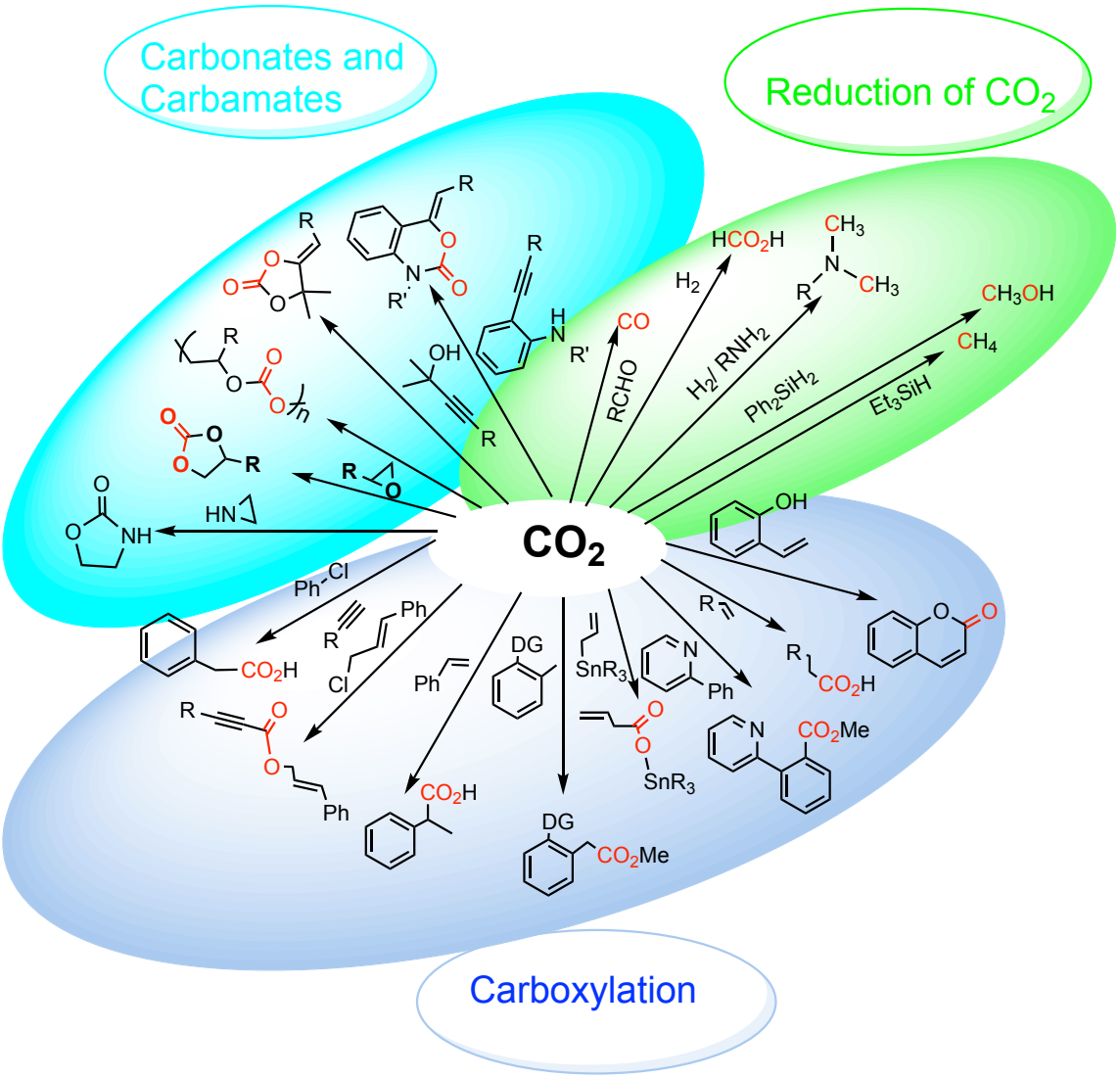

Figure 1.14. Chemical transformation of CO_2 into commodity chemicals

1.2.2 Chemical activation of carbon dioxide

Carbon dioxide (O=C=O) has a linear shape and contains 16 valence electrons. Although it contains two polar C-O bonds, CO_2 is a nonpolar molecule with two sets of π orbitals. Although CO_2 was thought to be a poor ligand initially, CO_2 possesses several coordination sites and exhibits diverse coordination abilities with various metals, and thus forms many complexes in a range of coordination modes.[78] In terms of coordination between CO_2 and the metal center, the CO_2 molecule exhibits several distinct modes that

display specific electronic properties as seen in Figure 1.15. CO_2 possesses two different reaction sites with: 1.) carbon atom LUMO electron density which makes it a lewis acidic site and can be described as an electrophilic center, or 2.) oxygen atoms are the sites of the HOMO electron density which can exhibit a weak Lewis base character and nucleophilic centers. The simultaneous acid-base activation is quite essential for most catalytic reactions involving CO_2, with the carbon atom and one of the oxygen atoms involved in the interaction with the metal. The two double C=O bonds contain π electrons that can interact with the d orbitals of transition metals. Generally, the catalyst's capability of weakening the C=O bonds to decrease the activation energy of the CO_2 conversion by specific chemical interactions is the fundamental factor of CO_2 conversion. To activate CO_2, electrons are added to the LUMO orbitals of CO_2 (via electron transfer), and the CO_2 molecule will minimize the energy by increasing the CO bond length and bending it until it reaches an OCO angle with an equilibrium angle of 130°. So, any interaction of carbon dioxide with a metal will induce a loss of linearity.[78] Consequently, the electronic structure of coordinated carbon dioxide is perturbed by bonding to a transition metal center and CO_2 becomes susceptible to reaction due to the weakening of the C=O bonds and contributes in lowering its activation energy for the CO_2 conversion. Thus, different types of altered reactivities have been observed for different coordination modes of CO_2.[69, 79]

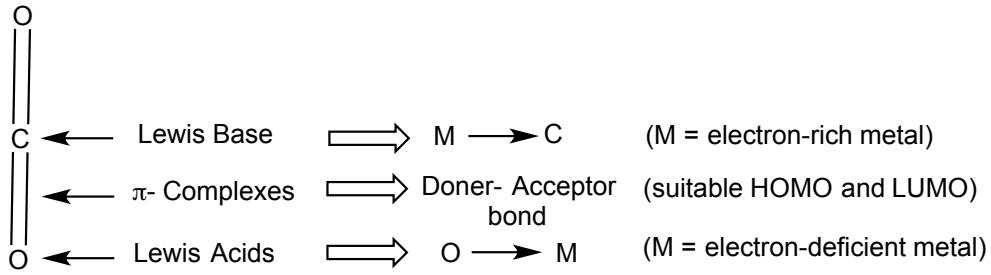

Figure 1.15. Type of metal and electronic properties and CO_2 dependence in metal-CO_2 bond

1.2.3 The Coordination Modes of CO_2

The initial, and an important step in the catalytic conversion of CO_2 into useful organic molecules is the coordination of CO_2 to a metal, where the electronic structure of the coordinated CO_2 is activated by bonding to the metal center. The first reports on CO_2-coordinated metal complexes were provided by Vol'pin et al. in 1969[80] and Jolly et al. in 1971.[81]

There are four basic modes of CO_2 coordination as described in Figure 1.16. The most common mode of bonding of CO_2 is the η^2-(C,O) bonding mode, in which there is a double bonding scheme with a σ bond from the π orbital of CO_2 to an empty d_z^2 (σ symmetry) metal orbital, together with back-bonding from a filled d_{xy} (π symmetry) metal orbital to the empty π^* orbital of CO_2. Several metal complexes having such a structure have been isolated and structurally characterized.[82] For the η^1-C coordination mode, when CO_2 acts as a sole C-electrophile, there is a strong charge transfer between a filled d_z^2 (σ symmetry) metal orbital and the anti-bonding π^* orbital of CO_2. This bonding mode is preferred with electronic-rich metals, probably due to an extra weak interaction between Lewis acid centers located in the coordination sphere of the metal with one or two oxygen atoms of CO_2[83] which is much more unstable than the η^2-(C,O) bonding mode. The η^1-O end-on coordination mode (linear η^1-O coordination) was first identified by Castro-Rodriguez in 2004.[84] The CO_2 molecule can remain linear or be weakly bent, which can be attributed to the weak interaction between the lone pair of only one oxygen atom and the metal center. This coordination mode is preferred with electron-poor metals. The η^2-(O,O) coordination mode is also known as a metal carboxylate with an ionic $M^+CO_2^-$ bond and is often common with alkali or alkaline-earth metals. The coordination of CO_2 to two or more metal centers is also very common and involves the coordination of the carbon to one metal and the bonding of one or two oxygen to a second (or third) metal center. The possible coordination modes are described in Figure 1.17, and these complexes are generally known as very stable complexes.[85]

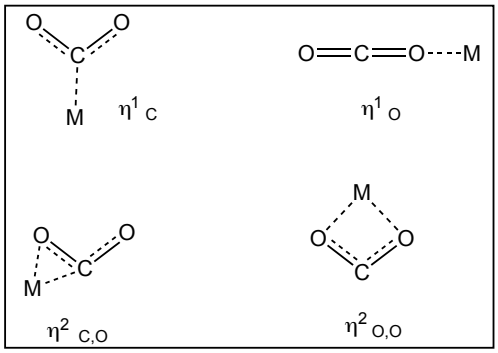

Figure 1.16. The CO_2 coordination modes to a single metal center

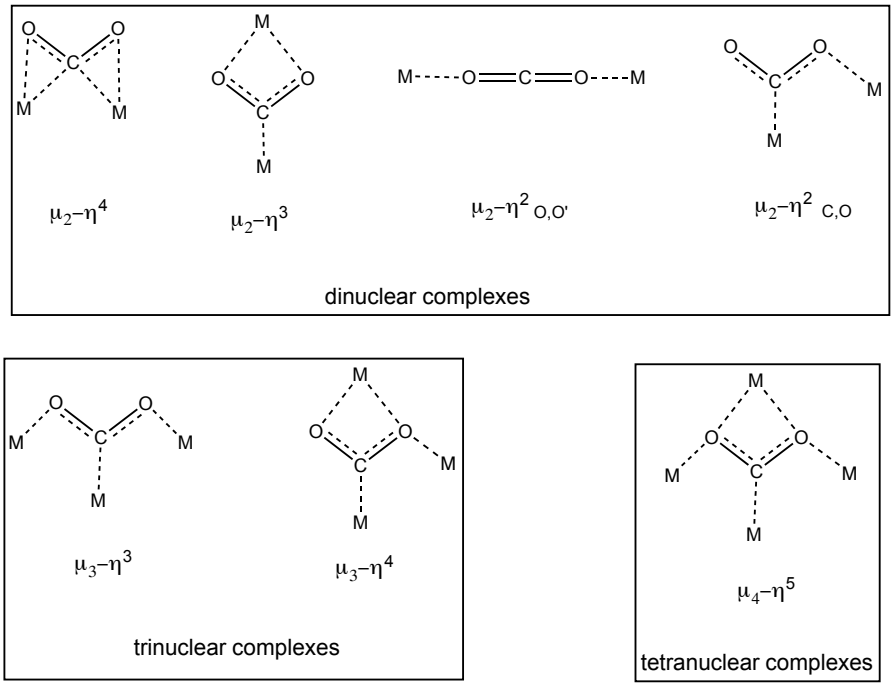

Figure 1.17. Coordination modes of CO_2 in multinuclear complexes with the metal centers bonded to O and C

1.2.4 Cyclic Carbonate Synthesis

Cyclic carbonates are organic compounds and in addition to their biodegradability[86] they have very interesting physical properties such as low toxicities, high solubilizing power, and high boiling points.[87] Therefore, their properties make

them useful for industrial or scientific applications such as green polar aprotic solvents and as electrolyte solvents in lithium-ion batteries.[88] In addition, they can be used as raw materials in the synthesis of polycarbonates [89]which have wide applications in the making CDs, DVDs, eyeglasses, aircraft windows, *etc.*[90], as fine chemical intermediates[91], fuel additives, plastic materials, and agricultural chemicals.[92] They are also found in various natural compounds present in fungi, bacteria, and/or plants[93] and potential pharmaceuticals.[94]

Cyclic carbonates can be prepared by the coupling reaction of CO_2 with strained heterocycles (epoxides or oxetanes), however, typically harsh reaction conditions and an efficient catalyst are required.[95] Five-membered rings are formed by the coupling reaction between CO_2 and epoxides, whereas the corresponding reaction with an oxetane leads to a six-membered ring derivative. The mid-1950s saw the first publication on the formation of propylene carbonate from propylene oxide and carbon dioxide.[96] Lewis acid or base catalysts were effective in catalyzing the cycloaddition reaction of propylene oxide (PO) and CO_2, which marked the advent of epoxide–CO_2 coupling chemistry. Although, the reaction occurs easily due to the high energy of the starting epoxides, the high pressure and temperature is still necessary for this reaction. Consequently, the process has some limitations and is associated with some energy and economic concerns. In early 1969, Inoue and co-workers discovered that a zinc-based heterogeneous catalyst was effective in catalyzing the alternating copolymerization of propylene oxide (PO) and CO_2 and is considered as the start of new routes for epoxide–CO_2 coupling chemistry.[97] This alternative "greener" synthetic approach to the preparation of cyclic carbonates and polycarbonate (PC) using CO_2 as renewable feedstocks (Scheme 1-18) contrasts with the conventional synthesis of polycarbonate made by the condensation of bisphenol-A (BPA) and phosgene, since they are considered highly toxic reagents**.** The coupling reaction of CO_2 with epoxides also has the advantage of being 100% atom economical reaction, making it a highly desirable transformation approach.[98] Following Inoue's report, the behavior of several zinc-based catalysts with different dihydric sources such as resorcinol, dicarboxylic acids and primary amines for the coupling reaction of propylene oxide and

CO_2 have been investigated.[99] With a growth in awareness of green chemistry practies, the number of environmentally-friendly approaches toward the coupling reactions of CO_2 and epoxides and the like has been increasing in recent decades. Several new greener approachs involve the utilizing of of ionic liquids,[100] organocatalysts,[101] supercritical CO_2,[102] or metal-based photocatalysts.[103] More specifically, the most commonly-used catalytic methodology for the synthesis of cyclic carbonates is the use of metal-based homogeneous catalysts. In recent years, many homogenous catalysts have been developed for this reaction, and many catalytic systems have appeared that address different reaction features such as chemoselectivity, sustainability, reactivity, reaction mechanism, and substrate scope.

On the basis of the different coordination and activation modes of CO_2 that were previously discussed, well-designed transition metal catalysts have been prepared that are able to promote the reactivity and also control the selectivity of CO_2 fixation reactions in organic synthesis. This promising research area still has many novelties to be discovered.

The cyclic carbonate formation reaction can be mediated by various Lewis acidic metal halides, carboxylate or alkoxide/aryloxide complexes and it is, accordingly, the most plausible proposed mechanism generally accepted to proceed *via* a coordination-insertion mechanism.[104] The Lewis base and Lewis acid work together to open the epoxide ring and then react with CO_2 to give the corresponding cyclic carbonate via a ring-opening and recyclization process as seen in (Scheme 1-17). Other reports also suggest the parallel requirement of both Lewis base activation of the CO_2 and Lewis acid activation of the epoxide.[75, 104]

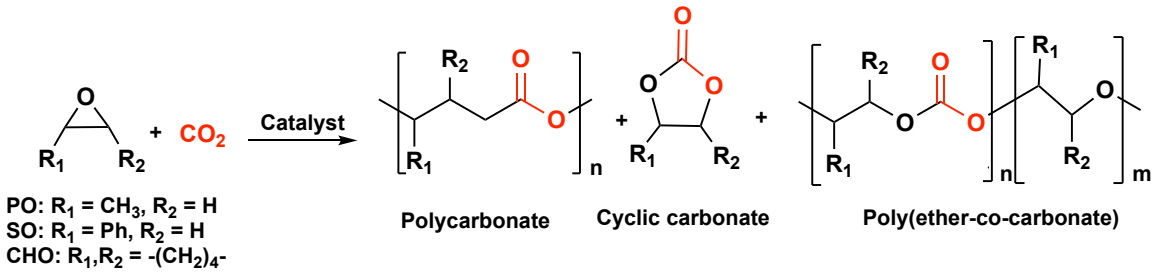

Scheme 1-17. General catalytic reaction of epoxides and CO_2 generating polycarbonate, cyclic carbonate and/or poly(ethercarbonate) [PO = propylene oxide; SO = styrene oxide; CHO = cyclohexene oxide]

The ligand electronic properties greatly affect both the bonding of the ligand to the metal and the electronic properties of the metal, which consequently affect their catalytic activity and selectivity. For example, the most common ligands used for the synthesis of these complexes for the cycloaddition of CO_2 to epoxides are porphyrin, salen and related ligands. Both ligands are tetradentate and can coordinate to the metal center in a planar fashion with the complex usually being able to accommodate an extra ligand in the axial position. These axial ligands are considered good leaving groups and they are generally labile, meaning they can be easily displaced from the coordination sphere during the reaction. It has been reported that a co-catalyst can improve the catalytic performance of the catalyst.[104-105] The co-catalyst provides the nucleophilic species and either attacks and opens the epoxide ring leading to the formation of a metal-bound alkoxide or it acts as a nucleophile that coordinates to the metal center (in the case of two nucleophiles involved), increasing its electron density and therefore weakening the bond with other nucleophilic species, which can be a polymeric (polycarbonate) chain in some of these systems. The co-catalyst should be a good nucleophile to open the ring of the epoxide and should be a good leaving group and not coordinate too strongly to the metal center. If it is a good leaving group, it should promote back biting reactions for the metal-bound carbonate intermediates, favouring the formation of cyclic carbonates, whereas poor leaving abilities would be more selective towards polycarbonate formation by supressing the back biting reaction. Several different types of co-catalyst are used in

these reactions. They can be neutral, like an organic base (e.g. substituted pyridines or imidazoles), or ionic, like an ammonium salt (e.g. tetrabutylammonium bromide). Common co-catalysts are shown in Figure 1.18. For ionic catalysts, the anion has a greater nucleophilicity towards the epoxide if the corresponding cation is bulky as it would exert lower ion-pair electrostatic attraction towards the anion.[106]

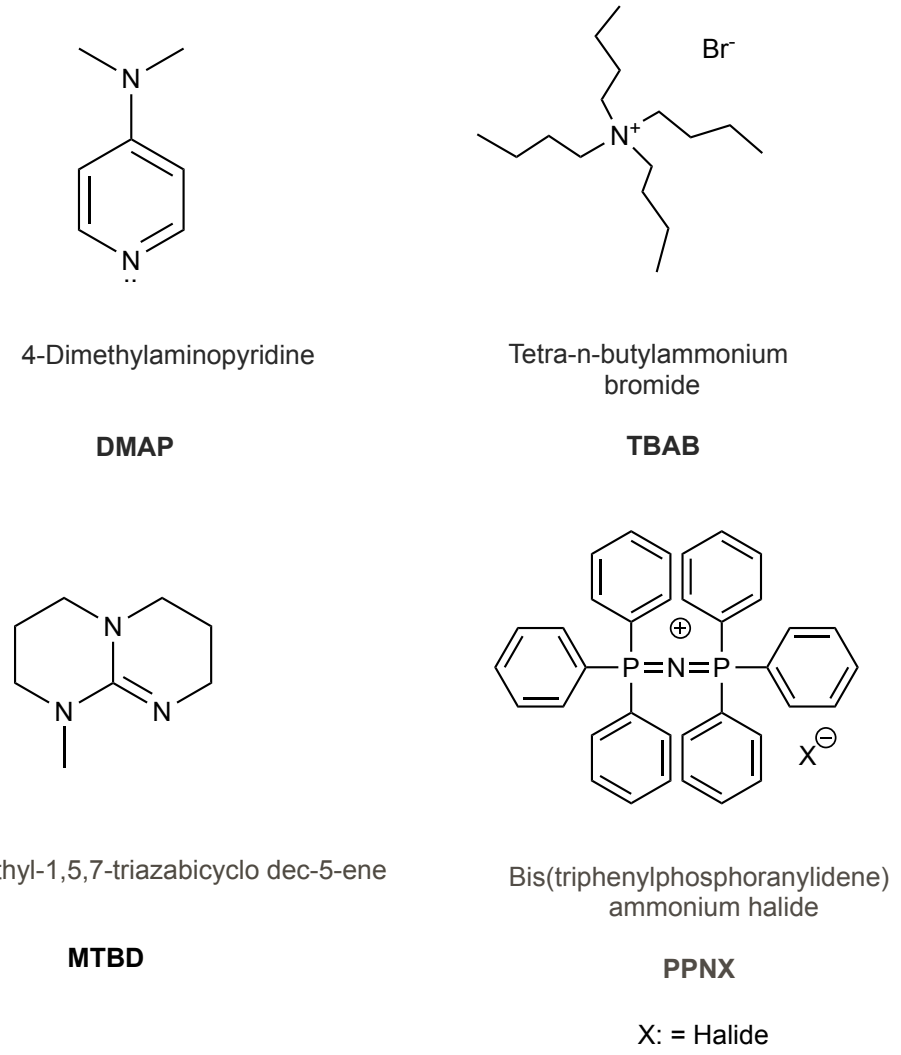

Figure 1.18. Common co-catalysts used in the reaction of carbon dioxide and epoxides

The selectivity of cyclic carbonate formation is strongly affected by the ratio between the catalyst and co-catalyst. The trend of higher selectivity towards cyclic carbonate at higher co-catalyst to metal ratios leads to displacement of the metal-carbonate intermediate, and, therefore, favors the back biting reaction for cyclization. In contrast, at lower co-catalyst to metal ratios a higher selectivity towards polycarbonate is observed.[104] Furthermore, the rate and selectivity of the cyclic carbonate formation depends on the epoxide substrate as a result of steric and electronic effects where the selectivity for cyclic or polycarbonates is also affected by the nature of the substituents on the epoxide ring. For terminal epoxides like propylene oxide, the nucleophilic attack mainly occurs at the least substituted carbon site (β-carbon) due to the higher accessibility and the electron-donating effect of the alkyl group. On the other hand, for epoxides like styrene oxide the nucleophilic attack occurs mainly at the electron deficient α-carbon instead of the β-carbon due to the consequence of the electron-withdrawing inductive effect of the phenyl group (Figure 1.19).[107] Moreover, for internal epoxides where there is more steric bulk around the epoxide ring such as cyclohexene oxide, it causes a lower conversion rate as nucleophilic attack is hindered by the co-catalyst.[108] Therefore, careful design and maintaining a good balance of the components discussed above including the nature of the metal center, substrate, and co-catalyst is very important to obtain the desired product selectively of this reaction.

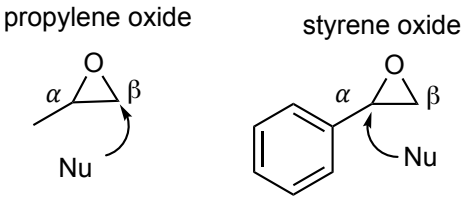

Figure 1.19. Most probable sites of nucleophillic attack for different epoxides

1.2.5 Plausible Mechanism on the Cycloaddition of CO_2 to Epoxide

The widely accepted mechanistic proposal that is invoked for binary systems in the synthesis of organic carbonates is explained in Scheme 1-18. The metal complex initiates the ring-opening of the epoxide by coordination of the epoxide to the Lewis acidic metal center followed by attack at the less hindered side of the epoxide (methine carbon) by a nucleophilic group (nucleophilic axial/leaving group or added co-catalyst e.g. chloride ion), which leads to the formation of a metal-bound alkoxide, Scheme1-18.[98a, 109] This causes the epoxide ring to open and allows for CO_2 insertion into the metal-alkoxide bond, forming a metal carbonate intermediate to give the corresponding cyclic carbonate via a recyclization process, known as back-biting. This mechanism has also been supported by X-ray crystallographic analysis (in the case of the resting state of some of the catalysts reported)[110] and computational studies[111] and a labelling experiment performed by Shi et al. in 2003.[112]

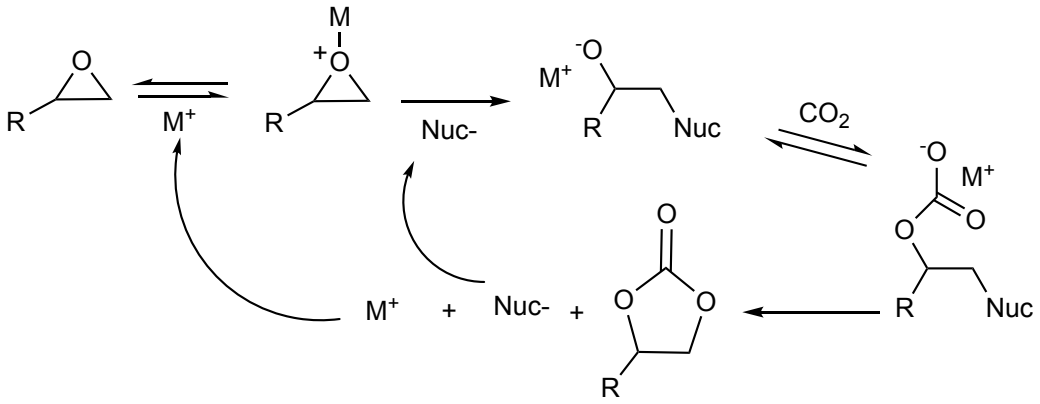

Scheme 1-18. Plausible Mechanism for the cycloaddition of CO_2 with epoxides catalyzed by acid-base bi-functional systems

1.2.6 Cyclic Carbonate Synthesis Catalyzed by Metal Complexes

As highlighted by recent detailed reviews[74b, h, 107, 113], cyclic carbonates can be obtained on a laboratory scale using a wide range of catalytic systems, such as ionic liquids, metal oxides, alkali metal salts, metal complexes, zeolites, organic bases, etc. However, there are a few challenges such as low selectivity towards the carbonates, the formation of side products, longer reaction times and the stability of the catalysts under an oxidizing environment and high temperature and pressure conditions. The metal complexes of first row transition elements, such as manganese and vanadium, are inexpensive, less toxic and biologically abundant[114], and thus are ideal when developing an alternate active catalytic system as a green catalyst.

1.2.6.1 Vanadium Catalysts for Coupling Reactions of Epoxides and CO_2

Lee and co-workers explored binary systems composed of a simple and commercially available vanadium trichloride catalyst in combination with various onium salts for the coupling reaction of CO_2 with a variety of epoxides.[115] A catalytic system such as VCl_3/n-Bu_4NOAc, VCl_3/(n-Bu_4NCl or PPNCl) was reported to be active to convert propylene oxide, epichlorohydrin, styrene oxide, and cyclohexene oxide to the corresponding cyclic carbonates without the use of organic solvents with over 90% yields under mild conditions of (90–120 °C) and pressures (1.5 MPa = 14.8 bar).[115]

Darensbourg *et al.* reported that a readily available vanadium complex, $VO(acac)_2$ (acac = acetylacetonato or 2,4-pentanedione) (**1.32**, Figure 1.20) along with *n*-Bu_4NBr as co-catalysts was an efficient system for the synthesis of trimethylene carbonate (TMC) from oxetane (trimethylene oxide) and CO_2 at 60 °C, 35 bar CO_2 for 8 h, yielding up to 95% conversion and 100% selectivity toward cyclic carbonate.[116]

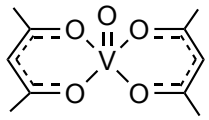

1.32

Figure 1.20. $VO(acac)_2$ (acac = acetylacetonate or 2,4-pentanedione)

Coletti *et al.* reported the synthesis of a set of catalysts based on vanadium complexes supported by salen and salphen ligands, bearing electron-donating and electron-withdrawing groups on the aromatic rings of the ligand framework (**1.33a–f** and **1.34a–f**, Figure 1.21). For the cycloaddition of CO_2 with epoxides the obtained results were compared to those gathered for the V^{IV} complex $[VO(acac)_2]$ (acac = acetylacetonate).[117] For comparison of data for the reactions with V^{IV}(O)salen **1.33d** and V^{IV}(O)salphen **1.33c**, and triflateV^{V} salphen species **1.33c** as potential catalysts for the cycloaddition reaction of CO_2 and 1,2-epoxyhexane in the presence of Bu_4NI as a co-catalyst under mild conditions (45 °C, 10 bar CO_2 pressure) for 18 h were also reported. It was observed that despite the variation in the nature of the vanadium center, the yields of cyclic carbonates proved to be generally low throughout the entire range of catalysts. For example, for the complex (**1.33c**) only 3% of cyclic carbonate was produced; however, its reactivity increased significantly when 1,2-epoxy-3-hydroxypropane (glycidol) was used as the substrate, giving rise to 55% yield for the corresponding cyclic product.[117] This is because glycidol is an activated epoxide and more susceptible to the ring-opening reaction.

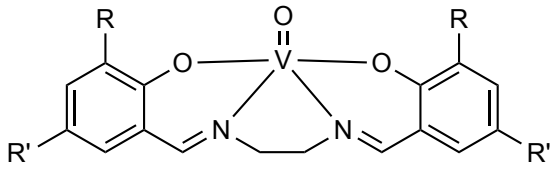

1.33a: R = R' = tBu
1.33b: R = H, R' = tBu
1.33c: R = R' = H
1.33d: R = H, R' = Cl
1.33c: R = R' = Cl
1.33f: R = H, R' = OMe

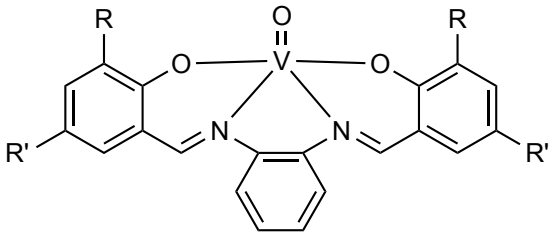

1.34a: R = R' = tBu
1.34b: R = H, R' = tBu
1.34c: R = R' = H
1.34d: R =H, R' = Cl
1.34c: R = R' = Cl
1.34f: R = H, R' = OMe

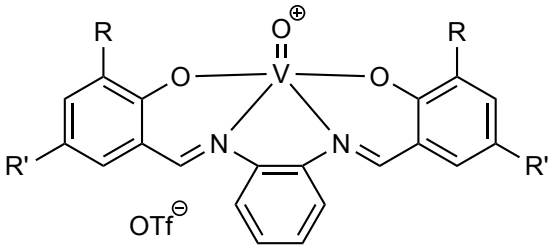

1.35a: R = R' = tBu
1.35b: R = R' = H
1.35c: R =H, R' = Cl
1.35d: R = R' = Cl

Figure 1.21. Vanadium salen and salphen complexes used as a catalyst for the cycloaddition of CO_2 to epoxide

More recently, Bai *et al.* reported complexes (VO(IV)) (**1.36a-c**, Figure1.22), bearing porphyrin ligands which were utilized along with both ionic and neutral bases as co-catalysts (e.g. *n*-Bu_4NBr > *n*-Bu_4NCl > *n*-Bu_4PBr > *n*-Bu_4NI > PTAT > *n*-Bu_4NF) for the cycloaddition of epoxides and CO_2.[118] The effect of the co-catalyst, ligand framework and the type of epoxides on coupling reaction was studied. For example, under the optimal reaction conditions (14 bar CO_2 pressure at 150 °C, 5 h) (**1.36a**) in conjunction with *n*-Bu_4NBr (1:2) catalyzed the reaction of propylene oxide and CO_2, and exhibited the highest catalytic activity (TOF = 396 h^{-1}) of all the catalysts.[118]

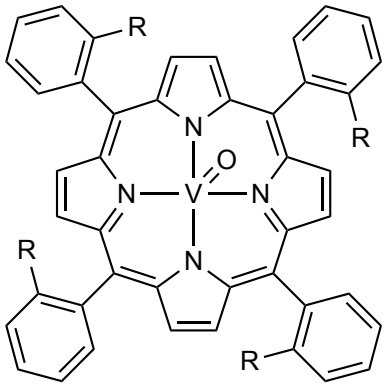

1.36a: R = H
1.36b: R = NO_2
1.36c: R = CH_3

Figure 1.22. Vanadium porphyrin complexes used as a catalyst for the cycloaddition of CO_2 to epoxide

Very recently Miceli *et al.*[119] reported the activity of vanadium(V) complexes (**1.37**) and 1.38, derived from aminotriphenolate ligands along with NBu_4X (X = I or Br) as a co-catalyst, for the cycloaddition reaction of various epoxides with CO_2 to afford a series of substituted organic carbonates in good yields, (Scheme 1-19). The best conversion of >99% was obtained using **1.37**/NBu_4I after a reaction time of 18 h for the coupling of CO_2 to 1,2-epoxyhexane A under 10 atm pressure at 50-85 °C. Terminal epoxides were also examined (styrene oxide B and epichlorohydrin C) and, surprisingly, in these cases the binary catalyst based on the chlorinated complex (**1.38**) was reported to be significantly less active than that derived from (**1.37**). In addition, they proposed a mechanism that starts off with coordination of the epoxide, to form a hexacoordinated V(V) complex of **1.38**-PO, which can occur with a higher tendency if the epoxide substituent is relatively small, (Scheme 1-19). Upon reactivation, (**1.38**) can re-enter the catalytic cycle in the presence of NBu_4X (X = Br, I), suggesting the subsequent formation of V(V) alkoxide intermediate species with the halide nucleophile X incorporated. Interestingly, (**1.38**) a V(V) complex bearing peripheral chloride groups on the ligand framework, was found to incorporate a ring-opened epoxide (*e.*g., **1.38**-PO and **1.38**-

ECH) with one of the phenolate-*O* atoms acting as a nucleophile and the metal center acting as a Lewis acidic site and forming a stable intermediate, which could be formed via a nucleophilic attack of the bromide onto the arylalkyl ether part of the unusual intermediate, subsequently followed by a nucleophilic displacement of the original phenolate.

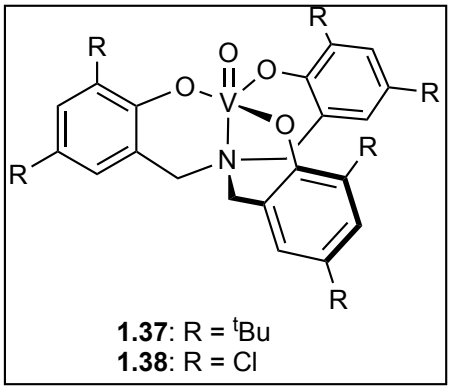

1.37: R = ^{t}Bu
1.38: R = Cl

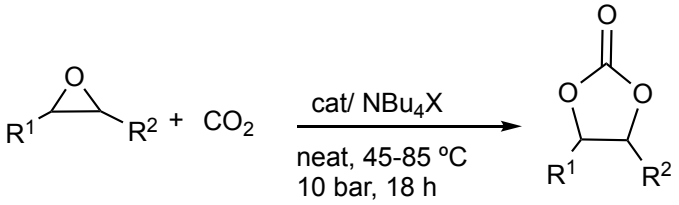

A: R^1 = nBu, R^2 = H
B: R^1 = -CH_2Cl, R^2 = H
C: R^1 = Ph, R^2 = H
D: R^1 = Ph, R^2 = Me

E: R^1 = nBu, R^2 = H
F: R^1 = -CH_2Cl, R^2 = H
G: R^1 = Ph, R2 = H
H: R^1 = Ph, R^2 = Me

Scheme 1-19. vanadium(V) complexes for the coupling of CO_2 and various epoxides

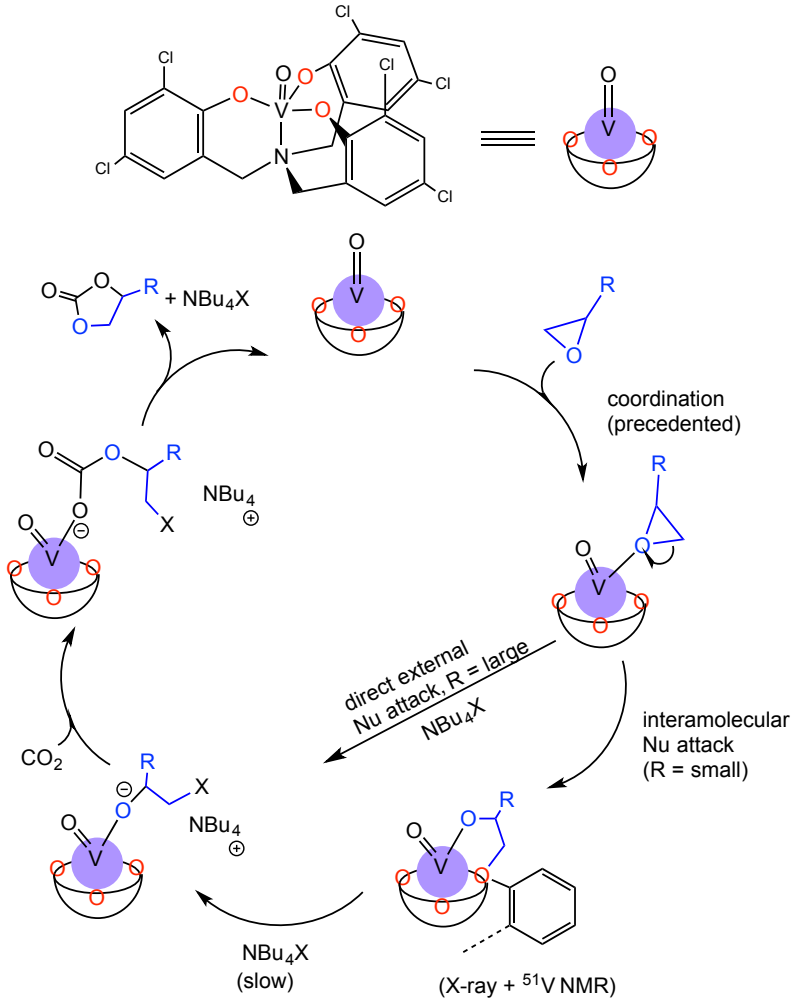

Scheme 1-20. Proposed mechanistic cycle for the formation of cyclic carbonates using the binary catalyst **1.37**/NBu_4X (X = Br, I)

1.2.6.2 Manganese Catalysts for Coupling Reactions of Epoxides and CO_2

In 2007, Darensbourg and co-workers reported the synthesis and utilization of several Schiff base complexes of the form (acacen)$Mn^{III}X$ (acacen = *N,N'*-bis(acetylacetone)-1,2-ethylenediimine), where X= OAc, Cl, N_3 or NO_3 (**1.39a-d**, Figure 1.23) which were used as catalysts to couple cyclohexene oxide and carbon dioxide in the

presence of a variety of co-catalysts to yield cyclic or polycarbonates.[120] They observed that these (acacen)MnX complexes exhibited a very limited tendency to couple epoxides and CO_2 to afford copolymer or cyclic carbonate products. The key reason for the catalytic inactivity is that the five-coordinate Schiff base derivatives of Mn(III) are essentially incapable of ring-opening epoxides because of the ineffectiveness of it to bind the epoxide ligands. However, the complexes were used as useful model complexes for the mechanistic study of the copolymerization reactions. As a consequence, this observation led to the conclusion that enhancing the electrophilicity of the metal center of manganese(III) acacen complexes should facilitate the binding and activation of epoxides. Therefore, Darensbourg reported the synthesis of a series of manganese(III) acacen derivative complexes bearing electron-withdrawing trifluoromethyl groups attached to the carbons α to the coordinated oxygen atoms of the ligand (**1.40a-d**, Figure 1.23).[121] Investigation of the increased tendency of the manganese (III) complexes of N, N'-bis(trifluoroacetylacetone)-1,2-ethylenediimine (tfacacen) to bind a sixth ligand was carried out. A kinetic study of the epoxide ring-opening process showed that cyclohexene oxide readily binds to (tfacacen)MnN_3.

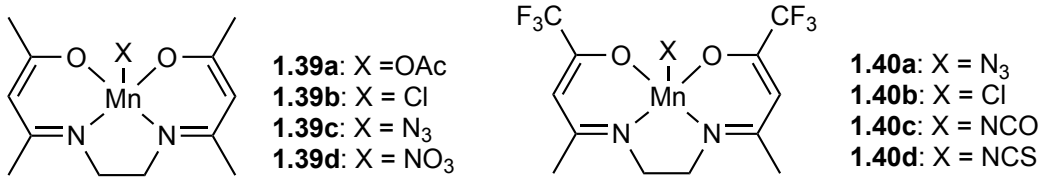

Figure 1.23. Manganese Schiff base complexes as catalysts for the coupling of CO_2 and epoxides **[120] [121]**

Salen complexes (bis(salicylidene)ethylenediamine) have the advantage of being cheap and easily prepared, as the highly modifiable ligand is able to coordinate to many different metals and stabilize them in various oxidation states. They have excellent thermal and chemical stability which allows for the use of salen base metal complexes in a large variety of useful catalytic transformations.[122] Cr(III)-salen and particularly Mn(III)-salen complexes have been extensively studied in related reactions, such as the

epoxidation of olefins, which usually precedes as a separate step in the production of the organic carbonates.[123] However, only Cr-salen complexes have been widely used as active species for the synthesis of cyclic carbonates[124] or the alternating copolymerization of epoxides and CO_2.[125] It is believed that the metal center of (salen)metalX complexes should be substitutionally inert, and electrophilic enough to bind and activate epoxides for ring-opening to be effective catalysts for the cycloaddtion or copolymerization processes. Also, it should be sufficiently nucleophilic to promote insertion of the poorly electrophilic CO_2 into the resulting metal–alkoxide bond. Furthermore, the cyclic carbonate formation is facilitated by the presence of an electron in the e_g anti-bonding d orbital of manganese(III).[74a, 120] Considering these observations, in 2008, the first successful Mn-salen complexes were reported by Baiker *et al.* to be an effective catalyst in the formation of cyclic organic carbonates.[126] Various homogeneous manganese-salen complexes (**1.41a-f**, Figure 1.24) were synthesized and tested as catalysts for the formation of cyclic organic carbonates from propylene oxide and styrene oxide and CO_2 in supercritical CO_2 for 3 h at 140 °C. The complexes showed excellent activity and very high selectivity (98%) towards the cyclic carbonate, and the highest TOFs measured were 233 h^{-1} with catalyst (**1.41f**) in the reaction of propylene oxide and 213 h^{-1} with catalyst (**1.41c**) in the reaction of styrene oxide.[126] Furthermore, a kinetics study under the same reaction conditions showed that the reaction rate is strongly influenced by the nature of the epoxide.[126]

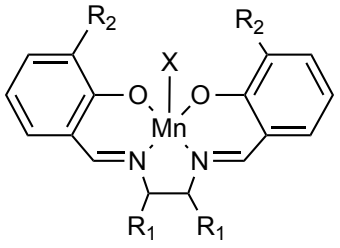

1.41a: $R_1 = R_2 = H$, X = Cl
1.41b: $R_1 = R_2 = H$, X = Br
1.41c: $R_1 = R_2 = H$, X = I
1.41d: $R_1 = C_6H_5$, $R_2 = H$, X = Cl
1.41e: $R_1 = C_6H_5$, $R_2 = H$, X = Br
1.41f: $R_1 = H$, $R_2 = C_6H_5$, X = Br

Figure 1.24. Manganese-salen complexes as catalysts for the formation of cyclic organic carbonates from epoxides and CO_2

In 2009, the same group reported an *in situ* XAS study of the synthesis of a series of Mn(III) salen bromide complexes (**1.42a-c**, Figure 1.25) with varying salen ligand structures and their utilization in the cycloaddition of CO_2 to propylene oxide and styrene oxide.[127] In the catalytic studies it was observed that propylene oxide usually reacted much faster than styrene oxide. This seems to be related to a faster coordination of propylene oxide to the Mn atom. Based on the experimental evidence, a mechanism was proposed (Scheme 1-21), which is similar to the previously studied trivalent Al, Co, and Cr salen systems.[128] In the first step, when the complex is dissolved in liquid epoxide, at least one epoxide molecule is coordinated to the Mn central atom, leading to octahedral coordination geometry. This is supported by the previous calculations of chromium salen complexes that show the free coordination site on a five-coordinate complex is rapidly occupied by an epoxide molecule.[128a] When propylene oxide is used as a substrate, the bromide ligand is quickly replaced by another epoxide molecule, whereas when styrene oxide is used, the replacement step takes a long time or needs a higher temperature. The following step is the insertion of CO_2, forming a coordinated carbonate species, which still contains a C-Br bond.[128a] Finally, the backbiting step takes place when there is an intramolecular attack of the manganese-bound oxygen atom onto the brominated carbon atom to form the cyclic carbonate and bromide as the leaving group.[128a]

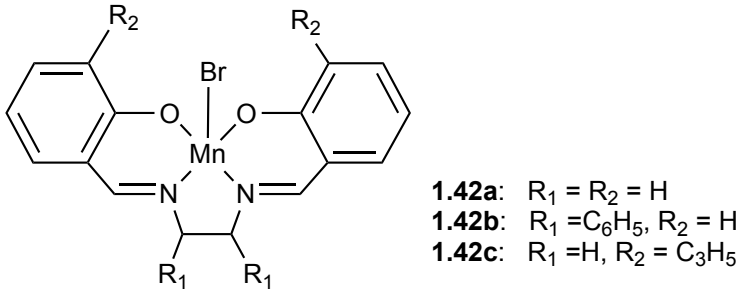

Figure 1.25. Manganese (III) salen bromide complexes as a catalyst for the cycloaddition of CO_2 to epoxides

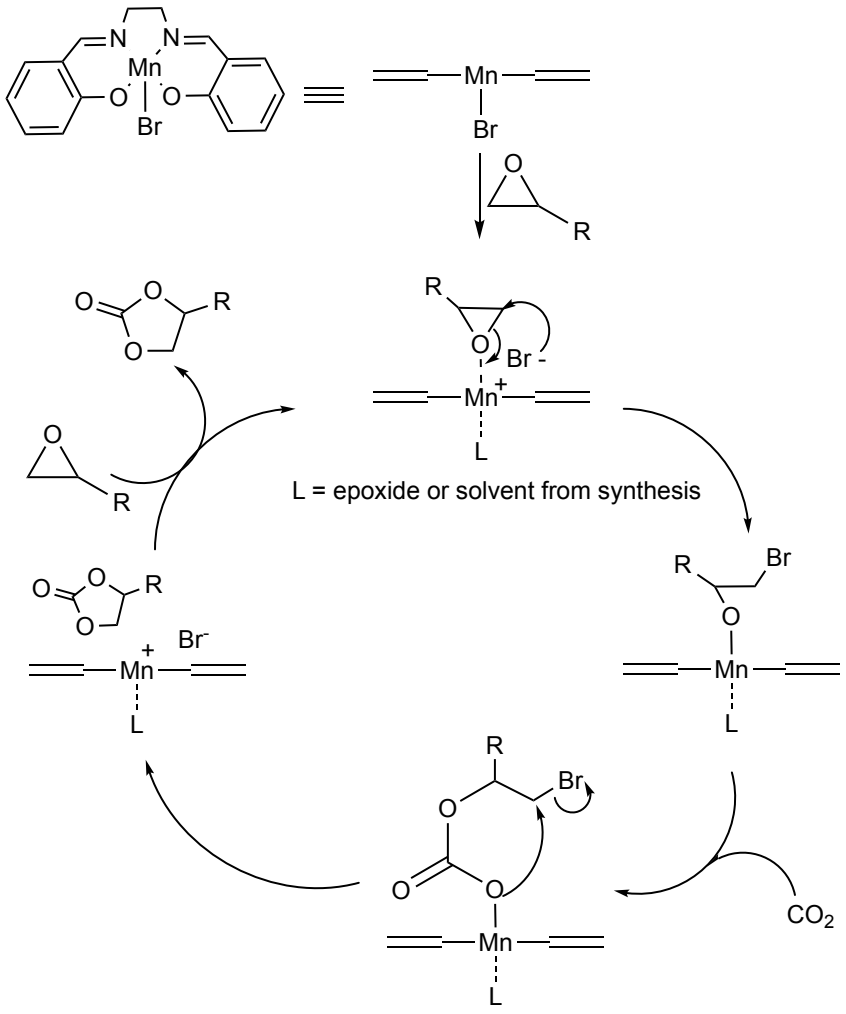

Scheme 1-21. Proposed mechanism of the catalytic cycle for the manganese salen complex

Although vanadium and manganese are environmentally benign and an attractive alternative for other transition metals, reports on vanadium and manganese-based catalysts in cyclic carbonate synthesis are rare, especially compared with other metals such as chromium and cobalt.

1.3 Objectives and Outline of the Thesis

The essential objective of this thesis was to develop new methods to generate useful chemicals from renewable sources, to create a chemical technology based on the use of biomass (lignocellulosic) and CO_2 as an alternative to petrochemistry. Therefore, the development of new homogeneous catalysts to selectively depolymerize lignin and provide lignin-derived aromatic feedstocks for chemical production, and use them for the transformation of CO_2 to cyclic carbonates using epoxides. That is to say that the research described in this thesis are to: (a) synthesize and characterize families of related potentially biocompatible catalyst systems; (b) apply these systems in aerobic oxidation reactions of alcohols and C–O bond cleavage reactions in simple lignin model compounds as well as in the cycloaddition reactions of CO_2 and epoxides.

Chapter 2 provides an overview of the synthesis and characterization of the series of amino-bis(phenolate) vanadyl complexes containing tetradentate tripodal ligands. The catalytic activities of the catalysts for the aerobic oxidation of alcohols and C–O bond cleavage reactions in simple lignin model compounds were also investigated. In Chapter 3, the catalytic activity of these vanadium complexes toward the cycloaddition of epoxides and CO_2 to synthesize cyclic carbonates is described as a first report on the reactivity of a vanadium aminophenolate complex in these reactions. Chapter 4 introduces the preparation and characterization of two Mn(III) complexes. The catalytic activity of these manganese complexes toward the cycloaddition of CO_2 with epoxides, and in the aerobic oxidation of 4-methoxybenzyl alcohol and 1,2-diphenyl-2-methoxyethanol is examined.

1.4 Co-Authorship Statement

This PhD thesis includes results of joint research that have been published in peer reviewed journals in the form of three full papers, as follows:

Chapter 2: Vanadium Aminophenolate Complexes and Their Catalytic Activity in Aerobic and H_2O_2-Mediated Oxidation Reactions

Authors: Ali Elkurethi, Andrew G. Walsh, Louise N. Dawe and Francesca M. Kerton

Journal: *Eur. J. Inorg. Chem*., **2016**, 3123–3130 *The principal author (Ali Elkurtehi)* contributed to all aspects of the project as the main researcher including: literature review, performing 90% of all the experiments, collecting and analyzing the data, designing some of the experiments, presenting and discussing the data and writing the first draft of the manuscript. *The co-author (Andrew G. Walsh)* assisted with ligand syntheses, purification of starting materials and recrystallizations. *The co-author (Dr. Louise Dawe)* was a crystallographer at Memorial University of Newfoundland, who collected XRD data and solved the structures for the complexes and wrote the crystallographic procedure section. *The corresponding author (Dr. Francesca M. Kerton)* was the principal investigator and developed the initial ideas for this research. She oversaw all aspects of the project, including supervision of the principal author (A. E.), the design of experiments, data analysis, revision of the draft manuscript and submission to the journal, and responding to the questions and comments from the peer reviewers.

Chapter 3: Coupling Reactions of Carbon Dioxide with Epoxides Catalyzed by Vanadium Aminophenolate Complexes.

Authors: Ali Elkurtehi and Francesca M. Kerton

Journal: *ChemSusChem*, **2017**, 10, 1249-1254. *The principal author (Ali Elkurtehi)* contributed to all aspects of the project as the main researcher including: literature review, performing of all the experiments, collecting and analyzing the data, designing some of the experiments, presenting and discussing the data and writing the first draft of the

manuscript. *The corresponding author (Dr. Francesca M. Kerton)* was the principal investigator and developed the original ideas for this research. She oversaw all aspects of the project, including supervision of the principal author (A. E.), the design of experiments, data analysis, and revision and submission of the revised manuscript, and responding to the questions and comments from the peer reviewers.

Chapter 4: Synthesis of Amino-Phenolate Manganese Complexes and Their Catalytic Activity in Carbon Dioxide Activation and Oxidation Reactions

Authors: Ali Elkurtehi and Francesca M. Kerton

Journal: Submitted to *Catalysis Science & Technology*. *The principal author (Ali Elkurtehi)* contributed to all aspects of the project as the main researcher including: literature review, performing of all the experiments, collecting and analyzing the data, designing some of the experiments, presenting and discussing the data and writing the first draft of the manuscript. *The corresponding author (Dr. Francesca M. Kerton)* was the principal investigator and provided the initial ideas for experiments performed. She oversaw all aspects of the project, including supervision of the principal author (A. E.), the design of experiments, data analysis, revision of the draft manuscript and submission to the journal, and responding to the questions and comments from the peer reviewers.

1.5 References

[1] A. Corma, S. Iborra and A. Velty, *Chem. Rev.* **2007**, *107*, 2411-2502.

[2] a) S. R. Collinson and W. Thielemans, *Coord. Chem. Rev.* **2010**, *254*, 1854-1870; b) J. Zakzeski, P. C. A. Bruijnincx, A. L. Jongerius and B. M. Weckhuysen, *Chem. Rev.* **2010**, *110*, 3552-3599; c) J. G. Linger, D. R. Vardon, M. T. Guarnieri, E. M. Karp, G. B. Hunsinger, M. A. Franden, C. W. Johnson, G. Chupka, T. J. Strathmann, P. T. Pienkos and G. T. Beckham, *Proc. Natl. Acad. Sci. U. S. A.* **2014**, *111*, 12013-12018; d) A. Rahimi, A. Ulbrich, J. J. Coon and S. S. Stahl, *Nature* **2014**, *515*, 249-252; e) C. S. Lancefield, O. S. Ojo, F. Tran and N. J. Westwood, *Angew. Chem., Int. Ed.* **2015**, *54*, 258-262.

[3] A. M. Ruppert, K. Weinberg and R. Palkovits, *Angew. Chem. Int. Ed.* **2012**, *51*, 2564-2601.

[4] C. R. Carere, R. Sparling, N. Cicek and D. B. Levin, *Int. J. Mol. Sci.* **2008**, *9*, 1342-1360.

[5] M. Ek, G. Gellerstedt and G. Henriksson, *Ljungberg Textbook: Pulp and paper chemistry and technology. Wood chemistry and wood biotechnology*, Fiber and Polymer Technology, KTH, **2007**.

[6] K. Kamide, *Cellulose and cellulose derivatives*, Elsevier, **2005**.

[7] J. D. McMillan, *Renewable Energy* **1997**, *10*, 295-302.

[8] E. Sjöholm, *Handbook of size exclusion chromatography and related techniques: Revised and expanded* **2003**, *91*, 311.

[9] D. Fengel and G. Wegener, *Wood: chemistry, ultrastructure, reactions*, Walter de Gruyter, **1983**.

[10] Y.-H. P. Zhang, S.-Y. Ding, J. R. Mielenz, J.-B. Cui, R. T. Elander, M. Laser, M. E. Himmel, J. R. McMillan and L. R. Lynd, *Biotechnol. Bioeng.* **2007**, *97*, 214-223.

[11] R. C. Schulz, *Berichte der Bunsengesellschaft für physikalische Chemie* **1981**, *85*, 1085-1085.

[12] Y. H. Zhang, *J. Ind. Microbiol. Biotechnol.* **2008**, *35*, 367-375.

[13] T. Timell, *Wood Sci. Technol.* **1967**, *1*, 45-70.

[14] C. Crestini, M. Crucianelli, M. Orlandi and R. Saladino, *Catal. Today* **2010**, *156*, 8-22.

[15] a) A. J. Ragauskas, C. K. Williams, B. H. Davison, G. Britovsek, J. Cairney, C. A. Eckert, W. J. Frederick, J. P. Hallett, D. J. Leak and C. L. Liotta, *Science* **2006**, *311*, 484-489; b) W. Boerjan, J. Ralph and M. Baucher, *Annu. Rev. Plant Biol.* **2003**, *54*, 519-546; c) C. Xu, R. A. Arancon, J. Labidi and R. Luque, *Chem. Soc. Rev.* **2014**, *43*, 7485-7500; d) A. J. Ragauskas, G. T. Beckham, M. J. Biddy, R. Chandra, F. Chen, M. F. Davis, B. H. Davison, R. A. Dixon, P. Gilna, M. Keller, P. Langan, A. K. Naskar, J. N. Saddler, T. J. Tschaplinski, G. A. Tuskan and C. E. Wyman, *Science* **2014**, *344*, 1246843.

[16] S. Son and F. D. Toste, *Angew. Chem. Int. Ed.* **2010**, *49*, 3791-3794.

[17] a) N. Yan, C. Zhao, P. J. Dyson, C. Wang, L. T. Liu and Y. Kou, *ChemSusChem* **2008**, *1*, 626-629; b) H. Wang, M. Tucker and Y. Ji, *J. Appl. Chem.* **2013**, *2013*, 9; c) M. D. Karkas, B. S. Matsuura, T. M. Monos, G. Magallanes and C. R. J. Stephenson, *Org. Biomol. Chem.* **2016**, *14*, 1853-1914; d) H. Lange, S. Decina and C. Crestini, *Eur. Polym. J.* **2013**, *49*, 1151-1173; e) W.-J. Liu, H. Jiang and H.-Q. Yu, *Green Chem.* **2015**, *17*, 4888-4907; f) B. A. Simmons, D. Loqué and J. Ralph, *Curr. Opin. Plant Biol.* **2010**, *13*, 312-319.

[18] T. Parsell, S. Yohe, J. Degenstein, T. Jarrell, I. Klein, E. Gencer, B. Hewetson, M. Hurt, J. I. Kim, H. Choudhari, B. Saha, R. Meilan, N. Mosier, F. Ribeiro, W. N. Delgass, C. Chapple, H. I. Kenttamaa, R. Agrawal and M. M. Abu-Omar, *Green Chem.* **2015**, *17*, 1492-1499.

[19] D. R. Vardon, M. A. Franden, C. W. Johnson, E. M. Karp, M. T. Guarnieri, J. G. Linger, M. J. Salm, T. J. Strathmann and G. T. Beckham, *Energy Environ. Sci.* **2015**, *8*, 617-628.

[20] A. Rahimi, A. Azarpira, H. Kim, J. Ralph and S. S. Stahl, *J. Am. Chem. Soc.* **2013**, *135*, 6415-6418.

[21] M. Tien and T. K. Kirk, *Proc. Natl. Acad. Sci.* **1984**, *81*, 2280-2284.

[22] J. I. Hedges and J. R. Ertel, *Anal. Chem.* **1982**, *54*, 174-178.

[23] T. P. Schultz and M. C. Templeton, *Holzforschung* **1986**, *40*, 93-97.

[24] a) R. A. Sheldon and I. W. C. E. Arends, *J. Mol. Catal. A: Chem.* **2006**, *251*, 200-214; b) B. L. Ryland and S. S. Stahl, *Angew. Chem. Int. Ed. Engl.* **2014**, *53*, 8824-8838.

[25] a) B. Sedai, C. Díaz-Urrutia, R. T. Baker, R. Wu, L. A. P. Silks and S. K. Hanson, *ACS Catal.* **2013**, *3*, 3111-3122; b) B. Sedai and R. T. Baker, *Adv. Synth. Catal.* **2014**, *356*, 3563-3574.

[26] B. Sedai, C. Díaz-Urrutia, R. T. Baker, R. Wu, L. A. P. Silks and S. K. Hanson, *ACS Catal.* **2011**, *1*, 794-804.

[27] J. J. Bozell, B. R. Hames and D. R. Dimmel, *J. Org. Chem.* **1995**, *60*, 2398-2404.

[28] B. Biannic and J. J. Bozell, *Org. Lett.* **2013**, *15*, 2730-2733.

[29] T. J. Collins, *J. Acc. Chem. Res.* **2002**, *35*, 782-790.

[30] F. Napoly, L. Jean-Gérard, C. Goux-Henry, M. Draye and B. Andrioletti, *Eur. J. Org. Chem.* **2014**, *2014*, 781-787.

[31] J. Mottweiler, T. Rinesch, C. Besson, J. Buendia and C. Bolm, *Green Chem.* **2015**, *17*, 5001-5008.

[32] a) V. Alves, E. Capanema, C.-L. Chen and J. Gratzl, *J. Mol. Catal. A: Chem.* **2003**, *206*, 37-51; b) P. Zucca, G. Mocci, A. Rescigno and E. Sanjust, *J. Mol. Catal. A: Chem.* **2007**, *278*, 220-227; c) Y. Cui, C.-L. Chen, J. S. Gratzl and R. Patt, *J. Mol. Catal. A: Chem.* **1999**, *144*, 411-417.

[33] C. Zhu, W. Ding, T. Shen, C. Tang, C. Sun, S. Xu, Y. Chen, J. Wu and H. Ying, *ChemSusChem* **2015**, *8*, 1768-1778.

[34] A. Oasmaa and A. Johansson, *Energy Fuels* **1993**, *7*, 426-429.

[35] R. G. Harms, I. I. E. Markovits, M. Drees, h. c. m. W. A. Herrmann, M. Cokoja and F. E. Kühn, *ChemSusChem* **2014**, *7*, 429-434.

[36] E. M. Oltz, R. C. Bruening, M. J. Smith, K. Kustin and K. Nakanishi, *J. Am. Chem. Soc.* **1988**, *110*, 6162-6172.

[37] D. Rehder, *Coord. Chem. Rev.* **1999**, *182*, 297-322.

[38] J. O. Nriagu, *Vanadium in the Environment, Part 1: Chemistry and Biochemistry*, Wiley **1998**.

[39] A. Butler, M. J. Clague and G. E. Meister, *Chem. Rev.* **1994**, *94*, 625-638.

[40] R. R. Chowdhury, A. K. Crane, C. Fowler, P. Kwong and C. M. Kozak, *Chem. Commun.* **2008**, 94-96.

[41] A. Butler and J. V. Walker, *Chem. Rev.* **1993**, *93*, 1937-1944.

[42] H. Kneifel and E. Bayer, *Angew. Chem. Int. Ed. Engl.* **1973**, *12*, 508-508.

[43] J. W. van Schijndel, E. G. Vollenbroek and R. Wever, *Biochim. Biophys. Acta* **1993**, *1161*, 249-256.

[44] M. Xie, L. Gao, L. Li, W. Liu and S. Yan, *J. Inorg. Biochem.* **2005**, *99*, 546-551.

[45] G. Wilkinson, R. D. Gillard and J. A. McCleverty, *Comprehensive coordination chemistry : the synthesis, reactions, properties, and applications of coordination compounds*, Oxford, England, **1987**.

[46] W. Zhang and H. Yamamoto, *J. Am. Chem. Soc.* **2007**, *129*, 286-287.

[47] T. Hirao, *Coord. Chem. Rev.* **2003**, *237*, 271-279.

[48] E. M. Page, *Coord. Chem. Rev.* **1998**, *172*, 111-156.

[49] a) D. Rabinovich, *J. Chem. Educ.* **2000**, *77*, 311; b) M.-N. Collomb and A. Deronzier in *Manganese: Inorganic & Coordination Chemistry*, John Wiley & Sons, Ltd, **2011**.

[50] a) L. P. Hager, D. R. Morris, F. S. Brown and H. Eberwein, *J. Biol. Chem.* **1966**, *241*, 1769-1777; b) R. L. Richards in *Vanadium: Inorganic & Coordination Chemistry*, John Wiley & Sons, Ltd, **2006**; c) A. G. J. Ligtenbarg, R. Hage and B. L. Feringa, *Coord. Chem. Rev.* **2003**, *237*, 89-101; d) E. Amadio, R. Di Lorenzo, C. Zonta and G. Licini, *Coord. Chem. Rev.* **2015**, *301–302*, 147-162.

[51] a) H. Mimoun, L. Saussine, E. Daire, M. Postel, J. Fischer and R. Weiss, *J. Am. Chem. Soc.* **1983**, *105*, 3101-3110; b) H. Mimoun, M. Mignard, P. Brechot and L. Saussine, *J. Am. Chem. Soc.* **1986**, *108*, 3711-3718.

[52] D. L. Thorn, R. L. Harlow and N. Herron, *Inorg. Chem.* **1996**, *35*, 547-548.

[53] S. K. Hanson, R. T. Baker, J. C. Gordon, B. L. Scott and D. L. Thorn, *Inorg. Chem.* **2010**, *49*, 5611-5618.

[54] a) B. N. Wigington, M. L. Drummond, T. R. Cundari, D. L. Thorn, S. K. Hanson and S. L. Scott, *Chem. Eur. J.* **2012**, *18*, 14981-14988; b) S. K. Hanson and R. T. Baker, *Acc. Chem. Res.* **2015**, *48*, 2037-2048.

[55] S. K. Hanson, R. Wu and L. A. P. Silks, *Org. Lett.* **2011**, *13*, 1908-1911.

[56] A. T. Radosevich, C. Musich and F. D. Toste, *J. Am. Chem. Soc.* **2005**, *127*, 1090-1091.

[57] G. Zhang, B. L. Scott, R. Wu, L. P. Silks and S. K. Hanson, *Inorg. chem.* **2012**, *51*, 7354-7361.

[58] J. M. W. Chan, *ACS Catal.* **2013**, *3*, 1369-1377.

[59] a) F. Cui, T. Wijesekera, D. Dolphin, R. Farrell and P. Skerker, *J. Biotechnol.* **1993**, *30*, 15-26; b) M. Kuwahara, J. K. Glenn, M. A. Morgan and M. H. Gold, *FEBS Lett.* **1984**, *169*, 247-250; c) M. Shimada, T. Habe, T. Umezawa, T. Higuchi and T. Okamoto, *Biochem. Biophys. Res. Commun.* **1984**, *122*, 1247-1252; d) T. Habe, M. Shimada, T. Okamoto, B. Panijpan and T. Higuchi, *J. Chem. Soc., Chem. Commun.* **1985**, 1323-1324.

[60] a) M. Hofrichter, R. Ullrich, M. J. Pecyna, C. Liers and T. Lundell, *Appl. Microbiol. Biotechnol.* **2010**, *87*, 871-897; b) L. Pollegioni, F. Tonin and E. Rosini, *FEBS j.* **2015**, *282*, 1190-1213.

[61] a) C. Crestini, A. Pastorini and P. Tagliatesta, *J. Mol. Catal. A: Chem.* **2004**, *208*, 195-202; b) C. Crestini, A. Pastorini and P. Tagliatesta, *Eur. J. Inorg. Chem.* **2004**, *2004*, 4477-4483.

[62] D. Cedeno and J. J. Bozell, *Tetrahedron Lett.* **2012**, *53*, 2380-2383.

[63] a) C. Baleizao and H. Garcia, *Chem. Rev.* **2006**, *106*, 3987-4043; b) W. Zhang and E. N. Jacobsen, *J. Org. Chem.* **1991**, *56*, 2296-2298; c) W. Zhang, J. L. Loebach, S. R.

Wilson and E. N. Jacobsen, *J. Am. Chem. Soc.* **1990**, *112*, 2801-2803; d) D. Fernández, S. Riaño and L. Fadini, *O. Cat. J.* **2009**, 101-109.

[64] T. Hattori, M. Shimada, T. Umezawa, T. Higuchi, M. S. A. Leisola and A. Fiechter, *Agric. Biol. Chem.* **1988**, *52*, 879-880.

[65] W. Sun, H. Wang, C. Xia, J. Li and P. Zhao, *Angew. Chem. Int. Ed.* **2003**, *42*, 1042-1044.

[66] a) H. R. Mardani and H. Golchoubian, *Tetrahedron Lett.* **2006**, *47*, 2349-2352; b) H. Golchoubian and S. E. Babaei, *Chin. J. Catal.* **2010**, *31*, 615-618.

[67] G. González-Riopedre, M. I. Fernández-García, E. Gómez-Fórneas and M. Maneiro, *Catalysts* **2013**, *3*, 232-246.

[68] a) J. D. Ward and W. P. Nel, *Energy Policy* **2011**, *39*, 7464-7466; b) W. P. Nel, *Energy Environ.* **2011**, *22*, 859-876; c) M. Hook and X. Tang, *Energy Policy* **2013**, *52*, 797-809.

[69] M. Aresta, *Carbon Dioxide as Chemical Feedstock, ed.*, John Wiley & Sons, **2010**, 56-58.

[70] *Energy Information Administration (Official Energy Statistics from the U.S. Government (*http://www.eia.doe.gov/iea/*))*

[71] a) *British Petroleum BP Statistical Review of World Energy* **2010**, ; b) *Renewable, Global Status Report, Renewable Energy Policy Network for the 21st Century* **2006**,

[72] T. M. Lenton, *Climatic Change* **2006**, *76*, 7-29.

[73] a) T. Sakakura, J.-C. Choi and H. Yasuda, *Chem. Rev.* **2007**, *107*, 2365-2387; b) T. Sakakura and K. Kohno, *Chem. Commun.* **2009**, 1312-1330.

[74] a) D. J. Darensbourg, *Chem. Rev.* **2007**, *107*, 2388-2410; b) M. North, R. Pasquale and C. Young, *Green Chem.* **2010**, *12*, 1514-1539; c) S. N. Riduan and Y. Zhang, *Dalton*

Trans. **2010**, *39*, 3347-3357; d) S. Klaus, M. W. Lehenmeier, C. E. Anderson and B. Rieger, *Coord. Chem. Rev.* **2011**, *255*, 1460-1479; e) M. Cokoja, C. Bruckmeier, B. Rieger, W. A. Herrmann and F. E. Kuhn, *Angew. Chem., Int. Ed.* **2011**, *50*, 8510-8537; f) Y. Tsuji and T. Fujihara, *Chem. Commun.* **2012**, *48*, 9956-9964; g) D. J. Darensbourg and S. J. Wilson, *Green Chem.* **2012**, *14*, 2665-2671; h) I. Omae, *Coord. Chem. Rev.* **2012**, *256*, 1384-1405; i) N. Kielland, C. J. Whiteoak and A. W. Kleij, *Adv. Synth. Catal.* **2013**, *355*, 2115-2138.

[75] D. H. Gibson, *Chem. Rev.* **1996**, *96*, 2063-2096.

[76] a) L.-N. He, J.-Q. Wang and J.-L. Wang, *Pure Appl. Chem.* **2009**, *81*, 2069-2080; b) M. Mikkelsen, M. Jørgensen and F. C. Krebs, *Energy Environ. Sci.* **2010**, *3*, 43-81; c) C. Maeda, Y. Miyazaki and T. Ema, *Catal. Sci. Technol.* **2014**, *4*, 1482-1497.

[77] a) http://www.chemicals-technology.com/projects/george-olah-renewable-methanol-plant-iceland/, ; b) M. Aresta and A. Dibenedetto, *Dalton Trans.* **2007**, 2975-2992; c) N. MacDowell, N. Florin, A. Buchard, J. Hallett, A. Galindo, G. Jackson, C. S. Adjiman, C. K. Williams, N. Shah and P. Fennell, *Energy Environ. Sci.* **2010**, *3*, 1645-1669.

[78] a) M. Bogey, C. Demuynck, J. L. Destombes and A. Krupnov, *J. Mol. Struct.* **1988**, *190*, 465-474; b) K. Hammami, N. Jaidane, Z. Ben Lakhdar, A. Spielfiedel and N. Feautrier, *J. Chem. Phys.* **2004**, *121*, 1325-1330; c) M. Sodupe, V. Branchadell, M. Rosi and C. W. Bauschlicher, *J. Phys. Chem. A* **1997**, *101*, 7854-7859; d) N. R. Walker, R. S. Walters and M. A. Duncan, *J. Chem. Phys.* **2004**, *120*, 10037-10045; e) G. Gregoire and M. A. Duncan, *J. Chem. Phys.* **2002**, *117*, 2120-2130; f) J. B. Griffin and P. B. Armentrout, *J. Chem. Phys.* **1997**, *106*, 4448-4462; g) B. L. Tjelta, D. Walter and P. B. Armentrout, *Int. J. Mass. Spectrom.* **2001**, *204*, 7-21; h) N. R. Walker, R. S. Walters, G. A. Grieves and M. A. Duncan, *J. Chem. Phys.* **2004**, *121*, 10498-10507; i) J. Herman, J. D. Foutch and G. E. Davico, *J. Phys. Chem. A* **2007**, *111*, 2461-2468.

[79] S. L. Suib, *New and future developments in catalysis: activation of carbon dioxide*, Newnes, **2013**.

[80] K. I. Vol'pin ME, Lobeeva TS., *Russ. Chem. Bull.* **1969**, *20*, 192.

[81] J. K. Jolly PW, Kruger C, Tsay Y-H., *J. Organomet.Chem.* **1971**, *109*,

[82] a) M. Aresta, C. F. Nobile, V. G. Albano, E. Forni and M. Manassero, *J. Chem. Soc. Chem. Commun.* **1975**, 636-637; b) T. Kégl, R. Ponec and L. Kollár, *J. Phys. Chem. C.* **2011**, *115*, 12463-12473; c) L. Contreras, M. Paneque, M. Sellin, E. Carmona, P. J. Pérez, E. Gutiérrez-Puebla, A. Monge and C. Ruiz, *New J. Chem.* **2005**, *29*, 109-115; d) G. S. Bristow, P. B. Hitchcock and M. F. Lappert, *J. Chem. Soc. Chem. Commun.* **1981**, 1145-1146; e) X. Yin and J. R. Moss, *Coord. Chem. Rev.* **1999**, *181*, 27-59; f) D. H. Gibson, *Coord. Chem. Rev.* **1999**, *185*, 335-355.

[83] a) J. Calabrese, T. Herskovitz and J. Kinney, *J. Am. Chem. Soc.* **1983**, *105*, 5914-5915; b) K. Tanaka and D. Ooyama, *Coord. Chem. Rev.* **2002**, *226*, 211-218.

[84] a) I. Castro-Rodriguez, H. Nakai, L. N. Zakharov, A. L. Rheingold and K. Meyer, *Science* **2004**, *305*, 1757; b) O. P. Lam, C. Anthon and K. Meyer, *Dalton Trans.* **2009**, 9677-9691.

[85] a) C. H. Lee, D. S. Laitar, P. Mueller and J. P. Sadighi, *J. Am. Chem. Soc.* **2007**, *129*, 13802-13803; b) X.-J. Hou, P. He, H. Li and X. Wang, *J. Phys. Chem. C* **2013**, *117*, 2824-2834; c) P. D. C. Dietzel, R. E. Johnsen, H. Fjellvag, S. Bordiga, E. Groppo, S. Chavan and R. Blom, *Chem. Commun.* **2008**, 5125-5127; d) C. C. Chang, M. C. Liao, T. H. Chang, S. M. Peng and G. H. Lee, *Angew. Chem. Int. Ed. Engl.* **2005**, *44*, 7418-7420.

[86] a) K. B. Beyer, W.; Berndt, W.; Carlton, W.; Hoffmann, D.; Schroeter, A.; Shank, R., *J. Am. Coll. Toxicol.* **1987**, *6*, 23; b) M. Yoshida and M. Ihara, *Chem. Eur. J.* **2004**, *10*, 2886-2893.

[87] P. Lenden, P. M. Ylioja, C. Gonzalez-Rodriguez, D. A. Entwistle and M. C. Willis, *Green Chem.* **2011**, *13*, 1980-1982.

[88] V. Aravindan, J. Gnanaraj, S. Madhavi and H. K. Liu, *Chem. Eur. J.* **2011**, *17*, 14326-14346.

[89] B. Nohra, L. Candy, J.-F. Blanco, C. Guerin, Y. Raoul and Z. Mouloungui, *Macromolecules* **2013**, *46*, 3771-3792.

[90] S. Fukuoka, M. Kawamura, K. Komiya, M. Tojo, H. Hachiya, K. Hasegawa, M. Aminaka, H. Okamoto, I. Fukawa and S. Konno, *Green Chem.* **2003**, *5*, 497-507.

[91] H. Yue, Y. Zhao, X. Ma and J. Gong, *Chem. Soc. Rev.* **2012**, *41*, 4218-4244.

[92] B. Schäffner, F. Schäffner, S. P. Verevkin and A. Börner, *Chem. Rev.* **2010**, *110*, 4554-4581.

[93] R. A. Davis, V. Andjic, M. Kotiw and R. G. Shivas, *Phytochem.* **2005**, *66*, 2771-2775.

[94] J. Y. Gauthier, Y. Leblanc, W. Cameron Black, C.-C. Chan, W. A. Cromlish, R. Gordon, B. P. Kennedey, C. K. Lau, S. Léger, Z. Wang, D. Ethier, J. Guay, J. Mancini, D. Riendeau, P. Tagari, P. Vickers, E. Wong, L. Xu and P. Prasit, *Bioorg. Med. Chem. Lett.* **1996**, *6*, 87-92.

[95] J. H. Clements, *Ind. Eng. Chem. Res.* **2003**, *42*, 663-674.

[96] W. J. Peppel, *Ind. Eng. Chem. Res.* **1958**, *50*, 767-770.

[97] a) S. Inoue, H. Koinuma and T. Tsuruta, *Macromol. Chem. Phys.* **1969**, *130*, 210-220; b) M. Kobayashi, S. Inoue and T. Tsuruta, *Macromolecules* **1971**, *4*, 658-659.

[98] a) X.-B. Lu and D. J. Darensbourg, *Chem. Soc. Rev.* **2012**, *41*, 1462-1484; b) G. Odian, *Principles of polymerization*, John Wiley & Sons, New Jersey, **2004**, 79.

[99] a) M. Kobayashi, S. Inoue and T. Tsuruta, *J. Polym. Sci., Part A: Polym. Chem.* **1973**, *11*, 2383-2385; b) S. Inoue, M. Kobayashi, H. Koinuma and T. Tsuruta, *Makromol. Chem.* **1972**, *155*, 61-73.

[100] Q. He, J. W. O'Brien, K. A. Kitselman, L. E. Tompkins, G. C. T. Curtis and F. M. Kerton, *Catal. Sci. Tech.* **2014**, *4*, 1513-1528.

[101] B. Chatelet, L. Joucla, J. P. Dutasta, A. Martinez, K. C. Szeto and V. Dufaud, *J. Am. Chem. Soc.* **2013**, *135*, 5348-5351.

[102] a) K. M. Doll and S. Z. Erhan, *Green Chem.* **2005**, *7*, 849-854; b) H. Kawanami and Y. Ikushima, *Chem. Commun.* **2000**, 2089-2090.

[103] N. Ishida, Y. Shimamoto and M. Murakami, *Angew. Chem. Int. Ed.* **2012**, *51*, 11750-11752.

[104] M. R. Kember, A. Buchard and C. K. Williams, *Chem. Commun.* **2011**, *47*, 141-163.

[105] M. North, M. Omedes-Pujol and C. Williamson, *Chem. Eur. J.* **2010**, *16*, 11367-11375.

[106] a) W.-M. Ren, G.-P. Wu, F. Lin, J.-Y. Jiang, C. Liu, Y. Luo and X.-B. Lu, *Chem. Sci.* **2012**, *3*, 2094-2102; b) F. Jutz, J.-M. Andanson and A. Baiker, *Chem. Rev.* **2010**, *111*, 322-353.

[107] P. P. Pescarmona and M. Taherimehr, *Catal. Sci. Technol.* **2012**, *2*, 2169-2187.

[108] S. Ghazali-Esfahani, H. Song, E. Paunescu, F. D. Bobbink, H. Liu, Z. Fei, G. Laurenczy, M. Bagherzadeh, N. Yan and P. J. Dyson, *Green Chem.* **2013**, *15*, 1584-1589.

[109] T. Kagiya and T. Matsuda, *Polym. J.* **1971**, *2*, 398-406.

[110] A. Decortes, M. Martinez Belmonte, J. Benet-Buchholz and A. W. Kleij, *Chem. Commun.* **2010**, *46*, 4580-4582.

[111] F. Castro-Gomez, G. Salassa, A. W. Kleij and C. Bo, *Chem. Eur. J.* **2013**, *19*, 6289-6298.

[112] Y.-M. Shen, W.-L. Duan and M. Shi, *J. Org. Chem.* **2003**, *68*, 1559-1562.

[113] a) W.-L. Dai, S.-L. Luo, S.-F. Yin and C.-T. Au, *Appl. Catal. A* **2009**, *366*, 2-12; b) N. A. M. Razali, K. T. Lee, S. Bhatia and A. R. Mohamed, *Renew. Sust. Energ. Rev.* **2012**, *16*, 4951-4964.

[114] a) K. Barnese, E. B. Gralla, J. S. Valentine and D. E. Cabelli, *Proc. Natl. Acad. Sci. U. S. A.* **2012**, *109*, 6892-6897; b) A. S. Tracey and D. C. Crans, *Vanadium compounds: chemistry, biochemistry, and therapeutic applications*, ACS Publications, **1998**.

[115] T. Bok, E. K. Noh and B. Y. Lee, *Bull. Korean Chem. Soc.* **2006**, *27*, 1171-1174.

[116] D. J. Darensbourg, A. Horn Jr and A. I. Moncada, *Green Chem.* **2010**, *12*, 1376-1379.

[117] A. Coletti, C. J. Whiteoak, V. Conte and A. W. Kleij, *Chem. Cat. Chem.* **2012**, *4*, 1190-1196.

[118] D. Bai, Z. Zhang, G. Wang and F. Ma, *Appl. Organomet. Chem.* **2015**, *29*, 240-243.

[119] C. Miceli, J. Rintjema, E. Martin, E. C. Escudero-Adán, C. Zonta, G. Licini and A. W. Kleij, *ACS Catal.* **2017**, 2367-2373.

[120] D. J. Darensbourg and E. B. Frantz, *Inorg. Chem. Commun.* **2007**, *46*, 5967-5978.

[121] D. J. Darensbourg and E. B. Frantz, *Inorg. Chem.* **2008**, *47*, 4977-4987.

[122] P. G. Cozzi, *Chem. Soc. Rev.* **2004**, *33*, 410-421.

[123] A. Heckel and D. Seebach, *Helv. Chim. Acta* **2002**, *85*, 913-926.

[124] D. J. Darensbourg, R. M. Mackiewicz, A. L. Phelps and D. R. Billodeaux, *Acc. Chem. Res.* **2004**, *37*, 836-844.

[125] D. J. Darensbourg and J. C. Yarbrough, *J. Am. Chem. Soc.* **2002**, *124*, 6335-6342.

[126] F. Jutz, J.-D. Grunwaldt and A. Baiker, *J. Mol. Catal. A: Chem.* **2008**, *279*, 94-103.

[127] F. Jutz, J.-D. Grunwaldt and A. Baiker, *J. Mol. Catal. A: Chem.* **2009**, *297*, 63-72.

[128] a) G. A. Luinstra, G. R. Haas, F. Molnar, V. Bernhart, R. Eberhardt and B. Rieger, *Chem. Eur. J.* **2005**, *11*, 6298-6314; b) D. J. Darensbourg, R. M. Mackiewicz, J. L. Rodgers, C. C. Fang, D. R. Billodeaux and J. H. Reibenspies, *Inorg. Chem.* **2004**, *43*, 6024-6034; c) X.-B. Lu and Y. Wang, *Angew. Chem. Int. Ed.* **2004**, *43*, 3574-3577.

CHAPTER 2

2 Vanadium aminophenolate complexes and their catalytic activity in aerobic and H_2O_2-mediated oxidation reactions

A version of this chapter has been published Ali Elkurethi, Andrew G. Walsh, Louise N. Dawe and Francesca M. Kerton *Eur. J. Inorg. Chem*., **2016**, 3123–3130

Some modifications were made to the original paper for inclusion as a chapter in this thesis.

2.1 Introduction

Nowadays, chemistry related to biomass (in particular, lignocellulose) is of significant interest because of the desire for renewable chemical and fuel production.[1] This has been brought about for a number of reasons including political conflicts, and the negative effects of petroleum on the environment and the advantages of renewable resources, such as their abundance, sustainability and often low cost. Among the three components of lignocellulose (cellulose, hemicellulose, and lignin), a large amount of research has been directed towards biofuel production (e.g. ethanol) from cellulose.[2],[3],[4],[5],[6],[7] In contrast, the utilization of lignin as a feedstock has been hampered due to lignin's structural complexity, which leads to challenges in its use as a feedstock.[8],[9] Further detail on this complexity can be found in Chapter 1 of this thesis (section 1.1.3). The development of new homogeneous catalysts to depolymerize lignin in a selective fashion may lead to efficient conversion technologies, which could provide lignin-derived aromatic feedstocks for chemical production.[10] Many of these catalysts perform aerobic oxidation or H_2O_2-mediated C-O bond cleavage reactions.

Recently, the field of aerobic oxidation catalysis has grown significantly as the search for new green oxidation processes continues. Many 3*d* transition metals (V, Mo, Fe, Cu) are attractive in terms of their abundance and low cost as the active centers for aerobic oxidation processes.[9],[11] In particular, vanadium complexes are well known as

an attractive class of catalysts,[12] mediating the aerobic oxidation of organic substrates including benzylic, allylic, and propargylic alcohols.[10b, 13] A growing number of vanadium(IV) and (V) complexes of multidentate N-O donor ligands including bis(phenolate) pyridine and amino-bis(phenolate) ligands have been reported as very active catalysts for C−O and C−C bond cleavage reactions in model compounds of lignin, which show a significant diversity of reactivity.[8a, 13a, 14] These were discussed in more detail in Chapter 1 of this thesis (section 1.1.5).

In this chapter, I describe the syntheses and structures of amino-bis(phenolate) vanadyl complexes containing tetradentate tripodal ligands $[ONOL]^{RR'}$ where L is a neutral N or O-containing donor group and R/R' are alkyl groups found in the *ortho* and *para* positions of the phenolate donor. I also report their use as catalysts for the aerobic oxidation of alcohols and C–O bond cleavage reactions in simple lignin model compounds, and compare these results with related systems in the scientific literature.

2.2 Results and Discussion

The amine-bis(phenol) protio ligands $H_2[O_2NO]^{BuMeMeth}$, $H_2[ON_2O]^{BuMe}$, $H_2[O_2NN]^{BuBuPy}$, and $H_2[O_2NO]^{BuBuFurf}$ were prepared according to previously reported procedures.[15] All ligands contain 2,4-alkyl-substituted phenols but contain different pendant donor groups (methoxy, pyridyl and furfuryl), or two tertiary amines situated in the backbone of the ligand. V(V) complexes **2.1**-**2.4** were synthesized *via* reaction of the protonated ligands in methanol with $VO(acac)_2$ for 24 h, affording dark black, purple or blue solids complex in 70-85% yield Scheme 2-1 and Scheme 2-2. The methoxide ligand is apparent in the NMR and MALDI-TOF mass spectra of the crude and purified products. In some cases, the compounds decompose upon recrystallization to form oxo-bridged complexes Scheme 2-1. Related oxo-bridged complexes have been prepared by others.[12e] **2.1**-**2.4** were characterized using ^{1}H NMR spectroscopy, MALDI-TOF mass spectrometry, X-ray crystallography, UV-vis spectroscopy and elemental analysis (see Appendix 2 for spectra). The absence of acetylacetonate ligands was confirmed by FT-IR spectroscopy. The ^{1}H NMR spectra of **2.1**-**2.4** contain the expected signals typical of

diamagnetic transition metal aminophenolate complexes. They also all contain a diagnostic signal close to δ 5.00, which was assigned to the methoxide ligand (δ 5.30, 5.05, 4.89, 5.33 for complexes **2.1-2.4** respectively).

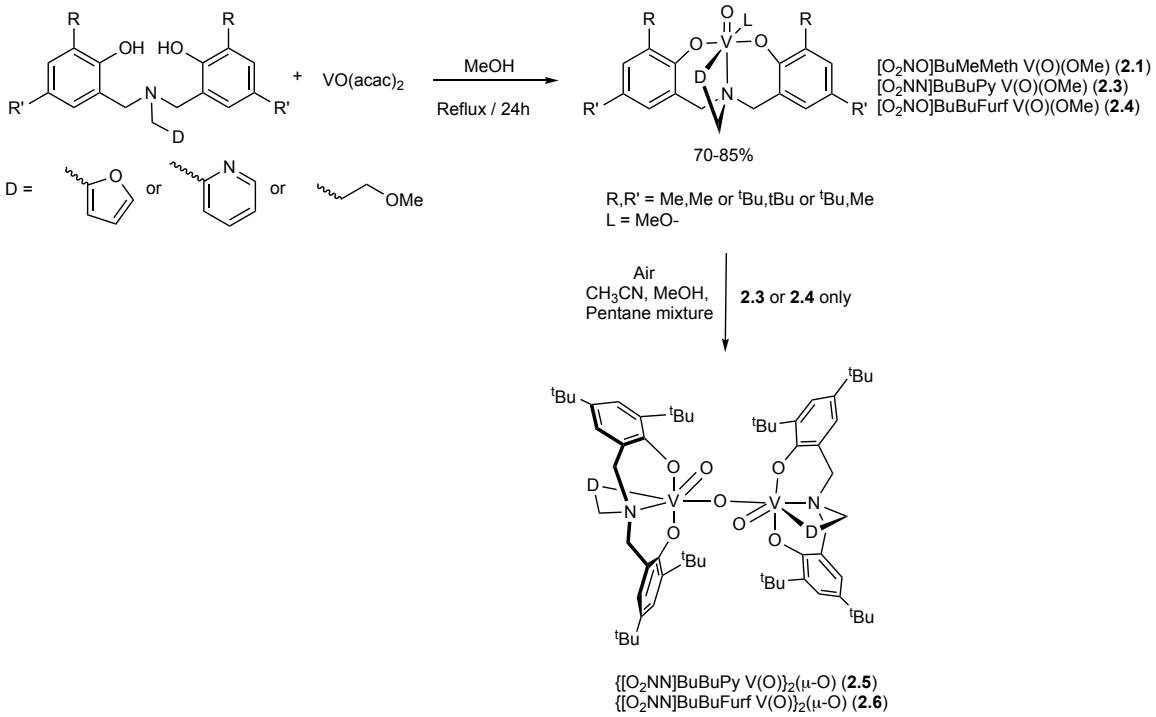

Scheme 2-1. Synthesis of vanadium complexes (**2.1**, **2.3**, and **2.4**) and oxo-bridged complexes (**2.5** and **2.6**)

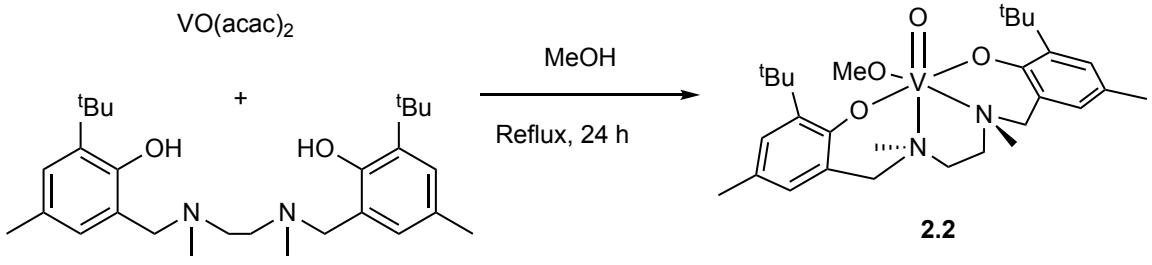

Scheme 2-2. Synthesis of vanadium complex **2.2**

The MALDI-TOF mass spectra were obtained via charge transfer ionization in the presence of the neutral UV-absorbent matrix, anthracene.[16],[17] The mass spectra generated for the V(V) complexes described herein showed characteristic fragment ions. In particular they exhibited $\{[O_2NO]^{BuMeMeth}\ V{=}O\}^{+\cdot}$ (**2.1**), $\{[ON_2O]^{BuMe}\ V{=}O\}^{+\cdot}$ (**2.2**), $\{[O_2NN]^{BuBuPy}\ V{=}O\}^{+\cdot}$ (**2.3**), $\{[O_2NO]^{BuBuFurf}\ V{=}O\}^{+\cdot}$ (**2.4**) fragments at *m/z* 492.16, 505.20, 609.24 and 602.25 respectively. The experimental isotopic distribution pattern for each of these ions shows good agreement with the theoretical patterns (Figures A1.1-A1.4). Additional peaks in the lower mass region of the spectra correspond to ligand fragments. For the oxo-bridged complexes (**2.5** and **2.6**), there are small peaks at *m/z* 1234.6 and 1212.6, which correspond to their respective molecular ions.

Electronic absorption spectra of complexes (**2.1**-**2.4**) in CH_2Cl_2 show multiple bands in the UV and visible regions (Table 2-1 and Figures A1.6- A1.9). The highest energy bands (<300 nm) result from ligand $\pi \rightarrow \pi^*$ transitions. Other intense bands also present in the UV region (300–350 nm) were assigned to charge-transfer from the out-of-plane $p\pi$ orbital (HOMO) of the phenolate oxygen to the empty d_{x2-y2}/d_{z2} orbitals of the V center. The lowest energy bands (visible region) arise from charge-transfer transitions from the in-plane π orbital of the phenolate to the empty d orbitals on V.

Table 2-1. UV–Vis spectral data of the vanadium complexes in CH_2Cl_2

Complex	$\pi \rightarrow \pi^*$	out-of-plane $p\pi \rightarrow d$	in-plane $p\pi \rightarrow d$
	λ /nm(ε/L $mol^{-1}cm^{-1}$)	λ/nm(ε/L $mol^{-1}cm^{-1}$)	λ /nm (ε/L $mol^{-1}cm^{-1}$)
2.1	248(10900)	276 (115000)	684 (34000)
2.2	243 (99000)	252 (92000)	601 (56000)
2.3	240 (98570)	275 (105000)	594 (10250)
2.4	240 (105000)	278(115000)	603 (47500)

Single crystals suitable for X-ray analysis were obtained after several weeks from a saturated methanol solution cooled to −20 °C (**2.1**, **2.2**) or a mixture of methanol, pentane and acetonitrile stored at 6 °C (**2.3**, **2.4**). ORTEP drawings are shown in Figure 2.1-Figure 2.4 with selected bond distances and angles given in Table 2-2.

Table 2-2. Selected Bond Lengths (Å) and Angles (°) for **2.1**, **2.2**, **2.5** and **2.6**

	2.1	**2.2**	**2.5**	**2.6**
V(1)−N(1)	2.244(2)	2.272(4)	2.377(3)	2.344(2)
V(1)−N(2)		2.355(4)	2.243(3)	
V(1)−O(1)	1.8994(20)	1.858(3)	1.865(3)	1.8576(18)
V(1)−O(2)	1.8860(18)	1.878(3)	1.896(3)	1.8525(18)
V(1)−O(3)	2.2567(16)	1.579(4)	1.620(3)	2.1655(19)
V(1)−O(4)	1.5851(16)	1.766(3)	1.8071(7)	1.7737(4)
V(1)−O(5)	1.7923(20)			1.6052(17)
O(1)−V(1)−O(2)	159.78(7)	164.06(15)	165.16(12)	164.71(8)
O(1)−V(1)−O(3)	83.68(7)	97.32(16)	94.86(14)	84.75(8)
O(2)−V(1)−O(3)	83.95(6)	94.00(15)	95.22(13)	83.75(8)
O(4)−V(1)−O(1)	95.16(9)	93.88(13)	94.79(9)	93.66(6)
O(4)−V(1)−O(2)	94.91(7)	93.62(14)	92.71(9)	94.26(6)
O(3)−V(1)−O(4)	172.13(8)	106.49(18	106.69(10)	162.40(5)
O(1)−V(1)−N(1)	83.35(7)	80.61(12)	83.25(12)	83.89(7)
O(2)−V(1)−N(1)	77.86(8)	87.85(12)	84.35(11)	83.08(7)
O(3)−V(1)−N(1)	73.65(7)	91.94(17)	166.04(13)	72.56(7)
O(4)−V(1)−N(1)	98.49(9)	161.33(17)	87.27(8)	89.83(5)
O(1)−V(1)−O(5)	97.79(7)			94.78(9)
O(2)−V(1)−O(5)	96.54(9)			95.59(9)
O(3)−V(1)−O(5)	83.20(7)			91.71(8)
O(4)−V(1)−O(5)	104.67(9)			105.90(7)
N(1)−V(1)−O(5)	156.59(7)			164.27(8)
O(1)−V(1)−N(2)		80.61(12)	87.44(12)	
O(2)−V(1)−N(2)		82.63(14)	81.22(12)	
O(3)−V(1)−N(2)		167.28(16)	92.80(13)	
O(4)−V(1)−N(2)		86.00(15)	160.09(10)	
N(2)−V(1)−N(1)		75.73(14)	73.33(12)	

The solid-state structures of **2.1** and **2.2** (VNO_5) and (VN_2O_4) confirm that the V^V centers reside in distorted octahedral environments. For **2.1** O(1)−V(1)−O(2), O(3)−V(1)−O(4) and N(1)−V(1)−O(5) angles are 159.78(7)°, 172.13(8)°, and 156.59(7)° respectively; for (**2.2**), O(1)−V(1)−O(2), O(4)−V(1)−N(1), and O(3)−V(1)−N(2), angles are 164.06(15)°, 161.33(17)° and 167.28(16)° respectively. The phenolate oxygen atoms are *trans* orientated for (**2.1** and **2.2**) with V(1)–O(1) distances, 1.899(20) and 1.858(3) Å and V(1)–O(2), distances, 1.886(18) and 1.878(3) Å respectively. The N1 atom in (**2.1**) is *trans* to the methoxide oxygen O(5) and *cis* to the oxo atom O(4). In (**2.2**), the methoxide bond (V−O4) is slightly shorter than the corresponding bond in (**2.1**) (V−O5). This might be due to steric considerations when the orientation of the *tert*-butyl groups are taken into account. The longer V(1)−O(3) distance in (**2.1**) (2.2567(16) Å) implies weak binding of the ether group in the sidearm to the vanadium, and also reflects the *trans* effect of the oxo group, as has been observed in other complexes.[18] The $V-O_{phenolate}$ distances are within the values that have been observed for these types of complexes previously.[18-19]

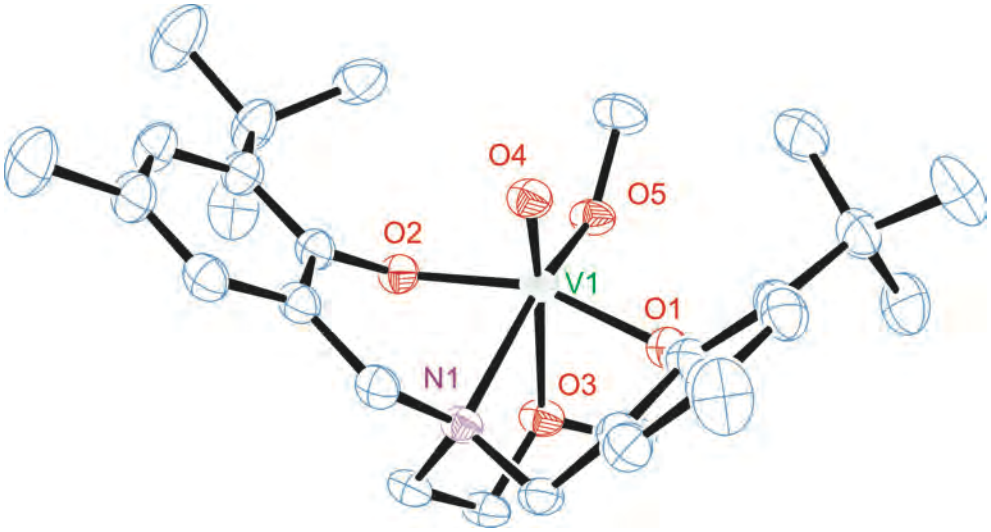

Figure 2.1. X-ray structure of (**2.1**) (thermal ellipsoids at 50% probability, H atoms omitted for clarity)

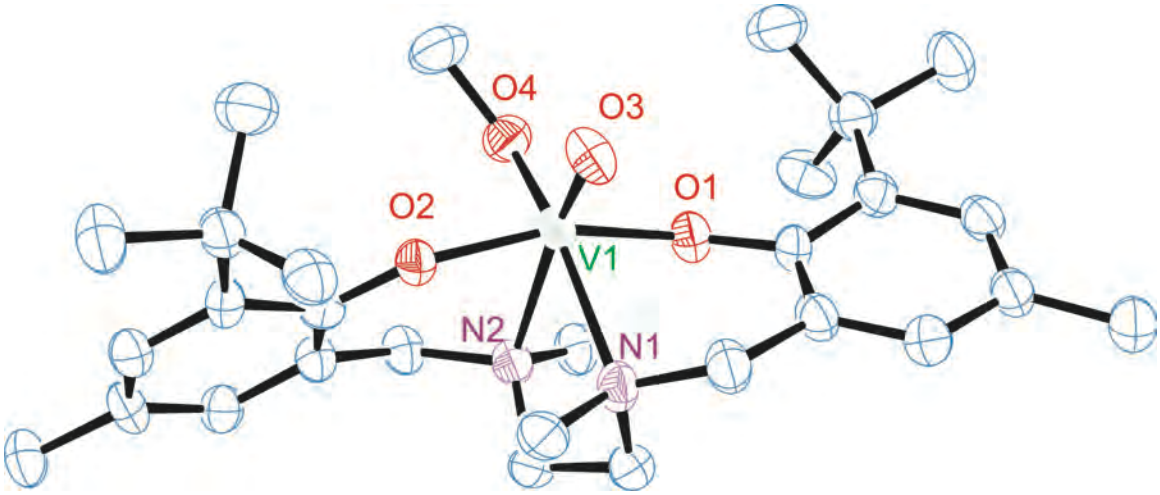

Figure 2.2. X-ray structure of (**2.2**) (thermal ellipsoids at 50% probability, H atoms omitted for clarity)

Upon recrystallization in air, (**2.3** and **2.4**) formed oxo-bridged complexes. The solid-state structures of the resulting compounds (**2.5** and **2.6**) confirm that the V^V centers reside in distorted octahedral environments Figure 2.3 and Figure 2.4. Although only small amounts of (**2.5** and **2.6**) were obtained, mass spectrometric and elemental analytical data confirmed their formulation. In (**2.5**), O(1)−V(1)−O(2), O(3)−V(1)−N(1) and N(2)−V(1)−O(4) angles are 165.16(12)°, 166.04(13)°, and 160.09(10)° respectively; in (**2.6**), O(1)−V(1)−O(2), O(4)−V(1)−O(3), and O(5)−V(1)−N(1), angles are 164.71(8)°, 162.40(5)° and 164.27(8)° respectively. For (**2.5**) atoms O(1), O(2), N(2), and O(4) lie in the plane and *cis* to the terminal oxo O(3) group and the nitrogen atom N(1), and for (**2.6**) atoms O(1), O(2), O(3), and O(4) lie in the plane and are *cis* to the terminal oxo O(5) group and the nitrogen atom N(1). The two vanadium centers are linked by a linear V−O−V bridge; both complexes (**2.5** and **2.6**) have nearly identical vanadium-oxo bond distances, which are longer than in a similar complex.[19] The terminal V=O bond distance for both complexes are also consistent, but moderately shorter than the values that were reported for similar complexes.[19] The $V-O_{phenolate}$ distances are in agreement with those of (**2.1**, **2.2**) and with those observed in related

complexes.[18-19] Unfortunately, we were not able to isolate sufficient quantities of (**2.5** and **2.6**) to study in detail their behaviour in subsequent catalytic reactions.

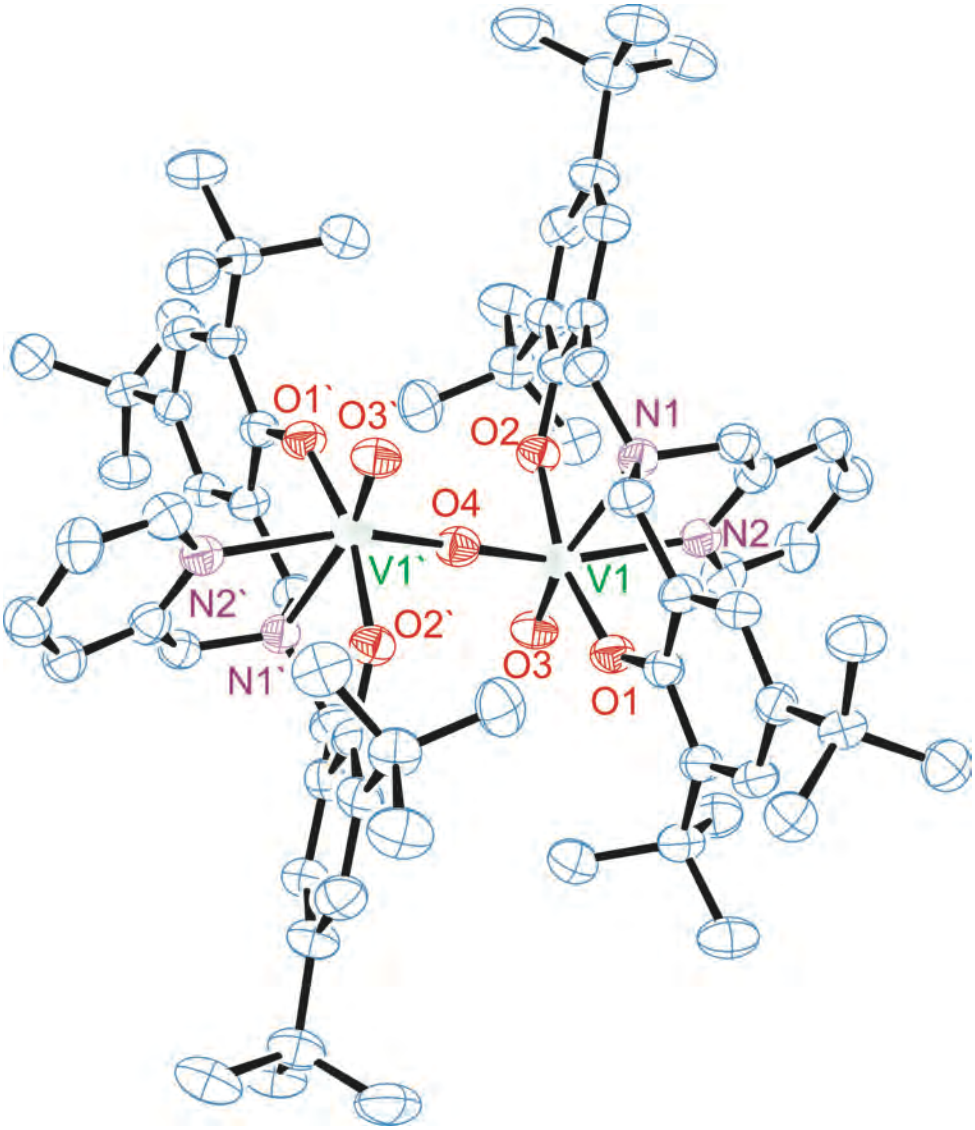

Figure 2.3. X-ray structure of **2.5** (thermal ellipsoids at 50% probability, H atoms omitted for clarity)

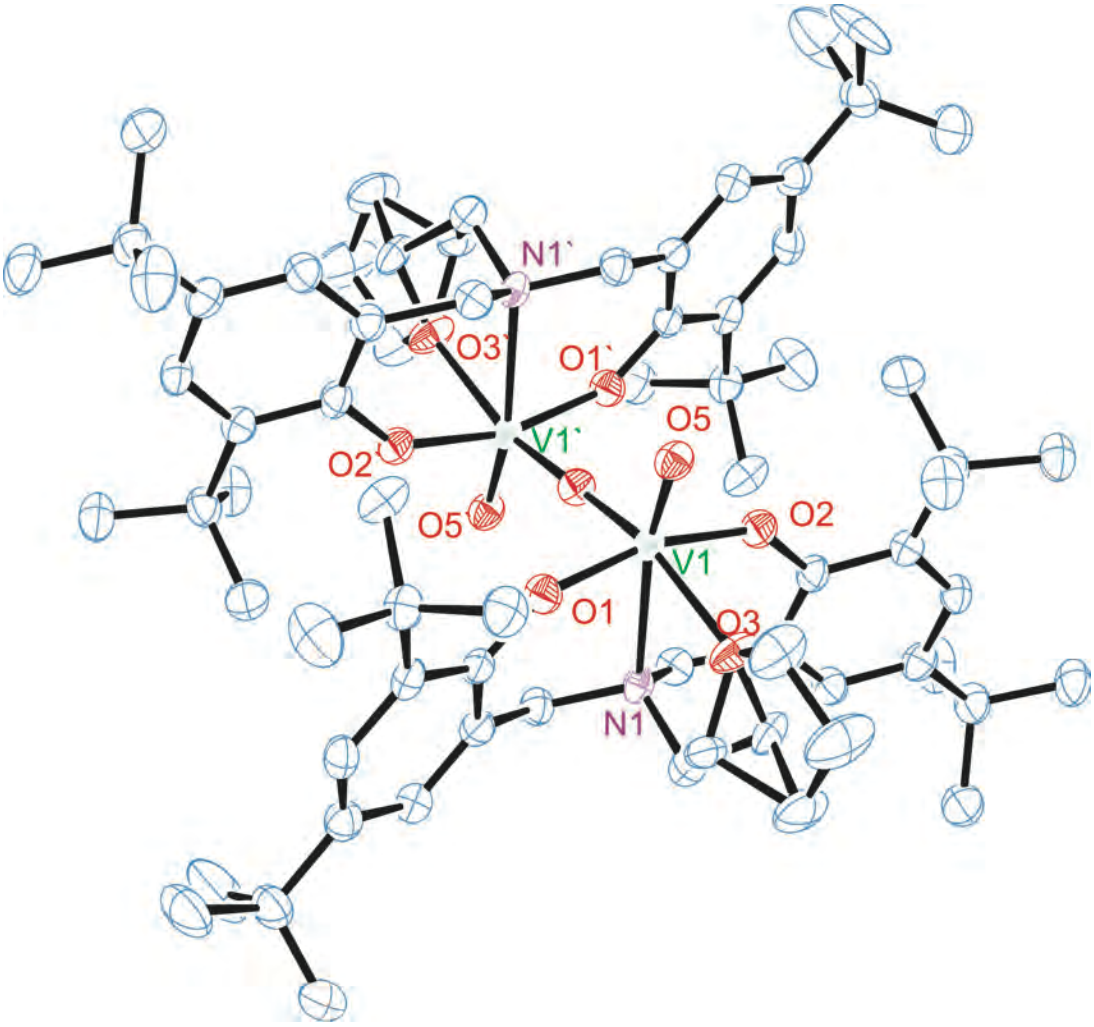

Figure 2.4. X-ray structure of **2.6** (thermal ellipsoids at 50% probability, H atoms omitted for clarity)

2.3 Catalytic Performance

2.3.1 Catalytic aerobic oxidation of *p*-methoxybenzylalcohol

Inspired by the recent results obtained by the group of Hanson,[13a] complexes (**2.1**-**2.4**) were screened for their activity in the aerobic oxidation of 4-methoxybenzyl alcohol at several different temperatures 80-140 °C using toluene as the solvent in the absence of a base additive. We postulated that in the case of **2.3** the pendant pyridyl group might act as an internal base. No significant oxidation of the substrate was observed under the following conditions: 0.5 mmol of alcohol, 2 mol% of V (**2.1**-**2.4**), in toluene-d_8 100 °C (Table 2-3, entry 1). However, addition of a base (NEt_3) facilitated the oxidation of 4-methoxybenzyl alcohol with conversions of up to 90% (Table 2-3, entry 2). It should be noted that at shorter reaction times there was little difference in activities between the four complexes studied. They all achieved approximately 30% conversion in 12 h. This suggests that complexes (**2.3** and **2.4**), which give lower conversions after 72 h compared with (**2.1** and **2.2**), are less stable catalysts. Based on the structures described above, we propose that they decompose to form catalytically inactive oxo-bridged compounds such as (**2.5** and **2.6**). Mechanisms proposed to date indicate that metal-alkoxide bonds are crucial in these reactions,[20] and these bonds do not exist in oxo-complexes (**2.5** and **2.6**). Increasing the reaction temperature from 80 to 100 °C led to moderate improvements in conversion (100%, 93% for (**2.1** and **2.2)**, respectively, after 60 h under air in toluene, (Table 2-3, entry 3). Data for the reactions at 140 °C is also reported (Table 2-3, entry 4) and similar conversions can be achieved after 36 h. A control reaction with 4-methoxybenzyl alcohol and base only (no vanadium) in toluene-d_8 under air showed no reaction when heated at 140 °C for 3 days. Reactions were also performed in acetonitrile-d_3, as it is a widely used solvent in oxidation chemistry. Conversion levels in this, even at longer reaction times, were significantly lower than in toluene (Table 2-3, entry 5). **(2.1** and **2.2**) are slightly less reactive than related compounds (**1.16**, **1.22** and **1.23**) previously studied by Hanson and co-workers (up to 99%, 60-80 °C, 24-48 h) respectively.[13a, 14c] These differences in activities are likely associated with the donor ability of the pendant group.

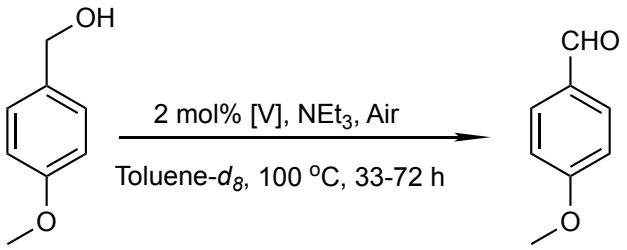

Scheme 2-3. Catalytic aerobic oxidation of *p*-methoxybenzylalcohol using vanadium complexes

Table 2-3. Aerobic oxidation of 4-methoxybenzylalcohol using vanadium complexes (**2.1** -**2.4**) [a]

Entry	Additive	T (^{o}C)	Time (h)	Conversion (%) [b]
1	none	80	72	trace (**2.1** -**2.4**)
2	NEt_3	80	72	(**2.1**) 90 (**2.2**) 85 (**2.3**) 70 (**2.4**) 75
3	NEt_3	100	60	(**2.1**) 100 (**2.2**) 93 (**2.3**) 77 (**2.4**) 85
4	NEt_3	140	36	(**2.1**) 100 (**2.2**) 100 (**2.3**) 84 (**2.4**) 95
5 [c]	NEt_3	120	106	(**2.1**) 52
6	NEt_3	80	65	(**1.22**) 99 (**1.23**) 80[13a]
7	NEt_3	60	24	(**1.16**) 99[21]

[a] Conditions: 2 mol% of (**2.1**, **2.2**, **2.3** or **2.4**), 10 mol% additive, in toluene-d_8. Vanadium complex identified in parentheses. [b] Conversion determined by ^{1}H NMR spectroscopy. [c] In acetonitrile-d_3. Two sets of conversion data in this table represent those reported by other researchers in this field and thus citations are provided

We propose that our homogeneous vanadium (V) catalysts perform these oxidations *via* a mechanism similar to that proposed by Hanson and co-workers, *i.e.* a two-electron base-assisted redox dehydrogenation mechanism.[22], [23] The alkoxide ligand on the vanadium complex exchanges readily with free benzyl alcohol in the first step. The base then deprotonates the benzyl alkoxide at the methylene, which leads to the formal

dehydrogenation of the benzyl alcohol and two-electron reduction of the metal center (V^{5+} to V^{3+}).

2.3.2 Catalytic aerobic oxidation of lignin model compounds

Studying model compounds of lignin instead of lignin itself is a good way to get a better understanding of the reactivity of corresponding lignin substructures because of the difficulty associated with the characterization of structural changes of lignin. In this study, 1,2-diphenyl-2-methoxyethanol, diphenylether, and benzylphenylether were chosen to represent the lignin model compounds, air and hydrogen peroxide were using as oxidizing agents under the catalytic influence of the vanadium complexes.

2.3.2.1 Catalytic aerobic oxidation of 1,2-diphenyl-2-methoxyethanol

After the promising results concerning the aerobic oxidation of 4-methoxybenzylalcohol, the vanadium complexes were evaluated as catalysts for the aerobic oxidation of the lignin model compound 1,2-diphenyl-2-methoxyethanol (Scheme 2-4). The substrate was heated with 5 mol% of vanadium complex (**2.1**-**2.4**) at 100 °C for 54 h. The product distribution for the catalytic oxidation differed in DMSO-d_6, pyr-d_5 and toluene-d_8 solvents but similar conversions were achieved (Table 2-4, data provided for (**2.4**), although (**2.1**-**2.3**) also gave similar yields of each product). Product identities were confirmed via GC-MS analyses. Control reactions with 1,2-diphenyl-2-methoxyethanol only (no vanadium) in DMSO-d_6, pyr-d_5 and toluene-d_8 solvents under air showed no reaction when heated at 140 °C for 3 days. Table 2-5 provides a direct comparison of compounds (**2.1**-**2.4**) for the conversion of 1,2-diphenyl-2-methoxyethanol over time. These data suggest that there is very little ligand effect in these catalytic reactions within this family of complexes. The nature of the amine used in preparing the ligand (leading to the presence or absence of a pendant arm, or the type of pendant donor) does not significantly influence the conversion levels achieved, which were in all cases 90-100%. As the substrate can yield multiple molecules upon oxidation via bond cleavage reactions, it should be noted that the sum of the product yields can be in excess

of 100%. In DMSO-d_6, (**2.4**) gave benzaldehyde (90%), methanol (46%), methyl benzoate (36%) and benzoin methyl ether (18%) as the major products and a small amount of benzoic acid (Table 2-4, entry 1). A different product distribution was observed when the catalytic reaction was run under the same reaction conditions in pyr-*d5* solvent. After 54 h, the starting material had been completely consumed, and the organic products consisted of, methyl benzoate (67%), benzoin methyl ether (15%), and methanol (2%). Benzaldehyde was detected as a minor product (1%) and no benzoic acid was detected (Table 2-4, entry 2). Whereas, when the catalytic reaction was run under the same reaction conditions in toluene-d_8 solvent, a third product distribution was observed (Table 2-4, entry 3). The major products were methyl benzoate (57%) and benzaldehyde (51%), and a small amount of benzoic acid (2%) was also detected. No benzoin methyl ether and methanol were not observed. For comparison, Hanson and co-workers under similar reaction conditions in DMSO-d_6 or pyr-d_5 as the solvent observed a different product distribution at conversion levels of 95%; benzaldehyde 73% (DMSO), 9% (pyr), methyl benzoate 69% (DMSO), 6% (pyr), benzoic acid 5% (DMSO), 85% (pyr), and methyl benzoate 5% (DMSO), 84% (pyr).

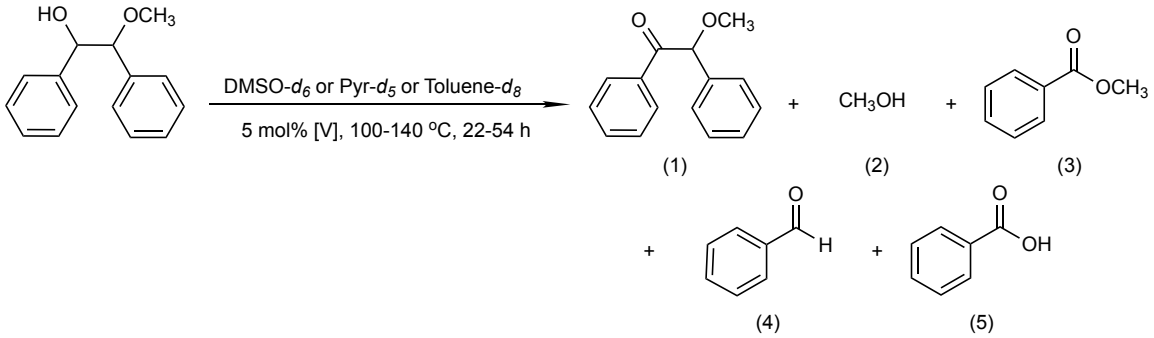

Scheme 2-4. Reaction of vanadium complexes with 1,2-diphenyl-2-methoxyethanol and potential products from aerobic oxidation

Table 2-4. Aerobic oxidation of 1,2-diphenyl-2-methoxyethanol using (**2.4**) in a range of solvents to afford products 1-5 (Scheme 2-4)[a]

Entry	Conv. [%]	Solvent	Yield of products[b]				
			1 [%]	2 [%]	3 [%]	4 [%]	5[%]
1	90	DMSO-d_6	18	46	36	90	0.2
2	99	Pyr-d_5	15	2	67	1	--
3	99	Toluene-d_8	--	--	57	51	2

[a] 0.5 mmol of lignin model (1,2-diphenyl-2-methoxyethanol), 5 mol% of (**2.4**), 54 h. All runs were carried out at 100 °C, using pyridine-d_5, DMSO-d_6, or toluene-d_8 as solvents, conversions and yields determined by integration against an internal standard (*p*-xylene). [b] Up to 5 products were identified as shown in Scheme 2.4

Table 2-5. Comparison of conversion levels for aerobic oxidation of 1,2-diphenyl-2 methoxyethanol using (**2.1**-**2.4**) at different time intervals[a]

Entry	**Time**	**2.1**	**2.2**	**2.3**	**2.4**
1	12 h	62	75	72	75
2	24 h	90	86	84	78
3	36 h	94	100	100	100

[a] 5 mol% (**2.1**-**2.4**), 0.5 mmol of lignin model (1,2-diphenyl-2-methoxyethanol), 140 °C, toluene-d_8. Conversion determined by integration against an internal standard (*p*-xylene).

2.3.2.2 Catalytic aerobic oxidation of diphenylether and benzylphenylether

Diphenylether and benzylphenylether were then studied as simple substrates for catalytic oxidation reactions using H_2O_2 as the oxidant to determine if benzylic ether cleavage was selective compared with aromatic, Ph-O-Ph, cleavage. A solution of H_2O_2 was added over a period of 1 h at 1 mL h^{-1} using a syringe pump to a solution of the

substrate and catalyst, (**2.1**-**2.4**) (2 mol%) at 80 °C. However, no significant oxidation of the substrate was observed under these conditions. Addition of a base (NEt_3) and use of a different solvent (acetone or toluene) did not prompt the oxidation of either compound. However, when acetonitrile was used as a solvent diphenylether, and benzylphenylether, gave 10% and 9% yield of phenol, and 15% yield of benzaldehyde for benzylphenylether, after stirring the reaction mixture at 80 °C for 72 h (Table 2-6). This shows that no selectivity in terms of C-O-C cleavage was observed and reactivity towards such bonds is poor especially when compared with reactions of 1,2-diphenyl-2-methoxyethanol using (**2.1**-**2.4**) in air. Control reactions showed no reaction when base, solution of H_2O_2 and diphenylether or benzylphenylether (no vanadium) were heated and stirred in acetonitrile under air at 80 °C for 3 days.

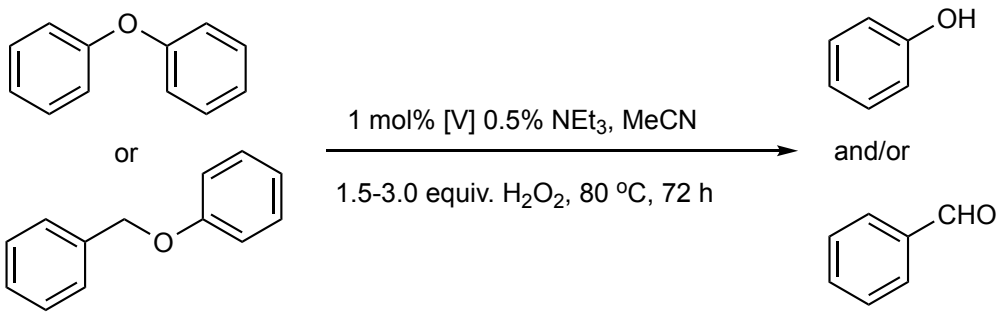

Scheme 2-5. Reaction of vanadium complexes in H_2O_2-mediated oxidation of aromatic ethers

Table 2-6. Catalytic oxidation of diphenylether and benzylphenylether using **2.1** -**2.4** with H_2O_2 [a]

Entry	Substrate	Additive	Yield [%]	
			Phenol	**Benzaldehyde**
1	Diphenyl ether	none	< 1	--
2	Benzylphenyl ether	none	< 1	--
3	Diphenyl ether	Et_3N	10	10
4	Benzylphenyl ether	Et_3N	15	9

[a] 0.5 mmol of ether, 2 mol% **2.4**, 10 mol% additive if used,1.5 mmol H_2O_2 in MeCN, 72 h, conversions determined by GC using dodecane as an internal standard. Note: similar reactivity was observed for compounds **2.1**-**2.3**.

2.4 Conclusions

Four new vanadium (V) complexes of amino-bis(phenolate) ligands have been synthesized and four structures determined by single crystal X-ray diffraction. Crystallography showed that some of the alkoxide derivatives decompose to yield oxo-bridged dimers upon storage in air. Their parent complexes were also less active in oxidation reactions of 4-methoxybenzylalcohol, which leads us to propose that the bridged complexes might be catalytically inactive species formed during oxidation processes. All complexes were also tested for catalytic aerobic oxidative C-C bond cleavage of 1,2-diphenyl-2-methoxyethanol, which afforded benzaldehyde and methyl benzoate as the major products. Catalytic, oxidative C-O bond cleavage of diphenylether, and benzylphenylether was also demonstrated, however, the conversions were quite low. Future work will focus on designing more active and stable catalysts for aerobic oxidation reactions as well as examining the reactivity of these species in other catalytic processes (see chapter 5).

2.5 Experimental Section

2.5.1 General methods and materials

Starting materials for all syntheses were purchased from Strem, Aldrich or Alfa Aesar and were used as received. Ligands were prepared via literature procedures.[15c] $CDCl_3$, toluene-d_8, DMSO-d_6 were purchased from Cambridge Isotope Laboratories and pyridine-d_5 from Aldrich. HPLC grade solvents were used as purchased. All syntheses were performed under ambient laboratory atmosphere unless otherwise specified. NMR spectra were recorded on Bruker Avance-500 or Avance III-300 spectrometers and referenced internally to TMS. MALDI-TOF mass spectra were recorded in reflectron mode on an Applied Biosystems Voyager DE-PRO equipped delayed ion extraction and high performance nitrogen laser (337 nm). Samples were prepared at a concentration of 0.02 mg L^{-1} in toluene. Anthracene was used as the matrix, which was mixed at a concentration of 0.02 mg L^{-1}. UV-vis spectra were recorded on an Ocean Optics USB4000+ spectrophotometer. GC-MS data were obtained on an Agilent Technologies 7890 GC with 5975 MSD. Elemental analyses were carried out by Canadian Microanalytical Service Ltd, Delta, BC, Canada. X-ray data were collected for single crystals of (**2.1**, **2.2**, **2.5**, and **2.6)** (details provided below).

2.5.2 Synthesis of vanadium complexes:

$[O_2NO]^{BuMeMeth}$ V(O)(OMe) (**2.1**): $H_2[O_2NO]^{BuMeMeth}$ (1.00 g, 2.25 mmol) and $[VO(acac)_2]$ (0.5970 g, 2.25 mmol) were placed in a flask, methanol (50 mL) was added and the mixture was heated to reflux overnight to yield a dark blue solution. The solvent was removed under vacuum and a dark blue solid (0.88 g) was obtained, 73% yield. Compounds (**2.2**-**2.4**) were prepared in a similar fashion. $[ON_2O]^{BuMe}$ V(O)(OMe) (**2.2**) was isolated as a dark blue solid 0.95 g, 80% yield. $[O_2NN]^{BuBuPy}$ V(O)(OMe) (**2.3**) was isolated as a black solid 0.92 g, 78 % yield. $[O_2NO]^{BuBuFurf}$ V(O)(OMe) (**2.4**) was isolated as a dark blue solid with yield 0.95 g, 80 % yield. Using a Johnson-Matthey magnetic susceptibility balance, all compounds were confirmed to be diamagnetic and did not give rise to any signals in EPR experiments. Upon recrystallization in air, crystals of (**2.1** and

2.2) suitable for X-ray structure determination were obtained. Upon storing in a refrigerator, solutions of (**2.3** and **2.4)** afforded oxo-bridged compounds (**2.5** and **2.6**).

(2.1) $C_{28}H_{45}NO_5V$: calcd. C 66.26, H, 8.34, N 2.76; found: C 65.88, H 8.12, N 2.99. IR: $\nu_{V=O}$, 951 cm^{-1}. ^1H NMR (300 MHz, $CDCl_3$) δ =7.11 (d, J = 1.8 Hz, 2H, ArH), 6.82 (d, J = 1.6 Hz, 2H, ArH), 5.30 (s, 3H, V-OCH_3), 4.57 (d, J = 13.7 Hz, 2H, OCH_2-C), 3.75 (d, *J* = 13.8 Hz, 2H, NCH_2-CH_2), 3.38 (s, 3H, C-OCH_3), 3.23 (s, 2H, ArC-CH_2-N), 2.82 (s, 2H, ArC-CH_2-N), 2.35 – 2.29 (m, 6H, $ArCH_3$), 1.47 (s, 18H, $ArC(CH_3)_3$.

(**2.2**) $C_{29}H_{45}N_2O_4V$: calcd. C 66.52, H 8.37, N 5.54; found: C 66.75, H 8.20, N 5.68. IR: $\nu_{V=O}$, 951cm^{-1}. ^1H NMR (300 MHz, $CDCl_3$) δ 7.12 – 7.03 (m, 2H, ArH), 6.73 (d, *J* = 1.6 Hz, 1H, Ar), 6.66 (d, *J* = 1.8 Hz, 1H, ArH), 5.05 (s, 3H, OCH_3), 4.67 (d, *J* = 14.6 Hz, 1H, N-CH_2-C), 4.43 (d, *J* = 13.6 Hz, 1H, N-CH_2-C), 3.75 – 3.62 (m, 1H, N-CH_2-C), 3.63 – 3.34 (m, 1H, N-CH_2-C), 3.11 (d, *J* = 13.6 Hz, 2H, ArC-CH_2-N), 3.08 – 2.97 (m, 2H, ArC-CH_2-N), 2.57 (s, 3H, NCH_3), 2.53 (s, 3H, NCH_3), 2.28 (s, 3H, $ArCH_3$), 2.27 (s, 3H, $ArCH_3$), 1.55 (s, 9H, $ArC(CH_3)_3$), 1.45 (s,9H, $ArC(CH_3)_3$).

(**2.3**) $C_{37}H_{53}N_2O_4V$: calcd. C 70.91, H 8.27, N 4.59; found: C 71.15, H 8.03, N 4.83. IR: $\nu_{V=O}$, 951 cm^{-1}. ^1H NMR (300 MHz, $CDCl_3$) δ 9.04 (d, *J* = 4.7 Hz, 1H, ArH), 7.35 (td, *J* = 7.7, 1.6 Hz, 1H, ArH), 7.08 (d, *J* = 2.4 Hz, 2H, ArH), 7.02 – 6.96 (m, 1H, ArH), 6.91 (d, *J* = 2.4 Hz, 2H, ArH), 6.49 (d, *J* = 7.8 Hz, 1H, ArH), 4.89 (s, 3H, OCH_3), 4.52 (d, *J* = 12.4 Hz, 2H, N-CH_2-C), 3.75 (d, *J* = 14.9 Hz, 2H, N-CH_2-C), 3.36 (d, *J* = 12.5 Hz, 2H, N-CH_2-C), 2.28 – 2.17 (m, 2H, N-CH_2-C), 1.38 (s, 18H, $ArC(CH_3)_3$), 1.24 (s, 18H, $ArC(CH_3)_3$).

(**2.4**) $C_{36}H_{52}NO_5V$: calcd. C 68.66, H 8.32, N 2.22; found: C 69.15; H 8.03; N 2.19. IR: $\nu_{V=O}$, 951 cm^{-1}. ^1H NMR (300 MHz, $CDCl_3$) δ 7.42 – 7.25 (m, 2H, ArH), 6.96 (dd, *J* = 20.3, 2.1 Hz, 2H, ArH), 5.33 (s, 3H, OCH_3), 4.97 (d, *J* = 15.0 Hz, 1H, $CH(CH_2)_2$), 4.50 – 4.21 (m,1H, ArH), 3.84 (d, *J* = 15.1 Hz, 1H, ArH), 3.56 (ddd, *J* = 30.2, 20.5, 8.4 Hz,4H, CH_2-N-CH_2), 3.02 – 2.18 (m, 2H, N-CH_2-C), 1.59 – 1.41 (m, 18H, $ArC(CH_3)_3$), 1.35 – 1.26 (m, 18H, $ArC(CH_3)_3$).

(**2.5**) $C_{72}H_{100}N_4O_7V_2$: calcd. C 70.00, H 8.16, N 4.53; found C 69.97, H 8.17, N 4.66.

(**2.6**) $C_{70}H_{98}N_2O_9V_2$: calcd. C 69.29, H 8.14, N 2.31; found C 69.46, H 8.21, N 2.52.

2.5.3 Experimental for single crystal X-ray determinations:

Crystals of (**2.1**, **2.2**, **2.5** and **2.6**) were mounted on a low temperature diffraction loops. All measurements were made on a Rigaku Saturn70 CCD diffractometer using graphite monochromated Mo-Kα radiation. For all four structures, all non-hydrogen atoms were located in difference map positions and were refined anisotropically, while all hydrogen atoms were introduced in calculated positions and refined on a riding model. In the structure of (**2.1**), no H-atoms were found on O5, which suggests that this is a methoxide ion (H_3CO^-), therefore, for charge balance, vanadium must be in the +5 oxidation state. Bond valence sum calculations were attempted with VaList in order to confirm this assignment, [24] however, V(V) cannot be unambiguously assigned using this method. Calculations for V(III) and V(IV) gave results that were high (~4.8), which does suggest that the species is most consistent with V(V) and this is supported by other experimental evidence (e.g. NMR spectroscopy). Crystals of (**2.2**) were irregular and appeared cracked. Multiple domains with the same unit cell were identified, but refinement using all components did not yield satisfactory results. A single domain was used for the reported results. Connectivity is similar to (**2.1**) around the vanadium center. Crystals of (**2.5**) were small and diffracted weakly. A solvent accessible void is present in the unit cell, however, application of a solvent mask did not improve the refinement statistics, and therefore this was left untreated. Finally, (**2.6**) exhibited three areas of disorder; one of the lattice solvent acetonitrile molecules was refined as two parts ([C38,N3]:[C38A,N3A] 0.136(11):0.864(11)). Distance and angle restraints were used to model this solvent molecule. H-atoms associated with this solvent were omitted form the model, but included in the formula for the calculation of intensive properties. Distance and angle restraints were applied to this molecule. Next, one of the ligand carbon atoms, and corresponding H-atoms, in the pendant THF was refined as two parts (C16:C16A, 0.553(9):0.447(9)). Finally, one of the ligand *t*-butyl groups, and corresponding H-atoms,

was also refined as two parts ([C25,C26,C27]:[C25A,C26A,C27A], 0.423(11):0.577 (11)]). Similar disorder has been seen in other metal complexes of this ligand.

Crystal Data for (**2.1**): $C_{28}H_{42}NO_5V$ (M =523.59 g/mol), monoclinic, space group C2/c (no.15), a =32.094(11) Å, b =11.055(3) Å, c =19.787(7) Å, β =127.184(3)°, V =5593(3) Å^3, Z =8, T =163(2) K, μ(MoKα) =0.391 mm^{-1}, D_{calc} =1.244 g/cm^3, 22592 reflections measured (5.24° ≤ 2Θ ≤ 53°), 5706 unique (and 5242 with I>2σ(I); R_{int} = 0.0610) which were used in all calculations. The final R_1 was 0.0569 (>2σ(I)) and wR_2 was 0.1623 (all data). CCDC no. 1419296

Crystal Data for (**2.2**): $C_{29}H_{45}N_2O_4V$ (M =536.61 g/mol): monoclinic, space group $P2_1/c$ (no.14), a =12.3406(8) Å, b =24.0686(19) Å, c =9.3036(7) Å, β =92.780(6)°, V =2760.1 (4) Å^3, Z =4, T =123.15 K, μ(MoKα) =0.396 mm^{-1}, D_{calc} =1.291 g/cm^3, 25008 reflections measured (3.304° ≤ 2Θ ≤ 59.586°), 6832 unique (and 3831 with I>2σ(I); R_{int} = 0.3546, R_{sigma}= 0.2006) which were used in all calculations. The final R_1 was 0.1163 (I > 2σ(I)) and wR_2 was 0.3179 (all data). CCDC no. 1410297

Crystal Data for (**2.5**): $C_{72}H_{100}N_4O_7V_2$ (M =1235.43 g/mol): monoclinic, space group $P2_1/c$(no.14), a =14.6760(11) Å, b =17.4805(9) Å, c =15.9994(11) Å, β =113.184(9)°, V = 3773.1(5) Å^3, Z =2, T =123.15 K, μ(MoKα) =0.297 mm^{-1}, D_{calc} =1.087 g/cm^3, 18149 reflections measured (5.16° ≤ 2Θ ≤ 50.054°), 6630 unique (and 4573 with I>2σ(I); R_{int} = 0.0688, R_{sigma} = 0.1240) which were used in all calculations. The final R_1 was 0.0895 (I > 2σ(I)) and wR_2 was 0.2301 (all data). CCDC no. 1410298

Crystal Data for (**2.6**): $C_{78}H_{118}N_6O_9V_2$ (M =1385.66 g/mol): monoclinic, space group I2/a (no.15), a =14.1027(3) Å, b =17.1339(5) Å, c =32.0775(7) Å, β =90.371(2)°, V =7750.9 (3) Å^3, Z =4, T =123.15 K, μ(MoKα) =0.298 mm^{-1}, D_{calc} =1.187 g/cm^3, 34379 reflections measured (5.08° ≤ 2Θ ≤ 53°), 8029 unique (and 6581 with I>2σ(I); R_{int} = 0.0596, R_{sigma} = 0.0459) which were used in all calculations. The final R_1 was 0.0747 (I > 2σ(I)) and wR_2 was 0.2223 (all data). CCDC no. 1410299

2.5.4 General procedure for the catalytic aerobic oxidation of 4-methoxybenzyl alcohol:

In a 25 mL round-bottom flask, or in a 20 mL microwave vial, 4-methoxybenzyl alcohol (69 mg, 0.50 mmol) was combined with vanadium complex (**2.1**-**2.4**) (0.01 mmol, 2 mol%), NEt_3 (7 μL, 0.05 mmol, 10 mol%), and *p*-xylene (5 μL, 0.041 mmol) as an internal standard. The mixture was dissolved in toluene-d_8 (1 mL) under air, and the flask equipped with a stir bar and an air condenser. If the reaction was performed in a microwave vial, it was sealed. The reaction mixture was heated with stirring in an oil bath at 80-140 °C for 36-60 h under air. The reaction mixture was cooled to room temperature, and the yield of oxidized product 4-methoxybenzaldehyde determined by integration of the ^{1}H NMR spectra against the internal standard.

2.5.5 General procedure for the catalytic aerobic oxidation of 1,2-diphenyl-2-methoxyethanol:

In a 25 mL round-bottom flask, or in 20 mL microwave vial, 1,2-diphenyl-2-methoxyethanol (29.8 mg, 0.131 mmol) was combined with a vanadium complex (**2.1**-**2.4**) (0.0066 mmol, 5 mol%), and *p*-xylene (5 μL, 0.041 mmol) as an internal standard. The mixture was dissolved in toluene-d_8 (1 mL) under air, and the flask equipped with a stir bar and an air condenser. If the reaction was performed in a microwave vial, it was sealed. The reaction mixture was heated with stirring in an oil bath at 100-140 °C for 12-36 h under air. The reaction mixture was cooled to room temperature, and the yields of oxidized products were determined by integration of the ^{1}H NMR spectra against the internal standard. Product identities were further confirmed via GC-MS analyses.

2.5.6 General Procedure for H_2O_2-mediated oxidation of diphenylether and benzylphenylether:

Acetonitrile (9 mL) was added to a vanadium complex (**2.1**-**2.4**) (0.005 mmol, 1 mol%), NEt_3 (7 µL, 0.05 mmol, 10 mol%), in a 50 mL of round bottom flask. The ether substrate (0.5 mmol) was added to the solution at room temperature in air. 30% aqueous H_2O_2 (170 µL, 1.5 mmol or 340 µL, 3.0 mmol) was dissolved in acetonitrile (870 µL or 1660 µL, respectively) and was added to the reaction mixture over a period of 1 or 2 h by a syringe pump. The flask was then equipped with a stir bar and an air condenser. The flask was heated with stirring in an oil bath at 80 °C for 48 h. The reaction was cooled to room temperature and the solvent was removed under vacuum. The residue of the reaction mixture was dissolved in diethyl ether and dodecane (100 or 50 µL as internal standard) was added, the mixture was analyzed by GC-MS and quantified using a calibration curve.

2.6 References

[1] A. Corma, S. Iborra and A. Velty, *Chem. Rev.* **2007**, *107*, 2411-2502.

[2] M. R. gen Klaas and H. Schone, *ChemSusChem* **2009**, *2*, 127-128.

[3] C. H. Zhou, X. Xia, C. X. Lin, D. S. Tong and J. Beltramini, *Chem. Soc. Rev.* **2011**, *40*, 5588-5617.

[4] S.P. Singh and D. Singh, *Renew. Sust. Energ. Rev.* **2010**, 578–597.

[5] G.D. Saratale, S.D. Chen, Y.C. Lo, R.G. Saratale and J. S. Chang, *J. Sci. Ind. Res.* **2008** , 962-979.

[6] D. Chiaramonti, M. Prussi, S. Ferrero, L. Oriani, P. Ottonello, P. Torre and F. Cherchi, *Biomass Bioenergy* **2012**, *46*, 25-35.

[7] L. Viikari, J. Vehmaanperä and A. Koivula, *Biomass Bioenergy* **2012**, *46*, 13-24.

[8] a) M. Aresta, *Carbon Dioxide as Chemical Feedstock, ed.*, John Wiley & Sons, **2010**, 56-58; b) J. Pérez, J. Muñoz-Dorado, T. de la Rubia and J. Martínez, *Int. Microbiol.* **2002**, *5*, 53-63; c) A. M. Boudet, S. Kajita, J. Grima-Pettenati and D. Goffner, *Trends Plants. Sci* **2003**, *8*, 576-581; d) J. G. Linger, D. R. Vardon, M. T. Guarnieri, E. M. Karp, G. B. Hunsinger, M. A. Franden, C. W. Johnson, G. Chupka, T. J. Strathmann, P. T. Pienkos and G. T. Beckham, *Natl. Acad. Sci. U. S. A.* **2014**, *111*, 12013-12018.

[9] J. Zakzeski, P. C. A. Bruijnincx, A. L. Jongerius and B. M. Weckhuysen, *Chem. Rev.* **2010**, *110*, 3552-3599.

[10] a) N. Yan, C. Zhao, P. J. Dyson, C. Wang, L. T. Liu and Y. Kou, *ChemSusChem* **2008**, *1*, 626-629; b) H. Wang, M. Tucker and Y. Ji, *J. Appl. Chem.* **2013**, *2013*, 9; c) C. Xu, R. A. Arancon, J. Labidi and R. Luque, *Chem. Soc. Rev.* **2014**, 7485–7500.

[11] a) M. R. Maurya, N. Saini and F. Avecilla, *RSC Advances* **2015**, *5*, 101076-101088; b) M. R. Maurya, N. Saini and F. Avecilla, *Inorganica Chimica Acta* **2015**, *438*, 168-178; c) M. R. Maurya, N. Saini and F. Avecilla, *RSC Advances* **2016**, *6*, 12993-13009.

[12] a) J. A. L. da Silva, J. J. R. F. da Silva and A. J. L. Pombeiro, *Coord. Chem. Rev.* **2011**, *255*, 2232-2248; b) P. Adao, S. Barroso, F. Avecilla, M. C. Oliveira and J. C. Pessoa, *J. Organomet. Chem.* **2014**, *760*, 212-223; c) P. Adao, M. L. Kuznetsov, S. Barroso, A. M. Martins, F. Avecilla and J. C. Pessoa, *Inorg. Chem.* **2012**, *51*, 11430-11449; d) S. Barroso, P. Adao, F. Madeira, M. T. Duarte, J. C. Pessoa and A. M. Martins, *Inorg. Chem.* **2010**, *49*, 7452-7463; e) M. R. Maurya, N. Chaudhary, F. Avecilla, P. Adao and J. C. Pessoa, *Dalton Trans.* **2015**, *44*, 1211-1232; f) M. R. Maurya, N. Chaudhary, A. Kumar, F. Avecilla and J. C. Pessoa, *Inorganica Chim. Acta* **2014**, *420*, 24-38; g) M. R.

Maurya, C. Haldar, A. Kumar, M. L. Kuznetsov, F. Avecilla and J. C. Pessoa, *Dalton Trans.* **2013**, *42*, 11941-11962.

[13] a) G. Zhang, B. L. Scott, R. Wu, L. P. Silks and S. K. Hanson, *Inorg. chem.* **2012**, *51*, 7354-7361; b) C. Parmeggiani, *Green Chem.* **2012**, *14*, 547-564.

[14] a) S. K. Hanson, R. T. Baker, J. C. Gordon, B. L. Scott, A. D. Sutton and D. L. Thorn, *J. Amer. Chem. Soc.* **2009**, *131*, 428-429; b) S. K. Hanson, R. T. Baker, J. C. Gordon, B. L. Scott and D. L. Thorn, *Inorg. Chem.* **2010**, *49*, 5611-5618; c) S. K. Hanson, R. Wu and L. A. Silks, *Org. Lett.* **2011**, *13*, 1908-1911; d) N. Jiang and A. J. Ragauskas, *Tetrahedron Lett.* **2007**, *48*, 273-276; e) M. Amin, L. Vogt, S. Vassiliev, I. Rivalta, M. M. Sultan, D. Bruce, G. W. Brudvig, V. S. Batista and M. R. Gunner, *J. Phys. Chem. B* **2013**, *117*, 6217-6226; f) B. Sedai, C. Díaz-Urrutia, R. T. Baker, R. Wu, L. A. P. Silks and S. K. Hanson, *ACS Catal.* **2011**, *1*, 794-804.

[15] a) S. Groysman, I. Goldberg, M. Kol, E. Genizi and Z. Goldschmidt, *Inorganica Chim. Acta* **2003**, *345*, 137-144; b) R. K. Dean, C. I. Fowler, K. Hasan, K. Kerman, P. Kwong, S. Trudel, D. B. Leznoff, H.-B. Kraatz, L. N. Dawe and C. M. Kozak, *Dalton Trans.* **2012**, *41*, 4806-4816; c) F. M. Kerton, S. Holloway, A. Power, R. G. Soper, K. Sheridan, J. M. Lynam, A. C. Whitwood and C. E. Willans, *Can. J. Chem.* **2008**, *86*, 435-443.

[16] N. Ikpo, S. M. Butt, K. L. Collins and F. M. Kerton, *Organometallics* **2009**, *28*, 837-842.

[17] M. D. Eelman, J. M. Blacquiere, M. M. Moriarty and D. E. Fogg, *Angew. Chem. Int. Ed.* **2008**, *47*, 303-306.

[18] O. Wichmann, H. Sopo, A. Lehtonen and R. Sillanpää, *Eur. J. Inorg. Chem.* **2011**, *2011*, 1283-1291.

[19] S. Barroso, P. Adão, F. Madeira, M. T. Duarte, J. C. Pessoa and A. M. Martins, *Inorg. Chem.* **2010**, *49*, 7452-7463.

[20] S.-S. Weng, M.-W. Shen, J.-Q. Kao, Y. S. Munot and C.-T. Chen, *P. Natl. Acad. Sci. USA* **2006**, *103*, 3522-3527.

[21] S. K. Hanson, R. Wu and L. A. P. Silks, *Org. Lett.* **2011**, *13*, 1908-1911.

[22] S. K. Hanson, R. T. Baker, J. C. Gordon, B. L. Scott, L. A. P. Silks and D. L. Thorn, *J. Am. Chem. Soc.* **2010**, *132*, 17804-17816.

[23] B. N. Wigington, M. L. Drummond, T. R. Cundari, D. L. Thorn, S. K. Hanson and S. L. Scott, *Chem. Eur. J.* **2012**, *18*, 14981-14988.

[24] V. A.S. Wills, Program available from http://www.ccp14.ac.uk,

CHAPTER 3

3 Coupling Reactions of Carbon Dioxide with Epoxides Catalyzed by Vanadium Aminophenolate Complexes

A version of this chapter has been published

Ali Elkurtehi, and Francesca M. Kerton

ChemSusChem, **2017**, 10, 1249-1254.

Some modifications were made to the original paper for inclusion as a chapter in this thesis.

3.1 Introduction

Carbon dioxide (CO_2) chemistry and the development of reactions utilizing CO_2 as a C1 feedstock have drawn significant attention because CO_2 is not only an abundant, inexpensive and non-toxic carbon source but also a major contributor to climate change.[1] One of the most promising reactions for using CO_2 is its transformation with epoxides to yield cyclic carbonates Scheme 3-1. Cyclic carbonates can be used as synthetic intermediates in the synthesis of fine or bulk chemicals. They have been used as a raw material for the synthesis of polycarbonates,[2] and can be found as components in other carbonate-containing materials and composites.[3] Cyclic carbonates can also be used as intermediates in the synthesis of other small molecules such as dimethylcarbonate.[4] It is also worth noting that carbonate structural motifs are also found in natural products.[5] An application of cyclic carbonates, which has grown significantly in recent years, is as green polar aprotic solvents,[1c, 6] because of their excellent solubilizing properties and relatively low toxicities. This has also led to their use as electrolyte solvents in lithium-ion batteries.[7]

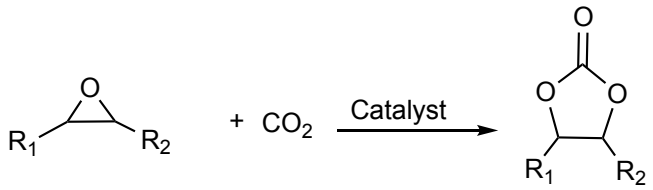

propylene oxide,	PO: $R_1 = CH_3$, $R_2 = H$	PC
styrene oxide,	SO: $R_1 = Ph$, $R_2 = H$	SC
cyclohexene oxide,	CHO: $R_1,R_2 = -(CH_2)_4-$	CHC

Scheme 3-1. General scheme for conversion of carbon dioxide to propylene carbonate (PC), styrene carbonate (SC), or cyclohexene carbonate (CHC) via reaction with the corresponding epoxides

Many homogeneous catalysts using a wide variety of ligand classes have been examined for the transformation of CO_2 to cyclic carbonates using epoxides. For porphyrin species, chromium,[8] manganese,[9] copper,[9a] iron,[9b] cobalt,[9b, 10] and zinc,[11]have all been investigated. In most cases, these complexes are combined with a nucleophilic co-catalyst, such as tetrabutylammonium bromide (TBAB), bis(triphenylphosphine)iminium chloride (PPNCl) or 4-dimethylaminopyridine (DMAP). At Memorial University, Kozak and co-workers have been investigating chromium complexes of amino-bis(phenolate) ligands as homogeneous catalysts for CO_2/epoxide copolymerization.[12] However, cobalt(II) and cobalt(III) complexes of these ligands were shown to couple CO_2 with propylene oxide under neat conditions to give propylene carbonate and not polymer,[13] but when closely related complexes were studied more recently poly(cyclohexene)carbonate was produced in the presence of DMAP.[14] Iron has also been studied with this class of ligand and such complexes have shown excellent reactivity for either cyclic carbonate or polycarbonate formation.[15] The use of the aminophenolate ligand class, as exemplified by the above examples, presents a number of advantages for homogeneous catalyst development among which are their ease of synthesis, simple electronic and steric variation, and tuneable complexation modes achieved by changing the substituents on the phenolate groups, the amine or any pendant

donors.[16] Catalytic transformations of CO_2 into cyclic carbonates are discussed in more detail in the introductory chapter of this thesis, Chapter 1.

In the current study, vanadium was chosen because it is an abundant and relatively non-toxic metal. In the first study including vanadium species for the coupling of CO_2 and epoxides, VCl_3 and other Lewis acids were examined as catalysts.[17] More recently, complexes containing vanadium(IV) metal centers involving a variety of ligand classes including salphen and salen,[18] and porphyrins,[19] have shown excellent activity towards cyclic carbonate synthesis. Herein, several oxo vanadium(V) amino-bis(phenolate) complexes (Figure 3.1) in conjunction with co-catalysts were screened in the hope of finding an efficient catalyst system for cycloaddition of epoxides and CO_2 to synthesize cyclic carbonates. I have recently reported the synthesis and characterization of these complexes, and their reactivity as oxidation catalysts (Chapter 2).[20] Furthermore, as far as we are aware, this is the first report on the reactivity of a vanadium aminophenolate complex in these reactions and activity of vanadium(V) complexes in such reactions is currently unknown.

3.2 Results and Discussion

Catalysts (**2.1**-**2.4**, Figure 3.1) were prepared as previously described – see Chapter 2.[20] They were previously studied in oxidation catalysis as described in Chapter 2 and add to the literature there.[21] Aminophenolate vanadium complexes have also been studied in olefin polymerization and copolymerization reactions.[22] They have also recently found application as anti-tumor agents.[23]

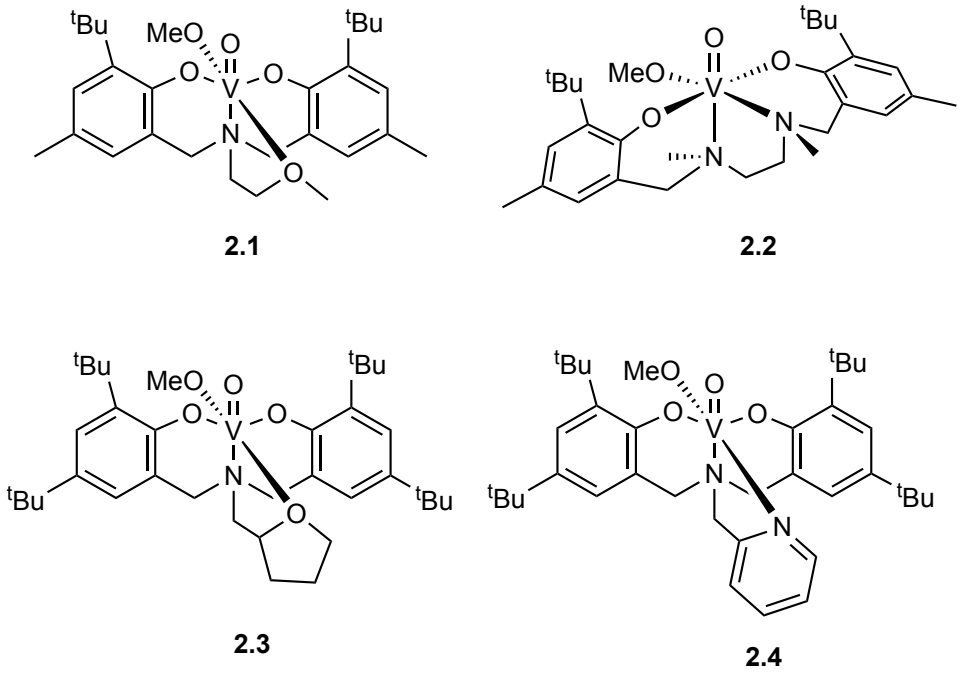

Figure 3.1 Homogeneous catalysts tested in this work

As (**2.1**-**2.4**) are soluble in the epoxides studied, the reactions were carried out without the addition of any organic co-solvent. The catalytic performance of complexes (**2.1–2.4**) in the cycloaddition of CO_2 to epoxides was initially investigated using PO as the model substrate. Reactions were performed in neat propylene oxide at 80 to 120 °C and under 20 or 40 bar of CO_2 pressure. They were monitored via *in situ* IR spectroscopy and Figure 3.2 displays a typical reaction profile, where a strong absorption just above 1800 cm^{-1} [ν(C= O) propylene carbonate] was observed for all catalyst systems**,** and no sign of a polycarbonate peak at 1750 cm^{-1} was seen. (**2.1**-**2.4**) were studied under identical conditions in order to determine if any of them showed superior reactivity towards propylene carbonate formation, PC (Figure 3.2 and Figure 3.3). Using TBAB as the co-catalyst at 120 °C and 20 bar CO_2, (**2.2** and **2.4**) appear to show an induction period of around 10 minutes whereas (**2.1** and **2.3**) immediately form PC. However, once the reaction started the rate of PC formation was significantly greater for (**2.2**) compared with the other three catalysts studied and was therefore chosen as the starting point for further investigations. It is worth noting that (**2.2**) has two amine donors in the backbone

of the ligand and no pendant ligand group unlike (**2.1**, **2.3** and **2.4**), and this might be the reason for the increased reaction rate observed for (**2.2**). However further studies would be needed to confirm this hypothesis.

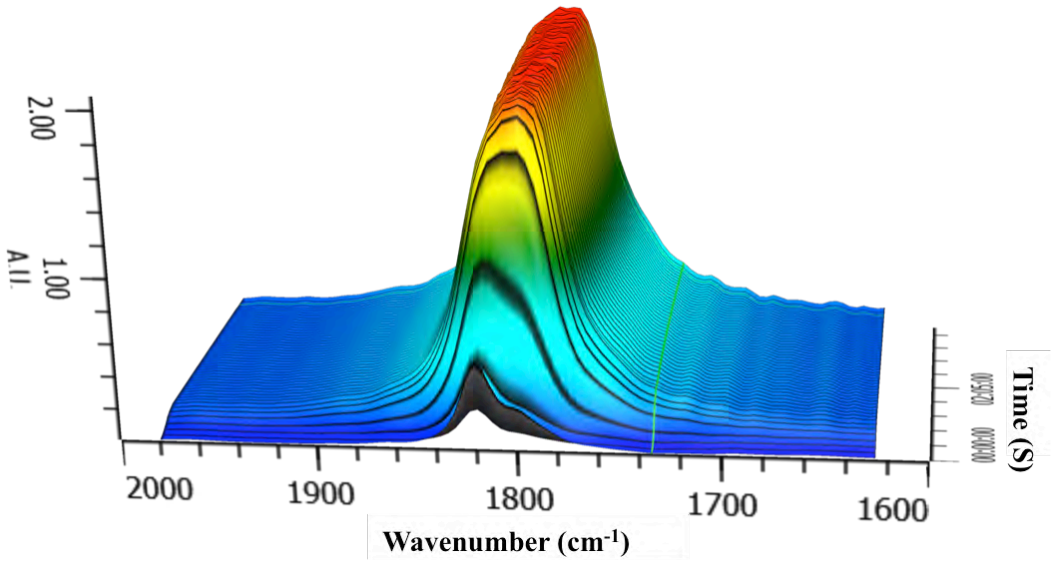

Figure 3.2. Typical surface diagram showing the growth of the cyclic carbonate group peak for propylene carbonate over time. No sign of polycarbonate peak at 1750 cm^{-1}

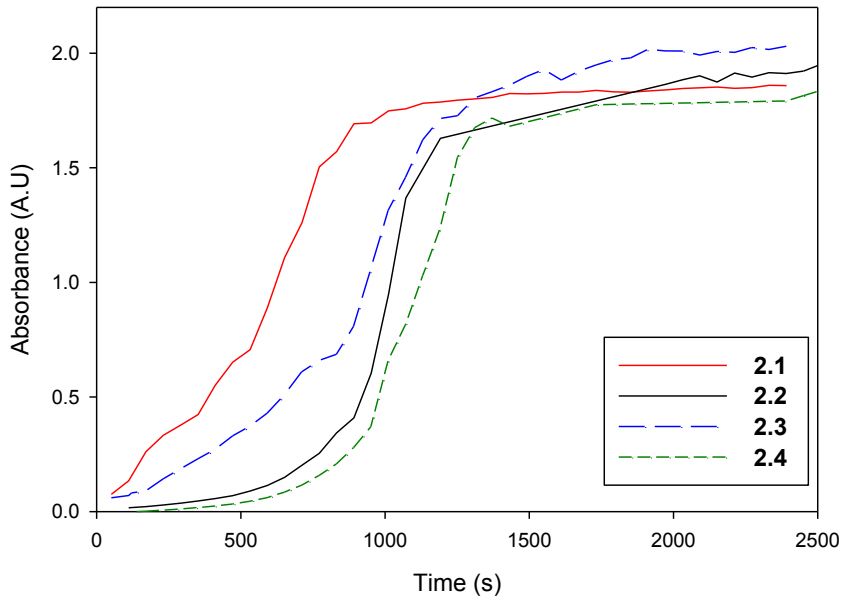

Figure 3.3. First hour of the reaction profiles showing the absorbance of the cyclic carbonate C=O band at 1810 cm^{-1} catalyzed by **2.1** (solid red line), **2.2** (solid black line), **2.3** (long dashed blue line), **2.4** (dashed green line). Reaction conditions: 20 bar CO_2, 120°C, [V]:[PO]:[TBAB] = 1:500:2

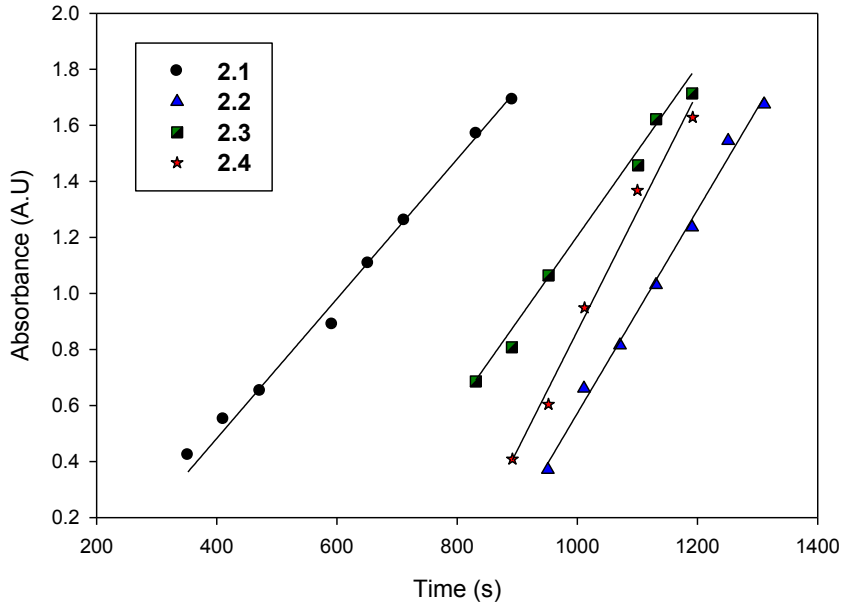

Figure 3.4. Initial rates of reactions during the first hour based on C=O absorbance of propylene carbonate. **2.1**(●)(y = 0.0025x - 0.5144, R^2 = 0.9835), **2.2** (▲)(y = 0.0043x – 3.39, R^2 = 0.9874), **2.3** (■) (y = 0.0030x – 1.8365, R^2 = 0.9822), **2.4** (☆) (y = 0.0036x – 3.0600, R^2 = 0.9934) Lines represent best fits of a linear model to the observed data

Table 3-1. Optimal reaction condition screening study for cyclic carbonate synthesis catalyzed by **2.2**[a]

Entry	Epoxide	Co-catalyst	[V]:[Epoxide]:[Co-cat]	P_{CO2} [bar]	T [°C]	time (h)	Conv. [%]	TON	TOF [h^{-1}]
1	PO	TBAB	0:500:1	40	80 or 100	18	0	0	0
2	PO	DMAP	1:500:1	40	80 or 100	18	0	0	0
3	PO	PPNCl	1:500:1	40	80	18	42	210	11.6
4	PO	TBAB	1:500:1	40	80	18	79	395	22
5	PO	TBAB	1:500:1	20	100	18	85	425	23.6
6	PO	TBAB	1:500:1	20	120	5	87	435	87
7	PO	TBAB	1:500:2	20	120	5	>99	>495	>99
8	PO	TBAB	1:500:3	20	120	5	85	425	23.6
9	PO	TBAB	1:2000:2	20	120	5	74	1480	296
10	PO	TBAB	1:4000:2	20	120	5	66	2640	528
11	PO	TBAB	1:4000:2	20	120	10	75	3000	300
12	PO	TBAB	1:4000:2	20	120	20	91	3640	182
13	PO	TBAB	1:4000:2	20	120	25	>99	>3960	>158
14	SO	TBAB	1:500:2	20	120	7	>99	>495	>71
15	CHO	TBAB	1:500:2	20	120	18	87	435	24.2

[a] Typical reaction conditions: 100 mL reactor volume, 50 mmol epoxide. (PO, propylene oxide, SO, styrene oxide and CHO, cyclohexene oxide). Conversions determined by ^{1}H NMR spectroscopy. TON = overall turnover number ($mol_{Epoxide\ converted}/mol_{Vanadium}$). TOF = overall turnover frequency (TON/reaction time).

3.3 Effect of Reaction Parameters on Conversion of PO

Results for reactions performed using (**2.2**) are summarized in Table 3-1 alongside a control reaction using TBAB and no catalyst (Table 3-1 entry 1). Among the different co-catalysts, TBAB showed greater activity compared with DMAP and PPNCl (Table 3-1 entries 2-4). It is worth noting that an ionic co-catalyst was critical in order to obtain catalytic turnovers, as no conversion was observed when DMAP was employed as the co-catalyst. The conversion of PO decreased if the **2.2**:TBAB mole ratio was increased or

decreased from the optimum 1:2 ratio (Table 3-1, entries 6–8). Similar trends have been noted for other vanadium catalysts studied.[19] Although PPNCl also functioned as an ionic co-catalyst for the cycloaddition of PO and CO_2, the PO conversion was lower than when TBAB was used (Table 3-1, entry 3 versus 4–13). This may be due to the fact that Br is both a better nucleophile and leaving group.[19] Catalyst loading was also varied (1:500- 1:4000) and the binary catalyst system could achieve high conversions after longer reaction times indicating that the catalysts are stable and can achieve high TON (Table 3-1, entries 9-13).

3.4 Cycloaddition Reaction of Styrene Oxide or Cyclohexene Oxide with CO_2 Catalyzed by 2.2/TBAB

The cycloaddition of CO_2 with other epoxides (styrene oxide, SO; cyclohexene oxide, CHO) using **2.2**/TBAB was examined at 120 °C and 20 bar (initial CO_2 pressure). Table 3-1 shows that the catalyst is active for all the selected substrates under the adopted conditions. For SO, the catalyst system is active and achieves 100% conversion to the corresponding cyclic carbonate within 7 h, (Table 3-1, entry 14). Reactivity towards CHO was also good; however, much longer reaction times were needed compared with PO and SO (Table 3-1, entry 15), which could be rationalized by the known lower rate of epoxide ring-opening for CHO due to its bicyclic nature which hinders the nucleophilic attack.

3.5 Kinetic Measurements

It is well known that cyclic carbonate is produced with increased selectivity over polycarbonate at elevated temperatures in the coupling reaction of PO and CO_2.[1d] The formation of cyclic carbonate is believed to occur via a backbiting mechanism from either an alkoxide or a carbonate group during the coupling reaction.[1d, 24] In order to develop a better understanding the of the mechanistic aspects of the formation of PC, the effect of reaction temperature on PC formation catalyzed by V/TBAB system was monitored by *in situ* infrared spectroscopy. At room temperature no PC formation was observed. By increasing the temperature to 30 °C, the absorbance at 1815 cm^{-1} which corresponds to

the cyclic carbonate carbonyl group started to slowly grow. The rate of formation of PC increases significantly as expected with increases in temperature Figure 3.5. Overall, it is clear that the activity of the catalyst is extremely sensitive to reaction temperature. From the kinetic data at variable temperatures, the activation energy for the PC formation can be obtained, Figure 3.6. The activation energy for PC formation in the **2.2**/TBAB catalyst system is 48.2 ± 0.16 kJ mol^{-1} at 20 bar of CO_2 pressure. This result under the present conditions was similar to those reported in the literature for the cycloaddition reaction using different catalysts - a range of values from 35 kJ mol^{-1} to 70 kJ mol^{-1} for a variety of other metals has been reported: Zn(II)[25], Al(III) [26], Co(III),[27] and Li.[28] However, there are examples where higher activation energies are reported around 100 kJ mol^{-1},[15b, 29] and this might be indicative of different rate determining steps between the catalytic systems being studied. Also, from the kinetic data at variable temperatures for SO and CHO conversions as illustrated in (Figures A3.1 and A3.3) the activation energies for the SC and CHC formations can be obtained (Figures A3.2 and A3.4). The activation energy for SC formation using the **2.2**/TBAB catalyst system was 45.6 ± 0.21 kJ mol^{-1}. The activation energy under the present conditions was in good agreement with those reported in the literature (35–70 kJ mol^{-1}) for this cycloaddition reaction using different catalysts. [25b],[26] For CHC formation using the **2.2**/TBAB catalyst system, the activation energy was 54.7 ± 0.22 kJ mol^{-1} at 20 bar of CO_2 pressure. This is higher than those for PC and SC formation and suggests that the rate-determining step for these reactions is dependent on the nature of the epoxide and the steric hindrance caused by using a non-terminal epoxide leads to a higher activation energy by CHO is the substrate.

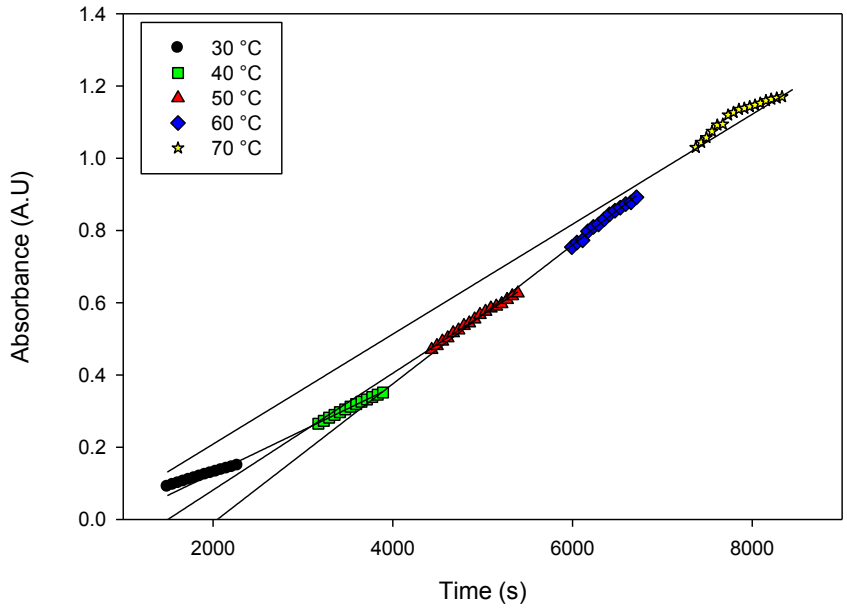

Figure 3.5. Temperature dependence of the initial rates of reaction based on the absorbance of the ν(C=O) of propylene carbonate (PC). Using **2.2** at 20 bar and [V]:[PO]:[Co-cat] 1:500:2, at 30 °C ● (y = 0.000039865x – 0.0200, R^2 = 0.9992), at 40 °C ■ (y = 0.00008028x – 0.1128, R^2 = 0.9977), at 50 °C ▲ (y = 0.0001x - 0.2421, R^2 = 0.9960), at 60 °C ♦ (y = 0.0001994x – 0.1128, R^2 = 0.9977), at 70 °C ☆ (y = 0.00040163x – 0.0200, R^2 = 0.9992)

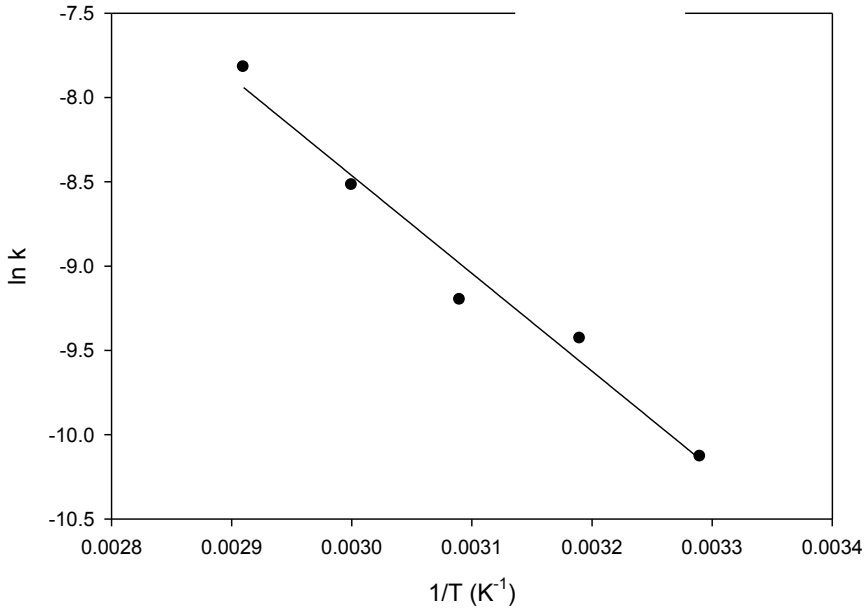

Figure 3.6. Arrhenius plot for the formation of propylene carbonate using variable temperature data presented in Figure 3.5. Straight line: $y = -5801.59x + 8.94$, $R^2 = 0.9736$

3.6 Conclusions

Vanadium amino-bis(phenolate) complexes (**2.1–2.4**) show very good catalytic performance for the selective coupling of epoxides and CO_2 in the presence of ionic co-catalysts (TBAB and PPNCl) to give cyclic carbonate with no evidence of any polymer formation. Under optimized conditions (120 °C and 20 bar CO_2), (**2.2**) could achieve a TOF of over 500 h^{-1} and a TON close to 4000 for propylene carbonate formation. Activation energies for the formation of PC, SC and CHC were determined. CHC formation had a significantly greater activation energy than PC and SC formation, which suggests that the rate determining step in these reactions is epoxide dependent, e.g. ring-opening of the epoxide, for this and related catalyst systems. However, we also note that reactions using other catalysts have reported significantly higher activation energies,[15b, 29] which implies that not all seemingly identical reactions progress with an identical rate

determining step. Further studies, including computational efforts, are needed to fully understand the reaction mechanisms and rate-determining steps in these and related reactions. Since this research was performed, another research group demonstrated that vanadium (V) complexes derived from amino-triphenolate ligands are also highly active catalysts for the coupling reaction of various epoxides with CO_2 to afford a series of organic carbonates in good yields.[30]

3.7 Experimental Section

3.7.1 Materials

Compounds (**2.1**-**2.4**) were prepared according to previously reported procedures (Chapter 2).[20] PO, SO and CHO were purchased from Aldrich and used as received. CO_2 was supplied from Praxair in a high-pressure cylinder equipped with a liquid dip tube. $CDCl_3$ was purchased from Cambridge Isotope Laboratories, Inc.

3.7.2 Instrumentation

^1H and ^{13}C NMR spectra were recorded on a Bruker AVANCE III 300 MHz NMR spectrometer. All coupling reactions, unless monitored *in situ* using a ReactIR system, were carried out in a 100 mL stainless steel Parr autoclave reactor (Parr Instrument Company) equipped with a motorized mechanical stirrer and a heating mantle. For monitored reactions, the pressure vessel was additionally equipped with a silicon ATR sensor (SiComp Sentinel). The ATR sensor was connected to a ReactIR 15 base unit (Mettler-Toledo) via a DS silver-halide Fiber-to-Sentinel conduit. Similar reaction monitoring systems have been described previously.[29b] It is important to note that caution should be taken when operating high-pressure equipment.

3.7.3 Typical procedure for catalytic coupling reaction of epoxides and CO_2

A solution of the catalyst in the epoxide was prepared and added *via* a long-needled syringe to a Parr autoclave, which was pre-dried under vacuum overnight at 80 °C. The appropriate pressure of CO_2 was then dosed into the reactor and heating and

stirring were started to achieve the desired temperature. After the desired time, the autoclave was slowly cooled down and after reaching room temperature, it was vented in a fume hood. This decompression was carried out very slowly, in order to allow the liquid phase to degas properly and to avoid loss of the reaction mixture. After this, the autoclave was opened and a sample was taken immediately for the determination of conversion by NMR spectroscopy.

3.8 References

[1] a) D. J. Darensbourg, C. C. Fang and J. L. Rodgers, *Organometallics* **2004**, *23*, 924-927; b) T. Sakakura, J.-C. Choi and H. Yasuda, *Chem. Rev.* **2007**, *107*, 2365-2387; c) W. Clegg, R. W. Harrington, M. North, F. Pizzato and P. Villuendas, *Tetrahedron: Asymmetry* **2010**, *21*, 1262-1271; d) X.-B. Lu and D. J. Darensbourg, *Chem. Soc. Rev.* **2012**, *41*, 1462-1484; e) C. Martín, G. Fiorani and A. W. Kleij, *ACS Catal.* **2015**, *5*, 1353-1370; f) C. Maeda, Y. Miyazaki and T. Ema, *Catal. Sci. Technol.* **2014**, *4*, 1482-1497; g) M. Cokoja, M. E. Wilhelm, M. H. Anthofer, W. A. Herrmann and F. E. Kuehn, *ChemSusChem* **2015**, *8*, 2436-2454; h) J. W. Comerford, I. D. V. Ingram, M. North and X. Wu, *Green Chem.* **2015**, *17*, 1966-1987; i) G. Fiorani, W. Guo and A. W. Kleij, *Green Chem.* **2015**, *17*, 1375-1389; j) M. Taherimehr and P. P. Pescarmona, *J. Appl. Polym. Sci.* **2014**, *131*, 41141/41141-41141/41117; k) M. Aresta, A. Dibenedetto and E. Quaranta, *J. Catal.* **2016**, *343*, 2-45.

[2] S. Fukuoka, M. Kawamura, K. Komiya, M. Tojo, H. Hachiya, K. Hasegawa, M. Aminaka, H. Okamoto, I. Fukawa and S. Konno, *Green Chem.* **2003**, *5*, 497-507.

[3] a) M. Yadollahi, H. Bouhendi, M. J. Zohuriaan-Mehr, H. Farhadnejad and K. Kabiri, *Polym. Sci. Ser. B* **2013**, *55*, 327-335; b) V. Besse, F. Camara, C. Voirin, R. Auvergne, S. Caillol and B. Boutevin, *Polym. Chem.* **2013**, *4*, 4545-4561; c) M. Fleischer, H. Blattmann and R. Mulhaupt, *Green Chem.* **2013**, *15*, 934-942; d) B. Nohra, L. Candy, J.-F. Blanco, C. Guerin, Y. Raoul and Z. Mouloungui, *Macromolecules* **2013**, *46*, 3771-3792.

[4] L. F. S. Souza, P. R. R. Ferreira, J. L. de Medeiros, R. M. B. Alves and O. Q. F. Araújo, *ACS Sustain. Chem. Eng.* **2014**, *2*, 62-69.

[5] a) S. Mizobuchi, J. Mochizuki, H. Soga, H. Tanba and H. Inoue, *J. Antibiot.* **1986**, *39*, 1776-1778; b) S. Chatterjee, G. C. Reddy, C. M. Franco, R. H. Rupp, B. N. Ganguli, H. W. Fehlhaber and H. Kogler, *J. Antibiot.* **1987**, *40*, 1368-1374; c) Z. Liu, P. R. Jensen and W. Fenical, *Phytochemistry* **2003**, *64*, 571-574.

[6] a) P. Lenden, P. M. Ylioja, C. Gonzalez-Rodriguez, D. A. Entwistle and M. C. Willis, *Green Chem.* **2011**, *13*, 1980-1982; b) B. Schäffner, F. Schäffner, S. P. Verevkin and A. Börner, *Chem. Rev.* **2010**, *110*, 4554-4581; c) J. Melendez, M. North and P. Villuendas, *Chem. Commun.* **2009**, 2577-2579; d) M. North and M. Omedes-Pujol, *Tetrahedron Lett.* **2009**, *50*, 4452-4454; e) M. North and M. Omedes-Pujol, *Beilstein J. Org. Chem.* **2010**, *6*, 1043-1055; f) C. Beattie, M. North and P. Villuendas, *Molecules.* **2011**, *16*, 3420-3432; g) H. L. Parker, J. Sherwood, A. J. Hunt and J. H. Clark, *ACS Sustain. Chem. Eng.* **2014**, *2*, 1739-1742; h) M. T. Reetz and G. Lohmer, *Chem. Commun.* **1996**, 1921-1922; i) B. Schäffner, J. Holz, S. P. Verevkin and A. Boerner, *ChemSusChem* **2008**, *1*, 249-253; j) B. Schäffner, J. Holz, S. P. Verevkin and A. Börner, *Tetrahedron Lett.* **2008**, *49*, 768-771.

[7] a) T. Ogasawara, A. Débart, M. Holzapfel, P. Novák and P. G. Bruce, *J. Am. Chem. Soc.* **2006**, *128*, 1390-1393; b) K. Xu, *Chem. Rev.* **2004**, *104*, 4303-4417; c) S. S. Zhang, *J. Power Sources* **2006**, *162*, 1379-1394; d) V. Aravindan, J. Gnanaraj, S. Madhavi and H. K. Liu, *Chem. Eur. J.* **2011**, *17*, 14326-14346.

[8] W. J. Kruper and D. D. Dellar, *J. Org. Chem.* **1995**, *60*, 725-727.

[9] a) R. Srivastava, T. H. Bennur and D. Srinivas, *J. Mol. Catal.* **2005**, *226*, 199-205; b) L. Jin, H. Jing, T. Chang, X. Bu, L. Wang and Z. Liu, *J. Mol. Catal. A: Chem.* **2007**, *261*, 262-266.

[10] a) R. L. Paddock, Y. Hiyama, J. M. McKay and S. T. Nguyen, *Tetrahedron Lett* **2004**, *45*, 2023-2026; b) D. Bai, Q. Wang, Y. Song, B. Li and H. Jing, *Catal. Commun.* **2011**, *12*, 684-688.

[11] T. Ema, Y. Miyazaki, S. Koyama, Y. Yano and T. Sakai, *Chem. Commun.* **2012**, *48*, 4489-4491.

[12] a) R. K. Dean, L. N. Dawe and C. M. Kozak, *Inorg. Chem.* **2012**, *51*, 9095-9103; b) R. K. Dean, K. Devaine-Pressing, L. N. Dawe and C. M. Kozak, *Dalton Trans.* **2013**, *42*, 9233-9244; c) H. Chen, L. N. Dawe and C. M. Kozak, *Catal. Sci. Technol.* **2014**, *4*, 1547-1555; d) C. M. Kozak, A. M. Woods, C. S. Bottaro, K. Devaine-Pressing and K. Ni, *Faraday Discuss.* **2015**, *183*, 31-46; e) K. Devaine-Pressing, L. N. Dawe and C. M. Kozak, *Polym. Chem.* **2015**, *6*, 6305-6315.

[13] L. N. Saunders, N. Ikpo, C. F. Petten, U. K. Das, L. N. Dawe, C. M. Kozak and F. M. Kerton, *Catal. Commun.* **2012**, *18*, 165-167.

[14] M. Reiter, P. T. Altenbuchner, S. Kissling, E. Herdtweck and B. Rieger, *Eur. J. Inorg. Chem.* **2015**, *2015*, 1766-1774.

[15] a) A. Coletti, C. J. Whiteoak, V. Conte and A. W. Kleij, *Chem. Cat. Chem.* **2012**, *4*, 1190-1196; b) D. Alhashmialameer, J. Collins, K. Hattenhauer and F. M. Kerton, *Catal. Sci. Technol.* **2016**, *6*, 5364-5373; c) M. Taherimehr, J. P. Serta, A. W. Kleij, C. J. Whiteoak and P. P. Pescarmona, *ChemSusChem* **2015**, *8*, 1034-1042.

[16] O. Wichmann, R. Sillanpää and A. Lehtonen, *Coord. Chem. Rev.* **2012**, *256*, 371-392.

[17] T. Bok, E. K. Noh and B. Y. Lee, *Bull. Korean Chem. Soc.* **2006**, *27*, 1171-1174.

[18] A. Coletti, C. J. Whiteoak, V. Conte and A. W. Kleij, *ChemCatChem* **2012**, *4*, 1190-1196, S1190/1191-S1190/1111.

[19] D. Bai, Z. Zhang, G. Wang and F. Ma, *Appl. Organomet. Chem.* **2015**, *29*, 240-243.

[20] A. I. Elkurtehi, A. G. Walsh, L. N. Dawe and F. M. Kerton, *Eur. J. Inorg. Chem.* **2016**, *2016*, 3123–3130.

[21] a) S. Barroso, P. Adao, F. Madeira, M. T. Duarte, J. C. Pessoa and A. M. Martins, *Inorg. Chem.* **2010**, *49*, 7452-7463; b) G. Zhang, B. L. Scott, R. Wu, L. P. Silks and S. K. Hanson, *Inorg. chem.* **2012**, *51*, 7354-7361; c) M. M. Hanninen, A. Peuronen, P. Damlin, V. Tyystjarvi, H. Kivela and A. Lehtonen, *Dalton Trans.* **2014**, *43*, 14022-14028; d) M. R. Maurya, N. Chaudhary, F. Avecilla, P. Adao and J. C. Pessoa, *Dalton Trans.* **2015**, *44*, 1211-1232.

[22] a) C. Lorber, F. Wolff, R. Choukroun and L. Vendier, *Eur. J. Inorg. Chem.* **2005**, 2850-2859; b) J.-Q. Wu, J.-S. Mu, S.-W. Zhang and Y.-S. Li, *J. Polym. Sci., Part A: Polym. Chem.* **2010**, *48*, 1122-1132; c) C. Lorber, E. Despagnet-Ayoub, L. Vendier, A. Arbaoui and C. Redshaw, *Catal. Sci. Technol.* **2011**, *1*, 489-494; d) J.-B. Wang, L.-P. Lu, J.-Y. Liu, H.-l. Mu and Y.-S. Li, *J. Mol. Catal. A: Chem.* **2015**, *398*, 289-296; e) Y. Phuphuak, F. Bonnet, L. Vendier, C. Lorber and P. Zinck, *Dalton Trans.* **2016**, *45*, 12069-12077.

[23] L. Reytman, O. Braitbard, J. Hochman and E. Y. Tshuva, *Inorg. Chem.* **2016**, *55*, 610-618.

[24] A. Buchard, M. R. Kember, K. G. Sandeman and C. K. Williams, *Chem. Commun.* **2011**, *47*, 212-214.

[25] a) F. Ono, K. Qiao, D. Tomida and C. Yokoyama, *J. Mol. Catal. A: Chem.* **2007**, *263*, 223-226; b) X. Pan, Z. Liu, R. Cheng, X. He and B. Liu, *J. Organomet. Chem.* **2015**, *775*, 67-75.

[26] S. Supasitmongkol and P. Styring, *Catal. Sci. Tech.* **2014**, *4*, 1622-1630.

[27] J. Liu, W.-M. Ren, Y. Liu and X.-B. Lu, *Macromolecules* **2013**, *46*, 1343-1349.

[28] Y. Ren, C.-H. Guo, J.-F. Jia and H.-S. Wu, *J. Mol. Catal. A: Chem.* **2011**, *115*, 2258-2267.

[29] a) J. E. Dengler, M. W. Lehenmeier, S. Klaus, C. E. Anderson, E. Herdtweck and B. Rieger, *Eur. J. Inorg. Chem.* **2011**, *2011*, 336-343; b) D. J. Darensbourg, J. C. Yarbrough, C. Ortiz and C. C. Fang, *J. Am. Chem. Soc.* **2003**, *125*, 7586-7591.

[30] C. Miceli, J. Rintjema, E. Martin, E. C. Escudero-Adán, C. Zonta, G. Licini and A. W. Kleij, *ACS Catal.* **2017**, 2367-2373.

Chapter 4

4 Synthesis of Amino-Phenolate Manganese Complexes and Their Catalytic Activity in Carbon Dioxide Activation and Oxidation Reactions

A version of this chapter has been submitted

Ali Elkurtehi, and Francesca M. Kerton

Submitted to Catalysis Science & Technology

Some modifications were made to the original paper for inclusion as a chapter in this thesis.

4.1 Introduction

Amino-phenolate ligands are easily tailored in terms of their electronic and steric properties, and with their combination of donors they are readily suited for coordination with metals from across the periodic table.[1] Group 4 complexes of these ligands have shown exceptional reactivity and control in olefin polymerization catalysis.[2] Similarly, catalysts for ring-opening polymerization of cyclic esters such as lactide have been extensively developed using this class of ligand.[3] More recently, rare earth and alkaline earth complexes of such ligands have been used in hydrophosphination reactions.[4]

There has been a growing trend towards the use of the lighter 3d transition metals in catalysis.[5] V, Cr, Fe and Co complexes of amino-phenolate ligands have been successfully used to catalyze the reaction of CO_2 with epoxides to yield either cyclic carbonates or polycarbonates.[6] Mn is widely used in catalysis,[7] and especially well-known for its catalytic reactivity towards the oxidation of alkenes.[8] Recently, Mn amino-phenolate complexes have been used in ring-opening polymerization of lactide,[3b] but such complexes have not been explored as catalysts in other types of reaction despite their air- and moisture-stable nature.

Using this type of ligand, we report herein the synthesis and characterization of two Mn(III) complexes and their catalytic reactivity in the cycloaddition of CO_2 with epoxides, and in aerobic oxidation of 4-methoxybenzyl alcohol and 1,2-diphenyl-2-methoxyethanol. Both of these catalysed reactions are important in terms of sustainable development, as the former uses CO_2 as a renewable C1-feedstock and the latter are important in terms of developing ways to convert lignin into a renewable source of aromatic molecules. These two topics have been reviewed previously.[9] To date, several Mn-containing catalysts bearing salen, porphyrin or cyclen ligands have shown good activity in the production of cyclic carbonates.[10] The highest TOFs reported to date for such complexes is 233 h^{-1} for the conversion of propylene oxide (PO) to propylene carbonate using a homogeneous Mn(salen)Br catalyst and 255 h^{-1} for a silica-immobilized version of said catalyst.[10c] Recently, a Mn(salen)Cl catalyst was studied towards lignin depolymerization.[11] In this work, Butler, Foston and co-workers showed that for both a β-O-4 lignin model substrate and organosolv lignin polymerization occurred and only small amounts of small molecule organic products from the desired cleavage reactions could be obtained. Previously, supported Mn-porphyrin complexes have been used in biomimetic catalytic approaches for lignin peroxidase-type reactivity and although good substrate conversions could be achieved, the yields of products (when reported) were from the trace level up to 11.3%.[12] In the current chapter, in order to avoid some of the side reactions that lead to polymerization, I focused on less complex lignin model substrates and air as the oxidant as opposed to hydrogen peroxide.

4.2 Results and discussion

4.2.1 Synthesis and characterization of Mn complexes

The amino-bis(phenol) protio ligands $H_2[O_2N]^{BuBuBn}$ and $H_2[O_2NO]^{BuMeMeth}$ were prepared according to previously reported procedures.[13] The ligands used in the current study contain 2,4-alkyl-substituted phenols but one is tridentate, as it was prepared using benzylamine, and the other is tetradentate, as it contains a pendant methoxy group. A related Mn complex containing a pendant pyridyl group was previously reported and structurally characterized by Bouwman and co-workers.[14] Mn(III) complexes (**4.1** and

4.2) were synthesized *via* the reaction of the protonated ligands in a methanol-toluene mixture with one equiv of $Mn(acac)_3$ (Scheme 4-1). After refluxing for a few minutes, complexation of the manganese center occurs, as evidenced by a colour change of the reaction mixture from black/brown to red/brown. Red coloured solids were obtained in 70-85% yield. MALDI-TOF mass spectrometry was used as an initial test to confirm ligand coordination due to the paramagnetic nature of the Mn(III) centers,[15] and the remaining acac ligand was apparent in the spectra of the crude products. The purified complexes were characterized using MALDI-TOF mass spectrometry, UV-vis spectroscopy, IR spectroscopy, melting point determinations, magnetic susceptibility measurements and elemental analysis (see Appendix for representative spectra). (**4.1** and **4.2**) are air stable and non-hygroscopic, but unfortunately crystals suitable for single crystal X-ray diffraction analysis could not be grown.

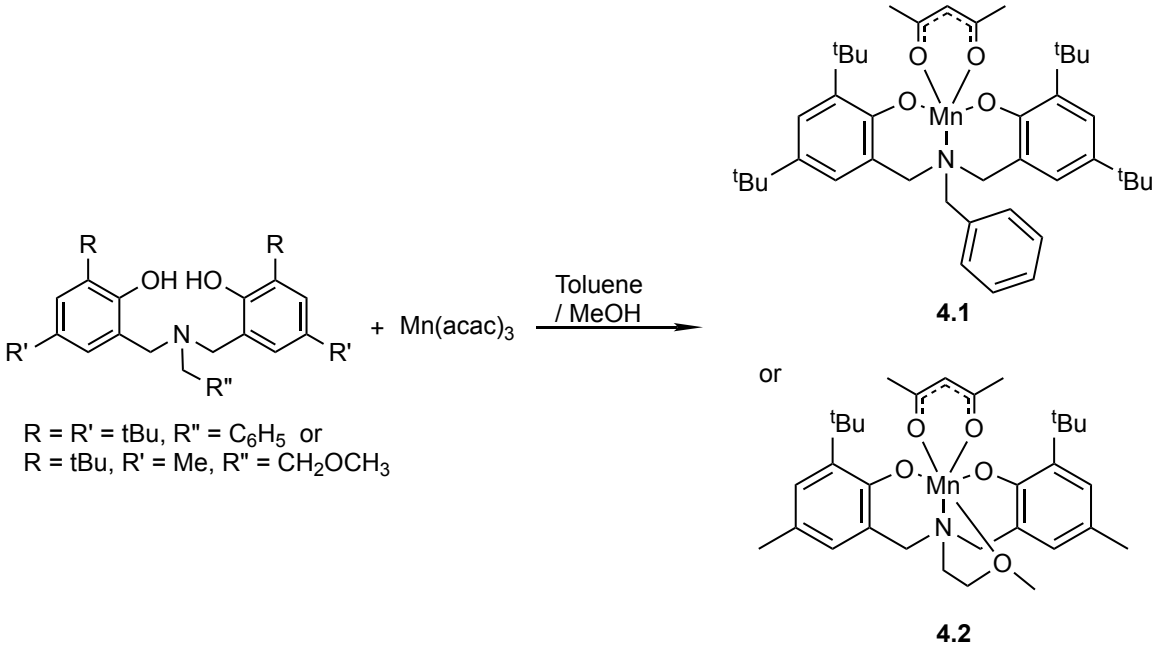

Scheme 4-1. Synthesis of manganese complexes **4.1** and **4.2**

The MALDI-TOF mass spectra were obtained via charge transfer ionization in the presence of the neutral UV-absorbent matrix anthracene.[15-16] The mass spectra generated for the Mn(III) complexes described herein showed characteristic fragment ions. In particular they exhibited peaks at *m/z* 696.31 and 579.19, which corresponded to the expected molecular ions for $\{Mn(acac)[O_2N]^{BuBuBn}\}^{+\cdot}$ (**4.1**) and $\{Mn(acac)[O_2NO]^{BuMeMeth}\}^{+\cdot}$ (**4.2**), respectively, thus indicating ligand coordination to the metal centers. The experimental isotopic distribution pattern for each of these ions shows good agreement with the theoretical patterns (Figures A4.1 and A4.2). Additional peaks in the lower mass region of the spectra correspond to ligand fragments.

Table 4-1. UV–Vis spectral data of the vanadium complexes in CH_2Cl_2

Complex	**$\pi \rightarrow \pi^*$** **λ /nm (ε /L mol^{-1}cm^{-1})**	**out-of-plane pπ →d** **λ /nm (ε /L mol^{-1}cm^{-1})**	**in-plane pπ →d** **λ /nm (ε /L mol^{-1}cm^{-1})**
4.1	248 (10900)	276 (115000)	684 (34000)
4.2	243 (99000)	252 (92000)	601 (56000)

The electronic absorption spectra for the complexes were recorded in CH_2Cl_2 and data are summarized in Table 4-1. The UV-vis spectra exhibit multiple intense bands in the UV and visible regions, and the electronic absorption spectra for the complexes are shown in (Figures A4.3 and A4.4). They exhibit intense absorptions energy bands at (<300 nm), attributed to $\pi \rightarrow \pi^*$ transitions involving the phenolate moieties and several ligand-to metal charge transfer (LMCT) transitions from the phenoxo to Mn(III) in the region 300–500 nm, which have also observed for a variety of other Mn(III) complexes with phenolate ligands.[17] Specifically these were assigned to charge transfer transitions from the out-of-plane pπ orbital (HOMO) of the phenolate oxygen to the ($3d^4$) $d_{x^2-y^2}/d_{z^2}$ orbital of Mn(III). The lowest energy bands (visible region) between 450 and 580 nm arise from charge-transfer transitions from the in-plane pπ orbital of the phenolate to the

($3d^4$) dπ* orbital of Mn(III) that are observed as a tail and result in the intense red-black colour of the complexes. In these complexes, the d–d transitions peaks are not visible due to their overlapping with the LMCT transitions.[18]

Infrared spectra of (**4.1** and **4.2**) show many strong bands within 400–1600 cm^{-1} and the assignment of all these vibrations has not been attempted. The protio ligands exhibit bands in the region 1251–1274 cm^{-1} which can be attributed to phenolic ν_{C-O} stretching vibrations. The coordination of the ligands through the phenolate oxygens to Mn is confirmed by an increase in ν_{C-O} stretching frequencies to ~1300 cm^{-1}. This was further supported by the disappearance of the ν_{OH} band in the range 3440–3445 cm^{-1} in the complexes and the presence of an intense band at ~1600 cm^{-1} assigned to the $\nu_{C=O}$ of the acac ligand. The bands at ~3000 cm^{-1} are assigned to aromatic C-H stretches. Further, the complexes show strong bands corresponding to ν_{Mn-N} and ν_{Mn-O} in the region 400–450 cm^{-1} and 500– 550 cm^{-1}, respectively. All these vibrations are in the normal range for similar linkages.[18-19]

Magnetic susceptibility data for powdered samples of compounds **(4.1** and **4.2)** were measured at room temperature using a Johnson-Matthey balance. Compound **(4.1)** exhibited a moment of 4.7μ_B, which is consistent with a high spin d^4 ions and within the normal range for a discrete high-spin octahedral Mn(III) complex having significant spin–orbit coupling.[17e, 20] However, strangely compound **(4.2)** exhibited a moment of only 3.4μ_B, which is significantly lower than that expected for high spin d^4 ions and higher than that expected for a low spin configuration. Further studies would be required to ascertain the origin of this behaviour, as elemental analysis and all other data suggest similar structures (and therefore electronic structures) for (**4.1** and **4.2**).

4.3 Catalytic Performance

4.3.1 Reaction of Epoxides with Carbon Dioxide

Complexes (**4.1** and **4.2**) were soluble in the neat substrate; therefore, the reactions were carried out without additional solvent. Initially, the catalytic activity of (**4.1** and **4.2**) in the coupling of propylene oxide (PO) with CO_2 to produce propylene carbonate (PC) was investigated as a model reaction. The formation rates of the cyclic carbonate were monitored by using in situ FT-IR spectroscopy, ν(C=O) of the cyclic carbonate at ~1815 cm^{-1} (Figure 4.1). Despite (**4.1**) containing a tridentate aminophenolate ligand and (**4.2**) containing a tetradentate ligand, they displayed almost identical catalytic activity (Figure 4.2). This many be due to the weak coordinating ability of the pendant methoxy group within (**4.2**), which means that the ligand behaves in a similar fashion to a formally tridentate ligand such as that in (**4.1**). Similar effects resulting from weakly coordinating ethereal donors in aminophenolate catalysts for this and related polymerization reactions have been reported previously.[6a, c] Using (**4.2**), to obtain optimum reaction conditions, the reaction parameters (effects of co-catalyst, temperature, catalytic loading and reaction time on the yield of cyclic carbonate) were varied. Neutral or ionic co-catalysts such as (4-dimethylamino)pyridine (DMAP), bis(triphenylphosphoranylidene)ammonium chloride (PPNCl) and tetrabutylammonium bromide (TBAB) were employed as co-catalysts. The initial reaction conditions assessed were 20 bar CO_2, 80 °C using a 0.2 mol% complex and 0.2 mol% co-catalyst over 18 h, as we had used similar conditions in vanadium catalyzed reactions.[6a] Both (**4.1** and **4.2**) in combination with TBAB catalyzed the coupling of CO_2 and PO (and the other epoxides tested) to produce the cyclic carbonate selectively. The reaction mixtures were analyzed by ^1H NMR spectroscopy in order to determine conversions. Catalytic results using (**4.2**) are summarized in Table 4-2.

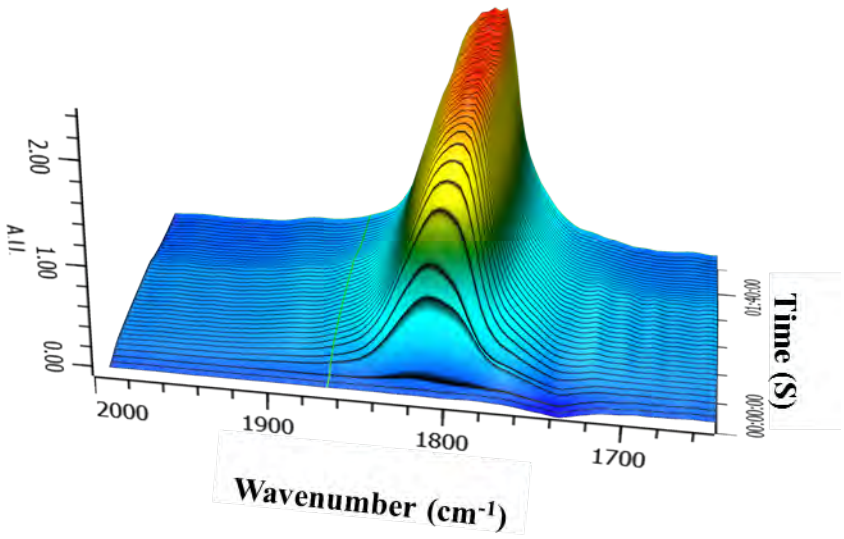

Figure 4.1. Surface diagram showing the growth over time of the carbonyl group of propylene carbonate at 1815 cm^{-1}. No sign of polycarbonate peak at 1750 cm^{-1}. Reaction conditions: 20 bar CO_2, 120 °C, [Mn]: [PO]: [TBAB] = 1:500:2

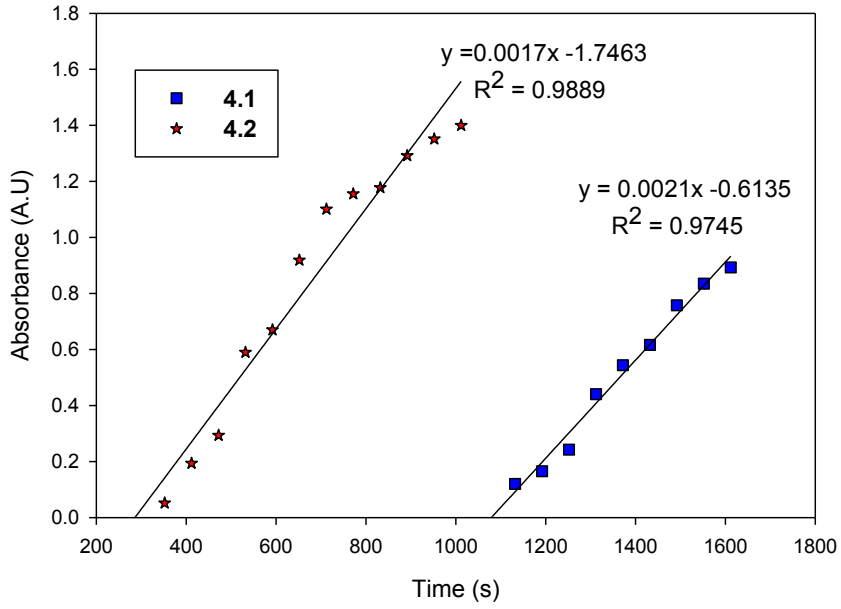

Figure 4.2 Initial rates of reactions during the first hour based on absorbance of the (C=O) of cyclic carbonate via monitoring of the absorbance band of the cyclic carbonate C=O band at 1810 cm^{-1}. **4.1** (■, y = 0.0017x - 0.5144, R^2 = 0.9889), **4.2** (★, y = 0.0021x – 0.6135, R^2 = 0.9745) represent best fits of a linear model. Reaction conditions: 20 bar CO_2, 120 °C, [Mn]: [PO]: [TBAB] = 1:500:2. Note: intercepts on x axis for **4.1** and **4.2** are different and neither through origin, as this represents the time taken for the autoclave to achieve the reaction temperature.

Table 4-2. Cyclic carbonate synthesis catalyzed by **4.2**.[a]

Entry	Epoxide, S	Co-catalyst	[Mn]:[S]:[Cocat]	T (°C)	Time (h)	Conv. (%)	TON	TOF (h^{-1})
1	PO	-	1:500:0	80/120	18	0	0	0
2	PO	TBAB	0:500:1	80/120	18	0	0	0
3	PO	DMAP	1:500:1	80(120)	18	35(55)	275	15
4	PO	PPNCl	1:500:1	80(120)	10	81(100)	500	50
5	PO	TBAB	1:500:1	80(120)	10	71(90)	500	50
6	PO	TBAB	1:500:2	120	5	100	500	100
7	PO	TBAB	1:500:3	120	5	80	400	80
8	PO	TBAB	1:2000:2	120	5	87	1740	348
9	PO	TBAB	1:4000:2	120	18	100	4000	222
10	PO	TBAB	1:6000:2	120	12	62	3720	310
11	PO	TBAB	1:6000:2	120	24	100	6000	300
12	SO	TBAB	1:500:2	120	7	100	500	71
13	CHO	TBAB	1:500:2	120	18	91	455	25

a. Reaction conditions: 100 mL Parr reactor, epoxide (50 mmol) at mol ratios indicated above [Mn]:[Substrate]:[Co-catalyst]. Conversions determined by 1H NMR spectroscopy. TON=overall turnover number ($mol_{epoxide\ converted}/mol_{Mn}$). TOF=overall turnover frequency (TON/reaction time).

4.3.2 Influence of reaction parameters on conversion of PO

It is well-known that Lewis basic (nucleophilic) co-catalysts play an essential role in these cycloaddition reactions;[21] therefore, the catalytic activity of various co-catalysts alongside (**4.2**) were evaluated (Table 4-2, entries 1-5). In the absence of either co-catalyst or catalyst (Table 4-2, entries 1-2), no conversion was observed even at 120 °C. Among the three co-catalysts, the highest conversion was observed using PPNCl, which showed greater activity with 100% conversion and total selectivity towards cyclic carbonate within 10 h. However, as TBAB leads to similarly active catalyst systems and

is soluble in the epoxides and PPNCl is not, TBAB was employed as the co-catalyst in all the other work reported herein. If the amount of TBAB was doubled to 2 equiv per Mn center, 100% PO conversion was achieved within 5 h at 120 °C (Table 4-2, entry 6). Further increasing the amount of TBAB used led to a decrease in conversion. This optimum ratio of Mn and TBAB is consistent with other work using a Mn complex for similar reactions.[22] On decreasing the catalyst loading from 1:500 - 1:6000 [Mn]:[PO] the binary catalyst system was still active albeit requiring a longer reaction time to achieve quantitative conversion (Table 4-2, entries 8-11). This suggests that the catalyst system is very stable and may be able to achieve TONs in excess of those observed in this study (i.e. > 6000) but the TOF will be limited to ~300 h^{-1}.

The effect of the reaction temperature on PO conversion catalyzed by the **4.2**/TBAB system was monitored by in situ infrared spectroscopy. At room temperature, no PO conversion was observed. By increasing the temperature to 40 °C, the absorbance at 1815 cm^{-1} started to grow in a very slow manner. From the kinetic data at this and subsequently increased temperatures, as illustrated in (Figure 4.3), the activation energy for the PC formation could be determined. The activation energy for PC formation using the **4.2**/TBAB catalyst system was 64.39 ± 0.16 kJ mol^{-1} at 20 bar of CO_2 pressure. This value was similar to others reported in the literature for the same reaction using different catalysts (range of about 35-70 kJ mol^{-1}).[6a, 23]

The cycloaddition of CO_2 with CHO and SO using the **4.2**/TBAB catalyst system was examined at 120 °C and 20 bar (initial CO_2 pressure). For SO (Table 4-2, entry 12), 100% conversion to the corresponding cyclic carbonate within 7 h was achieved, which is only a slightly longer reaction time than that needed to achieve a similar conversion of PO. In contrast, 91% conversion of CHO could only be achieved after 18 h (Table 4-2, entry 13). This is typical for catalysts in this in field and is due to the decreased rate of epoxide ring-opening resulting from the bicyclic nature of this substrate – see Chapter 3 for data on a related vanadium-containing catalyst system.

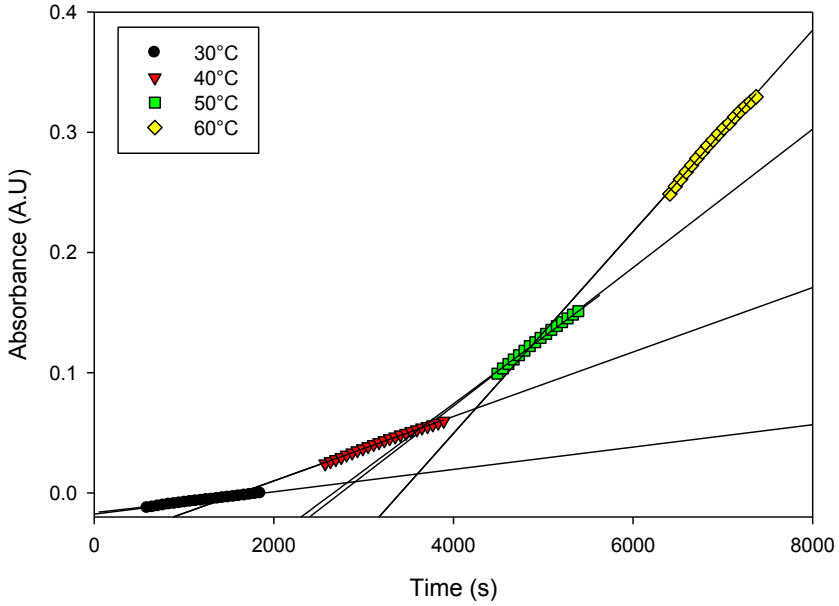

Figure 4.3. Temperature dependence of the initial rates of reaction based on the C=O absorbance of PC. Using 4.2 at 20 bar and [V]:[PO]:[Co-cat] 1:500:2, at 30 °C ● (y = 0.000008372x – 0.0164, R^2 = 0.9358), at 40 °C ▼ (y = 0.00002681x – 0.0436, R^2 = 0.9973), at 50 °C ■ (y = 0.00005545x - 0.1477, R^2 = 0.9974), at 60 °C ♦ (y = 0.00008388x – 0.2861, R^2 = 0.9964)

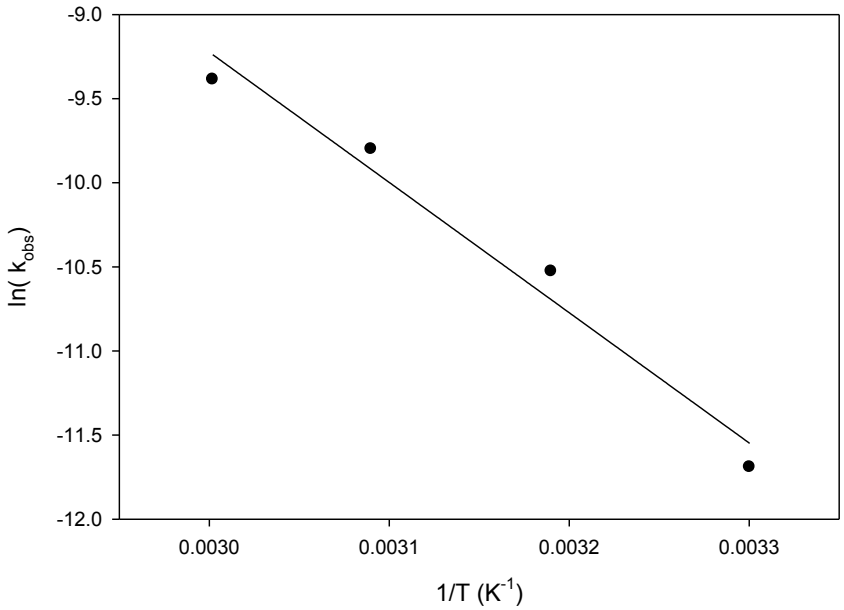

Figure 4.4. Arrhenius plot for the formation of propylene carbonate using variable temperature data presented in Figure 4.3. Straight line: y = -7744.92x + 14.01, R^2 = 0.9724

4.3.3 Catalytic aerobic oxidation reactions

The catalytic activities of (**4.1** and **4.2**) for oxidation reactions were also investigated. Even though (**4.1** and **4.2**) exhibited good performances in the reactions of epoxides and CO_2, their activities in catalytic oxidation reactions were somewhat disappointing given the precedence of Mn catalysts in this field. Two reactions were explored, namely aerobic oxidation of a benzylic alcohol to yield the corresponding aldehyde and oxidative C-C bond cleavage in 1,2-diphenyl-2-methoxyethanol, which is commonly used as a model compound for lignin. In both reactions, the complex containing the tridentate ligand, (**4.1)**, was moderately more reactive than (**4.2**), which contained a tetradentate aminophenolate ligand.

Inspection of the results for the oxidation of 4-methoxybenzylalcohol in Table 4-3 clearly showed the importance of an additional base as well as temperature on the

catalytic performance. The highest yield of aldehyde was observed using (**4.1**) at 140 °C, which afforded 40% yield after 72 h (Table 4-3, entry 4). To assess the potential influence of the solvent on the oxidation reactions, the aerobic oxidation was also performed in acetonitrile-d_3 and 20% yield of aldehyde was obtained even after a longer reaction time compared with reactions in toluene-d_8 (Table 4-3, entry 5). These results contrast with the results we obtained for reactions using V(V) catalysts under similar conditions where quantitative conversions were obtained.[24]

Table 4-3. Aerobic oxidation of 4-methoxybenzylalcohol using 4.1 or 4.2

Entry [a]	Additive	T (°C)	Time (h)	Yield (%)[b]
1	none	80	72	trace
2	NEt_3	80	72	(**4.1**) 15 (**4.2**) 10
3	NEt_3	100	72	(**4.1**) 20 (**4.2**) 18
4	NEt_3	140	72	(**4.1**) 40 (**4.2**) 35
5[c]	NEt_3	120	106	(**4.1**) 20

[a.] Conditions: 2 mol% **4.1** or **4..2**, 10 mol% NEt_3 (as appropriate), toluene-d_8. Mn complex identified in parentheses. [b.] Yield determined by ^{1}H NMR spectroscopy (internal standard *p*-xylene). [c.] Acetonitrile-d_3 used in place of toluene-d_8.

For the aerobic oxidation of the simple lignin model, 1,2-diphenyl-2-methoxyethanol, the two Mn(III) catalysts showed similar performances in terms of conversion to V(V) catalysts previously explored.[24] It should be noted that in such reactions, the total theoretical yield of aromatic products sums to 200% because of the two phenyl groups in the lignin model. In the current study, the best result was obtained using (**4.1**) (5 mol% loading, 100 °C, toluene-d_8) and the reaction cleanly converted the model compound to methyl benzoate **C** (46%) and benzaldehyde **D** (90%) with no evidence of the ketone intermediate and negligible quantities of benzoic acid **E** (0.3%), Scheme 4-2. These results contrast with those of the previously reported aminophenolate V(V) catalysts, where approximately equimolar amounts of **C** and **D** were obtained and 3% **E**,[24] and dipicolinate V(V) catalysts where the ketone intermediate **A** was always observed and the major products were either **D** (in DMSO) or **C**/**E** (in pyridine).[25] These data suggest that the Mn(III) catalysts are less efficient at oxidizing the aldehyde to the carboxylic acid, which leads to a build up in the amount of aldehyde produced.

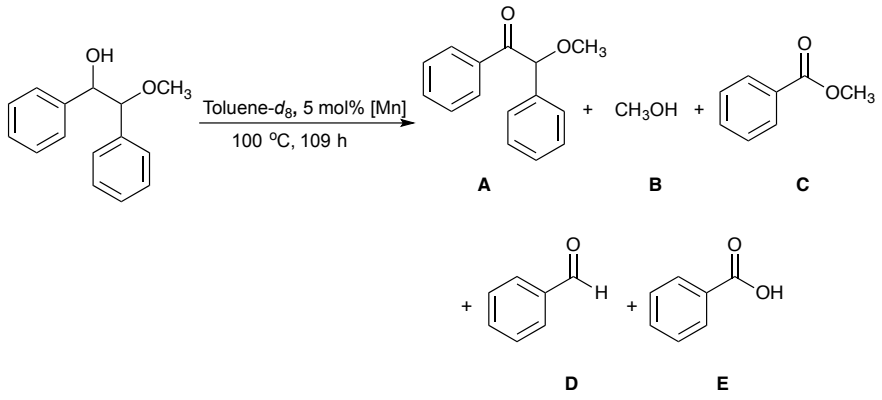

Scheme 4-2. Possible products produced during aerobic oxidation of 1,2-diphenyl-2-methoxyethanol

Table 4-4. Aerobic oxidation of 1,2-diphenyl-2 methoxyethanol using **4.1** or **4.2**

Entry [a]	Conv (%)	Cat	Yield of products [b]				
			A	**B**	**C**	**D**	**E**
1	95	**4.1**	-	-	46	90	0.3
2	85	**4.2**	-	-	33	88	0.2

[a.] Conditions: 5 mol% **4.1** or **4.2**, 100 °C, 109 h, toluene-d_8. [b.] Yield determined by ^{1}H NMR spectroscopy (internal standard *p*-xylene). Up to 5 potential products can be formed as identified in Scheme 2.

4.4 Conclusions

TONs of up to 6000 were achieved for the production of PC from PO and CO_2. This high TON reflects the stability of Mn amino-phenolate complexes towards air, moisture and temperature. Although the highest TOF achieved herein was ~350 h^{-1}, this is significantly higher than values reported for other Mn catalysts in this reaction and shows that this metal holds promise for future catalyst developments in this field. For example, one can envisage a Mn catalyst capable of both alkene epoxidation and carbonate formation in a single-pot process. For aerobic oxidation reactions, the catalysts showed sluggish reactivity but displayed selectivity contrasting to existing catalyst systems in the oxidative C-C bond cleavage of 1,2-diphenyl-2-methoxyethanol where an aldehyde was formed as the major product. Interestingly, the complexes containing tridentate and tetradentate ligands showed similar reactivity, which we suggest is due to the weak coordinating ability of the methoxy group within the tetradentate ligand.

4.5 Experimental

4.5.1 General methods and materials

Starting materials for all syntheses were purchased from Strem, Aldrich or Alfa Aesar and used as received. Ligands and the reagent 1,2-diphenyl-2-methoxyethanol were prepared via literature procedures.[13, 25] PO, SO and CHO were purchased from Aldrich. CO_2 was supplied from Praxair in a high-pressure cylinder equipped with a liquid dip tube. HPLC grade solvents were used as purchased. All syntheses were performed under ambient laboratory atmosphere unless otherwise specified. All coupling reactions were carried out in a 100 mL stainless steel Parr® 5500 autoclave reactor with a Parr® 4836 controller. *N.B.* Caution should be taken when operating high-pressure equipment. All ^{1}H and ^{13}C NMR spectra were obtained in $CDCl_3$ purchased from Cambridge Isotope Laboratories, Inc. NMR spectra were recorded on a Bruker Avance III-300 spectrometer and referenced internally to TMS. MALDI-TOF mass spectra were recorded in reflectron mode on an Applied Biosystems 4800 MALDI TOF/TOF instrument equipped delayed ion extraction and high performance nitrogen laser (355 nm). Samples were prepared at a concentration of 0.02 mg L^{-1} in toluene. Anthracene was used as the matrix, which was mixed at a concentration of 0.02 mg L^{-1}. UV-vis spectra were recorded on an Ocean Optics USB4000+ spectrophotometer. GC-MS data were obtained on an Agilent Technologies 7890 GC with 5975 MSD. Elemental analyses were carried out by Canadian Microanalytical Service Ltd, Delta, BC, Canada. Room temperature magnetic measurements were made using a Johnson-Matthey magnetic susceptibility balance.

4.5.2 Synthesis of manganese complexes

Synthesis of (**4.1**) $H_2[O_2N]^{BuBuBn}$ (1.00 g, 1.84 mmol) was dissolved in a mixture of methanol and toluene (50/50 v/v, 20 mL) in an Erlenmeyer flask. $[Mn(acac)_3]$ (0.648 g, 1.84 mmol) was dissolved in 20 mL of methanol in another Erlenmeyer flask. The ligand solution was added to the $[Mn(acac)_3]$ solution with stirring. The solution immediately darkened and the mixture was heated to reflux overnight to yield a red-black solution. Volatiles were removed under vacuum and a dark black solid was obtained, which could

be further purified by dissolution in CH_2Cl_2 and precipitation using pentane (0.934 g, 73%). mp 187-190 ºC. Anal. calc'd for $C_{42}H_{58}MnNO_4$: C 72.18; H 8.42; N 1.97. Found: C 72.40; H, 8.80; N 2.00. UV-vis (CH_2Cl_2) λ_{max}, nm (ε, $Lmol^{-1}cm^{-1}$) : 248 (10900), 276 (115000), 684 (34000). MS (MALDI-TOF) *m/z*: 695.31, $M^{+\cdot}$. μ_{eff} (solid, 25 ºC) = 4.7 μ_B.

Synthesis of (**4.2**) Compound (**4.2**) was prepared in a similar fashion to (**4.1**). It was isolated as a red-black solid (1.085 g, 80%). mp 175-178 ºC. Anal. calc'd for $C_{32}H_{46}MnNO_5$:C 66.31; H 8.00; N 2.42. Found: C 65.99; H 8.12; N 2.76. UV-vis (CH_2Cl_2) λ_{max}, nm (ε, $Lmol^{-1}cm^{-1}$) : 243 (99000), 252 (92000), 601 (56000). MS (MALDI-TOF) *m/z*: 579.19, $M^{+\cdot}$. μ_{eff} (solid, 25 ºC) = 3.4 μ_B.

4.5.3 General Procedure of Coupling Reaction of Epoxides and CO_2

The appropriate amounts of the liquid epoxide and the catalyst were added *via* a long-needled syringe to a 100 mL Parr® reactor, which was pre-dried under vacuum overnight at 80 °C. The appropriate pressure of CO_2 was then added into the reactor. The autoclave was heated to the desired temperature with stirring. After the desired time, the autoclave was slowly cooled down and after reaching room temperature, it was vented in a fume hood. This decompression was carried out very slowly, in order to allow the liquid phase to degas properly and to avoid the loss of reaction mixture. After this, the autoclave was opened and a sample was taken immediately for the determination of conversion by NMR (by integration of the peaks from the product relative to the starting epoxide).

4.5.4 General procedure for the catalytic aerobic oxidation of 4-methoxybenzyl alcohol.

In a 20 mL microwave vial equipped with a stir bar, 4-methoxybenzyl alcohol (69 mg, 0.50 mmol) was combined with the Mn complex (**4.1** or **4.2**, 0.01 mmol, 2 mol%, prepared as a standardised solution in toluene-d_8), NEt_3 (7 μL, 0.05 mmol, 10 mol%), and *p*-xylene (5 μL, 0.041 mmol) as an internal standard. The mixture was dissolved in

toluene-d_8 (1 mL) under air and was sealed. The reaction mixture was heated with stirring using an oil bath at the appropriate temperature for the desired time. The reaction mixture was cooled to room temperature, and the yield of oxidized product (4-methoxybenzaldehyde) was determined by integration of its peaks in the ^{1}H NMR spectra relative to those of the internal standard.

4.5.5 General procedure for the catalytic aerobic oxidation of 1,2-diphenyl-2-methoxyethanol

In a 20 mL microwave vial equipped with a stir bar, 1,2-diphenyl-2-methoxyethanol (29.8 mg, 0.131 mmol) was combined with a Mn complex (**4.1** or **4.2**, 0.0066 mmol, 5 mol%, prepared as a standardised solution in toluene-d_8), and *p*-xylene (5 μL, 0.041 mmol) as an internal standard. The mixture was dissolved in toluene-d_8 (1 mL) and the vial was sealed. The reaction mixture was heated with stirring using an oil bath for the desired time at the appropriate temperature. The reaction mixture was cooled to room temperature, and the yields of oxidized products were determined by integration of the ^{1}H NMR spectra. Product identities were further confirmed via GC-MS analyses.

4.6 References

[1] O. Wichmann, R. Sillanpää and A. Lehtonen, *Coord. Chem. Rev.* **2012**, *256*, 371-392.

[2] a) E. Y. Tshuva, I. Goldberg and M. Kol, *J. Am. Chem. Soc.* **2000**, *122*, 10706-10707; b) E. Y. Tshuva, I. Goldberg, M. Kol, H. Weitman and Z. Goldschmidt, *Chem. Commun.* **2000**, 379-380; c) E. Y. Tshuva, I. Goldberg, M. Kol and Z. Goldschmidt, *Organometallics* **2001**, *20*, 3017-3028; d) S. Groysman, I. Goldberg, M. Kol, E. Genizi and Z. Goldschmidt, *Organometallics* **2003**, *22*, 3013-3015; e) S. Groysman, E. Y. Tshuva, I. Goldberg, M. Kol, Z. Goldschmidt and M. Shuster, *Organometallics* **2004**, *23*, 5291-5299; f) S. Segal, I. Goldberg and M. Kol, *Organometallics* **2005**, *24*, 200-202.

[3] a) J.-M. E. P. Cols, C. E. Taylor, K. J. Gagnon, S. J. Teat and R. D. McIntosh, *Dalton Trans.* **2016**, *45*, 17729-17738; b) P. Daneshmand and F. Schaper, *Dalton Trans.* **2015**, *44*, 20449-20458; c) L. Wang, C. E. Kefalidis, S. Sinbandhit, V. Dorcet, J.-F. Carpentier, L. Maron and Y. Sarazin, *Chem. - Eur. J.* **2013**, *19*, 13463-13478; d) S. C. Rosca, D. A. Rosca, V. Dorcet, C. M. Kozak, F. M. Kerton, J. F. Carpentier and Y. Sarazin, *Dalton Trans.* **2013**, *42*, 9361-9375; e) B. Liu, T. Roisnel, L. Maron, J.-F. Carpentier and Y. Sarazin, *Chem. - Eur. J.* **2013**, *19*, 3986-3994; f) V. Poirier, T. Roisnel, S. Sinbandhit, M. Bochmann, J.-F. Carpentier and Y. Sarazin, *Chem. - Eur. J.* **2012**, *18*, 2998-3013; g) Y. Sarazin, D. Rosca, V. Poirier, T. Roisnel, A. Silvestru, L. Maron and J.-F. Carpentier, *Organometallics* **2010**, *29*, 6569-6577; h) V. Poirier, T. Roisnel, J.-F. Carpentier and Y. Sarazin, *Dalton Trans.* **2009**, 9820-9827; i) N. Ikpo, C. Hoffmann, L. N. Dawe and F. M. Kerton, *Dalton Trans.* **2012**, *41*, 6651-6660; j) M. A. Sinenkov, G. K. Fukin, A. V. Cherkasov, N. Ajellal, T. Roisnel, F. M. Kerton, J. F. Carpentier and A. A. Trifonov, *New J. Chem.* **2011**, *35*, 204-212; k) M. P. Blake, A. D. Schwarz and P. Mountford, *Organometallics* **2011**, *30*, 1202-1214; l) H. E. Dyer, S. Huijser, N. Susperregui, F. Bonnet, A. D. Schwarz, R. Duchateau, L. Maron and P. Mountford, *Organometallics* **2010**, *29*, 3602-3621.

[4] I. V. Basalov, B. Liu, T. Roisnel, A. V. Cherkasov, G. K. Fukin, J.-F. Carpentier, Y. Sarazin and A. A. Trifonov, *Organometallics* **2016**, *35*, 3261-3271.

[5] R. M. Bullock in *Catalysis without Precious Metals*, *Vol.* Wiley-VCH Verlag GmbH & Co. KGaA, Weinheim, Germany, **2010**.

[6] a) A. I. Elkurtehi and F. M. Kerton, *ChemSusChem* **2017**, *10*, 1249-1254; b) D. Alhashmialameer, J. Collins, K. Hattenhauer and F. M. Kerton, *Catal. Sci. Technol.* **2016**, *6*, 5364-5373; c) K. Devaine-Pressing, L. N. Dawe and C. M. Kozak, *Polym. Chem.* **2015**, *6*, 6305-6315; d) H. Chen, L. N. Dawe and C. M. Kozak, *Catal. Sci. Tech.* **2014**, *4*, 1547-1555; e) A. Coletti, C. J. Whiteoak, V. Conte and A. W. Kleij, *Chem. Cat. Chem.* **2012**, *4*, 1190-1196; f) L. N. Saunders, N. Ikpo, C. F. Petten, U. K. Das, L. N. Dawe, C. M. Kozak and F. M. Kerton, *Catal. Commun.* **2012**, *18*, 165-167.

[7] a) J. R. Carney, B. R. Dillon and S. P. Thomas, *Eur. J. Org. Chem.* **2016**, *2016*, 3912-3929; b) D. A. Valyaev, G. Lavigne and N. Lugan, *Coord. Chem. Rev.* **2016**, *308*, 191-235.

[8] P. Saisaha, J. W. de Boer and W. R. Browne, *Chem. Soc. Rev.* **2013**, *42*, 2059-2074.

[9] a) C. Li, X. Zhao, A. Wang, G. W. Huber and T. Zhang, *Chem. Rev.* **2015**, *115*, 11559-11624; b) J. W. Comerford, I. D. V. Ingram, M. North and X. Wu, *Green Chem.* **2015**, *17*, 1966-1987; c) C. Maeda, Y. Miyazaki and T. Ema, *Catal. Sci. Technol.* **2014**, *4*, 1482-1497; d) N. Kielland, C. J. Whiteoak and A. W. Kleij, *Adv. Synth. Catal.* **2013**, *355*, 2115-2138; e) P. P. Pescarmona and M. Taherimehr, *Catal. Sci. Technol.* **2012**, *2*, 2169-2187; f) I. Omae, *Coord. Chem. Rev.* **2012**, *256*, 1384-1405; g) B. Acharya, I. Sule and A. Dutta, *Biomass Convers. Biorefin.* **2012**, *2*, 349-369; h) D. J. Darensbourg and S. J. Wilson, *Green Chem.* **2012**, *14*, 2665-2671; i) D. J. Darensbourg, *Chem. Rev.* **2007**, *107*, 2388-2410; j) S. K. Hanson and R. T. Baker, *Acc. Chem. Res.* **2015**, *48*, 2037-2048; k) M. S. Singhvi, S. Chaudhari and D. V. Gokhale, *RSC Adv.* **2014**, *4*, 8271-8277; l) G. Chatel and R. D. Rogers, *ACS Sustain. Chem. Eng.* **2014**, *2*, 322-339; m) S. Feng, S. Cheng, Z. Yuan, M. Leitch and C. Xu, *Renew. Sust. Energ. Rev.* **2013**, *26*, 560-578; n) P. Azadi, O. R. Inderwildi, R. Farnood and D. A. King, *Renew. Sust. Energ. Rev.* **2013**, *21*, 506-523; o) D. M. Alonso, S. G. Wettstein and J. A. Dumesic, *Chem. Soc. Rev.* **2012**, *41*, 8075-8098; p) J. C. Hicks, *J. Phys. Chem. Lett.* **2011**, *2*, 2280-2287.

[10] a) R. Srivastava, T. H. Bennur and D. Srinivas, *J. Mol. Catal.* **2005**, *226*, 199-205; b) L. Jin, H. Jing, T. Chang, X. Bu, L. Wang and Z. Liu, *J. Mol. Catal. A: Chem.* **2007**, *261*, 262-266; c) F. Jutz, J.-D. Grunwaldt and A. Baiker, *J. Mol. Catal. A: Chem.* **2008**, *279*, 94-103; d) F. Jutz, J.-D. Grunwaldt and A. Baiker, *J. Mol. Catal. A: Chem.* **2009**, *297*, 63-72.

[11] S. D. Springer, J. He, M. Chui, R. D. Little, M. Foston and A. Butler, *ACS Sustainable Chem. Eng.* **2016**, *4*, 3212-3219.

[12] a) C. Crestini, A. Pastorini and P. Tagliatesta, *J. Mol. Catal. A: Chem.* **2004**, *208*, 195-202; b) C. Crestini, A. Pastorini and P. Tagliatesta, *Eur. J. Inorg. Chem.* **2004**, 4477-4483.

[13] F. M. Kerton, S. Holloway, A. Power, R. G. Soper, K. Sheridan, J. M. Lynam, A. C. Whitwood and C. E. Willans, *Can. J. Chem.* **2008**, *86*, 435-443.

[14] R. van Gorkum, J. Berding, A. M. Mills, H. Kooijman, D. M. Tooke, A. L. Spek, I. Mutikainen, U. Turpeinen, J. Reedijk and E. Bouwman, *Eur. J. Inorg. Chem.* **2008**, 1487-1496.

[15] N. Ikpo, S. M. Butt, K. L. Collins and F. M. Kerton, *Organometallics* **2009**, *28*, 837-842.

[16] M. D. Eelman, J. M. Blacquiere, M. M. Moriarty and D. E. Fogg, *Angew. Chem. Int. Ed.* **2008**, *47*, 303-306.

[17] a) M. Hirotsu, M. Kojima, W. Mori and Y. Yoshikawa, *Bull. Chem. Soc. Japan* **1998**, *71*, 2873-2884; b) H. Biava, C. Palopoli, C. Duhayon, J.-P. Tuchagues and S. Signorella, *Inorg. Chem.* **2009**, *48*, 3205-3214; c) L. Dubois, D.-F. Xiang, X.-S. Tan, J. Pécaut, P. Jones, S. Baudron, L. Le Pape, J.-M. Latour, C. Baffert, S. Chardon-Noblat, M.-N. Collomb and A. Deronzier, *Inorg. Chem.* **2003**, *42*, 750-760; d) C. Hureau, L. Sabater, F. Gonnet, G. Blain, J. Sainton and E. Anxolabéhère-Mallart, *Inorg. Chim. Acta* **2006**, *359*, 339-345; e) G. N. Ledesma, H. Eury, E. Anxolabéhère-Mallart, C. Hureau and S. R. Signorella, *J. Inorg. Biochem.* **2015**, *146*, 69-76.

[18] N. Noshiranzadeh, M. Emami, R. Bikas, K. Ślepokura and T. Lis, *Polyhedron* **2014**, *72*, 56-65.

[19] a) A. Bartyzel, *J. Coord. Chem.* **2013**, *66*, 4292-4303; b) S. Brooker, S. S. Iremonger and P. G. Plieger, *Polyhedron* **2003**, *22*, 665-671; c) S. Kannan, K. N. Kumar and R. Ramesh, *Polyhedron* **2008**, *27*, 701-708.

[20] a) C.-M. Che and W.-K. Cheng, *J. Chem. Soc., Chem. Commun.* **1986**, 1443-1444; b) S. Biswas, K. Mitra, S. K. Chattopadhyay, B. Adhikary and C. R. Lucas, *Transit. Metal Chem.* **2005**, *30*, 393-398.

[21] W. Clegg, R. W. Harrington, M. North, F. Pizzato and P. Villuendas, *Tetrahedron: Asymmetry* **2010**, *21*, 1262-1271.

[22] P. Ramidi, C. M. Felton, B. P. Subedi, H. Zhou, Z. R. Tian, Y. Gartia, B. S. Pierce and A. Ghosh, *J. CO_2 Util.* **2015**, *9*, 48-57.

[23] a) G. W. Huber and A. Corma, *Angew. Chem. Int. Ed. Engl.* **2007**, *46*, 7184-7201; b) S. Supasitmongkol and P. Styring, *Catal. Sci. Tech.* **2014**, *4*, 1622-1630; c) S. Ghazali-Esfahani, H. Song, E. Paunescu, F. D. Bobbink, H. Liu, Z. Fei, G. Laurenczy, M. Bagherzadeh, N. Yan and P. J. Dyson, *Green Chem.* **2013**, *15*, 1584-1589; d) Y. Ren, C.-H. Guo, J.-F. Jia and H.-S. Wu, *J. Mol. Catal. A: Chem.* **2011**, *115*, 2258-2267; e) S. Gazi, W. K. Hung Ng, R. Ganguly, A. M. Putra Moeljadi, H. Hirao and H. S. Soo, *Chem. Sci.* **2015**, *6*, 7130-7142.

[24] A. I. Elkurtehi, A. G. Walsh, L. N. Dawe and F. M. Kerton, *Eur. J. Inorg. Chem.* **2016**, *2016*, 3123–3130.

[25] S. K. Hanson, R. T. Baker, J. C. Gordon, B. L. Scott and D. L. Thorn, *Inorg. Chem.* **2010**, *49*, 5611-5618.

Chapter 5

5 Conclusions and Future Work

Chapter 1 included an overview of the chemistry and literature reviews related to the research reported in this thesis. This includes the use of renewable feedstocks for chemical processes, which falls within the context of Green Chemistry. It presents a survey of the selective catalytic oxidation of lignin model compounds. Specifically, focusing on the oxidative cleavage of Cα-Cβ bonds as a means to depolymerize lignin and obtain useful aromatic compounds using transition metal complexes such as vanadium and manganese. In addition an introduction to CO_2 chemistry and literature overview on the advancement in catalytic coupling reaction of expoxides with CO_2 using transition metal complexes such as vanadium and manganese is included. Chapter 2 describes a set of four new vanadium (V) complexes of amino-bis(phenolate) ligands (**2.1**-**2.4**) and four structures determined by single crystal X-ray diffraction. Crystallography showed that some of the alkoxide derivatives decompose to yield oxo-bridged dimers (**2.5** and **2.6**) upon storage in air. All complexes showed great potential as catalysts for the aerobic oxidation of 4-methoxybenzylalcohol, affording 4-methoxybenzaldehyde. The results showed that **2.1** and **2.2** were more active catalysts, than the **2.3** and **2.4** and that could be due to formation of the bridged complexes during oxidation processes that might be catalytically inactive species. It should be noted that the base additive plays a pivotal role in the oxidation reaction. The vanadium complexes were tested for the oxidative C-C bond cleavage of 1,2-diphenyl-2-methoxyethanol, which afforded high conversion and benzaldehyde and methyl benzoate as the major products. It should be noted that the product distribution for the catalytic oxidation is dependent on the reaction solvents. In DMSO-d_6, pyr-d_5 or toluene-d_8 respectively **2.4** gave benzaldehyde in 90%, 1%, or 51% yield, methanol in 46%, 2%, or 0% yield, methyl benzoate in 36%, 67%, or 57% yield, and benzoin methyl ether in 18%, 15%, or 0% yield. Furthermore, the vanadium complexes the presence of H_2O_2 as the oxidant were also evaluated for the catalytic oxidative C-O bond cleavage of diphenylether, and

benzylphenylether. However, no selectivity in terms of C-O-C cleavage was observed and reactivity towards such bonds was poor; affording 10% and 9% yield of phenol, and 15% yield of benzaldehyde for benzylphenylether. Time-permitting, it would have been desirable to isolate larger quantities of **2.5** and **2.6**, and study the reactivity of these oxo-bridged complexes in more detail (i.e. confirm that they are not active catalysts).

Using base-metal catalysts and air as the oxidant for breaking carbon−carbon or carbon-oxygen bonds of lignin model compounds provides new opportunities to optimize activity and selectivity in transformations of the lignin. The results in this thesis provide more evidence for the potential utility of vanadium complexes in the selective oxidative disassembly of lignin. Future work should focus on more the detailed experimental and computational investigations to give information on possible detailed reaction mechanisms. Extension of this catalytic oxidation reaction to more complex model systems and actual lignin samples e.g. organosolv lignin should also be pursued.

Utilization of CO_2 is beneficial as it is an inexpensive, abundant feedstock with low toxicity, and it can react with epoxides to produce polycarbonates or cyclic carbonates. Cyclic carbonates can act as polar aprotic green solvents as well as chemical intermediates for the synthesis of other small molecules and polymers. Polycarbonates can be used to synthesize several biodegradable plastics. Many research groups have had success in this area using inexpensive, earth abundant metals with amino-phenolate ligands, and these complexes can be readily modified to control steric and electronic properties. Use of vanadium is desirable for this process as it is cheap, relatively abundant, non-toxic, and biocompatible. The activity of vanadium amino-bis(phenolate) complexes **2.1**–**2.4** towards cyclic carbonate formation in the coupling reactions of epoxides and CO_2 was described in Chapter 3. The influence of the CO_2 pressure, temperature, co-catalyst and of the catalyst:co-catalyst ratio were studied. The catalytic systems showed very good catalytic performance for the selective coupling of epoxides and CO_2 in the presence of ionic co-catalysts (TBAB and PPNCl) yielded the cyclic carbonate with no evidence of any polymer formation. However, no conversion was observed when DMAP was employed as the co-catalyst. Under optimized conditions

(120 °C and 20 bar CO_2), **2.2** could achieve a TOF of over 500 h^{-1} and a TON close to 4000 for propylene carbonate formation. The cycloaddition of CO_2 with other epoxides (styrene oxide, SO; cyclohexene oxide, CHO) using **2.2**/TBAB under the adopted conditions was also examined and the results showed that the catalyst is active for all the selected substrates and yielded the corresponding cyclic carbonate with high conversion and could achieve a TON of over 400 for both reactions. Furthermore, the kinetic measurements for the formation of PC, SC and CHC were undertaken. The activation energies for cyclic carbonate formation in the **2.2**/TBAB catalyst system are 48.2 ± 0.16 kJ mol^{-1}, 45.6 ± 0.21 kJ mol^{-1} and 54.7 ± 0.22 kJ mol^{-1} respectively. Further studies, including computational efforts, are needed to fully understand the reaction mechanisms and rate-determining steps in these and related reactions, and it would be interesting discoverg these catalytic systems for the oxidative coupling of ethylene or styrene and CO_2.

The activity of manganese (III) amino-bis(phenolate) complexes (**4.1**–**4.2**) towards cyclic carbonate formation in the coupling reactions of epoxides and CO_2 was described in Chapter 4. These complexes are air stable, easily synthesized, and cheap. They be used as catalysts in the absence of co-solvent and can tolerate multiple substrates and reaction conditions. The manganese catalysts in combination with different co-catalysts (TBAB and PPNCl) provided a highly efficient synthesis of propylene carbonate with 6000 TON value. In contrast to what was observed when DMAP employed as the co-catalyst along with vanadium complexes, the Mn-DMAP system showed moderate activity. In addition, a kinetic study for the coupling reaction of the formation of PC was performed. The activation energy for PC formation in the **4.2**/TBAB catalyst system was 64.39 ± 0.16 kJ mol^{-1} at 20 bar of CO_2 pressure. Although the two catalysts showed very good activity for the conversion of CO_2 and epoxides into cyclic carbonates, the catalysts showed poor reactivity toward the aerobic oxidation reactions. Interestingly, the aldehyde was formed as the major product and showed different catalytic selectivity toward the oxidative C-C bond cleavage of 1,2-diphenyl-2-methoxyethanol compared with other catalytic systems. Furthermore, there was no significant reactivity difference

between the complexes containing tridentate and tetradentate ligands, which we attribute due to the weak coordinating ability of the methoxy group within the tetradentate ligand. Further work is needed, both experimental and computational to clarify the relationship between ligand design (sterics and electronics, rigidity, denticity and donor lability), metal (including oxidation state) and catalyst activity for CO_2 and epoxide coupling reactions. The electronic and steric properties of amino-phenolate ligands can be tuned by adding various substituents to the backbone or the phenolate groups of the ligand. For example, the electron density at the metal center can be reduced by introducing electron-withdrawing groups (e.g. chloro, trifluoromethyl) as substituents on the phenolate rings. One can hypothesize that metal complexes of such ligands will have increased Lewis acidity at the metal center. This in turn will increase the extent of activation of the incoming reagent (epoxide) by the metal center and increase the rate of ring-opening.

6 Appendices

6.1 Appendix for Chapter 2

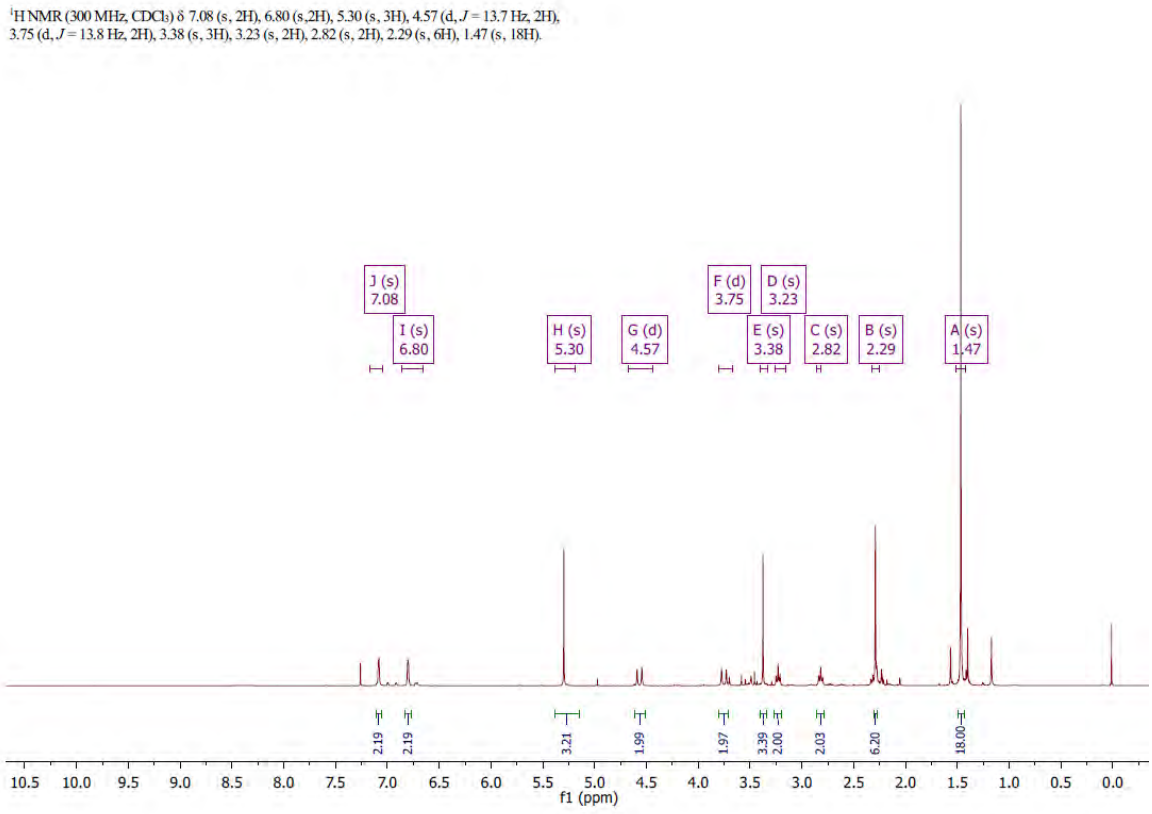

Figure A2. 1. ^{1}H-NMR of complex **2.1**

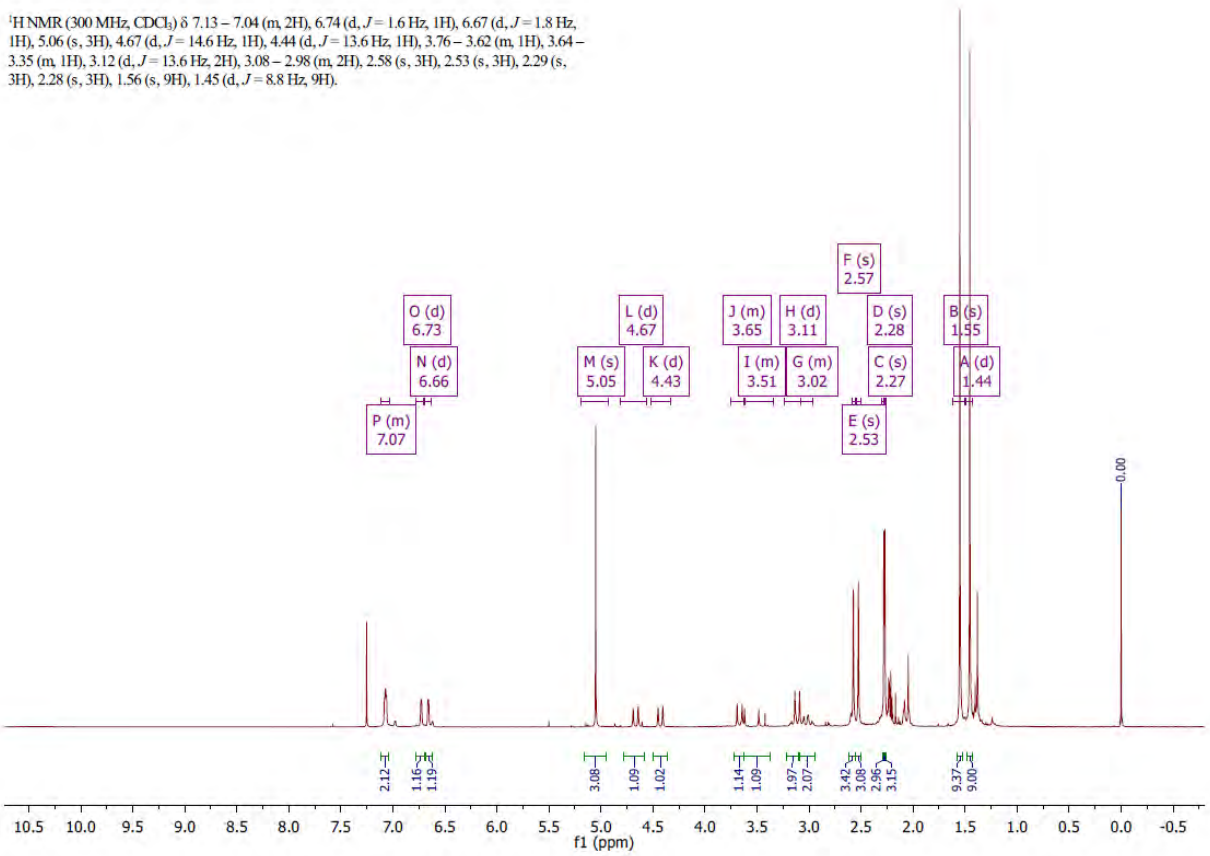

Figure A2. 2[1]H-NMR of complex **2.2**

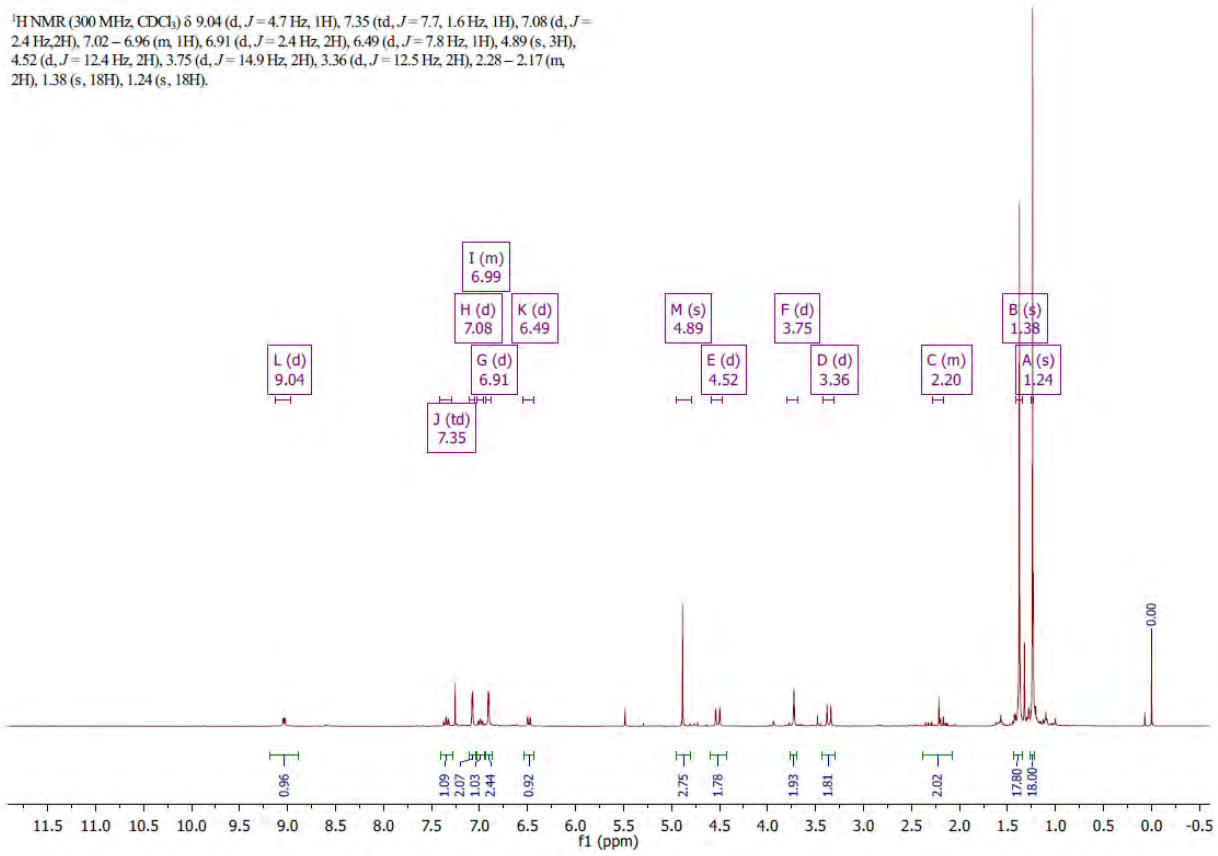

Figure A2. 3. ^{1}H-NMR of complex **2.3**

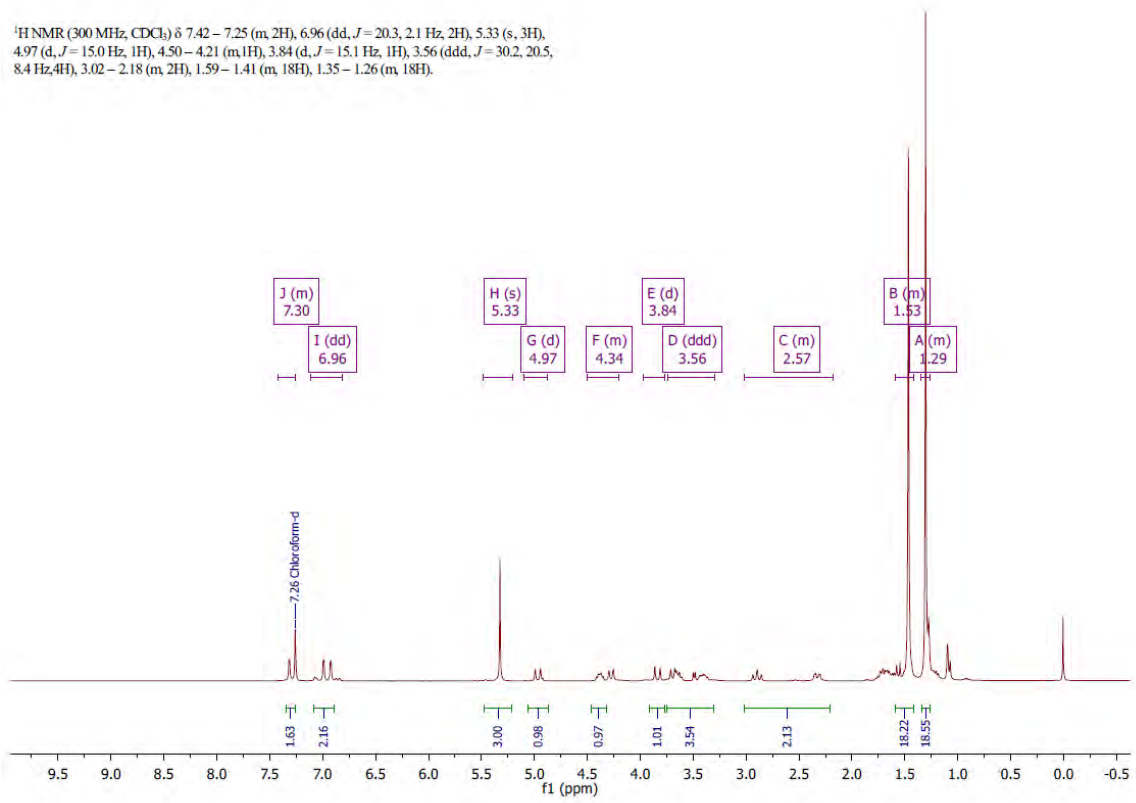

Figure A2. 4. [1]H-NMR of complex **2.4**

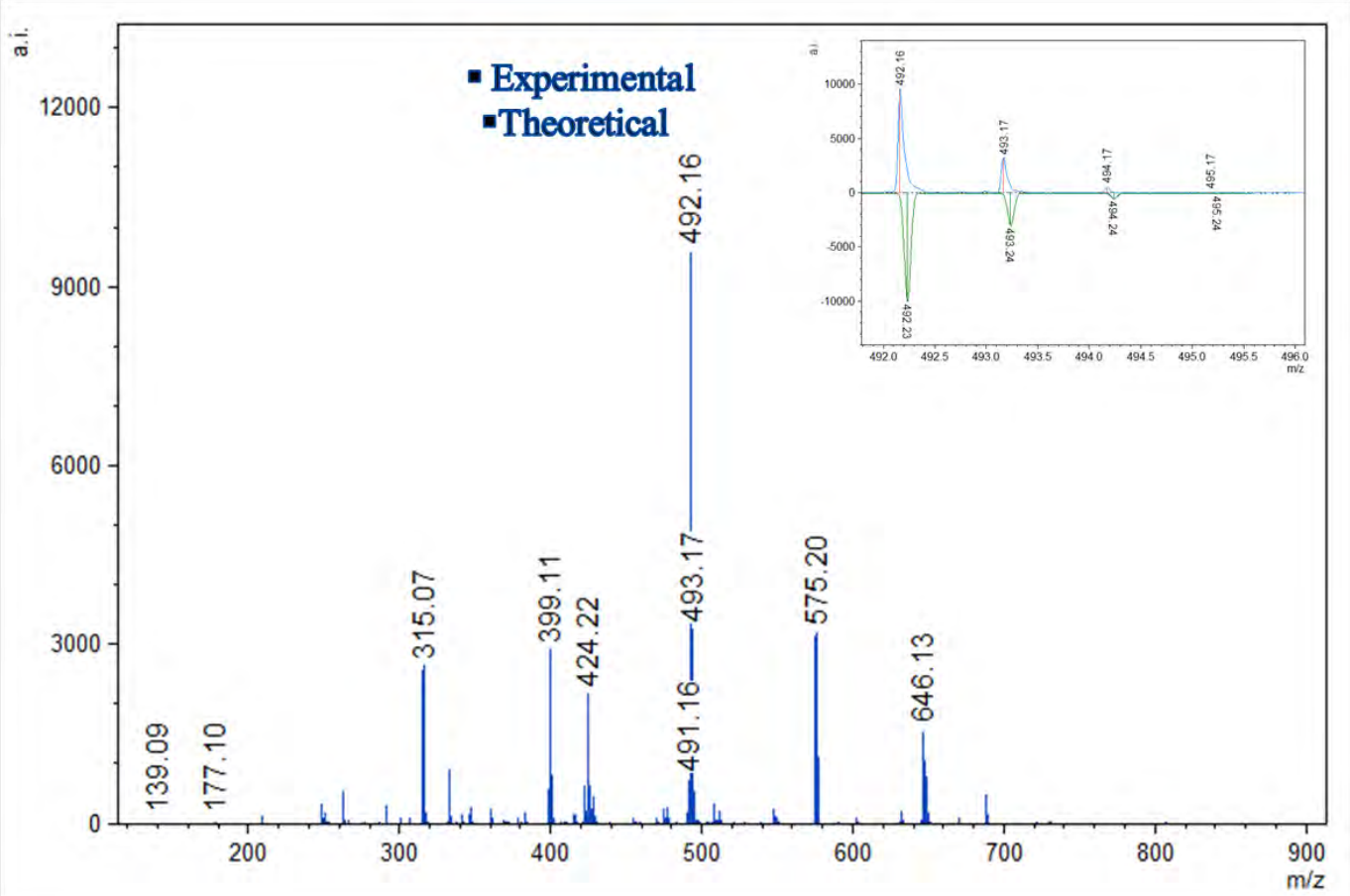

Figure A2. 5. MALDI-TOF mass spectrum of complex **2.1**

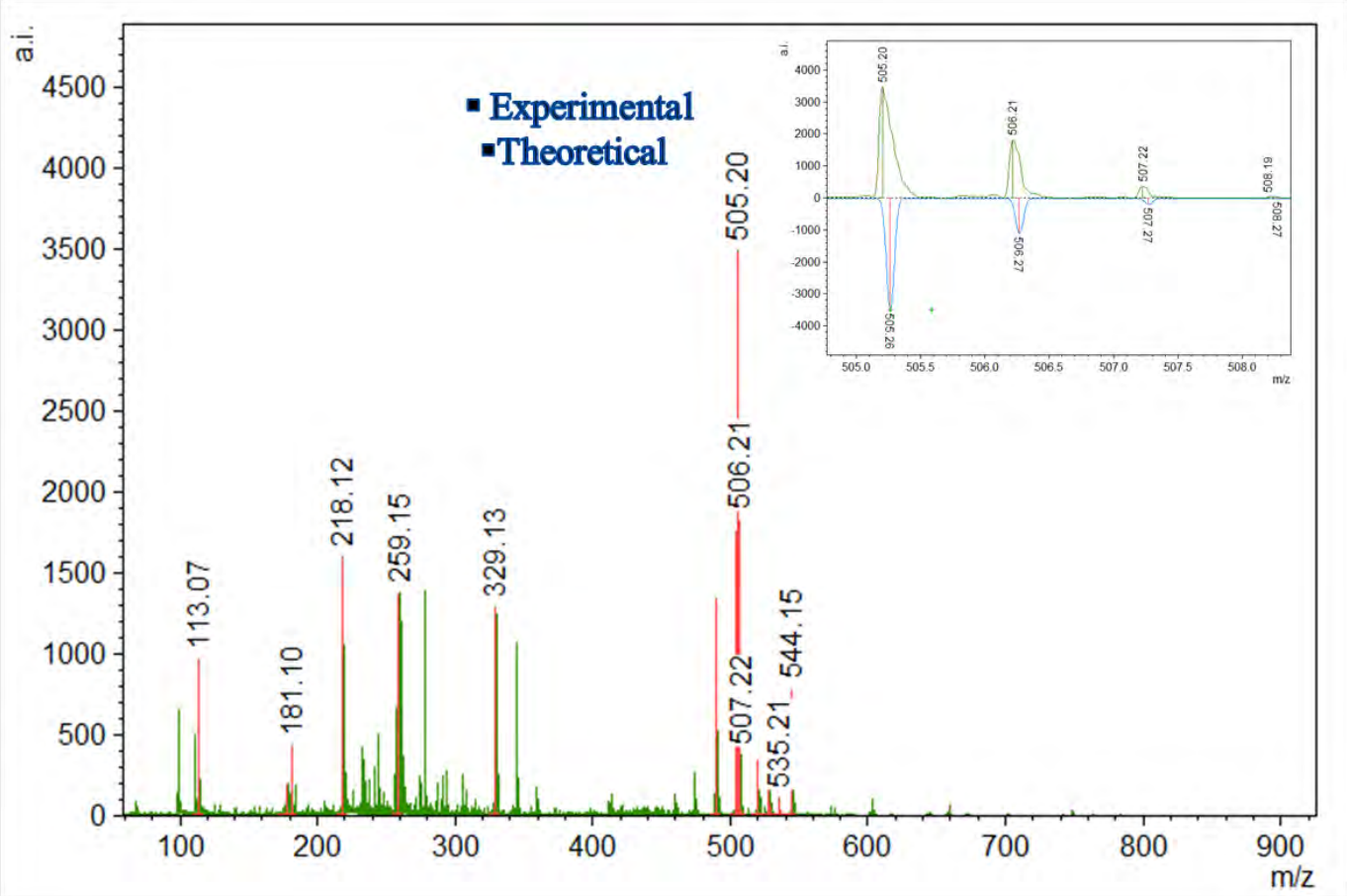

Figure A2. 6. MALDI-TOF mass spectrum of complex **2.2**

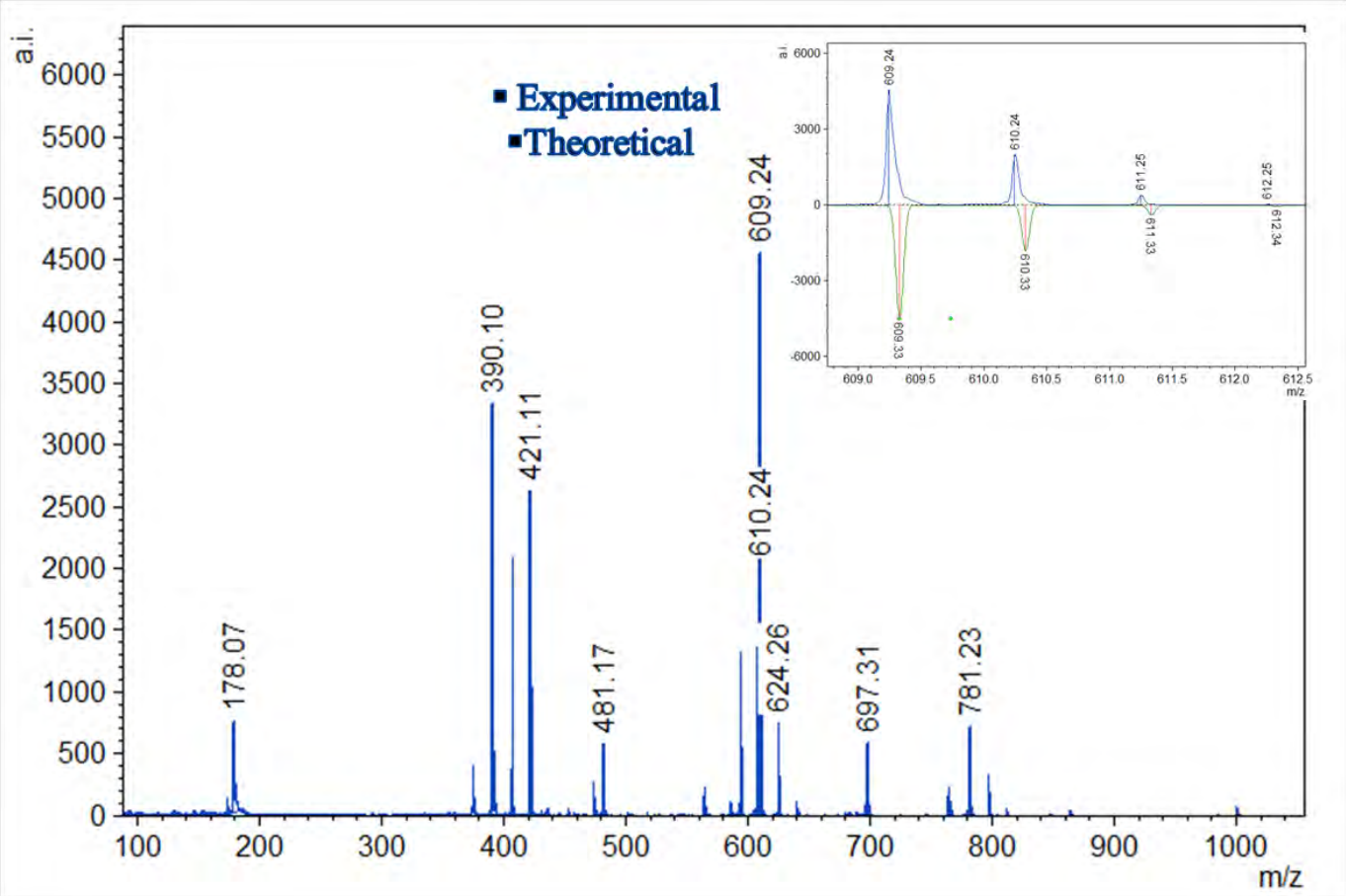

Figure A2. 7. MALDI-TOF mass spectrum of complex **2.3**

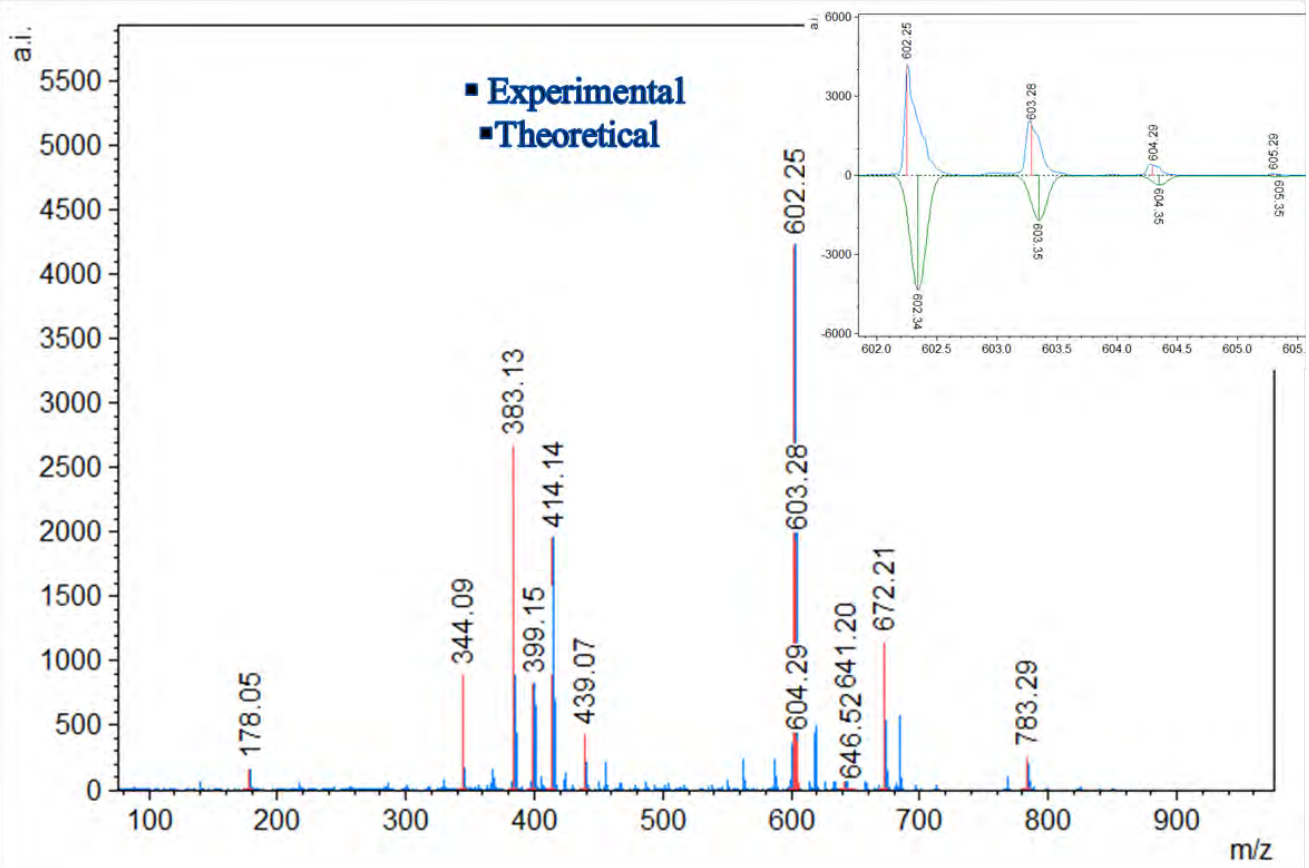

Figure A2. 8. MALDI-TOF mass spectrum of complex **2.4**

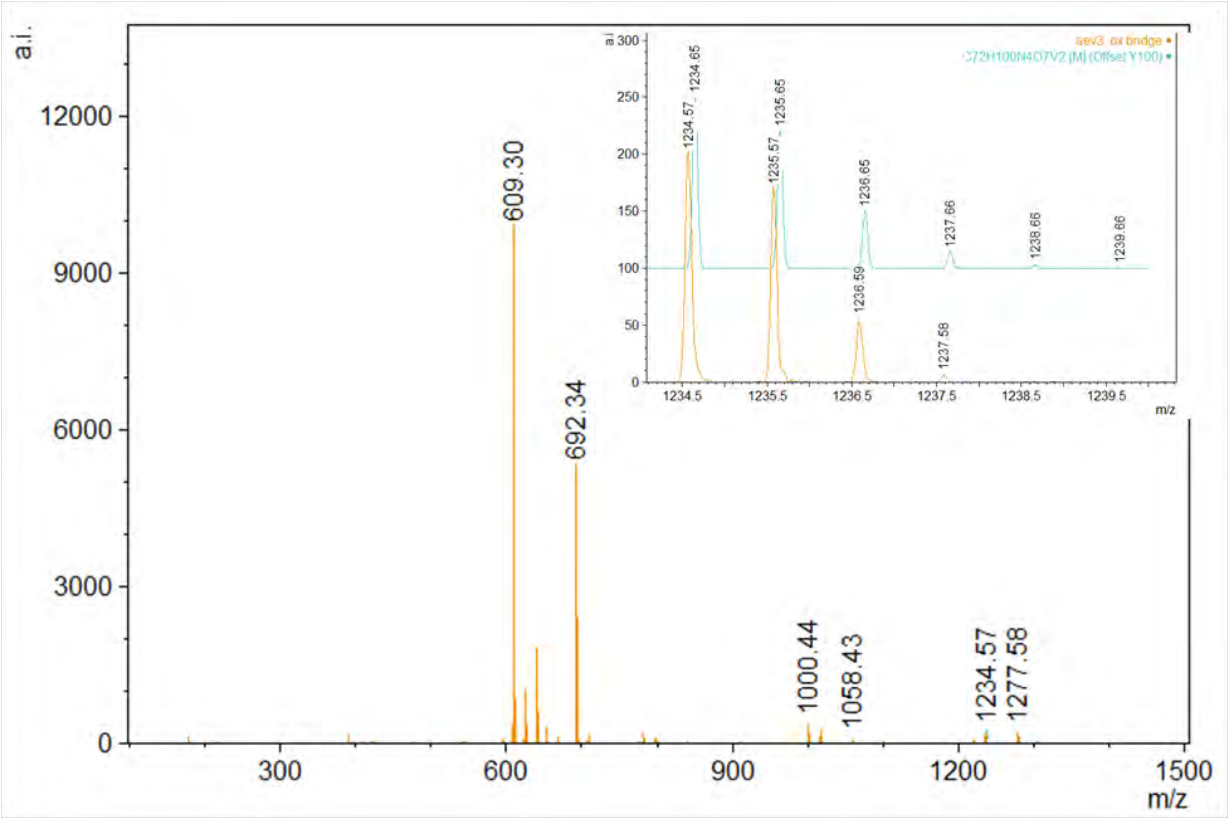

Figure A2. 9. MALDI-TOF mass spectrum of complex **2.5**

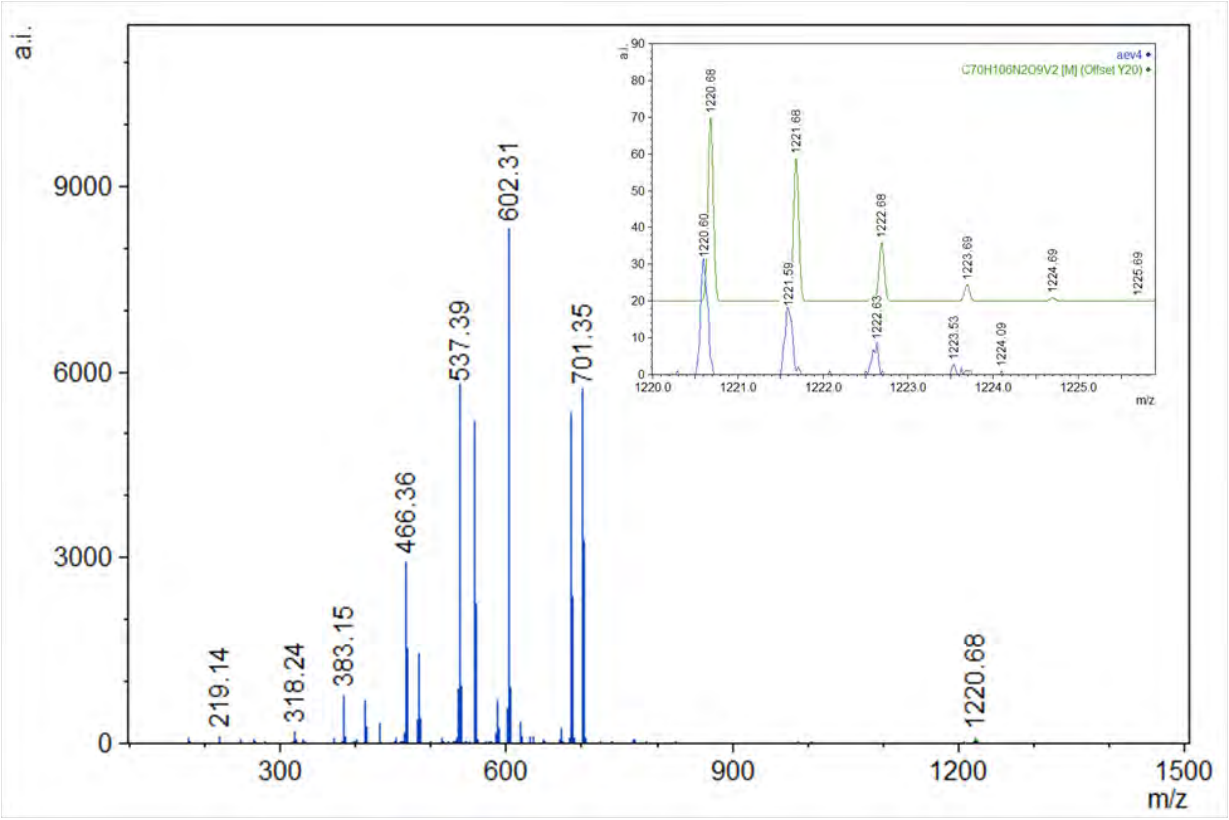

Figure A2. 10. MALDI-TOF mass spectrum of complex **2.6**

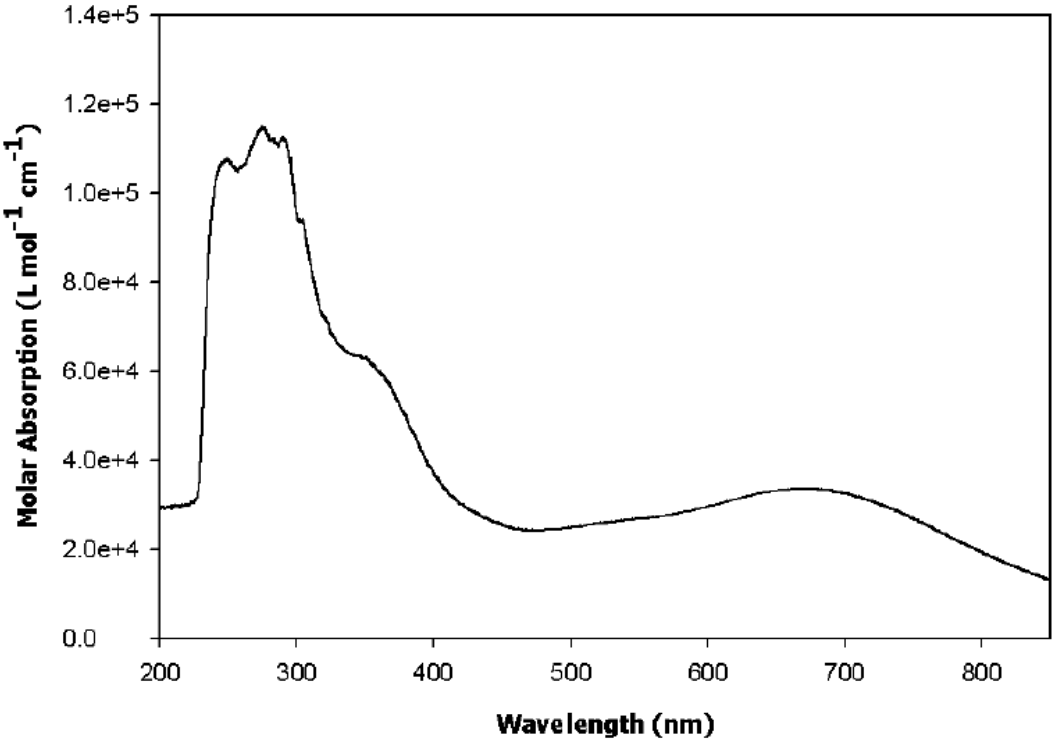

Figure A2. 11. UV-Vis absorption spectrum of complex **2.1**

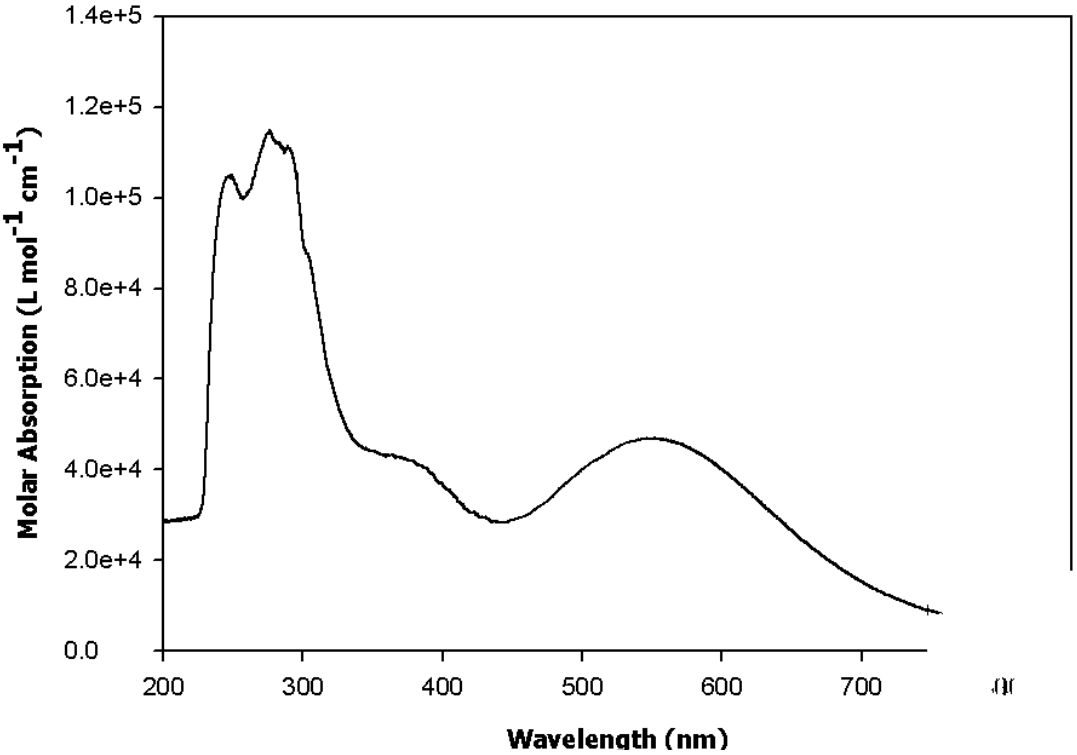

Figure A2. 12. UV-Vis absorption spectrum of complex **2.2**

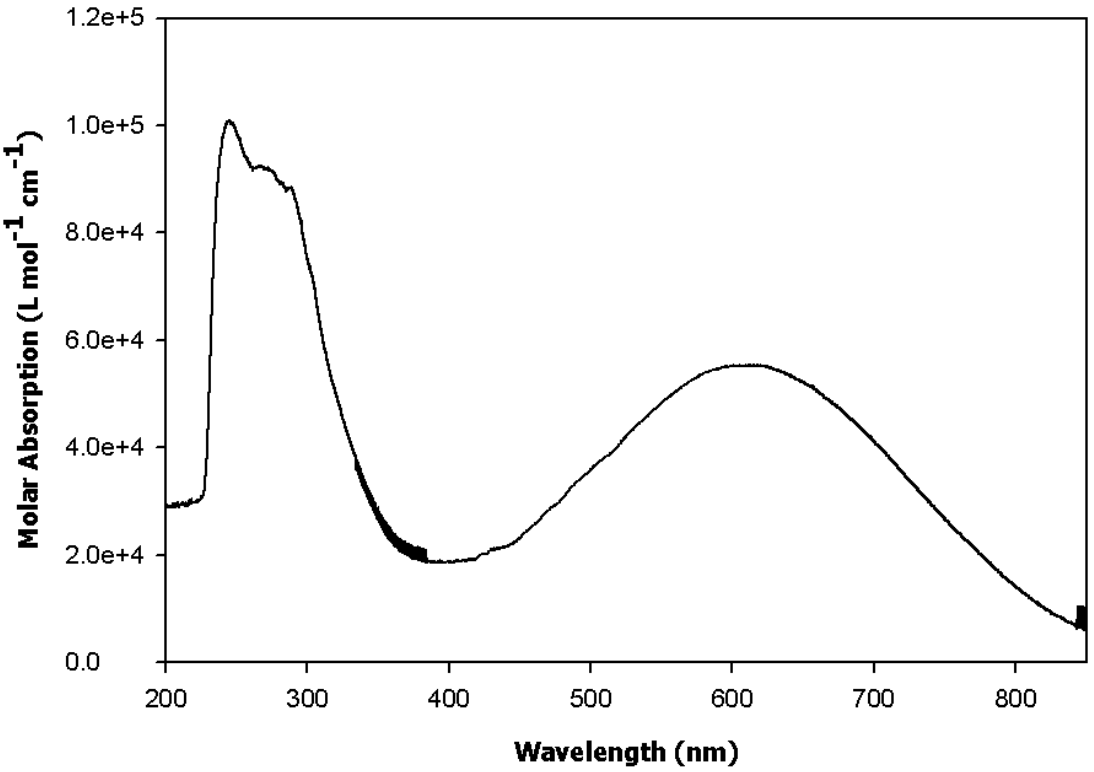

Figure A2. 13. UV-Vis absorption spectrum of complex **2.3**

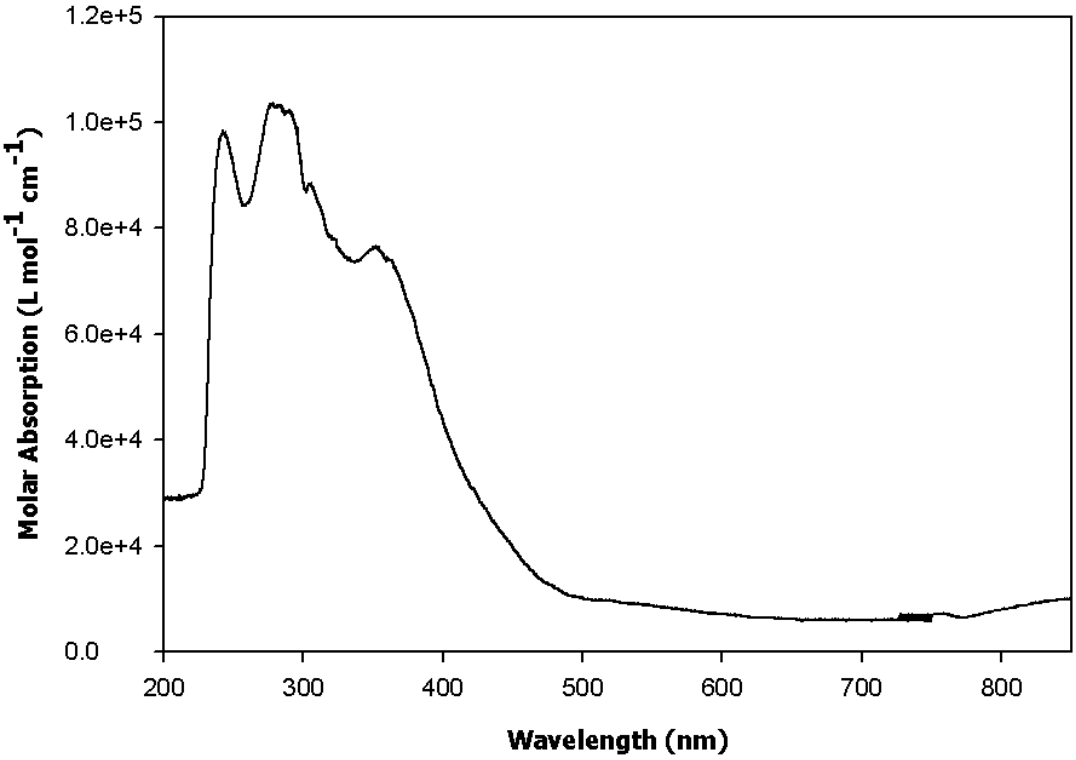

Figure A2. 14. UV-Vis absorption spectrum of complex **2.4**

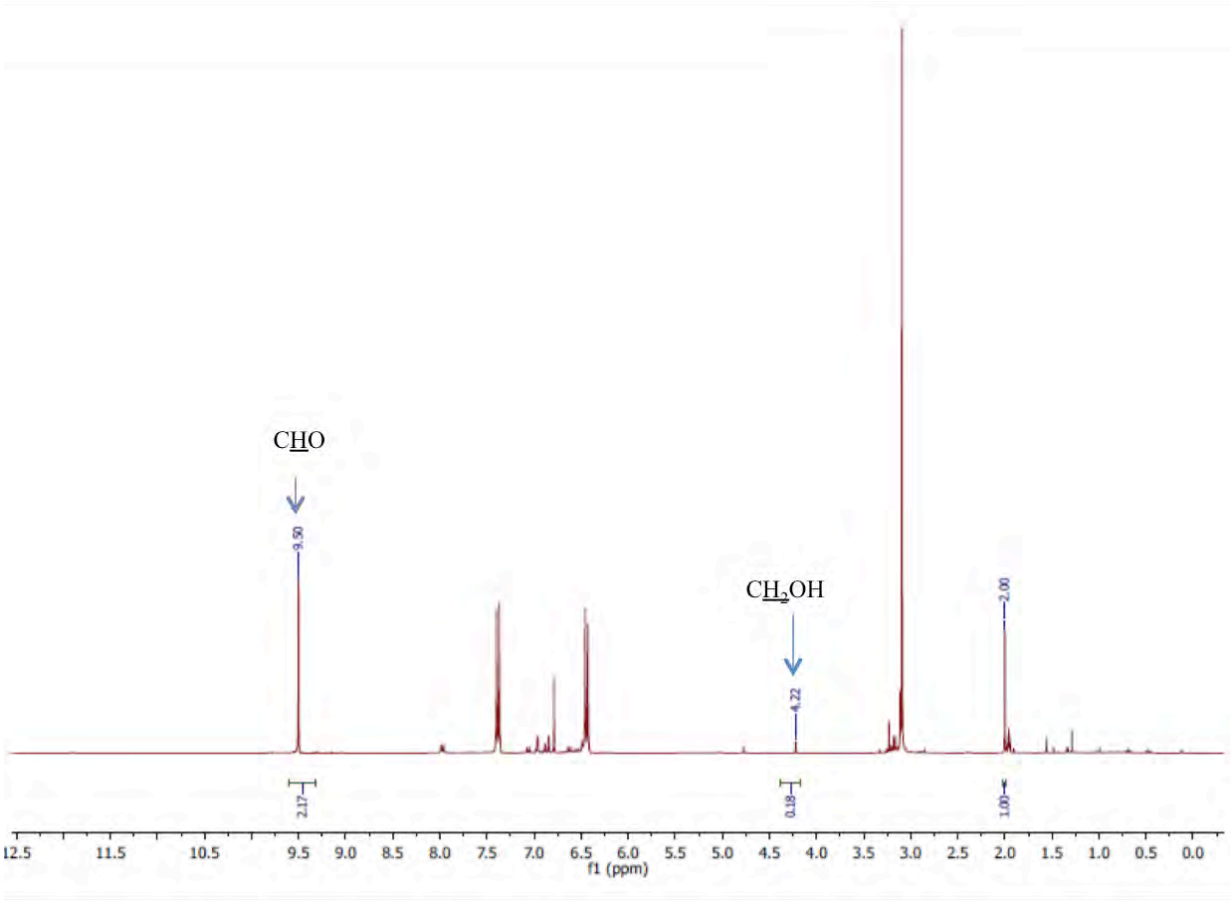

Figure A2. 15. ^{1}H-NMR of 4-methoxybenzyl alcohols with **2.1** corresponding to Table 2.3

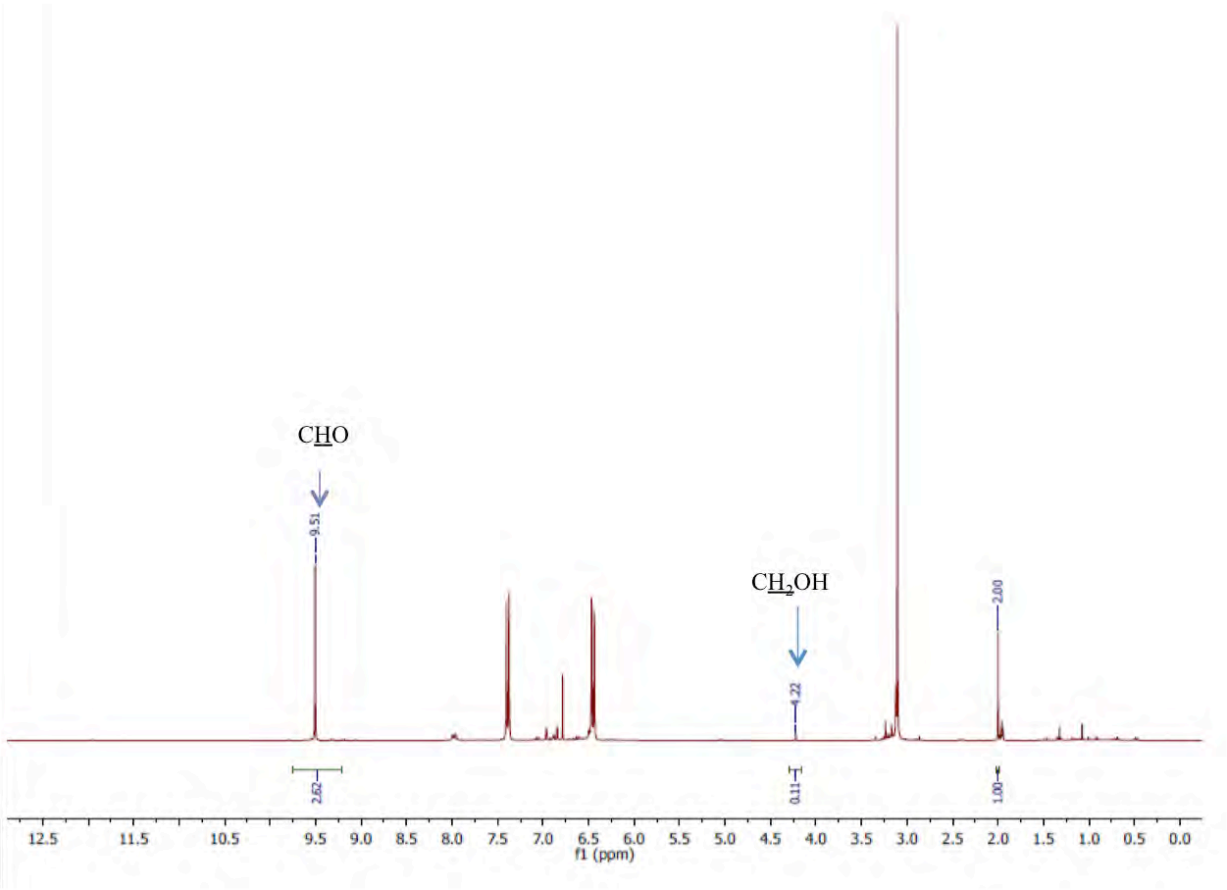

Figure A2. 16. ^{1}H-NMR of 4-methoxybenzyl alcohols with **2.2** corresponding to Table 2.3

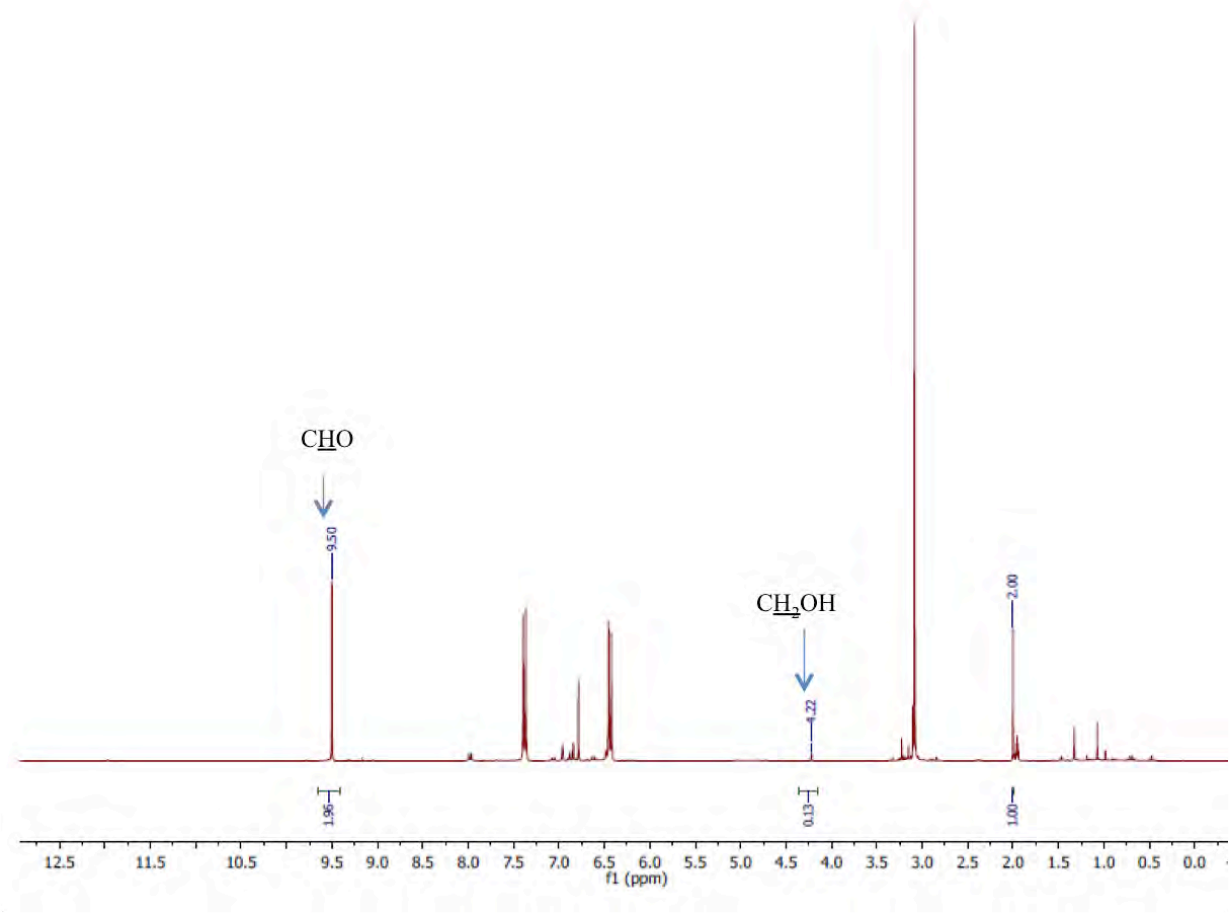

Figure A2. 17. [1]H-NMR of 4-methoxybenzyl alcohols with **2.3** corresponding to Table 2.3

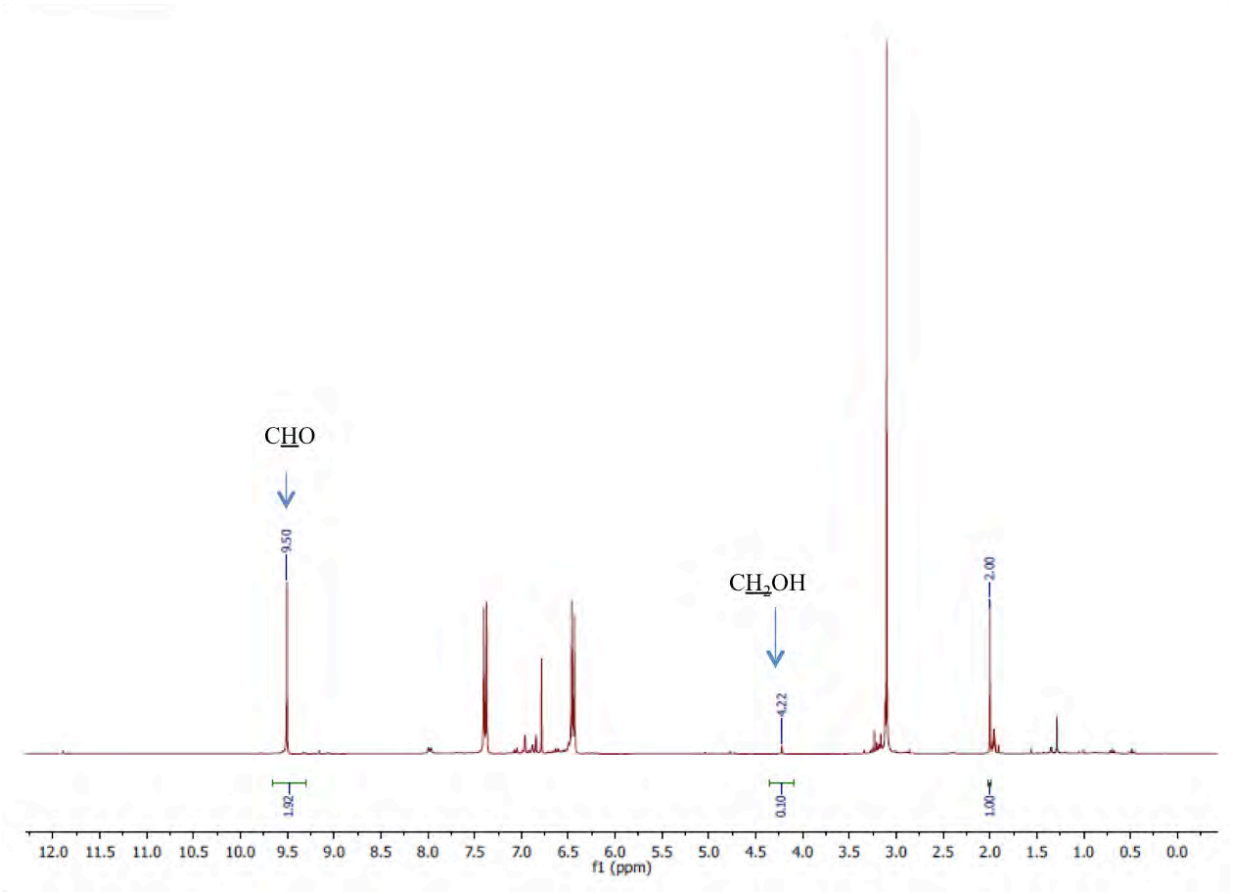

Figure A2. 18. ^{1}H-NMR of 4-methoxybenzyl alcohols with **2.4** corresponding to Table 2.3

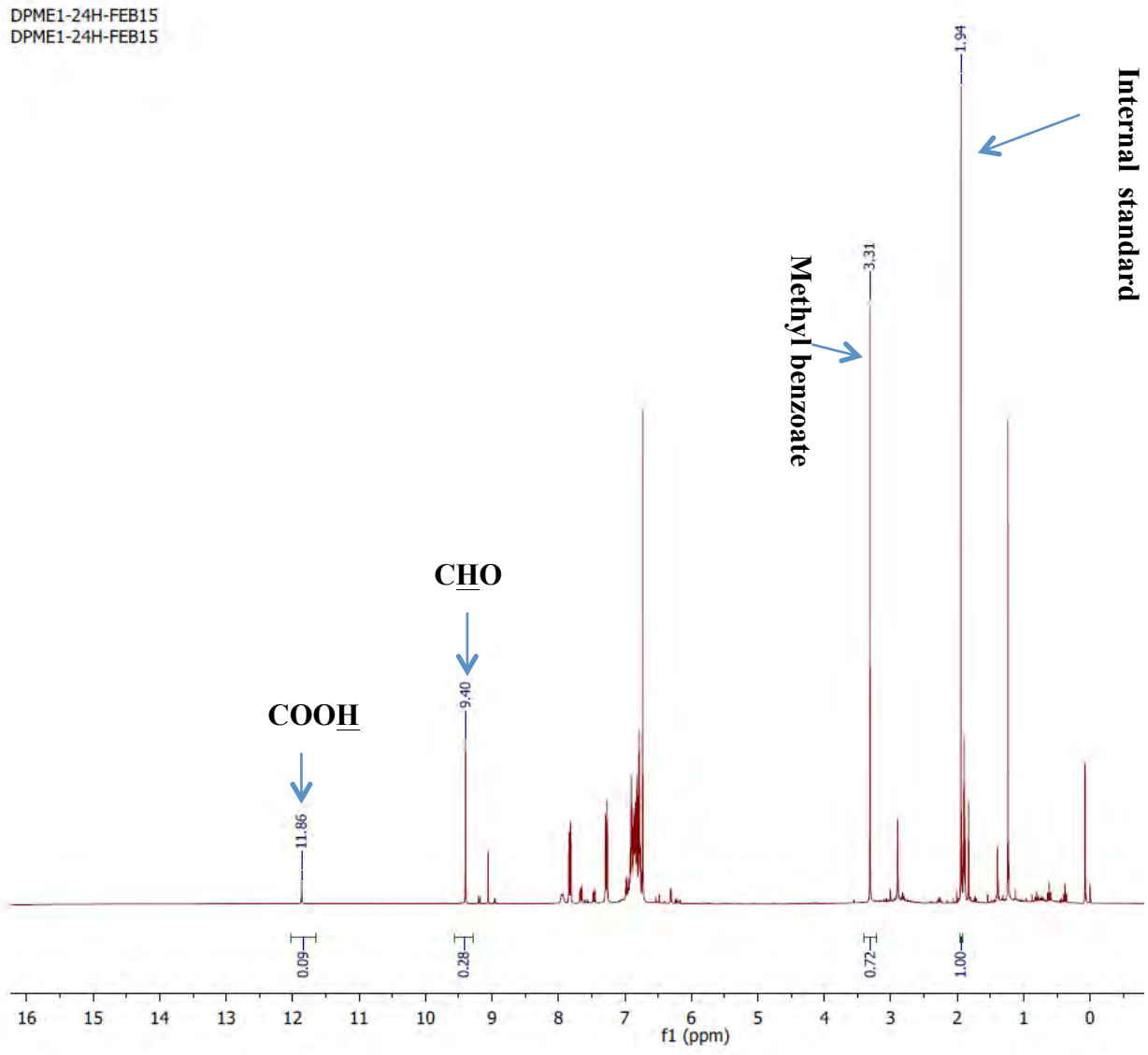

Figure A2. 19. [1]H-NMR of oxidation of 1,2-diphenyl-2 methoxyethanol using **2.1** corresponding to Table 2.5

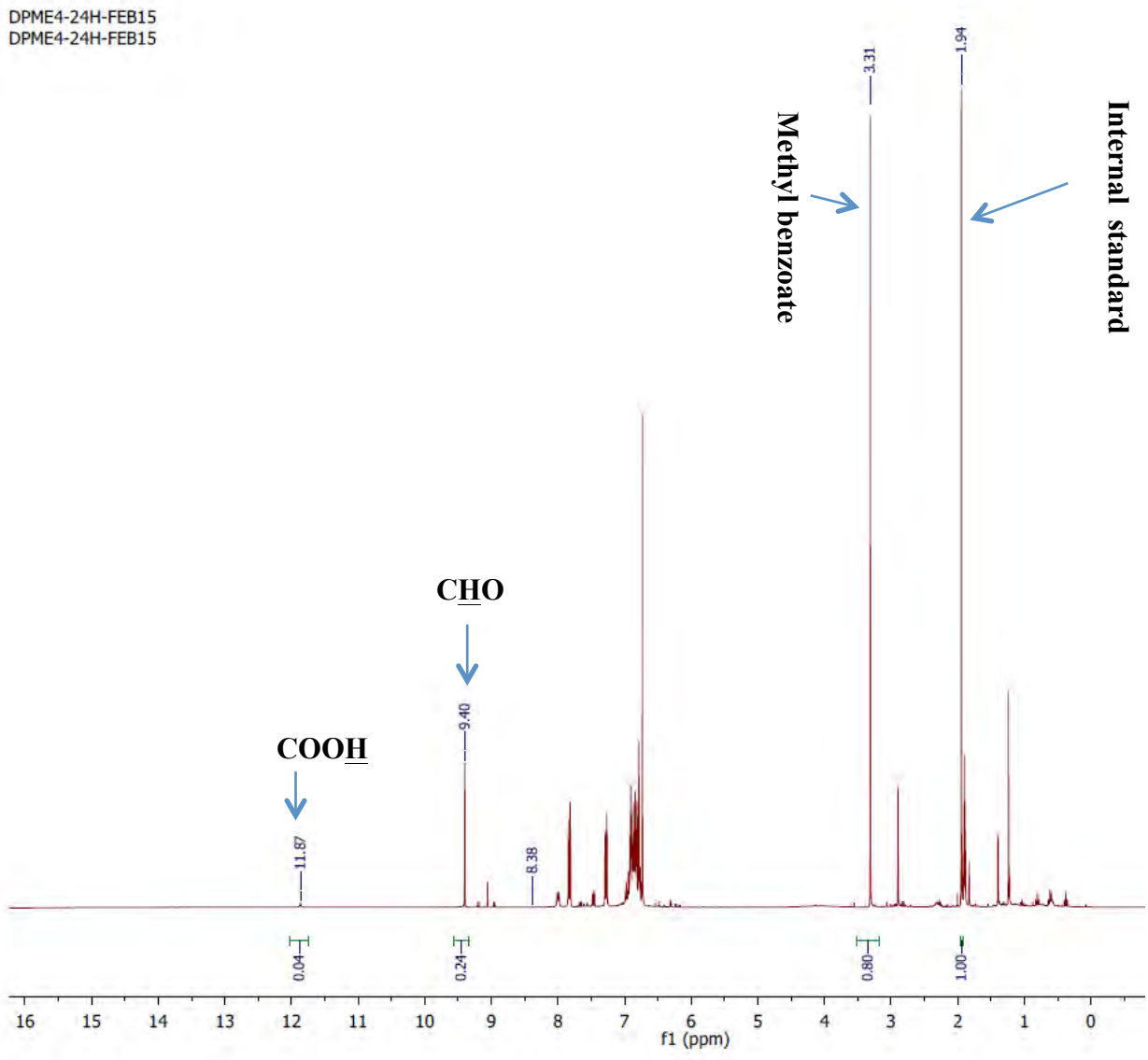

Figure A2. 20. ^{1}H-NMR of oxidation of 1,2-diphenyl-2 methoxyethanol using **2.2** corresponding to Table 2.5

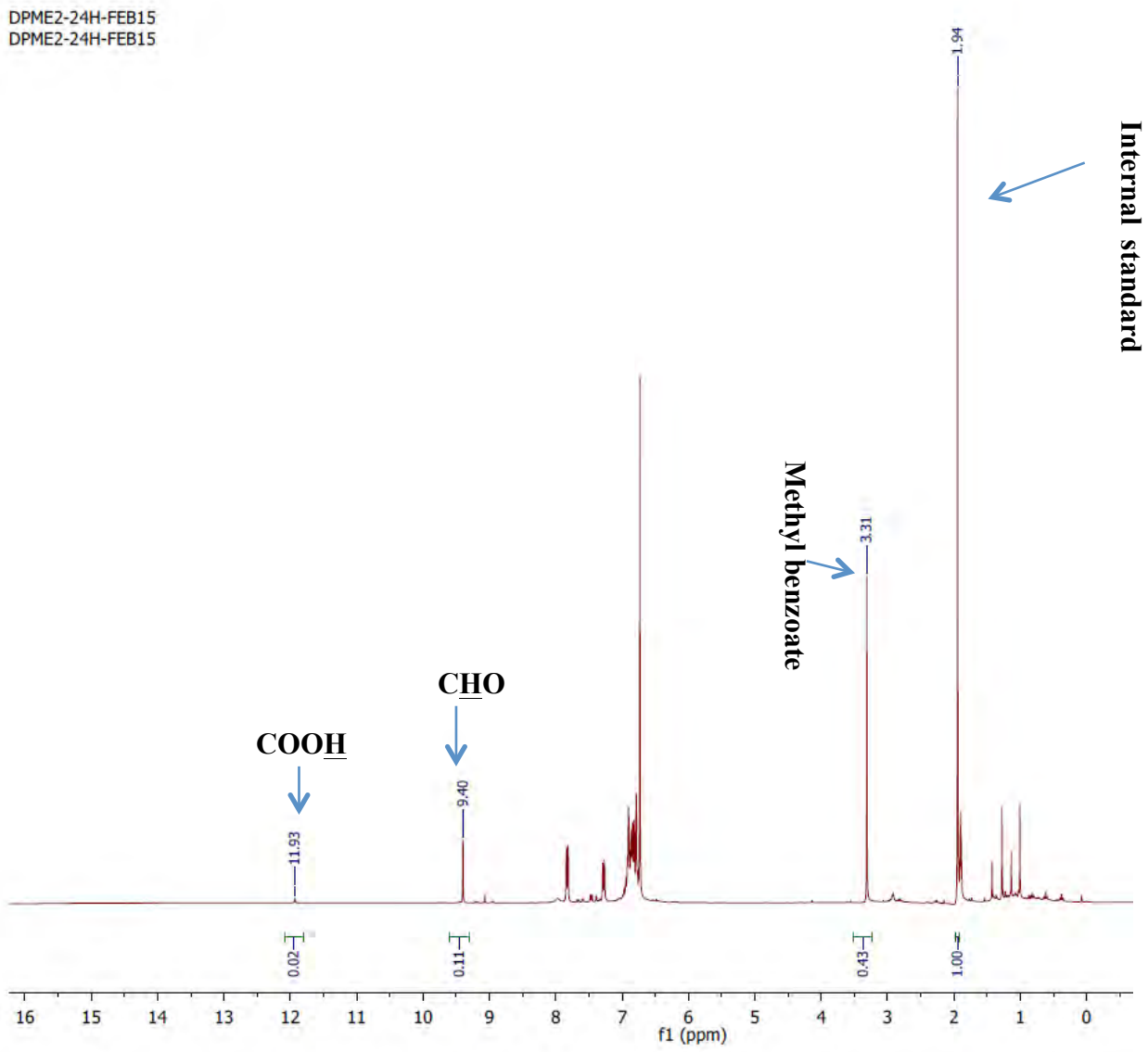

Figure A2. 21. [1]H-NMR of oxidation of 1,2-diphenyl-2 methoxyethanol using **2.3** corresponding to Table 2.5

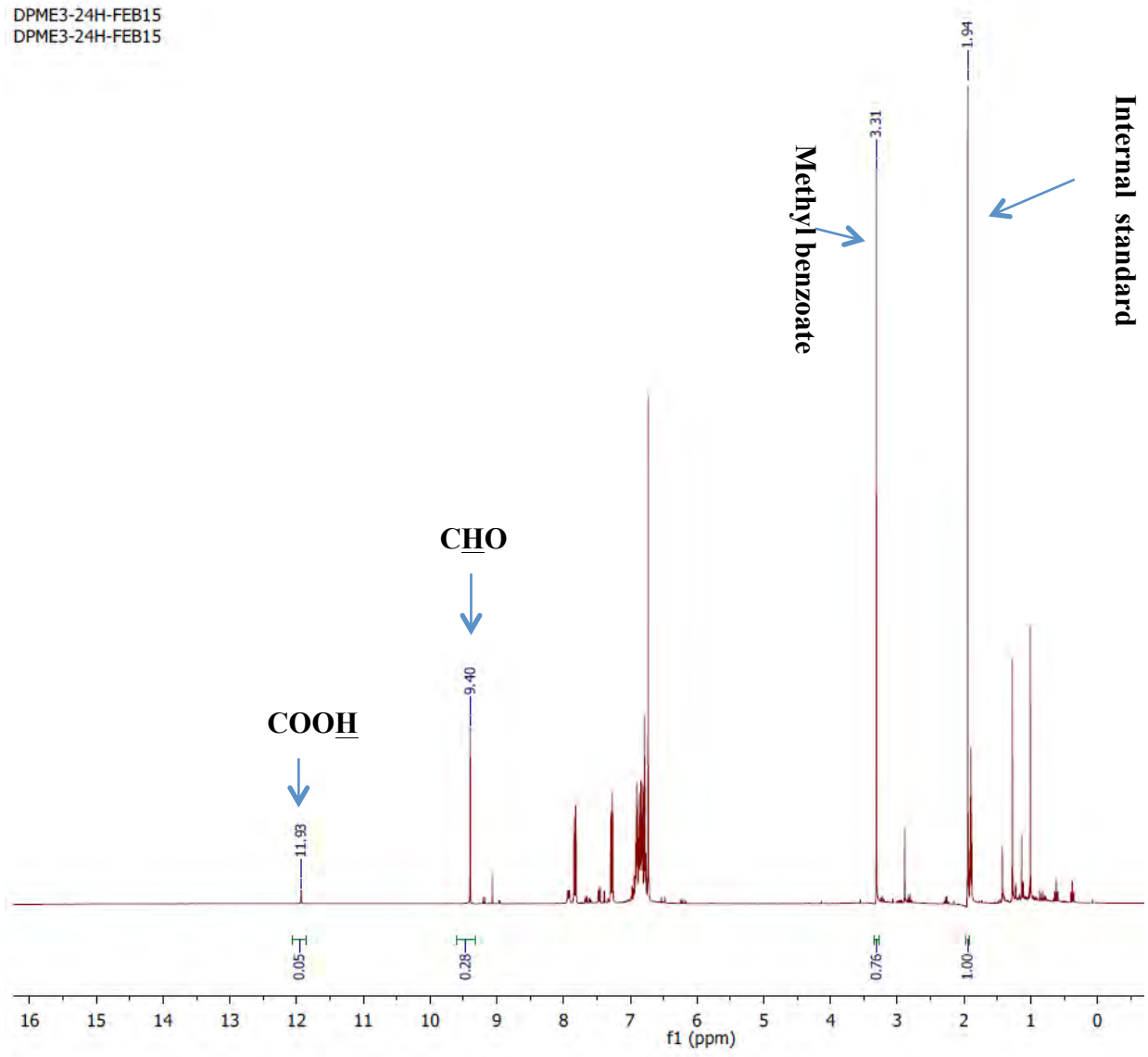

Figure A2. 22. ^{1}H-NMR of oxidation of 1,2-diphenyl-2 methoxyethanol using **2.4** corresponding to Table 2.5

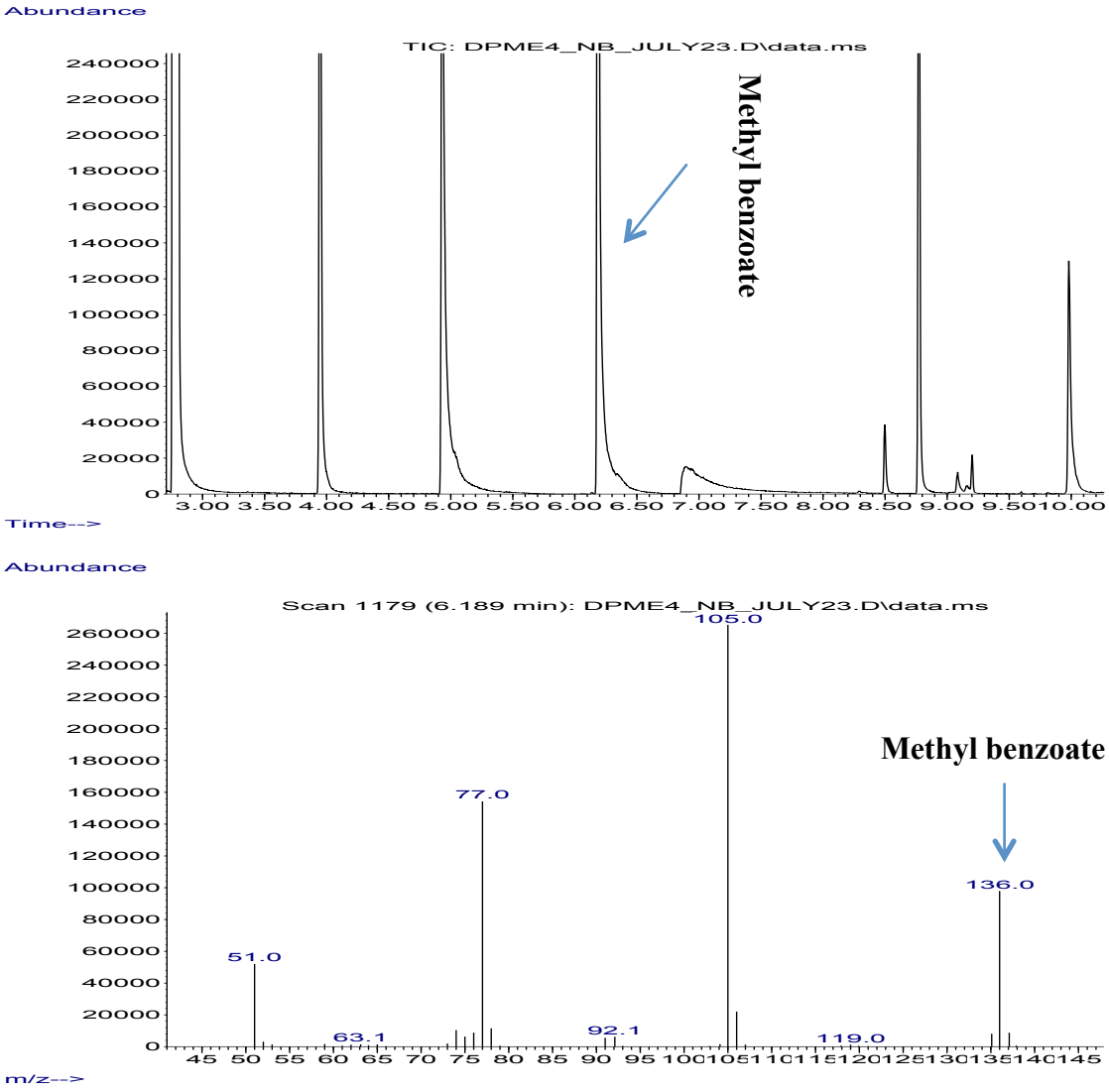

Figure A2. 23. GC-MS of reaction mixture produced from 1,2-diphenyl-2 methoxyethanol

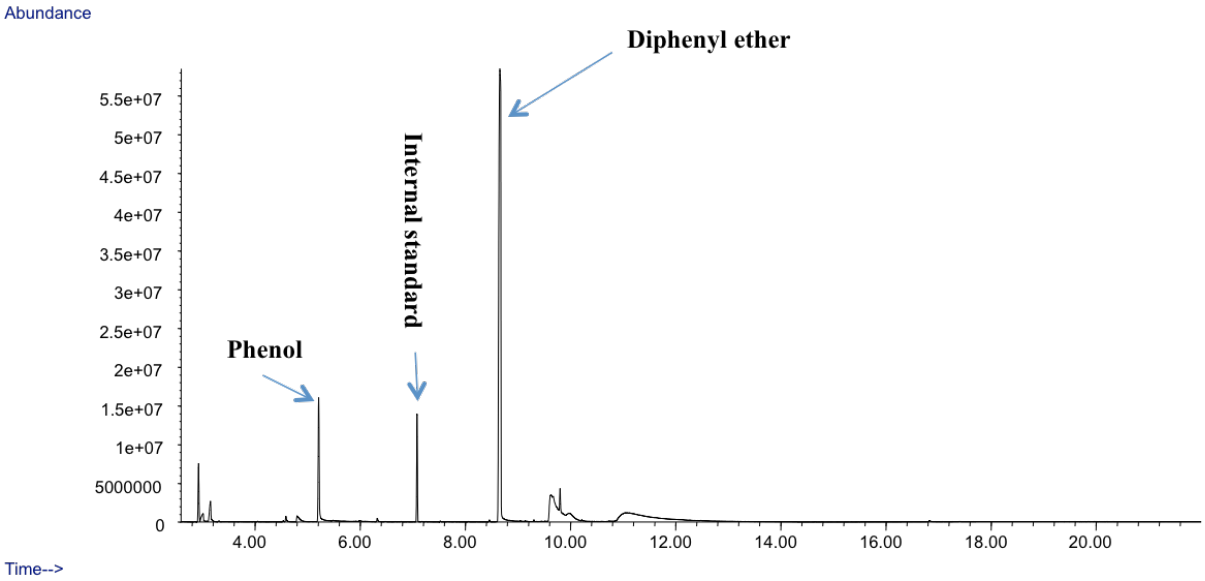

Figure A2. 24. GC of reaction mixture produced from diphenyl ether

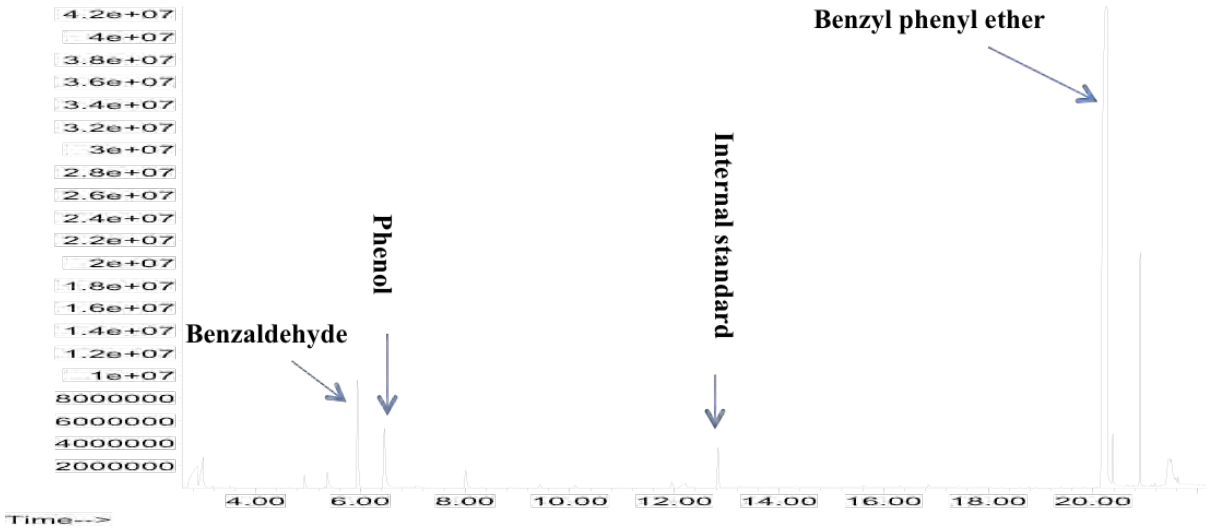

Figure A2. 25. GC of reaction mixture produced from benzyl phenyl ether

6.2 Appendix for Chapter 3

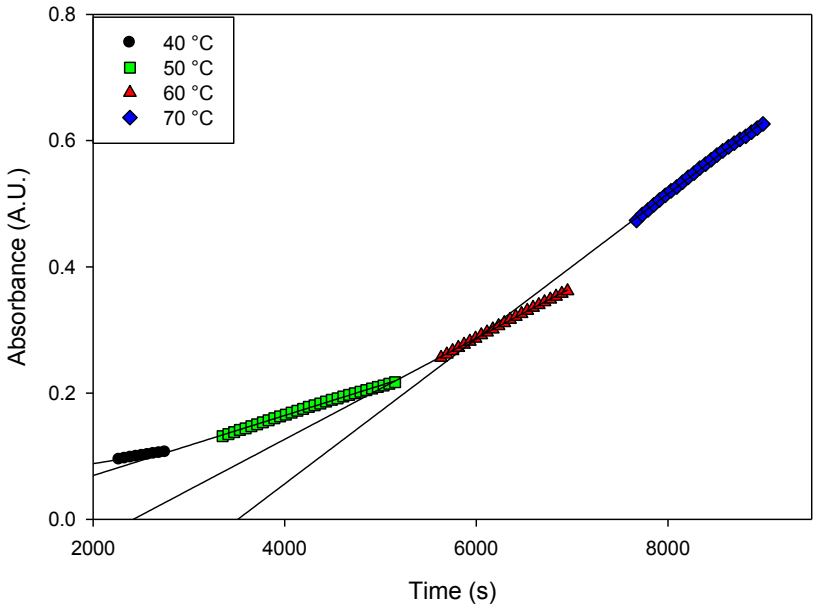

Figure A3. 1. Temperature dependence of the initial rates of reaction based on the absorbance of the ν(C=O) of styrene carbonate (SC). Using **2.2** at 20 bar, and [V]:[SO]:[Co-cat] 1:500:2 at 40 °C ● (y = 0.00002432x + 0.0395, R^2 = 0.9987), at 50 °C ■ (y = 0.00004606x − 0.0259, R^2 = 0.9981), at 60 °C ▲ (y = 0.00008019x -0.1940, R^2 = 0.9994) at 70 °C ◆, (y = 0.0001x − 0.4033, R^2 =0.9980)

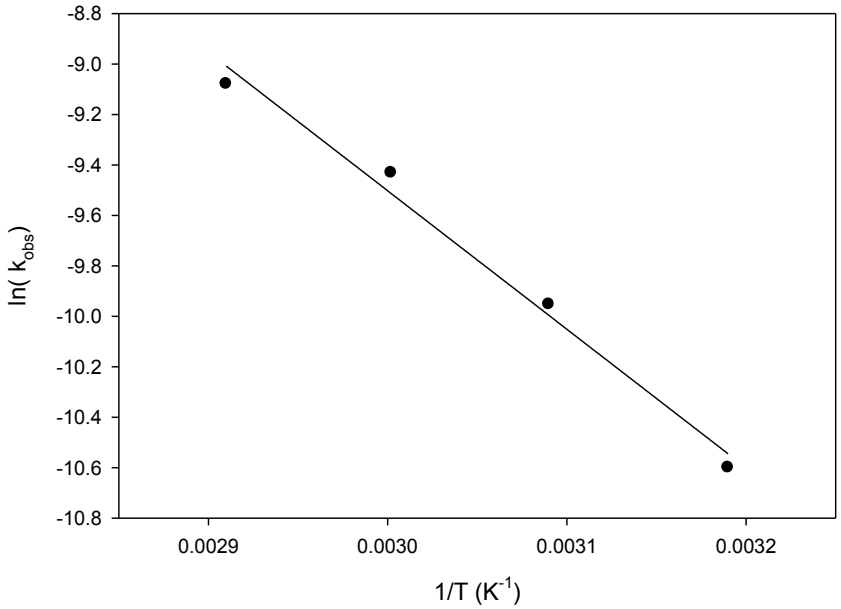

Figure A3. 2. Arrhenius plot for the formation of cyclic styrene carbonate based on data presented in figure (AppendiceStraight line: $y = -5488.72x + 6.96$, $R^2 = 0.9873$

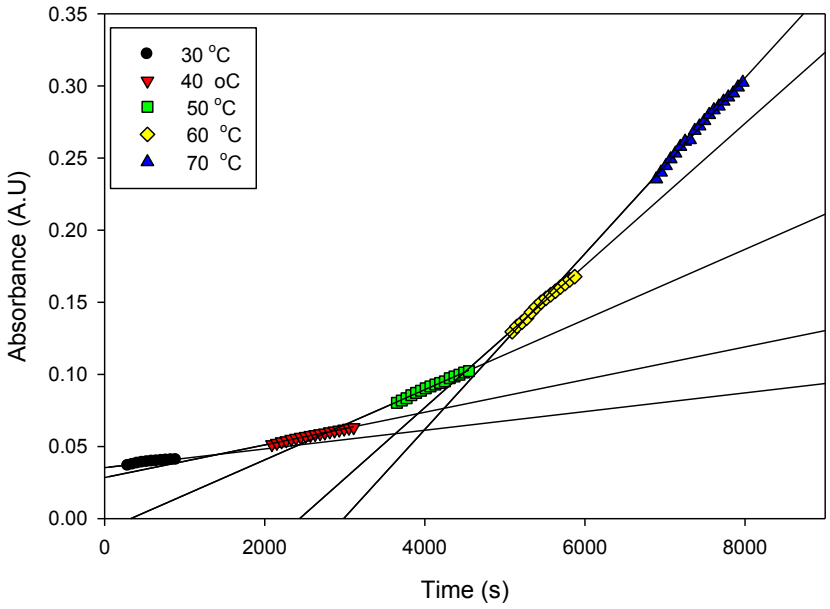

Figure A3. 3. Temperature dependence of the initial rates of reaction based on the absorbance of the ν(C=O) of cyclohexene carbonate (CHC). Using **2.2** at 20 bar, and [V]:[CHO]:[Co-cat] 1:500:2. at 30 °C ● (y = 0.0000648x + 0.0353, R^2 = 0.9268), 40 °C ▼ (y = 0.00001132x + 0.0284, R^2 = 0.9935), at 50 °C ■ (y = 0.00002434x − 0.0079, R^2 = 0.9964), at 60 °C ◆ (y = 0.00004924x − 0.1199, R^2 =0.9945), at 70 °C ▲ (y = 0.00006095x -0.1820, R^2 = 0.9956).

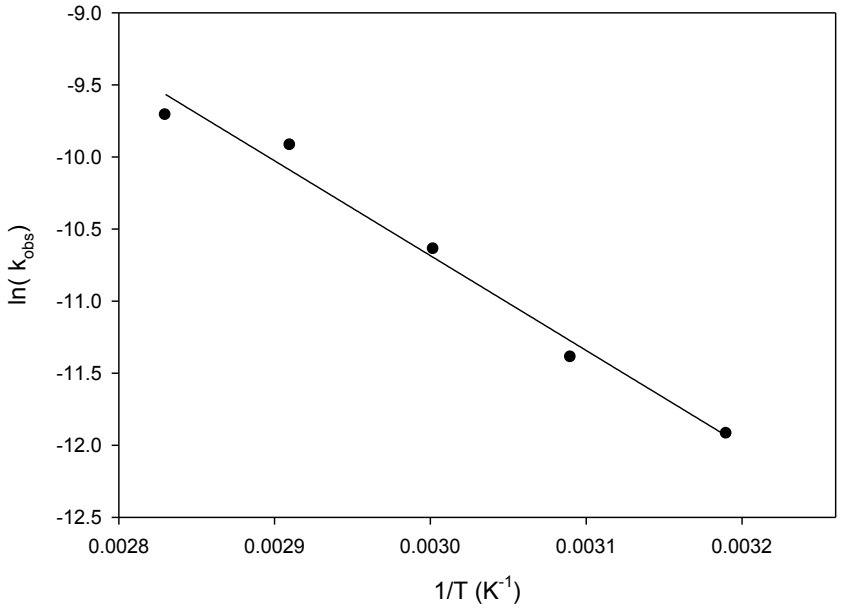

Figure A3. 4. Arrhenius plot for the formation of cyclic cyclohexene carbonate (CHC) based on data presented in Appendice 2.4. Straight line: $y = -6579.83x + 9.05$, $R^2 = 0.9821$

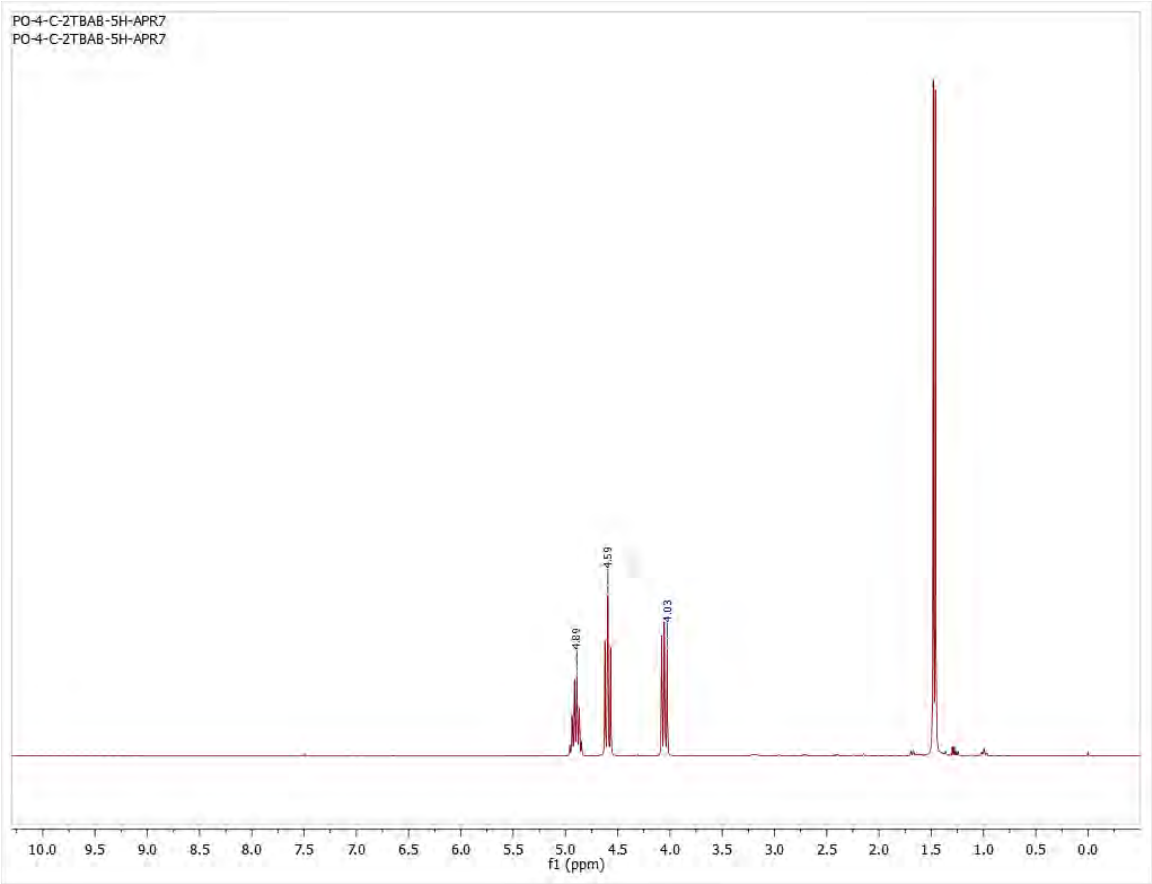

Figure A3. 5. ^{1}H NMR spectrum of propylene carbonate (PC) formation corresponding to Table 2.1, entry 13

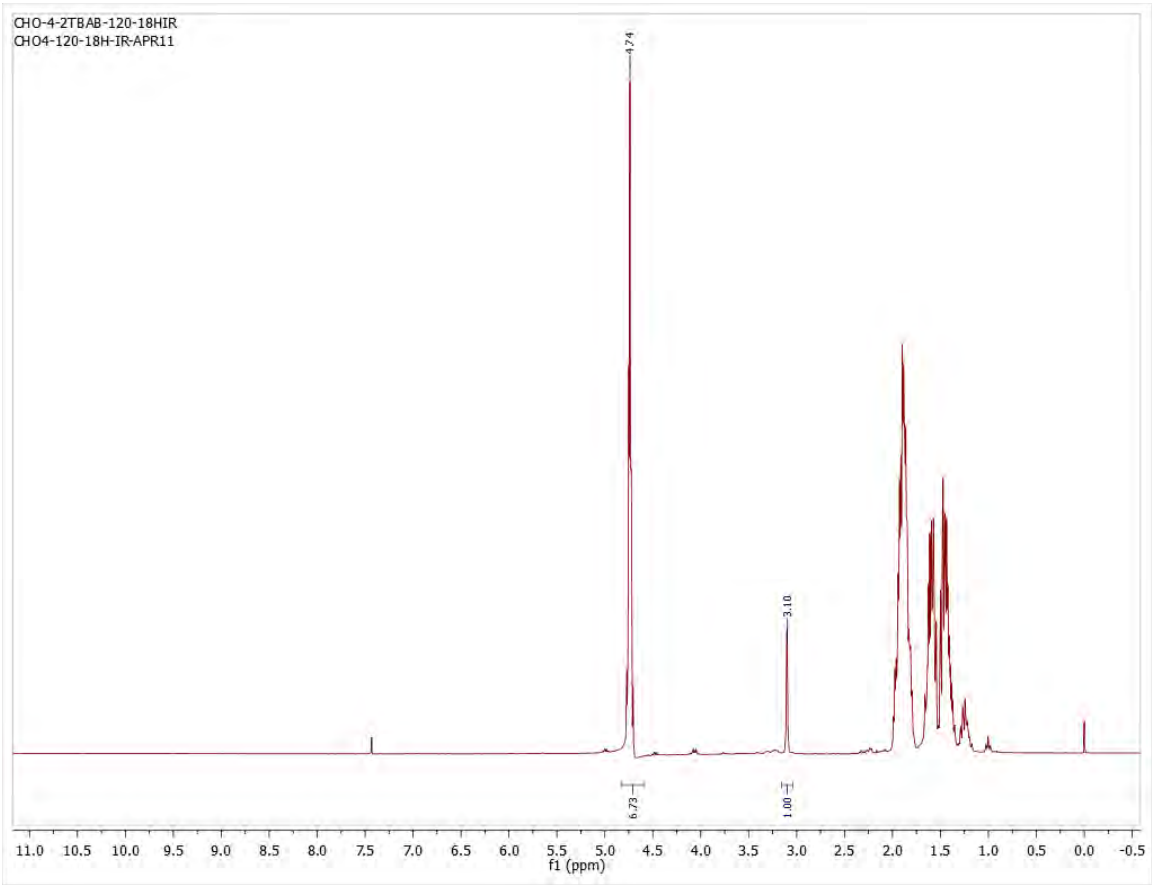

Figure A3. 6. ^{1}H NMR spectrum of cyclohexene carbonate (CHC) formation corresponding to Table 2.1, entry 15

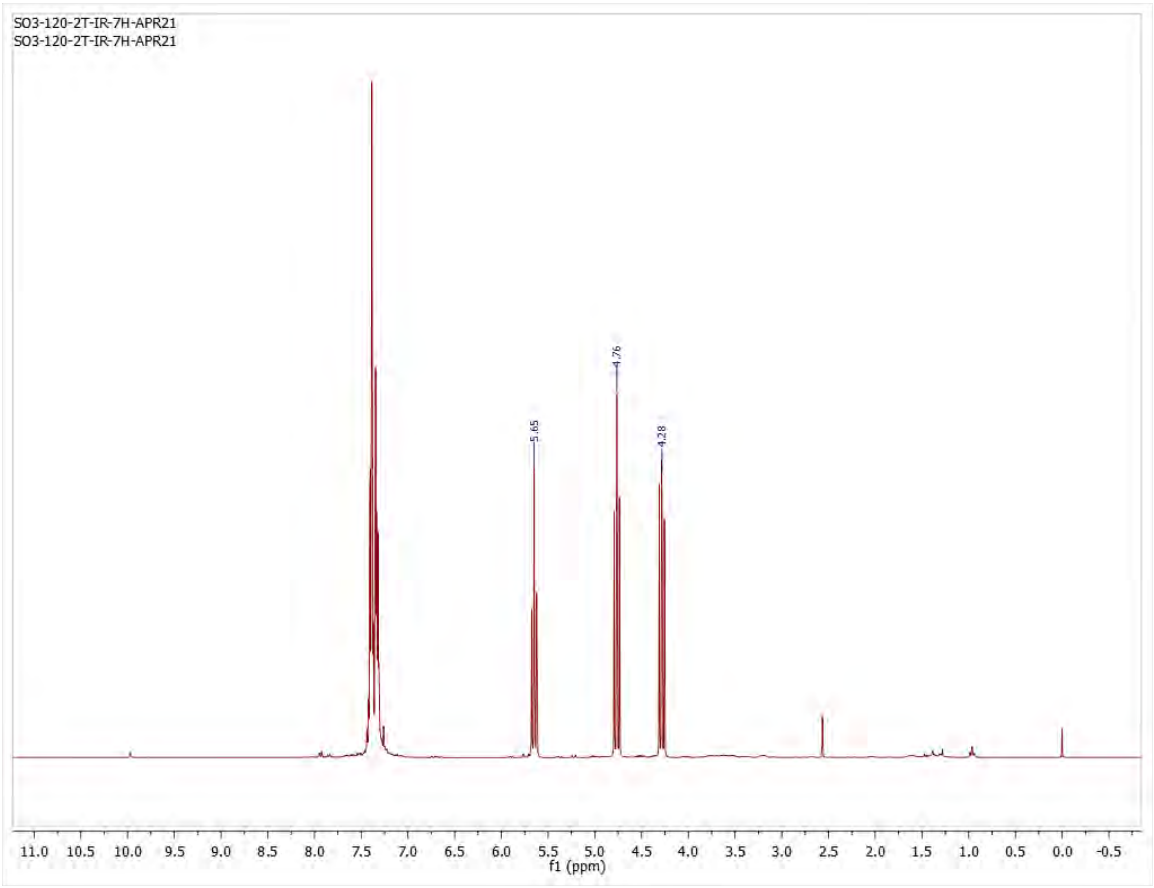

Figure A3. 7. ^{1}H NMR spectrum of styrene carbonate (SC) formation corresponding to Table 2.1, entry 14

6.3 Appendix for Chapter 4

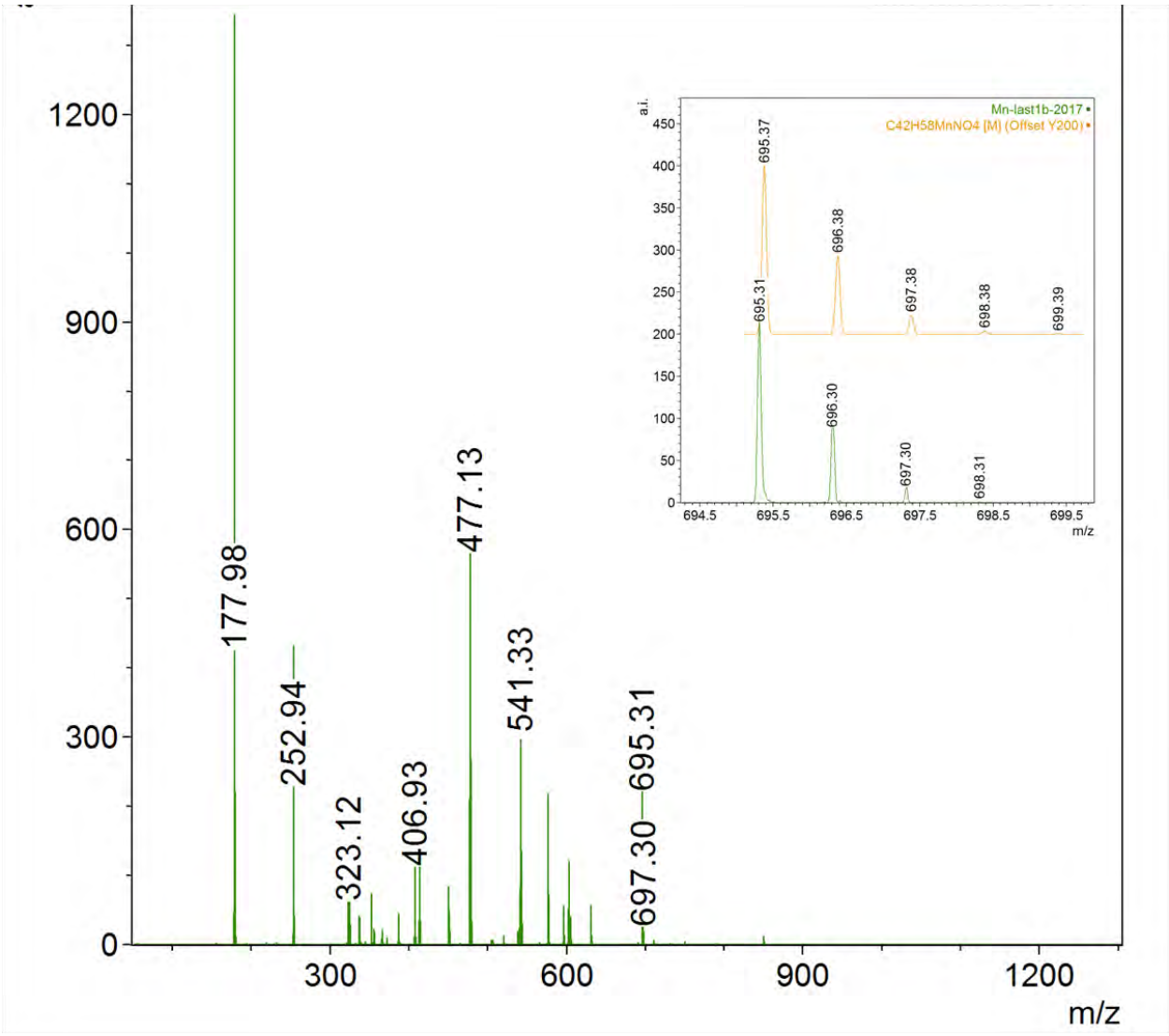

Figure A4-1. MALDI-TOF mass spectrum of complex **4.1**

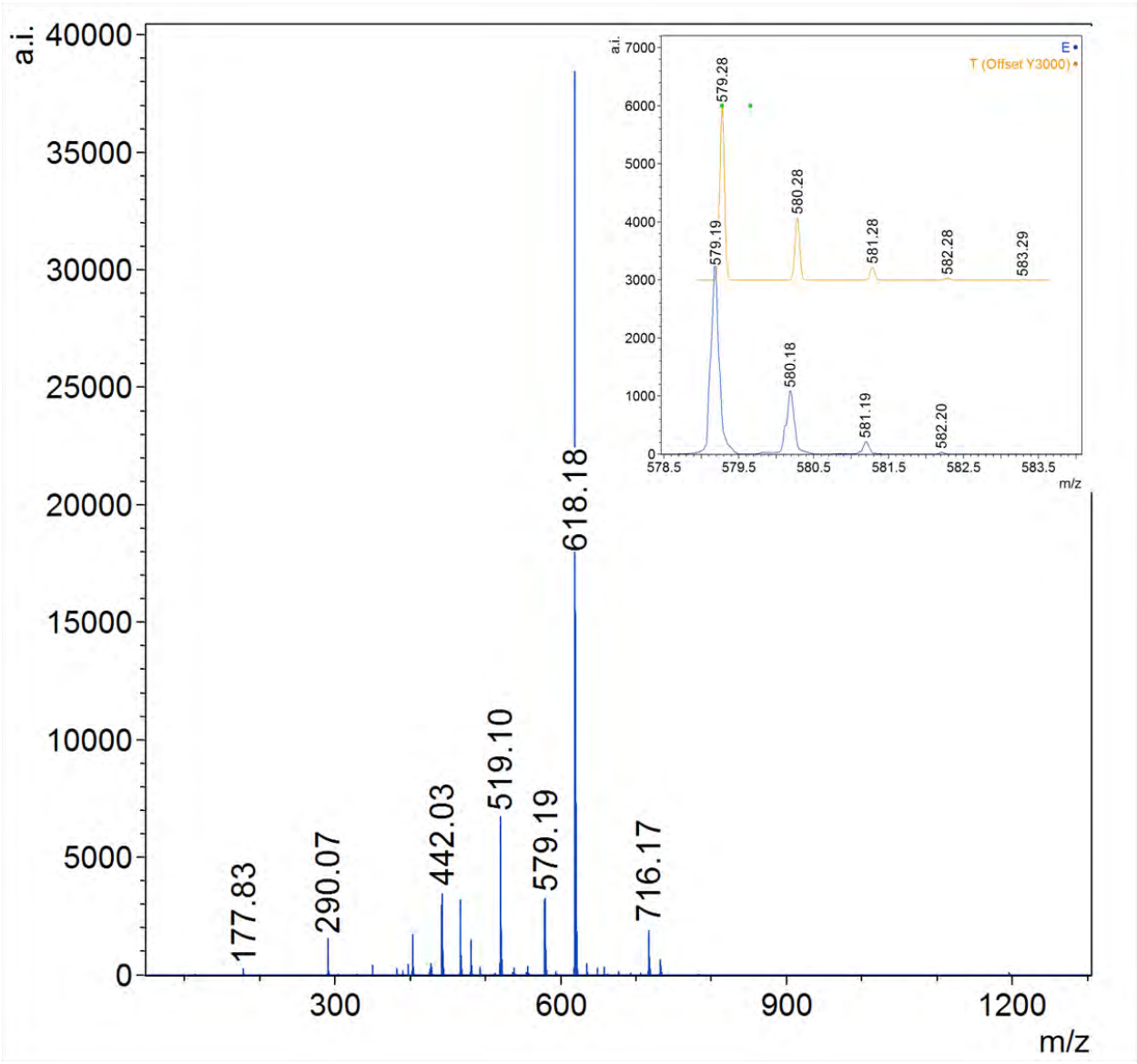

Figure A4-2. MALDI-TOF mass spectrum of complex **4.2**

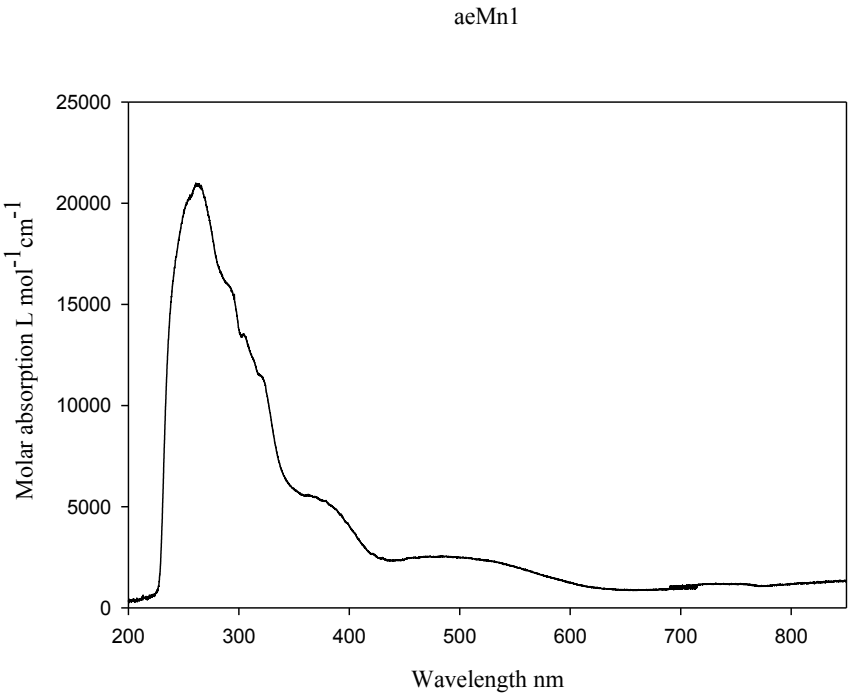

Figure A4-3. UV-Vis absorption spectrum of complex **4.1**

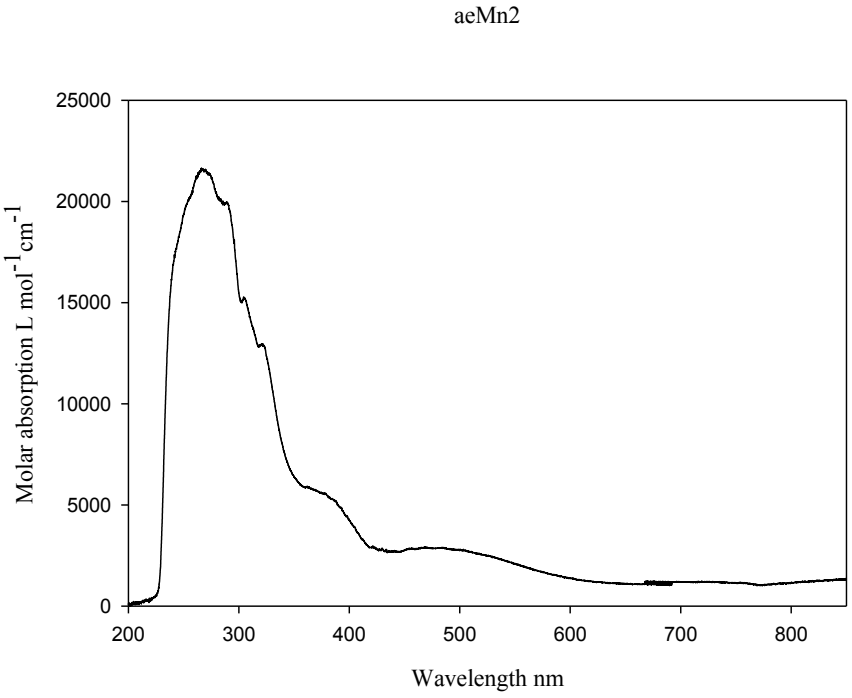

Figure A4-4. UV-Vis absorption spectrum of complex **4.2**

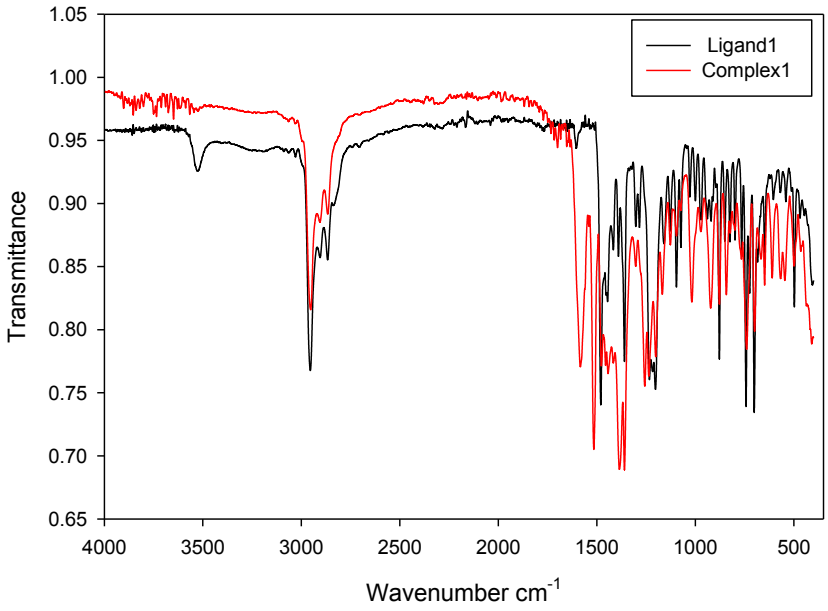

Figure A4-5. IR spectrum of complex **4.1**

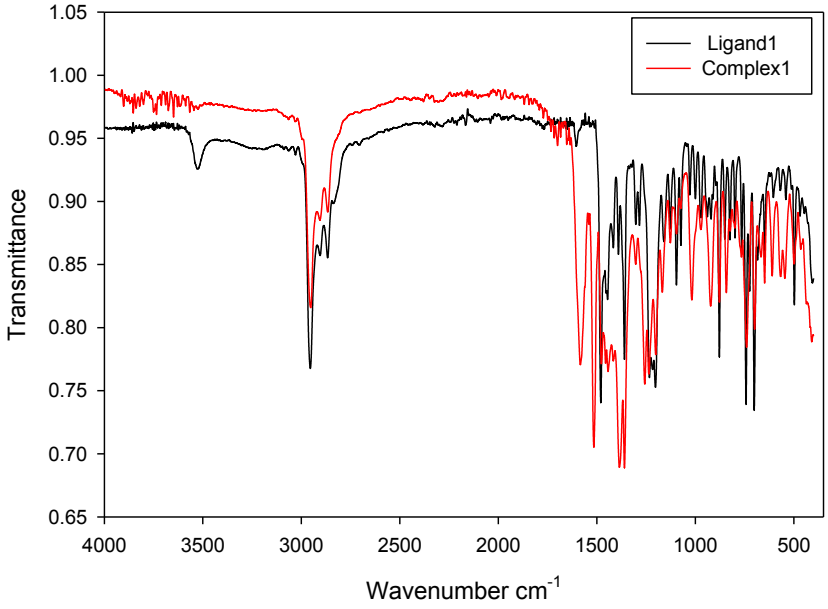

Figure A4-6. IR spectrum of complex **4.2**

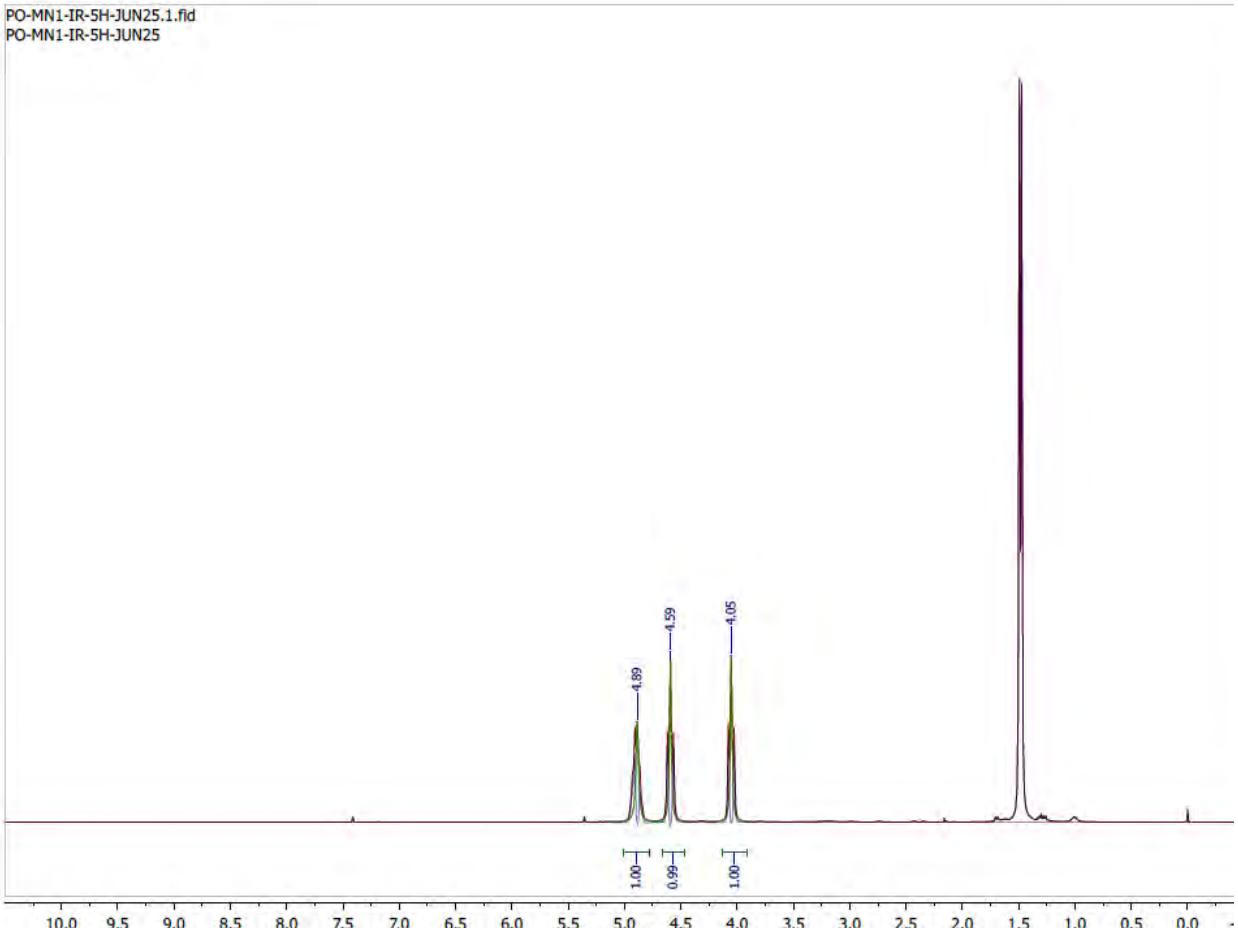

Figure A4-7. ^{1}H-NMR spectrum of propylene carbonate (PC) corresponding to Table 4.2

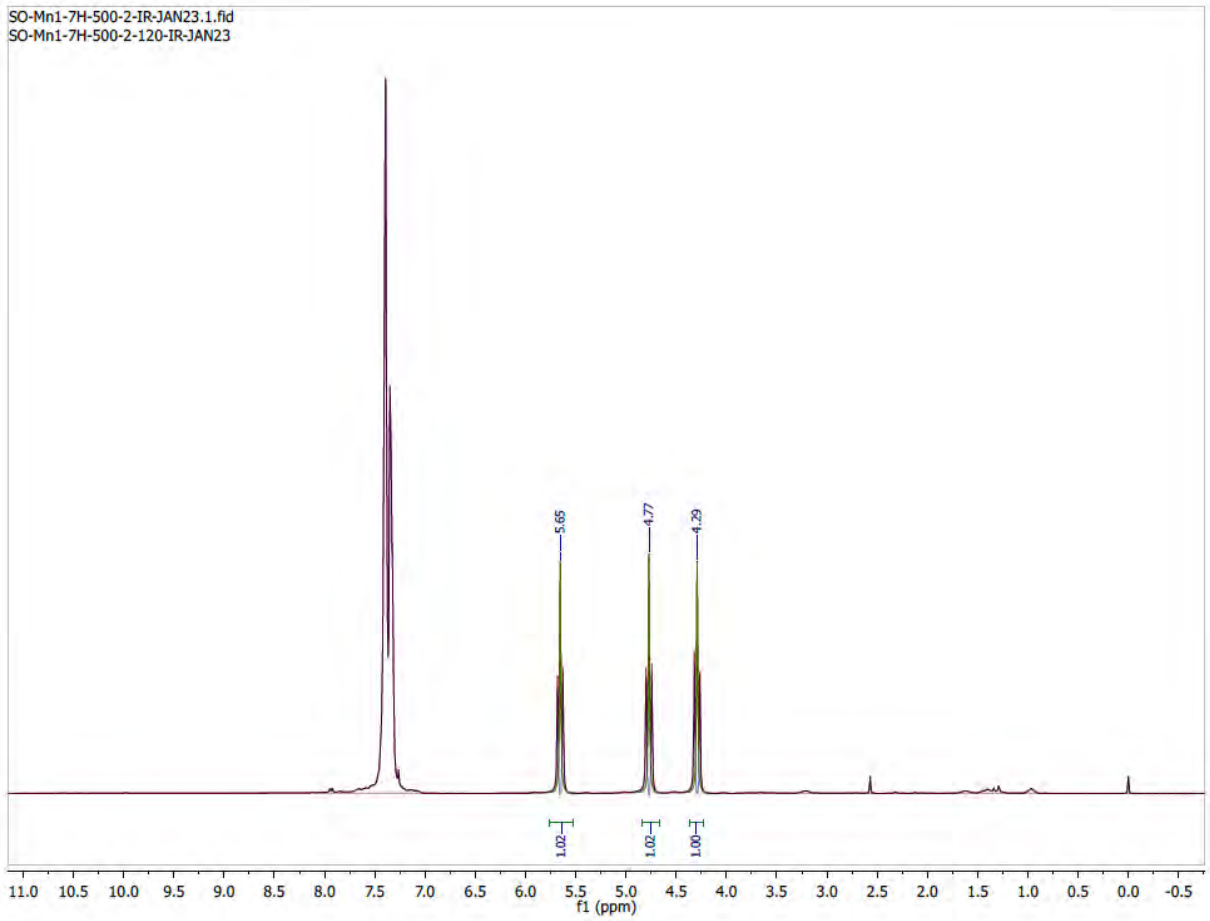

Figure A4-8. ^{1}H-NMR spectrum of styrene carbonate (SC) corresponding to Table 4.2

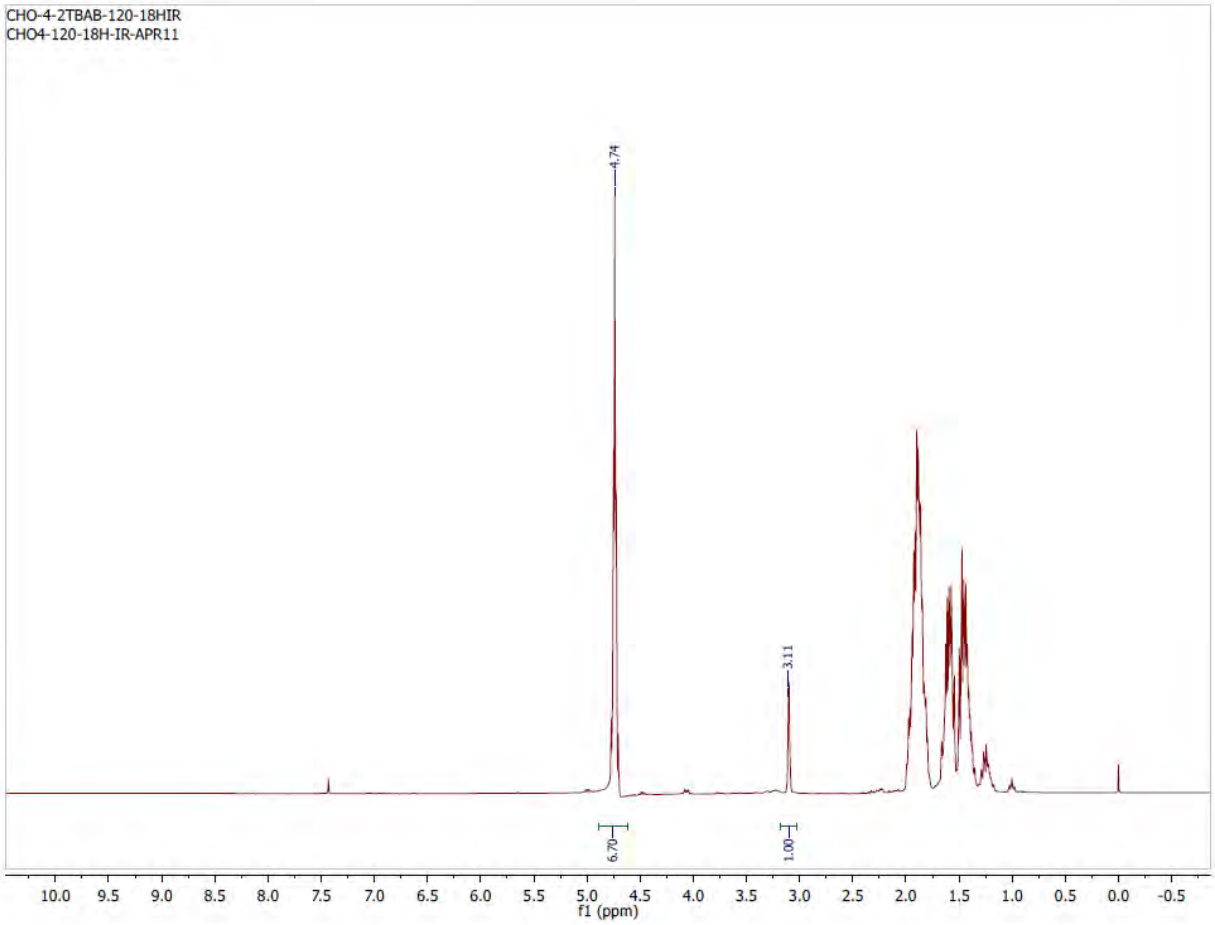

Figure A4-9. [1]H-NMR spectrum of cyclohexane carbonate (CHC) corresponding to Table 4.2

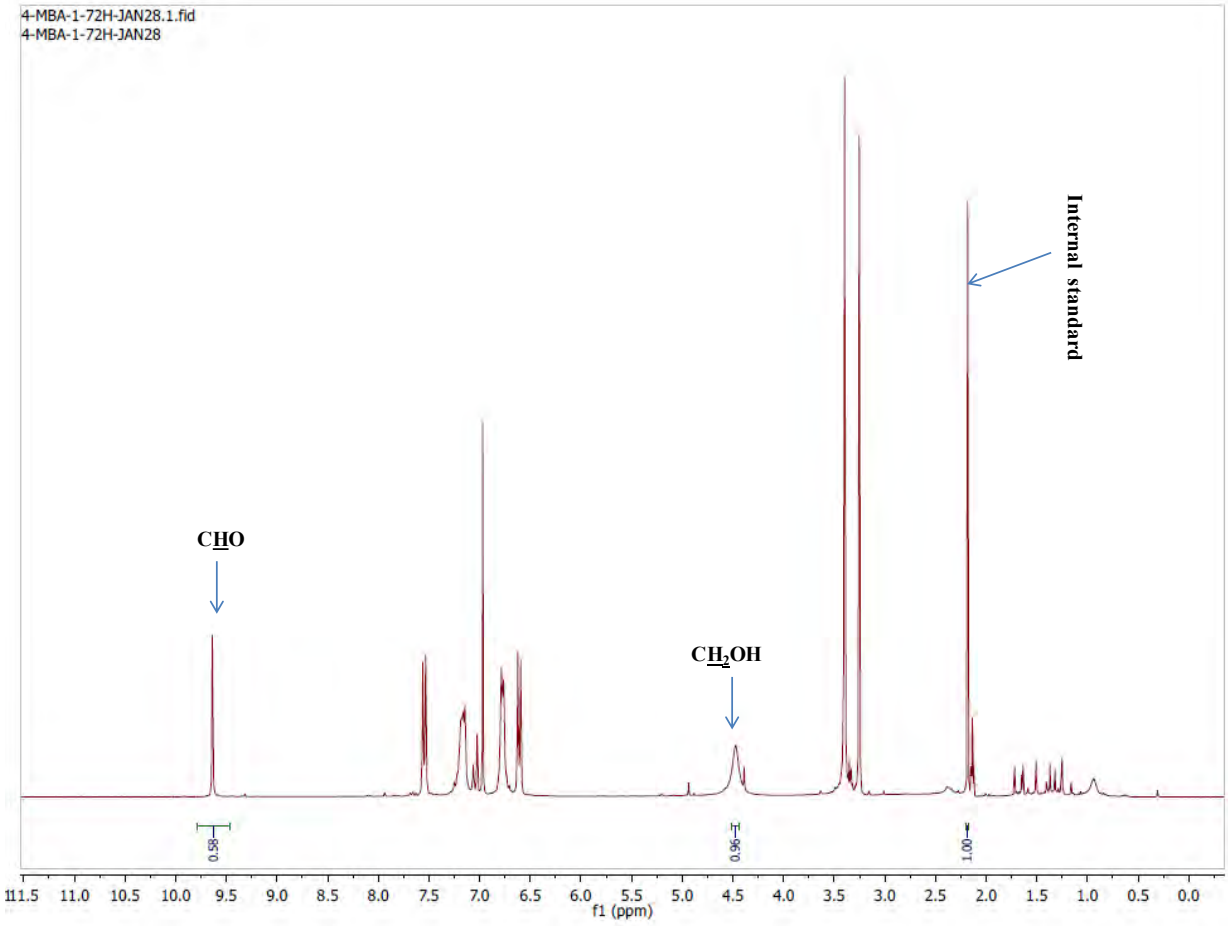

Figure A4-10. [1]H-NMR spectrum of reaction mixture from aerobic oxidation of 4-methoxybenzyl alcohol using **4.1** corresponding to Table 4.3

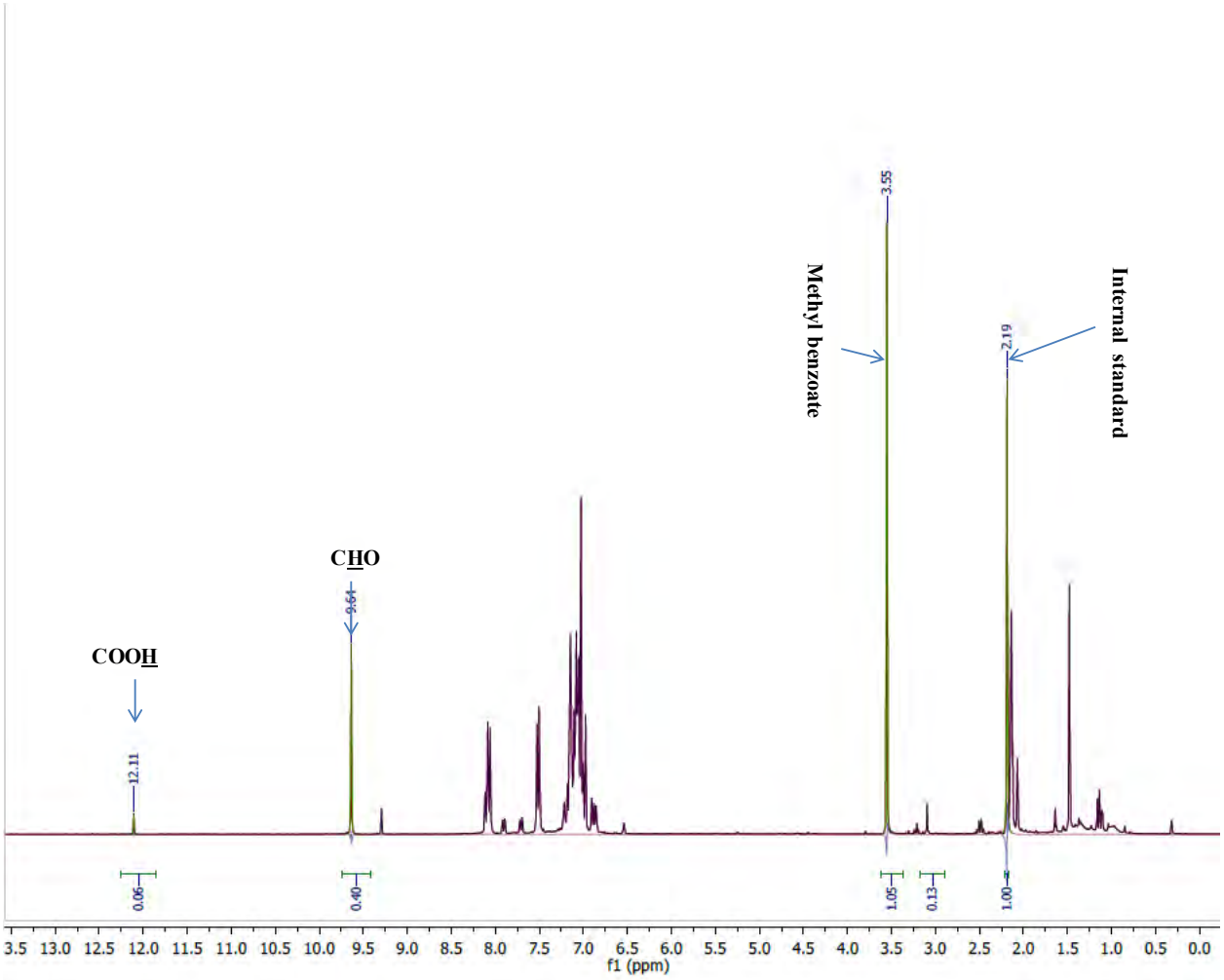

Figure A4-11. ^{1}H-NMR spectrum of products from oxidation of 1,2-diphenyl-2 methoxyethanol using **4.1** corresponding to Table 4.4